Fluorescent Lipopolyamines in Non-Viral Gene Therapy

Adjimatera, Noppadon

Award date:
2005

Awarding institution:
University of Bath

Fluorescent Lipopolyamines in Non-Viral Gene Therapy

Noppadon Adjimatera

A thesis submitted for the degree of Doctor of Philosophy

University of Bath

Department of Pharmacy and Pharmacology

October 2005

ProQuest LLC
789 East Eisenhower Parkway
P.O. Box 1346
Ann Arbor, MI 48106-1346

Abstract

In this work, lipopolyamine gene vectors have been designed and synthesised for non-viral gene therapy (NVGT) applications. N^4,N^9-Dioleoylspermine and N^1-cholesteryl spermine carbamate were designed based on tetracationic spermine conjugated to two C18 oleoyl chains and cholesterol respectively to mimic membrane lipids. Ethidium bromide fluorescence quenching and UV light scattering assays are used to assess the DNA-binding affinity and quality of DNA condensation.

The gene delivery efficacy of both vectors in primary cells and in a carcinoma cell culture model is demonstrated. High efficiency in gene delivery is reported in both cell models. Particularly, the new non-liposomal system with N^4,N^9-dioleoylspermine has the ability to transfect primary skin cells more efficiently than the commercially available liposomal Lipofectin. These vectors show low toxicity and high cell survival while maintaining their high transfection efficiency.

DNA condensation processes are studied at a single nanoparticle (equivalent to a single molecule) level by using the technique of fluorescence correlation spectroscopy (FCS) using PicoGreen (PG). The interaction of lipopolyamine vectors and plasmid DNA is monitored through DNA nanoparticle formation. Time-resolved FCS is also introduced to monitor the dynamics of PG in interactions with DNA duplex. A reliable and novel PG-based platform to monitor the formation of a single DNA nanoparticle has been established and validated, based on detailed understanding of the behaviour of this fluorescent probe.

The NVGT mechanism is also investigated, focusing on the cellular membrane barriers in lipopolyamine-mediated gene delivery. The membrane activity of NVGT vectors is demonstrated by reference to polyalkylpyridinium salt (a marine sponge polymer) as a model of a membrane-active NVGT vector. Fluorescent lipospermidine probes have been designed and synthesized to use as tools to gain a better understanding of each step in gene delivery. Additionally, fluorescently-labelled DNA is also prepared as a useful tracking molecule in NVGT research and development. A refereed paper, two edited book chapters, and several abstracts from presentations of the studies at international meetings are included in an Appendix.

Acknowledgements

I would like to thank Dr. Ian S. Blagbrough for his valuable guidance, supervision and support without which this work would not have been possible. I would also like to thank Dr. Charareh Pourzand for her advice and support in cell biological studies. I am also grateful to Dr. Adrian P. Neal for discussion of his previous work in fluorescence studies in the polyamine research group in the Department.

I would like to thank Prof. Martin Hof and Dr. Teresa Kral at the Czech Academy of Sciences in Prague, for their support in the biophysical studies in this thesis. I would also like to thank Dr. Roderick H. Scott at the University of Aberdeen for his advice in mechanistic aspects of cellular entry and for the kind provision of polyAPS.

I also gratefully acknowledge the Universities UK for an ORS award for financial support of this work. I thank the research and technical staff at the University of Bath: Kevin Smith, Jo Carter, Don Perry, Dr. Anthie Yiakouvaki, and Patricia Holley.

Finally, I would like to thank my family, and my friends in the Department of Pharmacy and Pharmacology, University of Bath for their continuing support.

Table of contents

Title i

Abstract ii

Acknowledgements iii

Table of contents iv

Abbreviations list viii

Chapter 1 Introduction to non-viral gene therapy 1

Introduction 2

Viral vectors 3

Non-viral (synthetic) vectors 4

Cellular polyamines in NVGT 5

Development of synthetic polyamine vectors in NVGT 7

Development of lipopolyamines for NVGT 10

Liposomal cationic lipids vectors 10

Self-assembly lipopolyamine vectors 11

Mechanism of gene delivery using NVGT vectors 15

DNA condensation - the first step in NVGT 15

Cellular uptake of DNA complexes 17

Endosomal escape of DNA 18

Nuclear localisation and entry 19

DNA dissociation and gene expression 20

Fluorescence techniques to determine the efficiency of lipopolyamines in gene delivery 20

Fluorescent lipopolyamines – probes derived from DNA delivery agents 21

Preparation of fluorescent macromolecules 24

Aims of this thesis 27

Chapter 2 Synthesis and testing of lipopolyamines for NVGT 28

Introduction 29

Synthesis of lipopolyamines as NVGT vectors 30

DNA condensation study 35

Effect of DNA type and their condensation 37

N^4,N^9-Dioleoylspermine-mediated DNA condensation study 39

N^1-Cholesteryl spermine carbamate-mediated DNA condensation study 42

Transfection of lipoplexes in a primary cell line 46

Transfection of lipoplexes in a carcinoma cell line 52

Toxicity study of lipoplex gene delivery 54

Optimisation of transfection efficiency and toxicity 57

Chapter 3 Fluorescence correlation spectroscopy studies of a single lipopolyamine-DNA nanoparticle 59

Introduction 60

Measurement of the confocal volume in FCS 61

Efficient probe in DNA condensation by FCS 61

Calf thymus DNA–PicoGreen interaction study 63

CT-DNA condensation by lipopolyamines 67

Point-like molecule detection in CT-DNA condensation 69

Plasmid DNA-PicoGreen labelling study 70

Diffusion behaviour of PG-labelled plasmid DNA 74

pGL3 and pEGFP condensation by lipopolyamines 75

Behaviour of PG during DNA condensation 79

PG intercalation in DNA plasmid and its fluorescence decay 81

FCS analysis of intercalated PG on plasmid DNA 83

FCS analysis of intercalated PG on plasmid DNA through the condensation process 87

Behaviour of PG on DNA undergoing condensation process 90

Conclusions 97

Chapter 4 NVGT mechanistic studies using fluorescent techniques and tools **99**

Introduction 100

Endocytosis of NVGT lipoplexes 101

Novel pore-forming NVGT vector 105

Potential membrane fusion/penetration activity of lipopolyamines 110

Membrane fusion modulation by spermine 111

Membrane lipids integrity disturbance by lipid molecules 112

Fusogenic lipopolyamines: possible synergistic effects from polyamines and lipid 114

Studies of interaction between lipopolyamines and cellular membrane 115

Fluorescent DNA as a tool in NVGT studies 121

Fluorescent lipopolyamine synthesis 123

Synthetic procedure of fluorescent lipospermidine 125

Conclusions 130

Chapter 5 Experimental **134**

General information about materials used in experiments 135

Synthesis of N^4,N^9-dioleoylspermine 137

Synthesis of N^1-cholesteryl spermine carbamate 140

Plasmid DNA amplification and purification 141

Study of lipopolyamine-mediated DNA condensation by ethidium bromide fluorescence quenching assay 144

Light scattering study of lipopolyamine-DNA complex 147

Human skin fibroblast (FEK4) transfection 148

HtTA-1 HeLa cells transfection 151

Fluorescent-activated cell sorting experiments 152

Bioluminescence assay of luciferase 153

Toxicity assessment of DNA condensing agents by MTT assay 154

General information on FCS experiments 155

Studies of DNA binding of PicoGreen using FCS 156

Studies of lipopolyamine-mediated DNA condensation using FCS 157

FCS data analysis 157

Time-resolved fluorescence correlation spectroscopy 159

FEK4 and HtTA-1 HeLa transfection at 12 °C 161

DNA condensation studies of polyalkylpyridinium salt 162
Light scattering study of DNA complexed with polyAPS 162
Fluorescein *O*-diacetate release assay of polyAPS 163
Propidium iodide uptake assay of polyAPS 165
Membrane integrity study of spermine and oleic acid 166
Membrane integrity study of synthetic lipopolyamines 167
Fluorescent labelling of plasmid DNA 167
Human skin fibroblast (FEK4) cells transfection with labelled DNA 168
Synthesis of fluorescent lipospermidine 169
Synthesis of N^1,N^{12}-di-trifluoroacetyl-N^4-oleoylspermine 172

References 174

Appendix Publications and presentations from this work

Abbreviations list

A	absorbance
AAV	adeno-associated virus
AF488	Alexa Fluor-488
BGTC	bis(guanidinium)-tren-cholesterol
Boc_2O	di-tert-butyl dicarbonate
bp	basepairs
br	broad
BSA	bovine serum albumin
CD	cyclodextrin
$C_{dye}/_{kbp}$	dye molecule/kilobasepair
CF	cystic fibrosis
CI	chemical ionisation
CMV	cytomegalovirus (promoter gene)
CR	count rate
CT-DNA	calf thymus DNA
CXR	5-carboxy-X-rhodamine
D	diffusion coefficient
Da	Dalton
DCC	1,3-dicyclohexylcarbodiimide
DC-Chol	3β-[*N*-(*N'*,*N'*-dimethylaminoethane)-carbamoyl]cholesterol
DCM	dichloromethane
DCU	1,3-dicyclohexylurea
DEAE	diethylaminoethanol
DMSO	dimethylsulfoxide
DNA	deoxyribonucleic acid
DNase	nuclease
DOGS	dioctadecylamidoglycyl-spermine
DOPE	dioleoylphosphatidylethanolamine
DOSPA	2,3-dioleyloxy-*N*-[2-(spermine carboxamido)ethyl]-*N*,*N*-dimethyl-1-propanaminium trifluoroacetate
DOSPER	1,3-dioleoyloxy-2-(6-carboxyspermine)propylamide
DOTMA	*N*-[1-(2,3-dioleyloxy)propyl]-*N*,*N*,*N*-trimethylammonium chloride

DPPES	dipalmitoylphosphatidylethanolaminyl-spermine
dsDNA	double-stranded DNA
D_w	diffusion coefficient in water
EDTA	ethylenediaminetetraacetic acid
EGFP	enhanced green fluorescent protein
EPC	egg phosphatidylcholine
EPE	egg phosphatidylethanolamine
eq	equivalent
ESM	egg sphingomyelin
EthBr	ethidium bromide
FAB	fast-atom bombardment
FACS	fluorescent-activated cell sorting
FCS	fluorescence correlation spectroscopy
FCS-EMEM	Earle's Minimal Essential Medium supplemented with foetal calf serum
FDA	fluorescein-*O*-diacetate
FDG	fluorescein-di-β-D-galactopyranoside
FITC	fluorescein isothiocyanate
Fmoc	fluoren-9-ylmethoxycarbonyl
FRAP	fluorescence-recovery after photobleaching
FRET	fluorescence resonance energy transfer
FSC	forward-scattered light
FT-IR	Fourier transform infrared
$G(\tau)$	autocorrelation function
GFP	green fluorescent protein
HEPES	2-[4-(2-hydroxyethyl)-1-piperazinyl]ethanesulfonic acid
HIV	human immunodeficiency virus
HOBt	*N*-hydroxybenzotriazole
HPLC	high performance liquid chromatography
HRP	horseradish peroxidase
IC_{50}	concentration at which cell viability is 50%
IR	infrared
IRF	instrument response function
K_b	binding constant
LB	Luria-Bertani

LC-MS	liquid chromatography-mass spectroscopy
λ_{em}	emission wavelength
λ_{ex}	excitation wavelength
log F_1	fluorescence intensity in log unit, using F_1 emission filter
log F_3	fluorescence intensity in log unit, using F_3 emission filter
LS	light scattering
LY	lucifer yellow carbohydrazide
m	multiplet
MOPS	3-[*N*-morpholino]propanesulfonic acid
MQ	milliQ
MS	mass spectroscopy
MTT	3-(4,5-dimethylthiazol-2-yl)-2,5-diphenyltetrazolium bromide
MW	molecular weight
NBD-PE	*N*-nitrobenzoxadiazole phosphatidylethanolamine
NLS	nuclear localisation signal
N-MANT	*N*-methylanthranilic acid
NMR	nuclear magnetic resonance
N/P	ammonium/phosphate
NPC	nuclear pore complex
N-Rh-PE	*N*-lissamine rhodamine phosphatidylethanolamine
NVGT	non-viral gene therapy
Opti-MEM	Minimal Essential Medium without serum
PA	phosphatidate
PBS	phosphate buffered saline
PC	phosphatidylcholine
PCR	polymerase chain reaction
PE	phosphatidylethanolamine
pEGFP	enhanced green fluorescent protein encoding plasmid
PEI	polyethylenimine
PG	PicoGreen
pGL3	firefly luciferase encoding plasmid
PI	propidium iodide
PLA	poly-L-arginine
PLH	poly-L-histidine

PLL	poly-L-lysine
PLO	poly-L-ornithine
PN	particle number
PolyAPS	polyalkylpyridinium salt
PS	phosphatidylserine
R6G	rhodamine-6G
R_f	retention factor
RLU	relative light unit
RNA	ribonucleic acid
RP-HPLC	Reversed-phase high performance liquid chromatography
s	singlet
SAINT	Synthetic Amphiphile INTeraction
S.D.	standard deviation
SDS	sodium dodecyl sulfate
SMS	single molecule spectroscopy
SPAD	single photon avalanche diode
SSC	side-scattered light
ssDNA	single-stranded DNA
SV40	simian virus 40 (promoter gene)
t	triplet
TCSPC	time-correlated single photon counting
τ_D	diffusion time
TE	Tris-EDTA
TEA	triethylamine
TFA	trifluoroacetic acid
TLC	thin layer chromatography
TMR	tetramethylrhodamine
t_R	retention time
TR-FCS	time-resolved fluorescence correlation spectroscopy
tTA	tetracycline-controlled transactivator
TTTR	time-tagged time-resolved
UV	ultraviolet
v	solvent volume
V	confocal volume

Chapter 1

Introduction to non-viral gene therapy

Introduction

Following the solving of the structure of DNA and its function in human life,[1] DNA technology has been used in many fields of biomedical science. Gene therapy, one example of gene technology, is a new treatment strategy which is primarily expected to treat genetic disorders, known as corrective gene therapy. Unlike conventional chemical-based medicines, the therapeutic DNA in gene therapy was used as the "pharmacologically-active" ingredient and formulated in proper forms for administration into patients' cells, aiming for desired gene expression. The desired outcome of therapy is not only limited to the missing proteins in patients (such as the chloride ion channel protein in cystic fibrosis (CF)), but also the inhibitory protein to stop the progression of disease or abnormal protein production.[2-6] Gene expression modulation using gene therapy is also useful in the treatment of other non-genetic diseases, especially cancer. The suicidal gene therapy strategy is exploited by the destruction of target cells using a cytotoxic pathway such as apoptosis and oncogene suppression.[7] "Suicide genes" can be also delivered to cancer cells to make them more susceptible to chemotherapeutics or toxins. Currently, cancer gene therapy dominates more than 60% of gene therapy clinical trials. Since 1989, the number of approved clinical trials has increased 10-times worldwide. Nevertheless, the success rate in gene therapy still drags behind expectations. Currently, most of the 630 completed or ongoing trials are in Phase I and II. There have been only 2% of clinical trials (from 1076 trials in total, data as of Aug 2005) proceeding through to Phase III.[8] Therefore, the development of safe and efficient gene therapy is still urgently required. A concise overview of gene therapy development and the major problems that hold back this technology are presented in this chapter.

There are two critical components in any successful gene therapy. Firstly, selection of the right therapeutic DNA, normally prepared in circular plasmid form, is important. The sequencing of the human genome offers many excellent opportunities for therapeutic gene selection for disease treatment. There are nearly 1,000 documented disease genes with correlations between the function of the gene product and features of the disease, such as age of onset, or mode of inheritance.[9] The other critical component is the gene vector with appropriate design to deliver the desired DNA into cells (either *in vivo* or *ex vivo*) efficiently and safely.[10] The development of suitable methods for gene delivery has been regarded as the greatest task in gene therapy.[10,11] The optimal vector design must incorporate these characteristics: specific cell targeting, long-term expression, high transfection, maximised DNA payload, and low immunogenicity/toxicity. The DNA delivery vector is the major research area in gene therapy and can be generally classified into 2 key groups, i.e. viral and non-viral vectors. Both gene vectors present their own distinctive advantages and disadvantages.[6]

Viral vectors

Viral delivery systems are derived from naturally evolved or recombinant viruses capable of transferring their genetic materials into host cells. Many viruses have been explored as transfection vectors. Viral vectors gain cell entry through their infectivity mechanisms, such as binding to cell membrane receptors. Both DNA and RNA viruses have been used in gene therapy. These viruses have been modified to eliminate their viral toxic genome and maintain their high gene transfer capability. Retroviruses were the first viral vectors used, whose RNA genome is converted into DNA in transfected cells. Retroviral vectors are capable of infecting only dividing cells. Lentiviral vectors such as human immunodeficiency virus (HIV), can infect both dividing and non-dividing cells. Lentiviruses offer longer periods of gene expression than retroviruses. Adenovirus is a family of DNA viruses causing benign respiratory tract infections in humans. It can infect cells in all stages of cell division. Their genomes contain more genes than other viral vectors typically used, and they do not usually integrate into the host DNA. The problems with adenovirus are transient gene expression (i.e. only for 1 week post-transfection) and high, undesirable immune responses. Adeno-associated virus (AAV) is a less toxic, single-stranded DNA virus with additional genes to replicate from other helper viruses (usually adenovirus). The size of the viral particle also limits the DNA payload in these vectors, for example, AAV can accommodate only DNA with 3.5-4.0 kilobasepair (kbp) size. Retrovirus and lentivirus have a bigger payload (DNA of 7.0-7.5 kbp), while adenoviral vectors can deliver DNA up to 30 kbp. Additionally, the production of viral vectors is very complicated, especially with regard to the control of toxic viral contamination in the manufacturing batch, low viral yield, and the high cost of production.[12-14]

Though viral vectors generally give high and sustained gene expression, they also cause safety concerns particularly immunogenicity. Viral vector toxicity is the major concern, especially the random integration of retroviral or lentiviral DNA into the host chromosome. As a process of gene delivery, the inserted viral gene (and transgene) will become a part of the host genome. This may alter the oncogenes' or tumour suppressor genes' function in host cells. Furthermore, expression of the viral protein (e.g. E2 protein in adenovirus) provokes inflammatory reactions and toxicities, both the cell-killing "cellular" response and the antibody-producing "humoral" response. In the cellular response, virally infected cells are killed by cytotoxic T-lymphocytes. Most of the human population also have antibodies to adenovirus from previous infections with naturally occurring viruses. This limits the repeated application of adenoviral vectors. It has been shown that the remaining low level of viral replication of first generation vectors induces CD4+ and CD8+ dependent immune

responses which lead to a reduced duration of gene expression *in vivo*. This immunity problem was also found in AAV vectors.[12-14]

Non-viral (synthetic) vectors

Considering the problems in virus-based gene therapy, an alternative approach called non-viral gene therapy (NVGT) has been intensively studied. The ideal NVGT vector would keep the high transfectivity demonstrated in viruses, but with no toxicity and no DNA payload limitation. Non-viral vectors are generally cationic compounds in nature which are typically polyamines. The simplicity of these chemical-based vectors permits chemical modification, such as addition of a lipophilic moiety, controlling the regiochemical distribution of positive charges, or conjugation to add desired functional groups. This expansive possibility has resulted in many classes of NVGT vectors. NVGT vectors have the advantages of safety, simplicity of preparation, and high gene encapsulation capability, though they are currently less efficient than viral vectors.[11]

In 1997, Felgner *et al.*[15] published the standardised NVGT vector classification and their nomenclature guidelines. The guidelines grouped these diverse synthetic gene delivery vectors into the two classes, which are lipoplex (cationic lipids-nucleic acid complex) e.g. lipopolyamines, cationic liposomes etc., and polyplex (cationic polymer-nucleic acid complex) e.g. polyethylenimine (PEI), poly-L-lysine (PLL) etc. Cationic lipid refers to all cationic amphiphiles, including cationic cholesterol and bile salt derivatives, as well as other micelle-forming cationic amphiphiles. In these guidelines, there is also an agreement on the expression of composition of DNA-vector complexes in the unit of charge ratios.

The effort to improve NVGT development is not only limited to chemical modification. There are many studies to find the right physico-chemical properties of DNA complexes to achieve high transfection. For example, the particle size and zeta potential are important to improve the cellular uptake of DNA complexes. The composition of lipid mixtures (e.g. cationic liposomal formulation) can also enhance gene delivery efficiency. Thus the addition of helper lipid may aid in the endosomal escape process for gene complexes.[11]

Recently, direct DNA delivery into the target cells or organ, by injection, has been introduced as a route for gene therapy without vectors (naked DNA).[16,17] Naked DNA (with no protection from vectors) goes through rapid degradation upon systemic administration and this causes low gene expression. Some direct-to-site delivery by physical techniques have been developed to resolve this low yield problem, e.g. gene gun, electroporation, ultrasound-mediated gene delivery, nucleus injection etc.[18] However, this improved result

has introduced complications in DNA administration requiring medical devices. Nevertheless, synthetic vector research is still the biggest group with intense competition in this NVGT research area.

Cellular polyamines in NVGT

Polyamines are polycationic at physiological pH and have many important roles in living cells, such as cell growth and differentiation control. Many mammalian cells also possess an active polyamine uptake system, but little is known about its function.[19] Spermine (Figure 1.1 (i)) and spermidine (Figure 1.1 (ii)) were firstly discovered in the nuclei of sperms, which help to package DNA. The phosphate anions of DNA, ($pK_a \sim 1.5$),[20,21] are fully ionized at physiological pH (7.4). For example, a 5 kbp DNA plasmid has a molecular weight of about 3.3 MDa and carries 10,000 negative charges. This highly negatively charged DNA is not able to cross the cell membrane (which is a lipophilic layer with a negatively charged surface). These polyamines ($pK_a = 8\text{-}10$) help neutralise the negative charges of the phosphate ions in DNA. This initiated the DNA helix's axis bending, resulting in DNA condensation into a compact (condensed) structure. In the NVGT applications of spermine, it was found that nanoparticles of DNA were formed on condensation by spermine. They are able to go across cell membranes and lead to the gene expression of delivered DNA.[22,23] The structure-activity relationships of DNA binding by polyamines are also critical to the efficiency of DNA condensation.[24-29]

However, most mammalian cells use histone proteins to condense nuclear DNA to form chromatin.[30] The histones are translated in the cytoplasm like other cellular proteins, though they are in need for DNA packaging in the nucleus. They undergo some post-translational modification, for example, acetylation, phosphorylation etc. Then, these histones are imported back into the nucleus. The histones found in chromatin are categorized as core histone (subunit H2A, H2B, H3, H4) and the linker histone (H1), forming an octamer (108 kDa) which binds to DNA. Lysine (Figure 1.1(iii)) and arginine (Figure 1.1(iv)), positively charged amino acids, are found in most histone proteins (an example of some part of histone H2A is shown in Figure 1.1(v)). Lysine (Lys, K) is the amino acid with $(CH_2)_4NH_3^+$ side chain, while arginine (Arg, R) contains a guanidine group. Both are basic amino acids and their side-chains are positively charged in the cell. The pK_as of lysine and of arginine are 10.0 and 12.0 respectively. The H1 subunit has about 20% of Lys/Arg, the biggest number among histone subunits, which is required for its nucleosomes linking responsibility. Histone is more efficient in DNA condensation than spermine or spemidine, due to its number and unique distribution of positive charges. The histone octamer is capable of condensing 200 bp DNA (67 nm length, 130 kDa).[31]

Histone proteins were also tried in NVGT applications. The IL-2 and single chain IL-12 (scIL-12, fusion protein) gene was delivered by 37-amino acid *N*-terminal peptide of histone H2A, with superior transfection compared to Superfect dendrimer.[32,33] The other study was on the transgene expression of luciferase gene (pCMV Luc) on ECV 304 human endothelial cells. Similarly, DNA complexed with histone H1, in toroidal forms, also gives high transfection efficiency. Cellular uptake is thought or presumed to be by phagocytosis.[34]

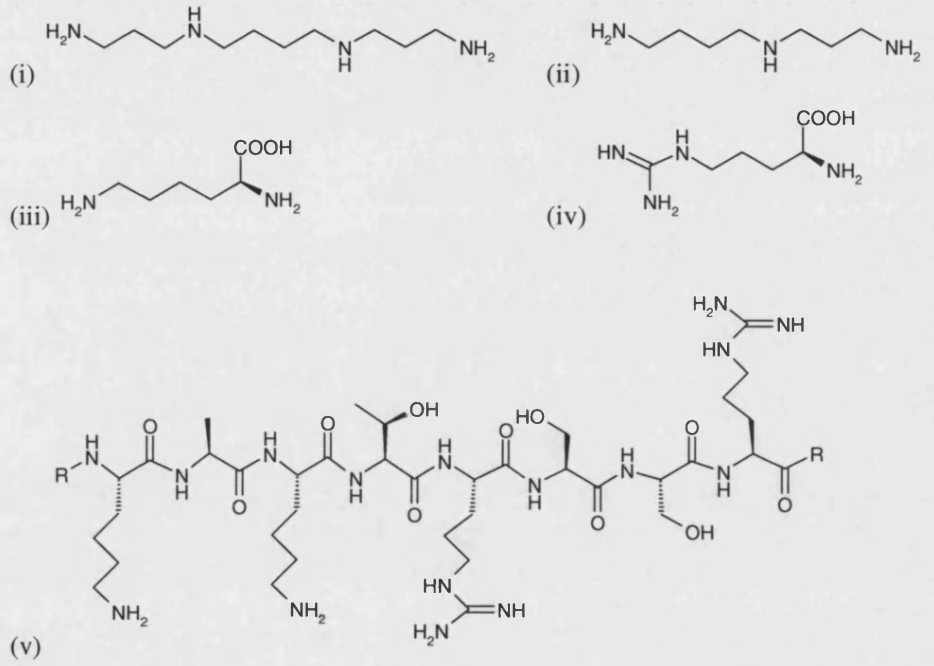

Figure 1.1 Natural DNA condensing agents: (i) spermine, (ii) spermidine, (iii) lysine, (iv) arginine, and (v) histone 2A K(13)AKTRSSR(20) (underlined amino acids indicate some DNA contact sites of histone 2A)[33]

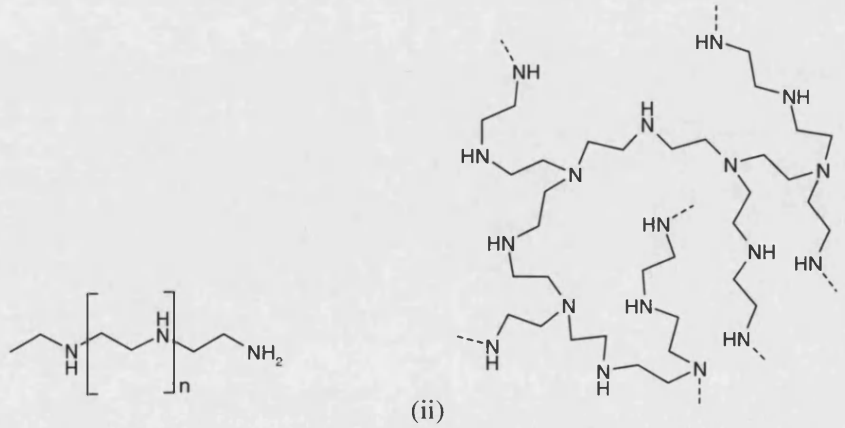

Figure 1.2 Polyethylenimine in (i) linear and (ii) branched form

Development of synthetic polyamine vectors in NVGT

A widely known synthetic polyamine in gene delivery, polyethyleneimine (PEI) (Figure 1.2), was first introduced by Behr and co-workers[35] in 1995. PEI has high positive charge number, with ammonium groups at every 3-7 nitrogen atoms at pH 7.[35-37] This enables PEI with high buffering capacity, known as a "proton sponge"[35] which is considered to be critical to endosomal escape of DNA complexes. From Godbey and co-workers' study, the endosomes containing PEI complexes were found to grow in number and size and were occasionally seen to lyse.[38] However, the charge density of PEI (particularly free PEI in polyplexes, typically found at 80% of total PEI) is also related to its high toxicity.[39]

PEI molecular weight (MW) and shape also play an important role in DNA delivery. Linear (Figure 1.2 (i)) and branched PEI (Figure 1.2 (ii)), with MW lower than 25 kDa, show better transfection than the higher MW PEI, possibly due to the higher DNA-PEI dissociation of low MW PEI.[40,41]

Apart from PEI, several cationic polymers have been synthesised for nucleic acid delivery, by employing building blocks from amino acids (e.g. Lys, Orn, Arg, Hist). For example, poly-L-lysines (PLL) (Figure 1.3 (i)) of varying molecular weight average (4, 24, 54, 224 kDa) were used to condense DNA and studied by ethidium bromide assay and photon correlation spectroscopy.[42] The size of nanoparticles obtained (37 - 207 nm diameter) is in linear relationship to the degree of PLL polymerization. Complexes based on larger PLL showed a sigmoidal destabilisation (more stable particles) by polyanion while complexes based on smaller PLL showed more linear disruption.[42]

The shape of PLL is also important in DNA delivery. Linear PLL is more efficient in condensing DNA than most dendritic PLL. Cellular uptake of PLL/DNA complexes was high. However, the overall transfection level of PLL is low, possibly due to inadequate endosomal escape or poor release of DNA from the complexes.[43] The addition of chloroquine was found to improve PLL transfection, presumably as an endosomolytic agent.[44]

Ornithine is an amino acid which is not used in mammalian peptide synthesis, but which has a similar pK_a to lysine. In a NVGT context, poly-L-ornithine (PLO),[45] Figure 1.3(ii), showed superior (10-times higher) *in vitro* transfection of DNA complexes compared to PLL. There is no difference in physico-chemical properties of both PLL- and PLO-DNA complexes. However, PLO is able to condense DNA at a lower mass ratio than PLL. This greater affinity of PLO for DNA may be related to the observed *in vitro* transfection efficiency.

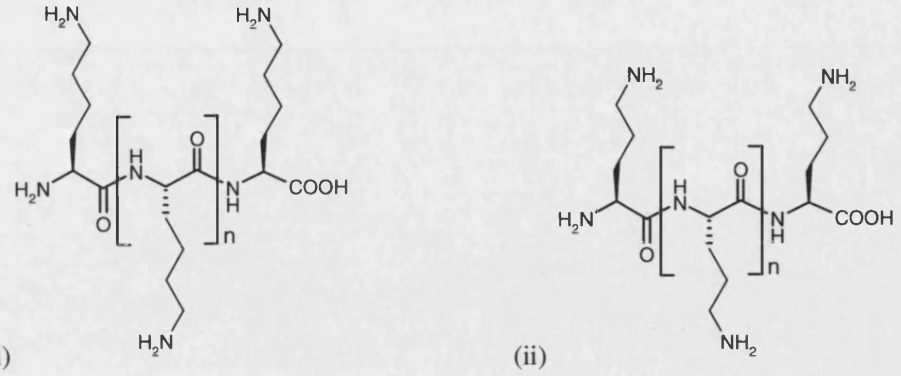

Figure 1.3 Synthetic polyamines based on basic amino acid monomers: (i) poly-L-lysine, (ii) poly-L-ornithine

Poly-L-arginine (PLA), Figure 1.4 (i), has been regarded as a potential gene cargo carrier. Apart from the presence of arginine in histones, many membrane-permeable peptides, for example HIV-1 Tat-(48-60) peptide, also contains this amino acid. PLA (MW 5-15 kDa) and oligoarginine (4-16 residues) were found to be able to transfect cells, similar to Tat protein when used as a gene delivery vector (comparable to Lipofectamine).[46] The higher molecular weight PLA (i.e. degree of polymerisation = 217) was also able to transfect cells, but less efficiently.[44] Homopolymers of L-arginine (6 arginines or more) entered cells far more effectively than polymers of equal length composed of other positively charged amino acids (i.e. lysine, ornithine and histidine). Rothbard, Wender and co-workers[47,48] found that the guanidine group of arginine is the critical moiety for this surprising biological activity which is ATP-dependent, but does not involve endocytosis.

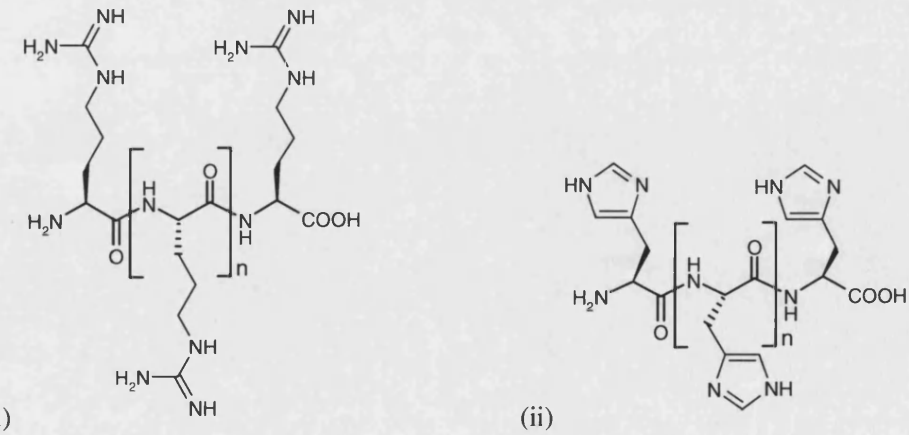

Figure 1.4 (i) Poly-L-arginine and (ii) poly-L-histidine

Histidine is another basic amino acid with the pK_a of its amino group at 9.2. Interestingly, the imidazole group in histidine (pK_a = 6.0) helps DNA delivery into the cytosol after their protonation in endosomes (which are acidified to pH 5.5) which mediates membrane destabilization. This imidazole protonation exhibits a buffer effect in an acidic medium, facilitating the swelling and destabilization of vesicles as the case of chloroquine and PEI.[49] Poly-L-histidine (PLH), Figure 1.4 (ii), is insoluble in aqueous solutions at pH > 6.0. The conjugation with water-soluble units, such as gluconic acid, or preparation in a co-polymer with lysine (known as HK-polymer), was reported to improve its solubility at physiological pH.[49,50]

Recently, there is some interest in bio-polyamines such as amino-sugars, especially for their biocompatibility and low toxicity. Chitin is a polysaccharide found in the exoskeleton of insects and crustaceans. When chitin is deacetylated in alkaline pH, chitosan which is a copolymer of D-glucosamine (Figure 1.5 (i)) (pK_a = 6.2-7.0) and *N*-acetyl-D-glucosamine (Figure 1.5 (ii)) is obtained. Transfection efficiencies of the DNA/chitosan complexes were dependent on the pH of the culture medium (acidic pH is required to enable protonation in chitosan) and on the molecular mass of chitosan. Chitosan of MW > 100 kDa gave poorer transfection than smaller chitosan polymers. It was also found that chitosan-DNA complexes had high resistance to serum and minimal cytotoxicity.[51-53]

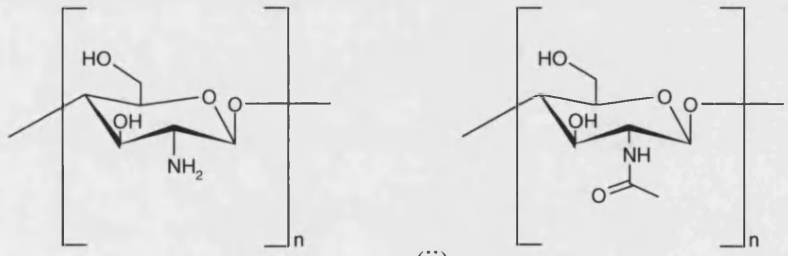

(i) (ii)

Figure 1.5 Chemical structures of (i) D-glucosamine and (ii) *N*-acetyl glucosamine.

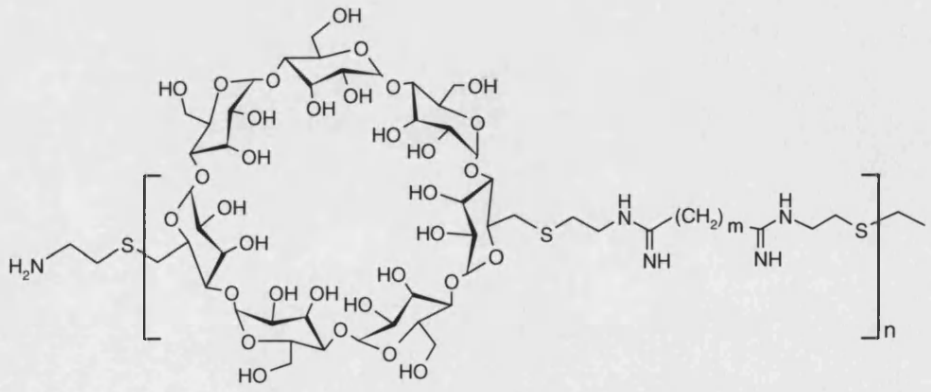

Figure 1.6 Example of β-cyclodextrin polyamine (m, n = 4-10)[54]

The carbohydrate moiety has been found to lessen the toxicity of NVGT vectors. Davis's research group demonstrated, through a series of β–cyclodextrin (CD)-polyamine conjugates (an example of these compounds is shown in Figure 1.6), that a shorter alkyl chain between the CD and the charge centres in the polycation backbone minimise toxicity. The CD unit also provides a unique property, with the ability to be modified by compounds that form inclusion complexes with CD, without disruption of the polymer-nucleic acid interactions.[54-56]

Development of lipopolyamines for NVGT

Polyamine vectors have been regarded as efficient DNA condensing agents, but the DNA delivery performance still needs improvement. The development of lipid-polyamine conjugates (called lipopolyamines) aims to keep the high DNA packaging function, and improve *in vivo* transfection results. These molecules have a lipophilic moiety (mainly long chain hydrocarbon or steroidal lipids) and positively charged amine group(s), such as spermidine, spermine, amino sugar, or synthetic polyamines as previously mentioned.[57] A more general term "cationic lipids" is sometimes used if they are conjugates of lipids and simple amine or quaternary ammonium ions. Currently, lipopolyamines are considered to be the major gene carriers among NVGT systems. Lipopolyamines can be either liposomal or non-liposomal non-viral delivery vectors.

Liposomal cationic lipids vectors

Liposomal delivery vectors usually contain two types of lipid, a cationic lipid and a neutral helper lipid. For example, in Figure 1.7, Lipofectin liposome is comprised of *N*-[1-(2,3-dioleyloxy)propyl]-*N*,*N*,*N*-trimethylammonium chloride (DOTMA)[58,59] for DNA condensation and cellular membrane interaction, and dioleoylphosphatidylethanolamine (DOPE) to increase transfection efficiency. DOPE is the helper lipid mainly used due to its membrane fusion promoting ability.[60-62]

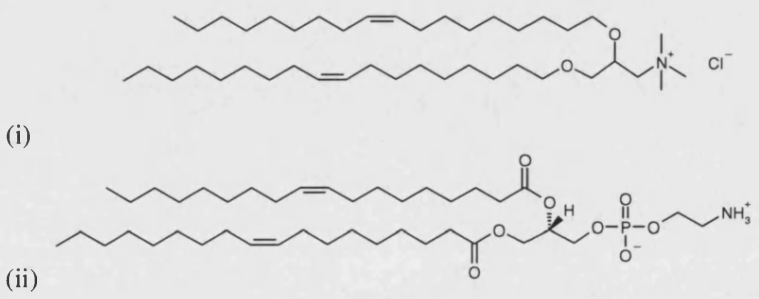

Figure 1.7 Lipofectin liposomal vector, a mixture of cationic lipid - (i) DOTMA and (ii) helper lipid - DOPE (1:1 w/w)

In 1991, Huang *et al.*[63] also introduced 3β-[*N*-(*N'*,*N'*-dimethylaminoethane)-carbamoyl]cholesterol (DC-Chol), as a first cholesterol-based cationic lipid for NVGT (Figure 1.8). The liposome formulation of DC-Chol:DOPE is highly efficient for delivering polynucleotides into various cell types *in vitro* and *in vivo*.[64]

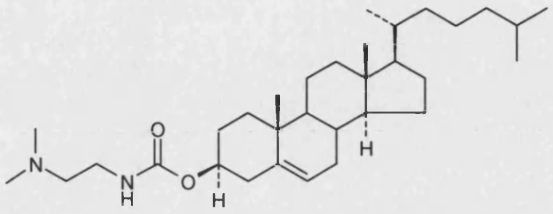

Figure 1.8 DC-Chol

Pyridinium compounds have also been utilized in cationic lipid design. From the previous study of Engbert's research group[65] on pyridinium-based transfection agents, the SAINT (Synthetic Amphiphile INTeraction) series was developed. This involved the conjugation of two fatty acid chains (tail groups) with pyridinium (head group), which results in high transfection efficiency when used in a liposomal formulation with DOPE. From structure-activity relationship studies, it was found that unsaturated fatty acids enhanced the transfection efficiency. Head-group modification, by introducing another pyridinium group linked with an alkyl spacer, also significantly improved the transfection efficiency. In the SAINT series, SAINT-2 (Figure 1.9) showed a 3-6-fold higher transfection than Lipofectin.[65]

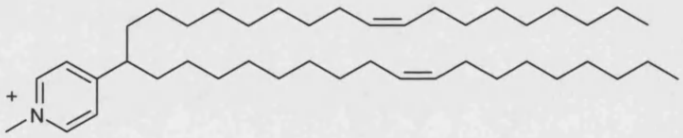

Figure 1.9 SAINT-2

Self-assembly lipopolyamine vectors

The efficiency of liposomal vectors is variable and DNA encapsulation is a lengthy and complicated process.[66] This inspires NVGT researchers to develop self-assembly lipopolyamine vectors which combine both the characteristics of cationic and helper lipids in one molecule. These lipopolyamines are believed to form a structured complex with DNA, which protects DNA from the external environment (such as DNAase) and assists in intracellular gene delivery. In 1989, the synthesis of non-liposomal lipopolyamines (or more precisely called lipospermine) dipalmitoylphosphatidylethanolaminyl-spermine (DPPES) (Figure 1.10 (i)) and dioctadecylamidoglycyl-spermine (DOGS or Transfectam) (Figure 1.10 (ii)) was carried out by Behr and co-workers[66] as effective transfecting agents.

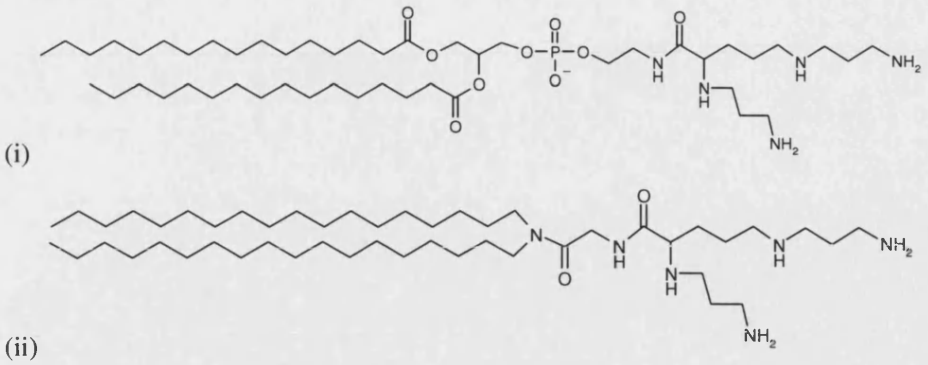

Figure 1.10 (i) DPPES and (ii) DOGS

This success led to more interest in the synthesis of novel lipospermines, e.g. RPR120535,[67] 1,3-dioleoyloxy-2-(6-carboxyspermine)propylamide (DOSPER)[68] and 2,3-dioleyloxy-*N*-[2-(spermine carboxamido)ethyl]-*N*,*N*-dimethyl-1-propanaminium trifluoroacetate (DOSPA, also used in Lipofectamine liposome which is a mixture of DOSPA:DOPE 3:1 w/w) (Figure 1.11). The design of a novel lipopolyamine formula for DNA condensation and cellular delivery relies on previous and continuing studies of the structure-activity relationships of DNA binding and condensation by polyamines. The effects of the distribution of positive charges along the polyamine moiety in DNA condensing agents were studied by Geall *et al.*[27,69] DNA condensation is dependent upon three characteristic properties of polyamines: number of positive charges, regiochemical distribution of charges (determined by the pK_a of each amino group), and local salt concentration.[24-29] Long-chain hydrophobic hydrocarbons, which mimic the fatty acids commonly found in cellular membrane's phospholipids (e.g. $C_{14\text{-}18}$, either saturated or unsaturated), are mostly used as the lipid moiety in the design.

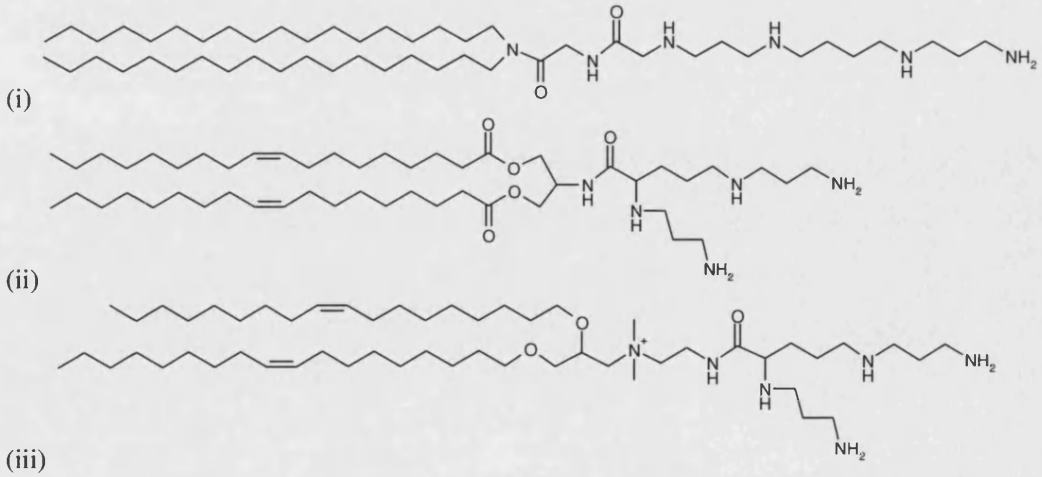

Figure 1.11 (i) RPR120535, (ii) DOSPER, and (iii) DOSPA

Vierling *et al.*[70] introduced the fluorinated double-chain lipospermines (an example is shown in Figure 1.12), one or both of these chains ending by a highly fluorinated tail of various lengths, which are close analogues of DOGS for NVGT. These fluorinated lipopolyamines are able to condense and transfect cells with and without DOPE. The modified lipid chain, which is both lipophobic and hydrophobic by nature, provided the protection of DNA from both lipophilic and hydrophilic biocompounds.[70]

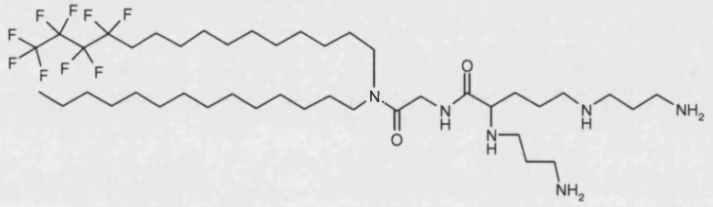

Figure 1.12 Example of fluorinated lipospermine [F4C11][C14]-GS

Steroid lipids are also of interest in lipopolyamine design. GL#67 (Figure 1.13 (i)) was developed by Genzyme,[71] consisting of a cholesterol anchor linked to a spermine head-group, apparently in a "T-shape" configuration. This lipid was used in combination with DOPE to replace the defective gene in CF patients. Lehn *et al.*[72,73] synthesised bis(guanidinium)-tren-cholesterol (BGTC) (Figure 1.13 (ii)) for gene therapy in airway epithelial cells for CF. This BGTC has been successfully used with or without DOPE. The multi-lamellar ordered structure of lipoplexes was detected by using transmission electron microscopy. This ordering may be associated to their high transfection efficiency.

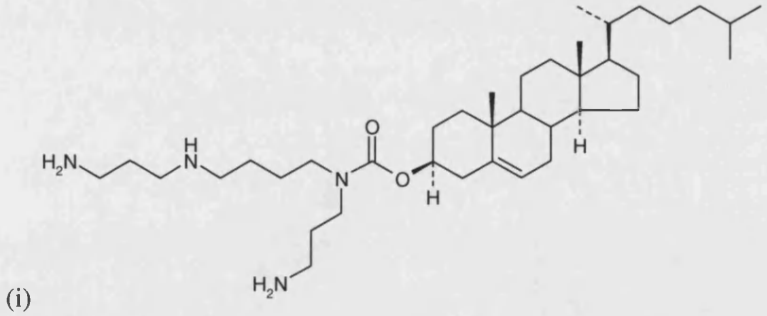

(i)

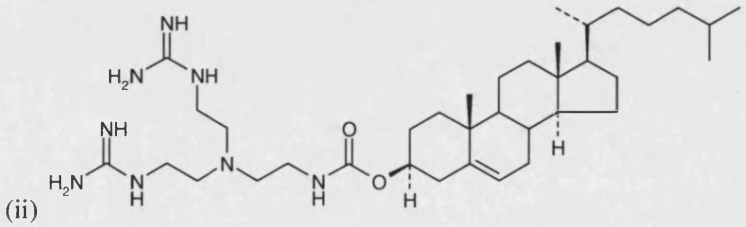

(ii)

Figure 1.13 Steroidal lipopolyamines (i) GL#67 and (ii) BGTC

Recently, the membrane-activity of steroidal lipopolyamines was shown in hemolytic experiments using bovine erythrocytes.[74] It was found that the steroid structure and its substituents, polyamine-chain length influenced this activity. This hemolysis observation support the fact of membrane interaction with steroidal lipids.[74] A series of cholesteryl spermine carbamates was also synthesised and used in DNA condensation and gene delivery.[27,69,75] Other steroids have been conjugated to spermine as a polyamine backbone; Blagbrough and co-workers reported that lithocholic acid gave more efficient gene packing ability than cholesterol, possibly due to its higher hydrophobicity.[76]

Cationic lipids are not only prepared from the conjugation of lipid moiety with linear polyamines. Lehn *et al.*[77] reported the use of cyclic polyamines, such as aminoglycoside kanamycin A, in lipopolyamine design. Aminoglycosides are natural polyamines known to bind to nucleic acids, provide a multifunctional scaffold for the synthesis of a variety of cationic lipids. KanaChol (Figure 1.14 (i)) was synthesised by the conjugation of kanamycin A and cholesterol through a carbamate functional group. The guanidinylated derivative of KanaChol (Figure 1.14 (ii)) was also produced. Both lipids are highly efficient for gene transfection into a variety of mammalian cell lines when used either alone or as a liposomal formulation with DOPE.[77]

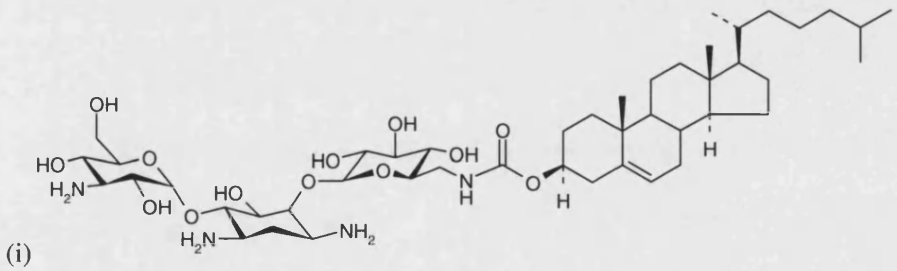

(i)

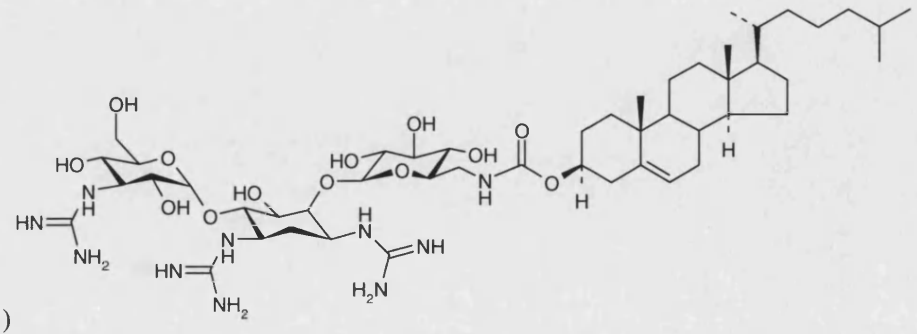

(ii)

Figure 1.14 (i) KanaChol and (ii) its guanidinylated derivative

Mechanism of gene delivery using NVGT vectors

Gene therapy is a complex drug delivery strategy, thus there are no conclusive general characteristics of efficient NVGT vectors. Vector design involves either the invention of new DNA condensing agents or the modification of existing condensing agents. *In vitro* transfection efficiency of polyplexes or lipoplexes depends on a variety of factors e.g. physico-chemical properties of complexes, cell types and their physiological activities, and incubation conditions. In addition, DNA has to be delivered across cellular barriers to reach its site of action (nucleus) and to attain the desired therapeutic effect. Moreover, the correlation between *in vitro* and *in vivo* transfection is unpredictable, and this is also viewed as a major hurdle in gene therapy. In general, for any vectors to reach the nuclei of target cells, there are 5 key steps involved: DNA condensation, cellular uptake, endosomal escape, nuclear localisation and nuclear entry, followed finally by gene expression (Figure 1.15).

DNA condensation - the first step in NVGT

Learning from viral vectors, a self-assembled complex is the most commonly used strategy in NVGT. Condensation can be achieved *in vitro* using the naturally occurring polyamines. As described in Manning's counterion theory,[78] negatively charged (due to the phosphate groups) DNA is neutralized by salt formation (titration) with the positively charged in vectors. This results in condensed nanometre-sized particles typically 50-150 nm in outer diameter.[23,79] DNA nanoparticles, toroidal in shape, were observed in polyamine-induced DNA condensation. As an example, toroidal condensates of circumferentially wrapped T5 phage DNA (120 kbp) were formed with spermine.[80] Similar toroidal shape particles were also found with T4 phage condensed by a high concentration of spermidine.[81] DNA condensation of a phage DNA with hexamine cobalt (III), investigated by cryoelectron microscopy, also resulted in toroidal DNA particles with hexagonal packing.[82,83]

Bloomfield[28,84] proposed statistical mechanics for the collapse of stiff polymer chains of DNA. From an experimental survey, DNA condensation occurs when about 90% of its charge is neutralized by counterions.[78] The collapse of the expanded wormlike coil causes the entropy loss and small change in free energy. The stiffness of DNA sets limits on tight curvature to form structured toroids. The main contributions were believed to be from salt (or bound multivalent ions) and water, which help overcome the electrostatic repulsions of phosphate groups. Hydration accommodates the water structure surrounding surface groups on the DNA helix as they approach the confined toroidal shape. The paths toward this morphology may include winding around a ring, along a chain, or folding through rod states.[85] This DNA compaction facilitates stability in extracellular compartments, cellular uptake, and other intracellular processes such as nuclear entry.[23,86]

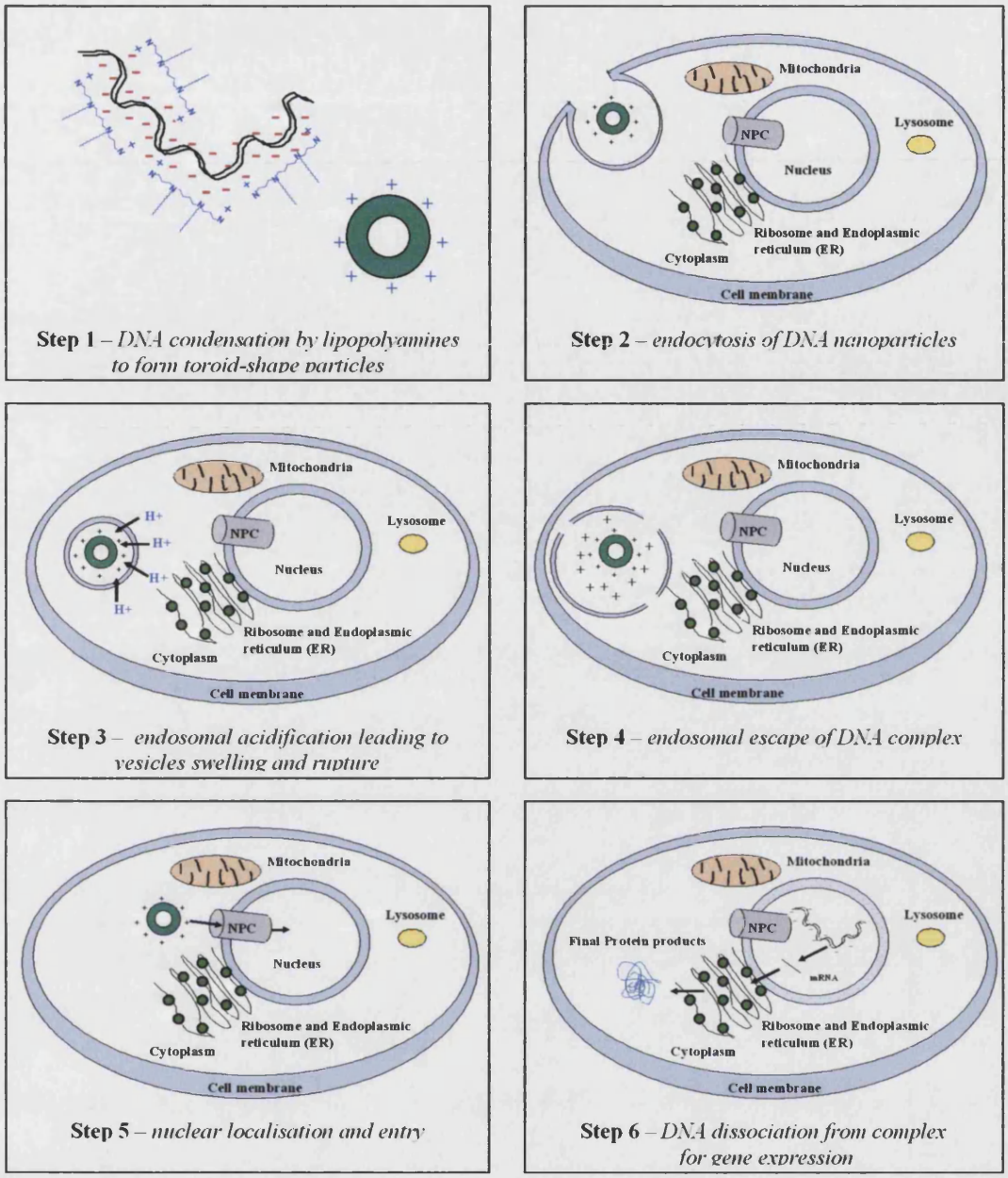

Figure 1.15 Mechanism of gene delivery using NVGT: DNA is typically complexed with vectors to form a nanoparticle. The DNA complex can be uptaken into cells by many routes, depending on its size and chemical design, including receptor-mediated entry, endocytosis and pore/channel formation etc. Typically, DNA complexes are encapsulated in the endosomal vesicles, which are susceptible to enzymatic degradation. These particles must be released from the endosomes before the lysosome is fused to the endosomes. Thus, this endosomal escape is regarded as a critical barrier in NVGT. Nuclear translocation into the nucleus is also required for successful gene expression.

Cellular uptake of DNA complexes

Cell membrane is a lipid bilayer with various integral proteins which selectively allows molecules to enter the cell. Cell surfaces are negatively charged, due to their content of glycoproteins, proteoglycans, and phospholipids. The electrostatic interactions between the surface of DNA particles and cell membranes are expected to be an initial process prior to cellular uptake.[87,88] Polycations are not all equal in their capacity to neutralize the cell surface. Flexible molecules were more effective in destabilising the membrane than ones with rigid structure.[89] Complex size is also another factor determining the mode of cell entry of NVGT vectors. Endocytosis, the major route of cell entry, is allowable for DNA complexes in the diameter range 50-200 nm.[23] Results were different between different cell lines. For example, hepatic cells engulfed 93 and 220 nm in diameter particles, but not 560 nm. The bladder carcinoma cell (ECV304) can ingest large particles of up to 1 μm in diameter. Confluent cells also allow less particle uptake or altogether lose their ability to ingest larger particles.[90]

Polyplexes, such as PEI, use adsorptive endocytosis following the clathrin coated pit mechanism.[38,91] Lipoplexes bind to the negatively charged cell surface, use endocytosis, possibly with fusion to cellular membranes.[92] Alternatively, a cholesterol-dependent clathrin-mediate might be a pathway.[87,88] The magnitude of binding both lipoplex and polyplex to the cell surface and high complexes internalisation does not necessarily correlate to the gene expression level.

DNA condensing agents conjugated to membrane receptors' ligands (e.g. integrin, transferrin, sugars, folate, B12) have also been used to target the entry to specific cells.[93] For example, gene delivery into parenchymal liver cells was found to be useful, because these cells can serve as a host of post-translational modifications for certain gene products. At the surface of hepatocytes, there are a large number of high-affinity asialoglycoprotein-binding receptors. Asialoglycoprotein (glycoproteins with clustered galactose residues, as a receptor recognition and binding unit) ligand was covalently bound to polylysine, and studied for its liver cells transfection by Wu *et al.*[93] The result shows high gene expression in rat's liver cells within 24 hour post-injection, but this effect declined within 2-3 days. Transferrin is another glycoprotein example (which carries iron into cells), and is efficiently taken up into cells by the receptor-mediated endocytosis. Transferrin receptors are found on the surface of most proliferating cells, but highly presented on many kinds of tumours. Transferrin conjugated to polylysine has been reported to deliver DNA molecules into targeted tumour cells successfully. Though cell targeting is improving the cellular uptake of gene, there is still a need to improve the duration of gene expression in those cells.[93]

Endosomal escape of DNA

It has been shown in many studies that endosome escape of the DNA is one major critical barrier to efficient transfection.[86] Early endosomes are formed by the inversed cell membrane upon DNA particles endocytosis, which are eventually degraded into late endosomes by internalization into lysosome vesicles. The "proton sponge" hypothesis has been proposed for endosome escape of polycation (such as PEI) or lipopolyamine (e.g. DOSPA).[94] The protons are pumped into endosomes (at pH 7.4) by V-ATPase proton pump at their membrane while polycations (pK_a of primary amine is around 10)[69] work as a pH buffer material. This results in an increased proton/water flux and finally pH is lowered to 5.5. Membrane disruption by swelling and finally osmotic lysis allows DNA complexes to escape from these vesicles prior to enzymatic degradation.

An alternative to this "proton sponge" is lipid membrane mixing between endosomal membrane and cationic lipid vectors.[86,95,96] Cationic lipids were found to promote the formation of non-bilayer lipid structures, preferentially adopting the inverted hexagonal (H-II) phase. Helper lipids or cholesterol also enhance the formation of the H-II phase.[97] The "flip-flop" mechanism was proposed by Zelphati *et al.*[98] Upon the contact of lipoplexes with anionic lipids from the cytoplasmic facing monolayer, endosomal anionic lipids laterally diffuse into the complex and form a charged neutralized ion-pair with the cationic lipids. This leads to displacement of the oligonucleotide from the cationic lipid and its release into the cytoplasm.

For high yield gene transfection, efficient escape of DNA from the endosome is required. In addition to helper lipids (DOPE), membrane disruptive peptides have also been used to help DNA complex pass through cellular membrane. Most of the membrane active peptide elements have an amphipathic character, with a distinctive stretch of apolar amino acids (called "fusion sequence"). These sequences vary from short stretches (3-6 amino acids) to longer sequences (24-36 amino acids) and are mostly located at the *N*-terminal of the fusion protein. The secondary peptide structure normally includes the amphipathic helices with hydrophobic amino acids on one helical face and the apolar residues on the other, or of stretches of apolar amino acids.[99] These membrane disruptive and fusogenic peptides have a tendency to undergo conformational change in a pH-dependent manner.[100] The presence of α-helical structure in at least part of the fusion peptide is strongly correlated with activity, whereas β-structure tends to be less prevalent, associated with non-native experimental conditions, and more related to vesicle aggregation than fusion.[101] Examples are either synthetic peptide (e.g. GALA,[102] KALA) [103] or natural toxin (e.g. influenza virus haemagglutinin).[104]

Nuclear localisation and entry

Released DNA complexes will be in the cytoplasm and translocate to the nucleus. Naked DNA has a half-life in cytoplasm shorter than 90 min,[105] so the DNA complex form offers the protection to nuclease. The compact DNA particles also diffuse faster than free DNA, resulting in less exposure to nuclease before reaching the nucleus. The mechanism of DNA nuclear translocation is not well understood. There are two processes by which delivered genes enter the nucleus. During mitosis, the nuclear membrane disassembles which allows large macromolecules including plasmids to gain access. During non-mitotic phases in cell division, nuclear envelope remains intact with double phospholipid layers and nuclear lamina, a fibrous meshwork that provides structural support to the nucleus. The lamina is thought to serve as a site of chromatin attachment at the inner side of membrane. The inner and outer membranes join together at the nuclear pore complex (NPC). The NPC is a large structure with an assembly of eight spikes attached to rings on the cytoplasmic and nuclear sides of the nuclear envelope, called "cytoplasmic ring" and "nuclear ring" accordingly, with a formed central channel. The central channel is approximately 40 nm in diameter for the transportation of large particles across the nuclear membrane.

NPC is really the only way for plasmids to gain entry to the nucleus. Passive diffusion is only possibly with small molecules of 9 nm diameter, and size less than 50 kDa. The bigger molecules including DNA are transported by energy-dependent mechanism through this NPC. This selective transport of these macromolecules to and from the nucleus requires the nuclear localisation signals (NLS) to direct their traffic through the NPC.[106]

NLS are small peptides which help delivered plasmids to reach the nucleus. NLS binds with the α- subunit of the importin receptor on the nuclear membrane, then the β-subunit of the importin binds to the nuclear pore with the help of GTP binding protein (called Ran). The β-subunit is retained at the inner face of pore complex.[106] According to the amino acid sequence analysis of NLS, e.g. SV40 T-antigen, HIV tat protein etc., positively charged amino acids are commonly found as their unique characteristic e.g. lysine and arginine.[106] Synthetic NLS (PKKKRKVEDPYC) was used by Behr *et al.*,[107] and it was found that transfection of cells with the NLS-DNA conjugate remained effective. Transfection was increased 10- to 1,000-fold as a result of this signal peptide, irrespective of the cationic vector or the cell type used. The study by Tachibana *et al.* revealed that the transfection efficiency measured is also related to the number of plasmid copies delivered into the nucleus.[108]

DNA dissociation and gene expression

DNA complex dissociation is critical to gene transcription and finally translation into the desired protein. Xu and Szoka presented a model which described that plasmid DNA is released from the complex on escaping from endosomes.[109] The nuclear microinjecion of cationic liposome–DNA complexes prevent the gene expression, thus this suggested that DNA cannot dissociate from the liposomal vector in the nucleus.[110] However, from Godbey and co-workers' study,[38] PEI was found in complexed form with DNA (and also in free form) inside the nucleus of successfully transfected cells, suggesting that PEI may dissociate from DNA in the nucleus. Histone H1 in active chromatin is also tightly bound to DNA, this may also support that the proposal of complex dissociation, polycation (Lys and Arg in H1) bound to DNA, takes place in the nucleus. Thus, the mechanism of the transfer of plasmid DNA, complexed with non-viral carriers, to the nucleus remains highly speculative.[111]

Another aspect of gene expression is the design of the DNA plasmid itself. The careful selection of gene sequence, e.g. promoter, is also critical to the magnitude of gene expression. The use of tissue-/tumour-specific promoter allows precise control of gene transcription, which will increase the efficacy and reduce the toxicity of treatment.[112]

Fluorescence techniques to determine the efficiency of lipopolyamines in gene delivery

The development of gene-based medicines as a new class of pharmaceuticals is clearly important. As previously discussed, lipopolyamines are good candidates for DNA delivery studies. The vectors can self-assemble with DNA, especially without a need to form liposomes. The safety profile of lipopolyamines is also more favourable than the commonly used polybasic polymeric amines (e.g. PEI, PLL).

Fluorescence spectroscopy and microscopy techniques are highly specific to the studied molecules or systems. They also allow a non-invasive way to gain insights into NVGT, and can aid in the development of high-throughput assays. In 1967, LePecq and Paoletti[113] introduced ethidium bromide (EthBr) (Figure 1.16) to study DNA binding. EthBr, intercalated in stacks of DNA base pairs, fluoresces at 600 nm by direct excitation at 546 nm, or more efficiently through energy transfer from DNA base by excitation at 260 nm. This EthBr assay was later applied to measure condensation efficiency of vector systems. This improved method by Geall and Blagbrough[114] offers a rapid and sensitive analysis of lipoplex formation. On DNA condensation, at increasing ammonium/phosphate (N/P) charge ratio,[15] a decrease in EthBr fluorescence intensity was measured.[114,115]

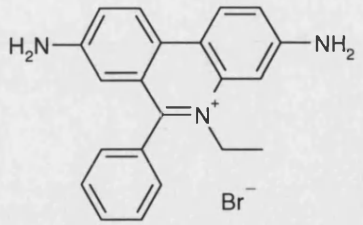

Figure 1.16 Ethidium bromide (DNA probe)

Fluorescamine, a non-fluorescent molecule, is also useful in studying NVGT.[53,116] Fluorescamine easily reacts with primary amine functional groups of polyamines, forming a fluorescent molecule (Figure 1.17). On salt formation between DNA phosphates and polyammonium ions, the reactivity to fluorescamine of these primary amine groups is eliminated. This observation allowed a study of DNA-polyamine interactions,[117] including polyamine-mediated DNA condensation. Thus, the reaction between free (i.e. unbound to DNA) primary amines on polyamines and added fluorescamine was used to determine the level of condensation. There is fluorescence from the product formed between fluorescamine and these amine groups, observed using λ_{ex} 392 nm and λ_{em} 480 nm.

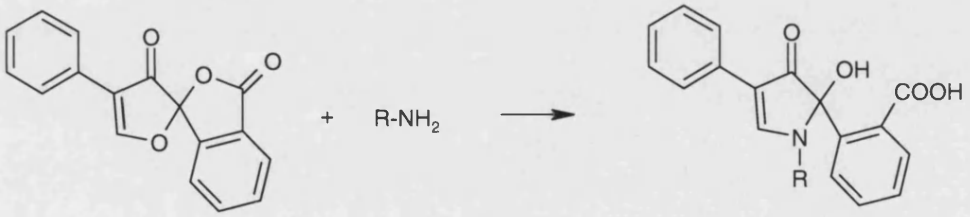

Figure 1.17 Fluorescamine (amine probe) and its fluorescent product from a reaction with a primary amino group.

Fluorescent lipopolyamines – probes derived from DNA delivery agents

Fluorescent lipopolyamine probes which maintain their DNA condensing properties, gene delivery ability, are useful tools in NVGT research. They can be detected by various fluorescence methods, such as: fluorescence steady-state spectroscopy, fluorescence resonance energy transfer (FRET),[98,118] and confocal fluorescence microscopy[38] etc. Thus, by introducing this probe to the DNA to be delivered, NVGT events can be followed spectroscopically and microscopically. The designed fluorescent lipopolyamines are important tools to study the intracellular fate of DNA nanoparticles.[119] An example of fluorescent lipopolyamine synthesised by employing Fmoc (fluoren-9-ylmethoxycarbonyl) chemistry in order to label a specific position with a chosen fluorophore is shown in Figure 1.18.[119,120]

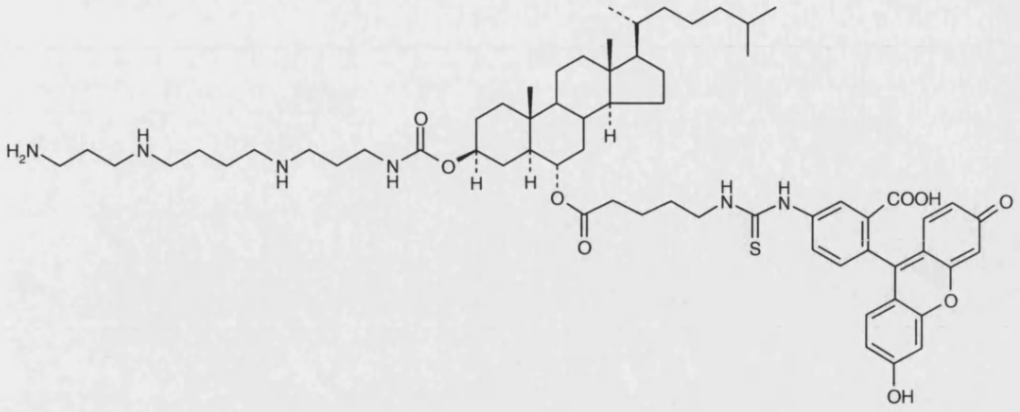

Figure 1.18 An example of our novel fluorescent lipopolyamine conjugates, carrying a DNA condensing moiety (from spermine), a lipophilic steroid (a *trans*-AB-oxygenated cholestane), and coupled to a fluorescent tag

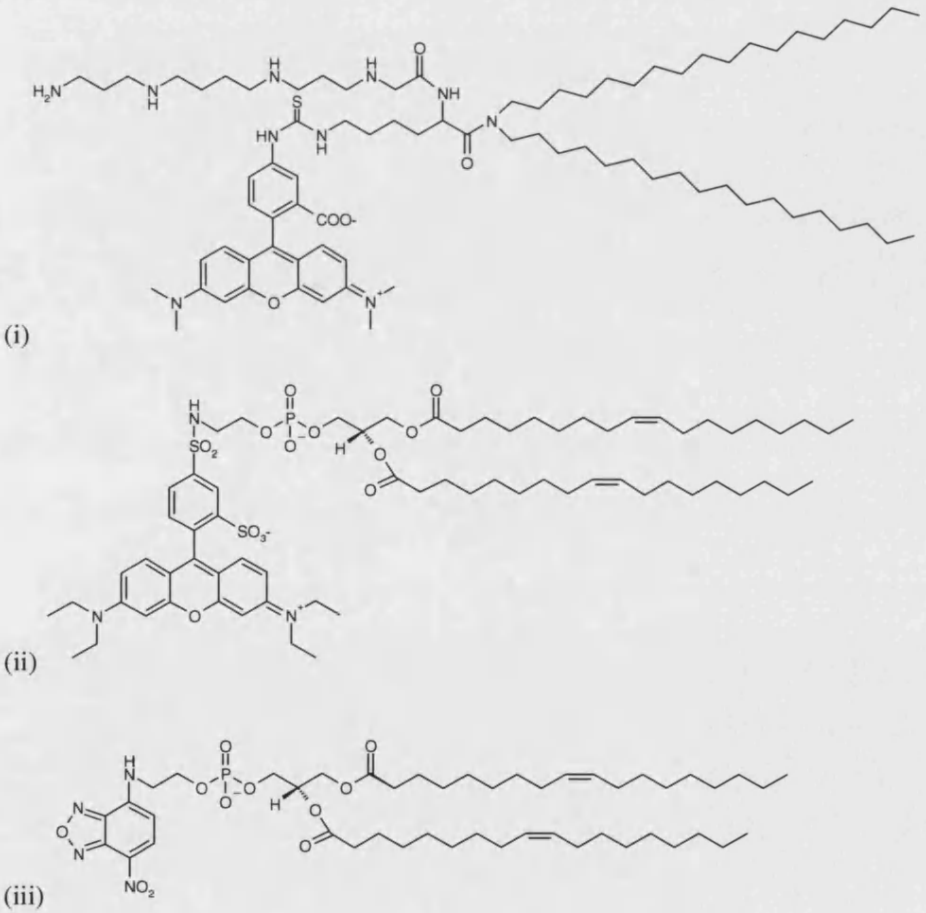

Figure 1.19 Recently reported fluorescent lipopolyamine and liposomal lipids: (i) RPR-121653, (ii) *N*-Lissamine rhodamine phosphatidylethanolamine (*N*-Rh-PE), (iii) *N*-nitrobenzoxadiazole-phosphatidylethanolamine (NBD-PE)

Byk, Scherman, and co-workers[67,121,122] have designed and synthesised polyamine-hydrocarbon lipid conjugates. A rhodamine derivative of a lipopolyamine (RPR 121653) was also synthesised and studied as an NVGT probe (Figure 1.19 (i)).[67] Structure-modification was also carried out by introducing a disulfide bridge (a reduction-sensitive functional group) at different positions in the backbone of the lipids. The disulfide is incorporated in order to afford another escape mechanism for the DNA from the lipopolyamine carrier, taking advantage of the cytosolic cellular reducing medium, such as the plasma membrane or by cytoplasmic reductases. Early reduction led to undesirable DNA release, i.e. total disruption of the particles in the early phase of delivery yielded total loss of transfection, but some positions for the disulfide bridge afforded increased transfection efficiency.[121,122]

Fluorescent derivatives of a small lipid molecule such as *N*-Rh-PE (1,2-dioleoyl-*sn*-glycero-3-phosphatidylethanolamine-*N*-lissamine rhodamine B sulfonyl) and NBD-PE (*N*-4-nitrobenzo-2-oxa-1,3-diazole phosphatidylethanolamine) are commercially available (Avanti Polar Lipids, AL, USA). These molecules (Figure 1.19 (ii) and (iii)), incorporated into cationic liposomes in NVGT, enable the ability to track fluorescently the progress of transfection from liposomes (*vide infra*).[98,123] Fluorescent labelling of polyplex NVGT carriers has also recently been reported, with Oregon Green-PEI[38] and Texas Red-chitosan (*vide infra*).[51]

Ideal fluorophores are primarily chosen for their photostability profile. Naylor *et al.*[124] showed in interesting experiments that the cellular uptake and metabolism of fluorescent fatty acid analogues were different. The polar fluorophore has poor cellular uptake, and anthracene or pyrene fluorophores (Figure 1.20) were regarded as the most extensively incorporated into cellular lipids. From these findings, it is expected that the molecular hydrophobicity of fluorophores may play an important role in fluorescent lipid-based NVGT vector design.

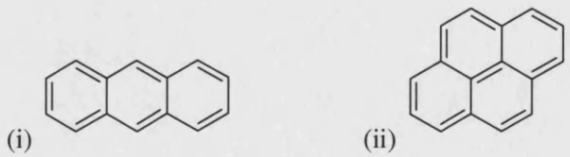

Figure 1.20 (i) Anthracene and (ii) pyrene fluorophore

Preparation of fluorescent macromolecules

DNA can be labelled with fluorescent molecules by chemical techniques such as photo-crosslinking (e.g. ethidium monoazide,[92,125] *p*-azido-tetrafluoro-benzyl-lissamine,[126] dinitrophenyl[127]). Aryl azides can be photoactivated with UV light to generate highly reactive aryl nitrenes which bind to the aromatic bases of DNA. Fluorescent DNA has also been used to study NVGT barriers, such as cell entry[92,128] and nuclear entry.[92,129]

In addition to using fluorescent plasmids as a probing strategy for NVGT, protein markers have been employed to follow the transfection outcome i.e. gene expression. Such protein markers include: green fluorescent protein (GFP) of the jellyfish *Aequorea victoria* which absorbs light λ_{ex} 395 nm, and emit fluorescence at λ_{em} = 510 nm. Comack *et al.*[130] studied the mutant form of GFP with 2 amino acid mutations (at position 64 from phenylalanine to leucine and at 65 from serine to threonine), and established (enhanced) green fluorescent protein (EGFP) which fluoresces naturally and more intensely (20- and 35-fold) than the wild GFP. The excitation maxima of the three mutants are red-shifted by about 100 nm, permitting efficient excitation at 488 nm which is a typical excitation laser used for fluorescent-activated cell sorting (FACS) to detect fluorescein. The chemistry which underpins the use of these reporter systems is highlighted below. By using pEGFP[130] as delivered DNA, the EGFP chromophore (a substituted 4-hydroxybenzylidene imidazolidinone, Figure 1.21) was detected in successfully transfected cells by FACS (fluorescent-activated cell sorting).

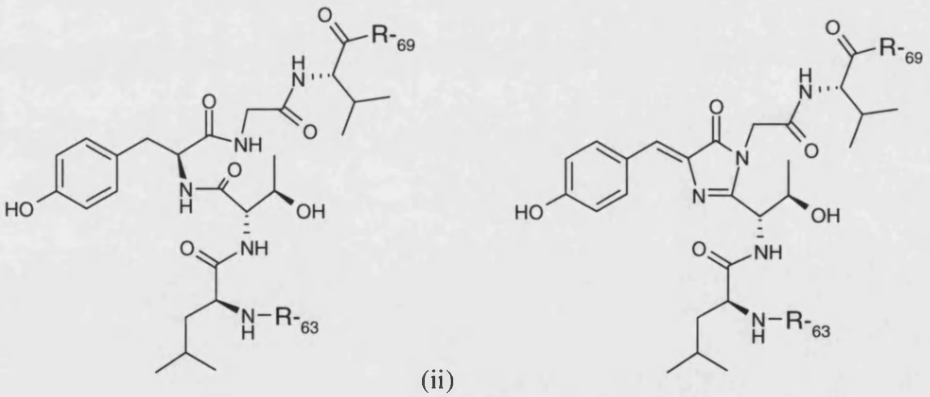

Figure 1.21 The fluorophore in EGFP (i) EGFP amino acid sequence L(64)TYGV(68) shown (ii) Post-translational cyclisation of amino acids 65-67 forming hydroxybenzylidene-imidazolidinone, an EGFP fluorophore with λ_{ex} = 488 nm (red-shifted from wild GFP protein) and λ_{em} = 507 nm

Apart from GFP, there are various other naturally fluorescent proteins which can be used as gene expression markers. DsRed,[131] as an example shown in Figure 1.22, is a red fluorescent protein found in coral reef *Discosoma spp.* The biosynthesis of DsRed's chromophore includes one more step that extends the conjugated π-system of the GFP chromophore. It was also found that a single amino acid replacement in GFP (T into Q) could convert it into Ds-Red-like protein. The multi-colour range of fluorescent protein allows researchers to study the interaction of bio-components using multiple spectra of fluorescence.

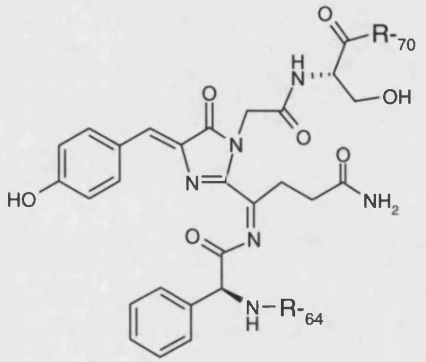

Figure 1.22 DsRed chromophore, amino acid sequence F(65)QYGS(69)

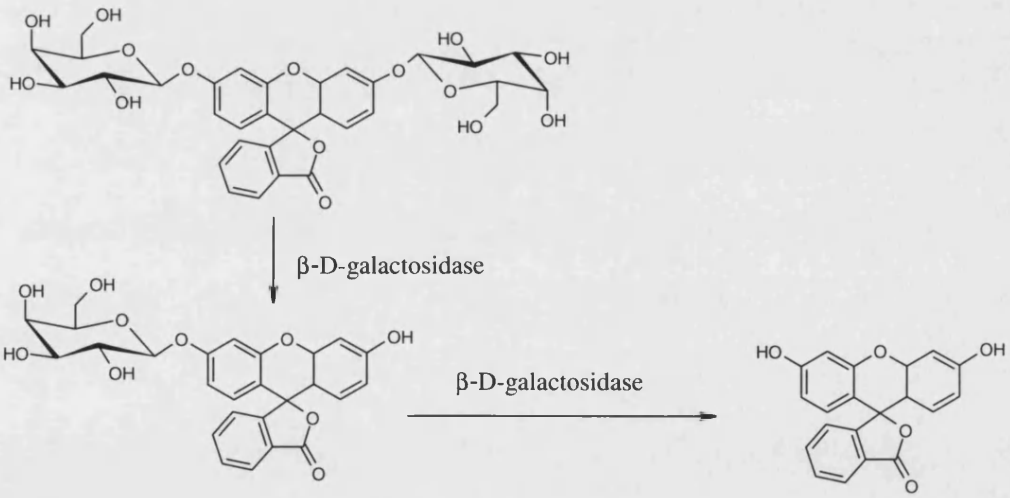

Figure 1.23 Fluorescein-di-β-D-galactopyranoside (FDG), its hydrolysed product (fluorescein monogalactoside), and finally fluorescein.

Gene expression markers such as enzymes are also widely used to determine the efficiency of transfection. For example, β-galactosidase is the gene product of pLacZ transfection. When cells are treated with a fluorogenic substrate, e.g. fluorescein-di-β-D-galactopyranoside (FDG) shown in Figure 1.23, cell transfection efficiency can be detected

fluorescently. Fluorescein was locked into the non-fluorescent spirolactone form by bis-*O*-glycosylation with two β-D-galactopyranoside sugars. β-galactosidase enzyme catalyses the sequential hydrolysis of β-glycosidic bonds, to obtain a fluorescein molecule. Nolan *et al.*[132] also reported the application of this FDG in cell sorting experiments of mammalian cells transfected with pLacZ. This FDG assay is very sensitive and as few as 5 copies of β-galactosidase per cell can be detected using FACS analysis.

Luciferase, the protein encoded by pGL3, drives luciferin oxidation and generates light. Luminescence involves chemical reactions producing structurally different products which emit light. This bioluminescence method has been also used to quantify the NVGT efficiency.[133] Firefly luciferase (*Photinus pyralis*),[133] which is widely used for gene expression, catalyses luciferin oxidation generating oxyluciferin and detectable yellow light. The reaction is shown in Figure 1.24.

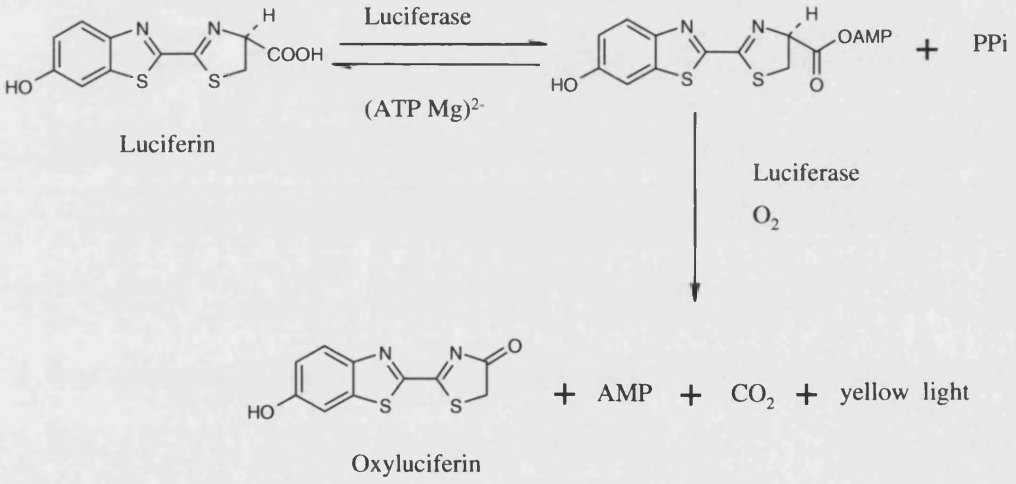

Figure 1.24 The biochemical reaction of luciferin oxidation by luciferase to oxyluciferin

Fluorescence techniques can potentially play important roles in all areas of NVGT research. EthBr and other DNA intercalating dyes (as a simple, rapid analytical screen) contribute to the discovery of novel DNA condensing agents. NVGT efficiency can be evaluated by using plasmids encoding for either fluorescent protein or luminescence-associated enzymes. In these studies, fluorescent lipopolyamines were designed and synthesised, enabling the intracellular tracking of DNA complexes to reveal spectroscopically the key steps and barriers in gene delivery. Moreover, fluorescent labelling of DNA can be used together with lipopolyamine probes for studies of fluorophore interactions, e.g. by fluorescence resonance energy transfer (FRET) for studies of the (diss-)association of DNA and its cationic carrier, NLS or other biomolecules or intracellular organelles.

Aims of this thesis

The aims of this thesis are to understand, design, and prepare lipopolyamines for NVGT. The thesis starts with a concise literature review of the period prior to the start of these studies. This provides the background in the chemistry and biology of NVGT vectors. The review is also focused on fluorescent techniques for NVGT research.

The research will focus on conjugates of naturally-occurring polyamines (e.g. spermine and spermidine) and lipid (long chain fatty acids and cholesterol) and evaluate them using fluorescence techniques. The study also extends to lipopolyamines with respect to the transportation of biomolecules across cell membranes. The first step in NVGT, DNA nanoparticle formation, will be studied for the synthesised compounds, to understand the effect of vector structure, e.g. lipid moiety and positive charge distribution, on the efficiency of DNA condensation. *In vitro* transfection and toxicity in both an immortalized cancer cell line (HtTA-1 HeLa) and a primary skin cell line (FEK4) will be investigated. The results will be used to develop safer and more efficient NVGT vectors.

In this study, the DNA condensation process will be also investigated at the single nanoparticle level by using fluorescence correlation spectroscopy (FCS). A small probe, such as PicoGreen, will be evaluated as a reporter for the interactions of lipopolyamines and polynucleotides. A technique to monitor the dynamics of such a probe interacting with the DNA duplex, time-resolved fluorescence correlation spectroscopy, will also be used. The aim of this part of the research is to establish a reliable and novel fluorescence-based platform for the study of a single DNA nanoparticle, as well as to understand such a monitoring mechanism.

There are several membrane-related steps in the gene delivery process, i.e. cellular uptake, endosomal escape, and nuclear entry. Membrane interaction models, e.g. endocytosis, membrane destabilisation, and pore-forming will be studied. This work aims to aid in the development of membrane-disruptive NVGT vectors, which will ultimately enhance the overall efficiency of non-viral gene delivery system.

To better understand the efficiency of gene delivery, more novel tracking molecules are needed. Fluorescent lipopolyamine probes were therefore designed and synthesised. The aim is to use them as biosensors in monitoring the intracellular processes of gene delivery. Additionally, fluorescent-labelled DNA will be also included in the study. Such a label may be suitable for use with selected fluorescent vectors as a complementary fluorescent pair.

Chapter 2

Synthesis and testing of lipopolyamines for NVGT

Introduction

Polyamines, such as spermine and spermidine, are natural condensing agents that mammals use to store DNA in the limited space of the nucleus. Their DNA neutralisation property has inspired researchers to try to use them as a vector for gene delivery without using viruses. Several studies have been carried out to understand and improve spermine in both DNA condensation and its applications in gene delivery. From the regiochemical distribution of positive charges along polyamines, it was found that a 3 or 4 carbon spacing between the amine groups in spermine and spermidine facilitates DNA condensation.[27] In our synthetic experiments, spermine was used as a backbone polycation for our lipopolyamines. The lipid moieties selected are inspired by the lipid membrane bilayer. Phospholipids typically contain two hydrocarbon fatty acid chains (an example is given in Figure 2.1(i)). Oleic acid is one of the fatty acids commonly found, with one (*cis*) double bond at C9-10 position creating a kink in the molecules. When oleic acid is placed in the bilayer membrane, it decreases lipid packing order and provides membrane fluidity.[134] DOPE (Figure 2.1 (ii)) is a membrane fusogenic lipid used as an adjuvant in lipoplexes. Cholesterol (Figure 2.1 (iii)) is also another abundant lipid found in mammalian cell membranes. The "planar" steroidal ring system and the hydrophobic tail direct cholesterol to be placed within the membrane core, and the 3-β-hydroxyl group of cholesterol will orient the molecule to the surface of the bilayer. The structure of cholesterol allows it to reduce the freedom of movement of phospholipid acyl chains, thus rigidifying the membrane, which can have a dramatic impact upon membrane function.[135] GL#67 (Figure 2.1 (iv))[71] is an example of cholesterol conjugated to spermine, used in a NVGT liposomal formulation.

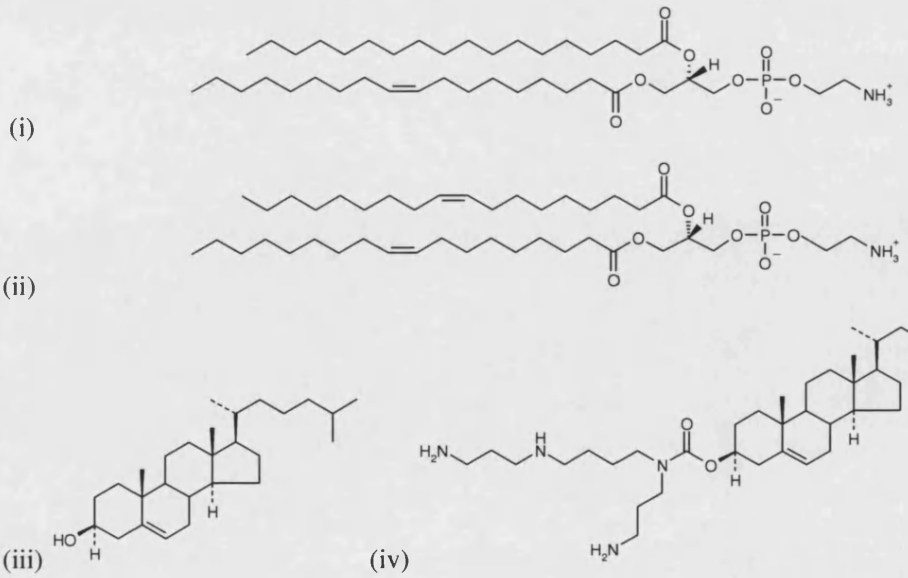

Figure 2.1 (i) Natural 1-stearoyl-2-oleoyl-*sn*-glycero-3-phosphoethanolamine, (ii) 1,2-dioleoyl-*sn*-glycero-3-phosphoethanolamine (DOPE), (iii) cholesterol, and (iv) GL-67

As described in the Experimental (Chapter 5), the lipospermines synthesized for DNA condensation and gene delivery studies are N^4,N^9-dioleoylspermine and N^1-cholesteryl spermine carbamate. Both lipopolyamines were compared to spermine, their parent molecule. The gene delivery transfection was performed to assess the ability of these NVGT vectors in cell cultures. The efficacy was also evaluated along with toxicity studies using the 3-(4,5-dimethylthiazol-2-yl)-2,5-diphenyltetrazolium bromide (MTT) assay.[136]

Synthesis of lipopolyamines as NVGT vectors

N^4,N^9-Dioleoylspermine (Figure 2.2) was prepared in a one-pot synthesis as shown in Figure 2.3. A selective protection strategy for primary amine functional groups (N^1 and N^{12}), by reaction with ethyl trifluoroacetate (2 eq to spermine) to yield N^1,N^{12}-ditrifluoroacetylspermine, was followed. The yield of trifluoroacetylated product was previously reported at 93%.[137] In this experiment, one major product on TLC analysis (MeOH/NH_4OH 4/1 v/v, R_f = 0.8) was also found and it stained purple with ninhydrin solution, with a small spot of unreacted spermine still near the baseline (R_f = 0.1, using the same mobile phase). Thus, the next step of oleic acid conjugation was continued without further purification of the N^1,N^{12}-di-protected spermine. Oleic acid conjugation (2.2 eq) to protected spermine was achieved by using 1,3-dicyclohexylcarbodiimide (DCC) and *N*-hydroxybenzotriazole (HOBt) as catalysts. The last stage of deprotection of di-trifluoroacetyl dioleoylspermine was carried out by adding to ammonium hydroxide solution (pH 11.0) and leaving for 20 h. N^4,N^9-Dioleoylspermine was obtained as a pale yellow oil (12 % yield overall).

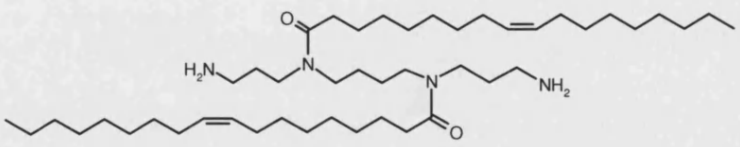

Figure 2.2 N^4,N^9-Dioleoylspermine

When this experiment was started, it was found that Kirby's research group previously reported the synthesis of gemini surfactant (N^1,N^{12}-di(Lys-Lys-Lys-Ser)-N^4,N^9-dioleoylspermine and N^1,N^{12}-di-Lys-N^4,N^9-dioleoylspermine) for luciferase gene delivery in CHO cells.[138,139] N^4,N^9-Dioleoylspmerine was published as an intermediate in their work to obtain these cationic surfactants. Their research paper did not report any intention to explore the use of this substance as an NVGT vector.[138,139] There are also no other research groups who have reported the synthesis or activity of N^4,N^9-dioleoylspermine in NVGT.

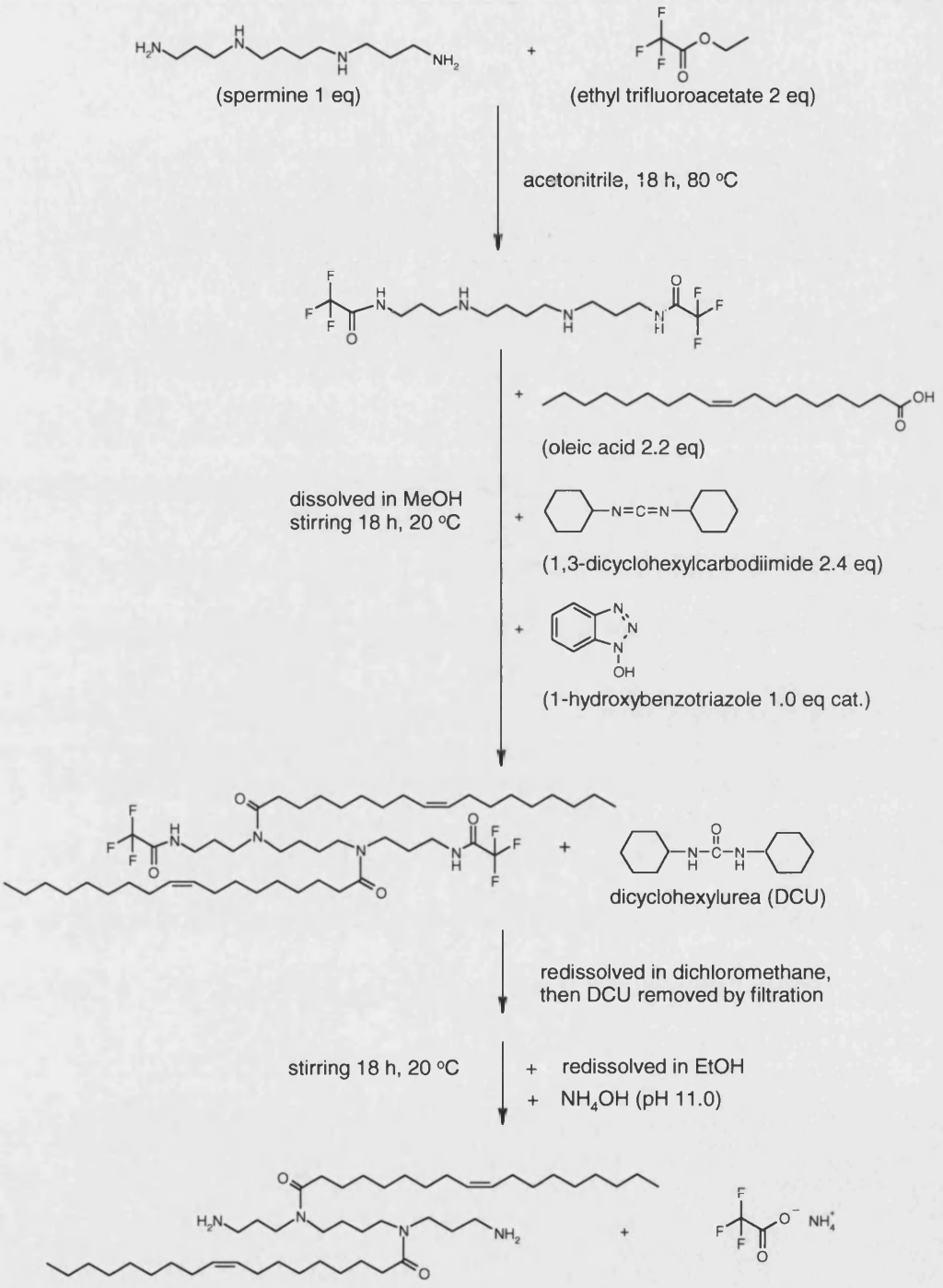

Figure 2.3 Synthetic scheme for N^4,N^9-dioleoylspermine

The synthetic detail used by Kirby and co-workers is also different from the synthetic scheme in this work. They use *N*-ethylcarboxyphthalimide to protect both primary amines and oleic acid chloride was used in the conjugation reaction. Whereas, we used ethyl trifluoroacetate as a primary amine protecting group and oleic acid (carboxylic acid) to conjugate with spermine in a DCC/HOBt catalysed system.

Dansylation reaction was then used to detect N^4,N^9-dioleoylspermine by HPLC-fluorescence. The reaction is shown in Figure 2.4. This analytical protocol for lipopolyamines is based on Escribano and Legaz's work,[140] and it was successfully applied to detect N^4,N^9-dioleoylspermine by a short and convenient reaction (11 min). Efficient resolution (Figure 2.5) was performed with a reversed-phase HPLC (ABZ+Plus) column to detect dansylated products (t_R = 11 min), using the conditions given in the Experimental. In Figure 2.5, N^1-dansyl-N^4,N^9-dioleoylspermine was eluted at 11 min (HPLC-fluorescence, MeOH/H_2O 95/5 v/v, 1.3 ml/min). The di-dansylated derivative was not eluted until MeOH was used to clean the column. Using LC-MS with a higher flow rate (1.6 ml/min) on the same column, N^1-dansyl-N^4,N^9-dioleoylspermine (t_R = 8.24 min) and N^1,N^{12}-didansyl-N^4,N^9-dioleoylspermine (t_R = 12.99 min) were resolved.

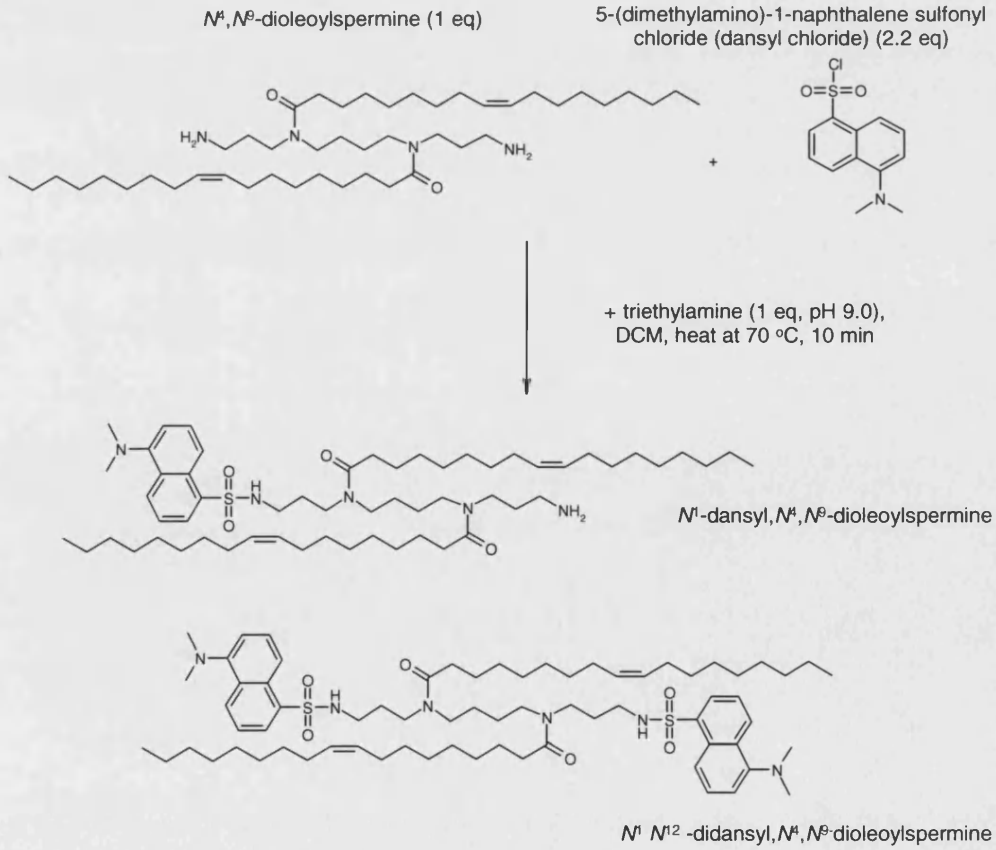

Figure 2.4 Dansylation reaction of N^4,N^9-dioleoylspermine

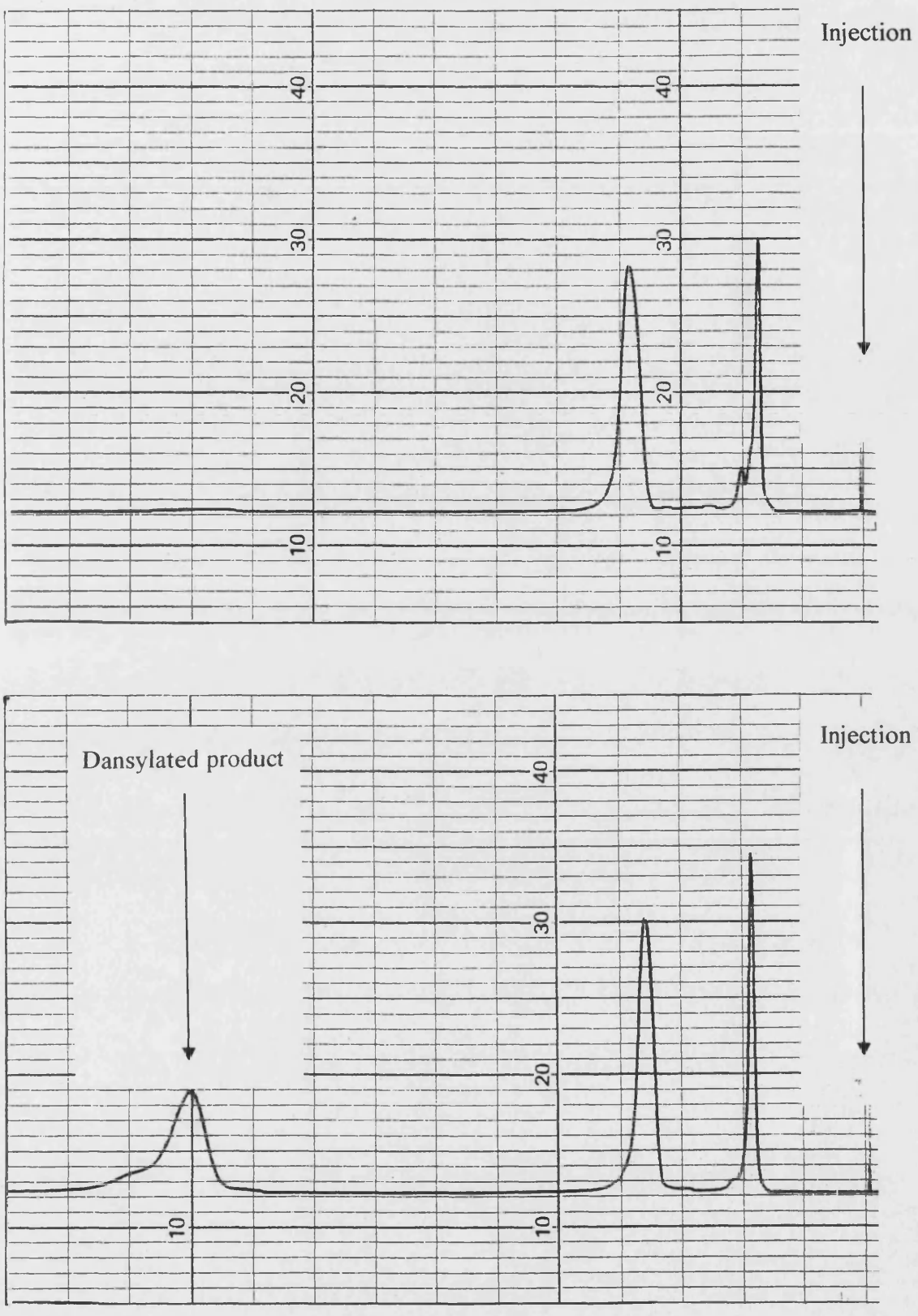

Figure 5 HPLC-fluorescence trace of dansylated N^4,N^9-dioleoylspermine using column Supercosil ABZ+ Plus, MeOH/H_2O (95/5 v/v, 1.3 ml/min), chart speed 1 cm/min, sample (top) blank reaction (without N^4,N^9-dioleoylspermine) and (bottom) dansylation of N^4,N^9-dioleoylspermine with a peak at 11 min which is N^1-dansyl-N^4,N^9-dioleoylspermine.

N^1-Cholesteryl spermine carbamate (Figure 2.6) is another lipopolyamine which was previously reported for its efficient DNA condensation by Blagbrough and co-workers.[69] The interesting aspects of this molecule are its cholesterol moiety (which is similar to DC-Chol) and the positive charge distribution found in the spermidine equivalent backbone. Below is the scheme for this synthetic strategy (Figure 2.7).

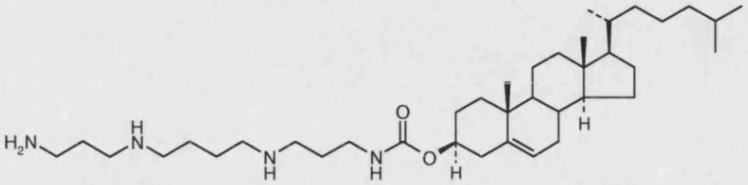

Figure 2.6 N^1-Cholesteryl spermine carbamate

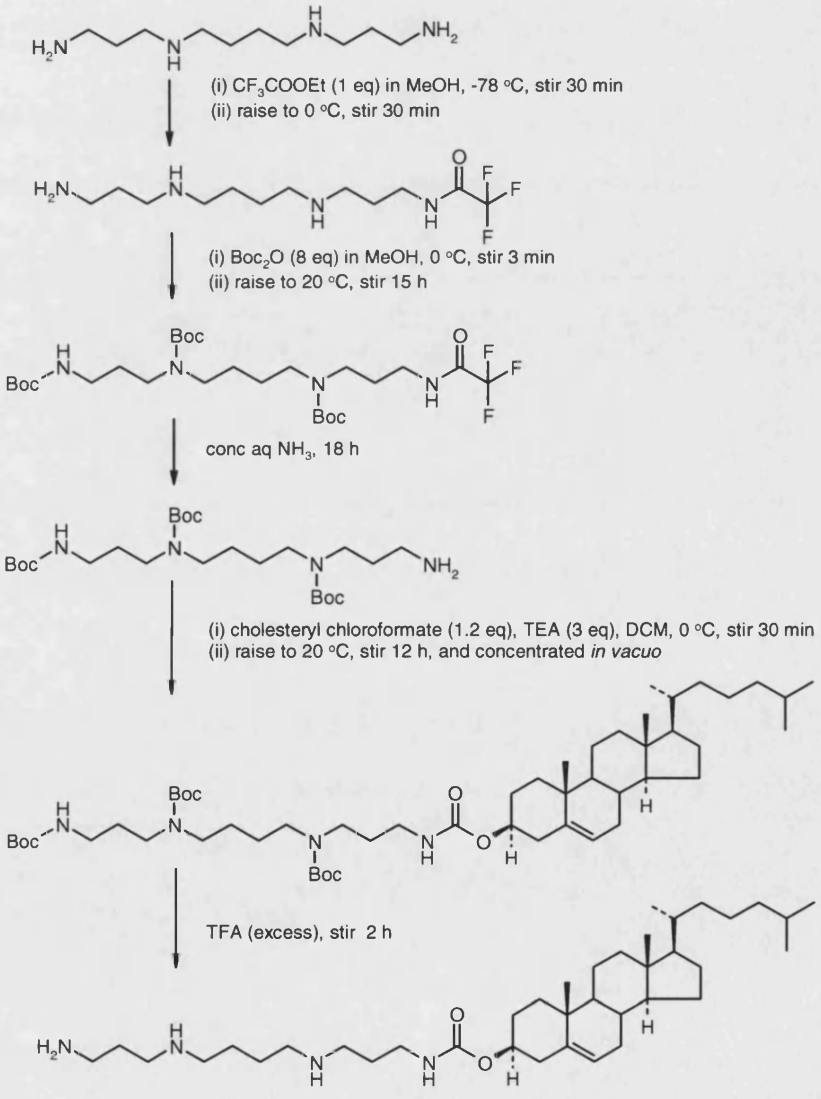

Figure 2.7 Synthetic scheme for N^1-cholesteryl spermine carbamate

Two protective reagents were used to achieve N^1,N^4,N^9-tri-Boc-spermine. Similar to our synthesis of N^4,N^9-dioleoylspermine, ethyl trifluoroacetate was chosen to protect the primary amine group. A single amine group protection (to yield N^1-trifluoroacetyl spermine) was performed stoichiometrically (at mole ratio 1:1 eq) at low temperature (-78°C) to minimize the N^1,N^4-ditrifluoroacetyl spermine byproduct. From this synthesis with $(Boc)_2O$ (8 eq) and trifluoroacetyl deprotection, a pale yellow oil of N^1,N^4,N^9-tri-Boc spermine was obtained by column chromatography in 43% yield. In this study, cholesteryl chloroformate was chosen to form a carbamate bond with an amine group of tri-Boc spermine. Tri-Boc cholesteryl spermine carbamate was purified over silica gel (75% yield), to remove the unreacted tri-Boc spermine. The Boc-protected cholesteryl spermine conjugate was finally deprotected by using a strong acid i.e. trifluoroacetic acid. The final step of purification was modified from Geall's work[69] by employing a simple re-crystallization technique, instead of HPLC-UV which faces the low sensitivity of UV wavelength (220 nm) used to detect a cholesterol chromophore. The final product was re-crystallized in EtOAc to yield a white powder (R_f= 0.2, DCM/MeOH/NH_3 50/10/1 v/v/v).

DNA condensation studies

Polycationic compounds such as polyamines or synthetic lipopolyamines interact with DNA by charge neutralization, leading to DNA condensation into nanoparticles. This is a first step to overcome the problem of DNA size and its high number of charges, which prevent translocalisation through membrane bilayers. DNA used in gene therapy is mostly prepared as a circular plasmid, which promotes DNA strength and stability, unlike linear forms which have a greater tendency to break or are more vulnerable to enzyme degradation. Two circular plasmids, pEGFP (4.7 kbp) and pGL3 (5.3 kbp) were amplified by Maxiprep as described in the Experimental. The production yields are in the range 1.1 – 5.5 mg/ml and A_{260}/A_{280} between 1.75-1.90.[141-143] Both plasmids were used in both DNA condensation and *in vitro* transfection studies.

To understand the effect of lipopolyamines in DNA condensation, a series of experiments was conducted. First, spermine (Figure 2.8 (i)), which is the polyamine used in our synthesis, was used to condense pEGFP. Ethidium bromide (EthBr) displacement assay[114] was employed to monitor the change in DNA conformation. EthBr (Figure 2.8 (ii)) is a cationic dye that displays a significantly increased fluorescence (λ_{ex} = 546 nm, λ_{em} = 600 nm) upon binding with DNA through intercalation of the phenanthridinium-moiety between adjacent base-pairs of DNA.[113,114] EthBr may be excited directly at 546 nm, or by energy transfer from nucleic bases following irradiation at 260 nm.

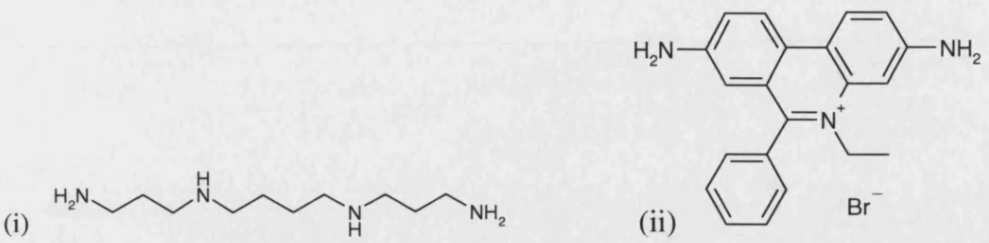

Figure 2.8 (i) Spermine and (ii) ethidium bromide

EthBr solution was added into HEPES (20 mM NaCl, pH 7.4), before the addition of pEGFP. The (background) fluorescence of free EthBr obtained is usually small and negligible. When pEGFP (6 μg, 1 μg/μl) was added into EthBr-HEPES buffer, significantly high fluorescence was recorded indicating that EthBr readily intercalated between base-pairs. The concentration of spermine added was expressed as N/P charge ratio. The positive charge equivalents of spermine (3.8 charges/molecule) to the negative charges of DNA phosphate (2 charges/DNA base-pair) were used in the N/P calculation. When spermine was added, the fluorescence started to decrease indicating its interactions with DNA, causing the displacement of EthBr from its binding sites (decreased fluorescence as less bound EthBr), or at least preventing re-intercalation of EthBr on bending the DNA during the condensation process, distorting the intercalation binding sites from parallel base-pairs.

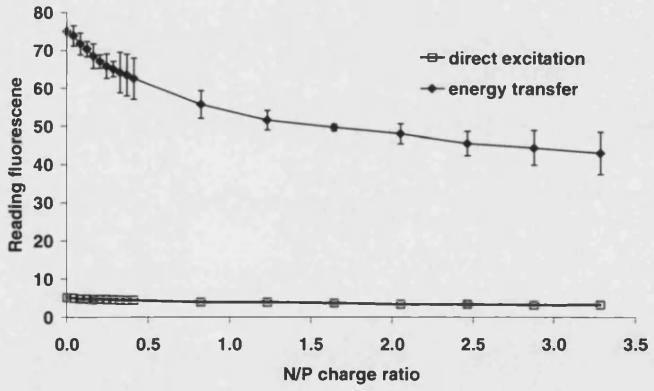

Figure 2.9 Spermine-mediated pEGFP condensation by EthBr displacement assay, by direct excitation at 546 nm, or by energy transfer from nucleic bases at 260 nm (n = 3, error bars are S.D.), monitored by the decrease of reading (absolute) fluorescence

As the energy of excitation light is reciprocal to its wavelength, the relative energy difference between 260 and 546 nm is approximately 2 times. However, in Figure 2.9, the indirect excitation of EthBr at 260 nm produces a much higher level of fluorescence at 10-15

times. We conclude that efficient energy transfer from DNA to EthBr may be related to the close proximity of intercalated nucleic bases and EthBr molecules.

Fluorescence data were normalised to percentages, shown in Figure 2.10. There is no difference in % fluorescence decrease between the two approaches. However, from Figure 2.9, the excitation through DNA is a more sensitive assay to detect fluorescence. This method was chosen for our further experiments especially when a low amount of DNA (6 μg) was used. In Figure 2.10, at N/P charge ratio 2.5, the residual fluorescence was approaching a plateau at 50% in all experiments. According to Bloomfield,[28] the full condensation of DNA occurs when about 90% of the charge on DNA is neutralised (i.e. 10% residual fluorescence). Thus, (free) spermine is not considered as an efficient DNA condensing agent, and the development of new synthetic gene vectors is required.

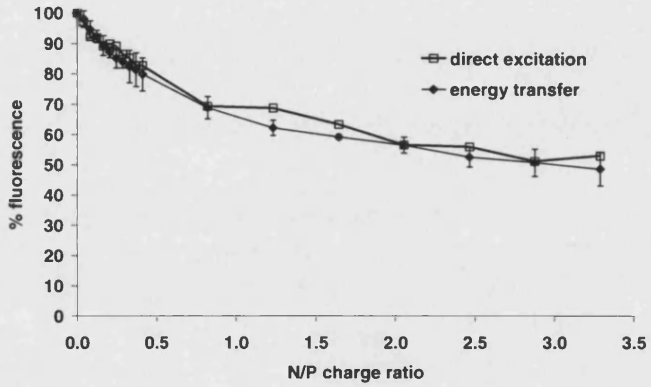

Figure 2.10 Spermine-mediated pEGFP condensation by EthBr displacement assay, by direct excitation at 546 nm, or by energy transfer from nucleic bases at 260 nm (n = 3, error bars are S.D.), reported in the units of % fluorescence

Effect of DNA type and their condensation

Preparation of circular plasmids is a complicated and time-consuming process. More importantly, these plasmids though in less than milligram amounts are generally expensive. Given this, an alternative DNA which is commercially available, such as linear calf thymus DNA (CT-DNA) was introduced in our study for initial experiments. Some DNA condensing agents show base selectivity, for example, spermine and its analogues induce structural changes specific to alternating A-T sequences.[22] Steroidal polyamines also show a preference to binding A-T rich sequences.[144] CT-DNA is comprised of random sequence double stranded polynucleotide with A-T (58%) and G-C (42%),[145] which make this DNA ideal for our studies.

CT-DNA is a polydispersed DNA with varied lengths of polynucleotide. For example, CT-DNA used in this experiment, as obtained from Sigma-Aldrich, UK (product code D4522), has the minimum size of 13 kbp. From the recent work by Yoshikawa *et al.*,[146] the polydispersity does not affect DNA condensation, for any DNA in the range 15-150 kbp. DNA conformational transition (from uncondensed to condensed DNA) is sharp and the coexistence of uncondensed and condensed DNA as reported by Yoshikawa *et al.* and Kleideiter *et al.* is within a narrow concentration range of DNA condensing agents used.[146,147]

An aim of this experiment is to validate the use of CT-DNA in DNA condensation studies. CT-DNA and two circular plasmids (pEGFP and pGL3) were condensed with spermine using similar EthBr experimental conditions. In Figure 2.11, the fluorescence decrease curves for all three DNA condensed by spermine are similar, especially at N/P 0.0-2.0. At N/P 2.5, CT-DNA condensation still continued until it reached 30% (at N/P 3.0), while at N/P 2.5 pEGFP and pGL3 had already reached their constant level at 50% EthBr fluorescence quenched. This may be related to the size of CT-DNA which is higher than both of the plasmids used. The collapse of DNA requires a higher amount of polycation (higher N/P) to reach the plateau than the theoretical N/P of 1.0. However, both 50% and 30% residual fluorescence are not regarded as complete DNA condensation, so (free) spermine is not an excellent DNA condensing agent.

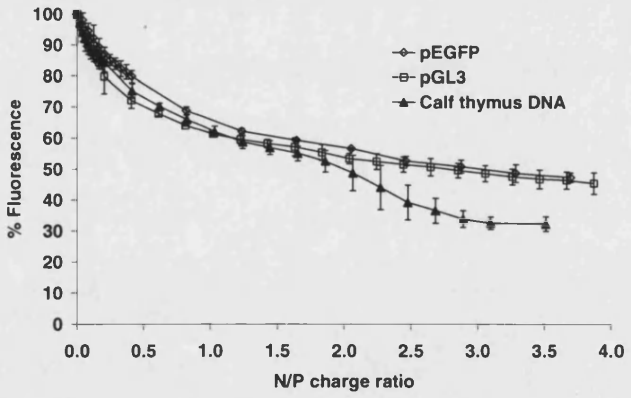

Figure 2.11 pEGFP, pGL3, and CT-DNA condensation studied by EthBr displacement assay (λ_{ex} = 260 nm and λ_{em} = 600 nm) (n = 3, error bars are S.D.), using spermine

Light scattering (LS) experiment, by measuring the apparent UV absorbance at 320 nm (where there is no DNA absorbance above 300 nm), was previously employed to identify DNA nanoparticle formation.[27,148,149] The concentration of DNA used in light scattering experiments is ten times the concentration used in fluorescence quenching experiments

which is mainly due to the lack of sensitivity of the light scattering experiment compared with the fluorescence assay. When the DNA particles are being formed, these particles cause the scattering of input light and this reduces light intensity at the UV detector. The "apparent" UV absorbance was measured until it reached a plateau.

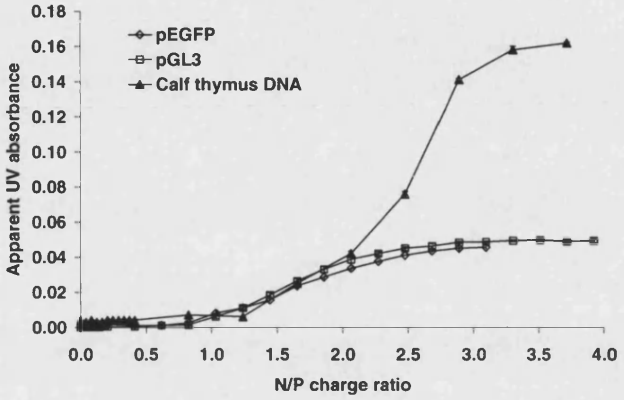

Figure 2.12 pEGFP, pGL3, and CT-DNA condensation studied by light scattering assay (λ = 320 nm) (n = 3, error bars are S.D.), using spermine

The upward curves in Figure 2.12 indicate the formation of DNA particles of pEGFP, pGL3, and CT-DNA upon interaction with spermine. Particle formation was also confirmed by LS assay with significantly increased apparent absorbance at N/P ratio 2.5-3.0. The condensation profiles of both plasmids were found to be similar, possibly relative to their similar plasmid sizes. Both plasmids reach their maximum absorption at N/P 2.5, which is similar to the range found in the corresponding EthBr assays. It was also found that CT-DNA complexed with spermine has higher UV absorbance at higher N/P. This could be due to its large DNA size, resulting in higher particle sizes and higher light scattering. Though the apparent UV absorbance is not an accurate way to determine the size of DNA complexes, it shows the formation of DNA complexes as particles capable of scattering light. We concluded that there is essentially no difference between linear and circular DNA plasmids in DNA condensation using (free) spermine.

N^4,N^9-Dioleoylspermine-mediated DNA condensation study

Spermine condensed DNA to the 30-50% residual fluorescence level in the EthBr assay. With an aim to improve the gene packing ability of spermine, lipophilic moieties were covalently bound to spermine to construct NVGT vectors, lipopolyamines. N^4,N^9-Dioleoylspermine is our synthetic lipopolyamine with two chains of C18 oleic acid, and two ammonium groups at pH 7.4 (pK_a = 10.8).[31] CT-DNA was used in the initial experiment to determine the DNA charge neutralisation effect of this compound.

Figure 2.13 shows the ability of the studied lipopolyamine to displace EthBr from CT-DNA. Lipophilicity modification of this structure led to efficient DNA condensation (6% residual fluorescence at N/P charge ratio 2.0) compared to the tetracationic spermine (50% DNA condensation at charge ratios more than 3.50).

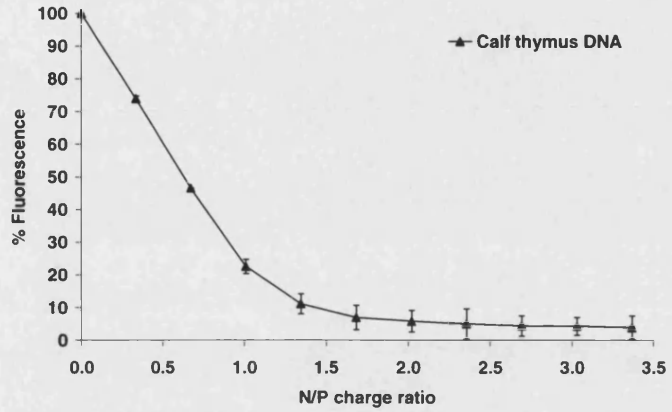

Figure 2.13 CT-DNA condensation studied by EthBr displacement assay (λ_{ex} = 260 nm and λ_{em} = 600 nm) (n = 3, error bars are S.D.), using N^4,N^9-dioleoylspermine

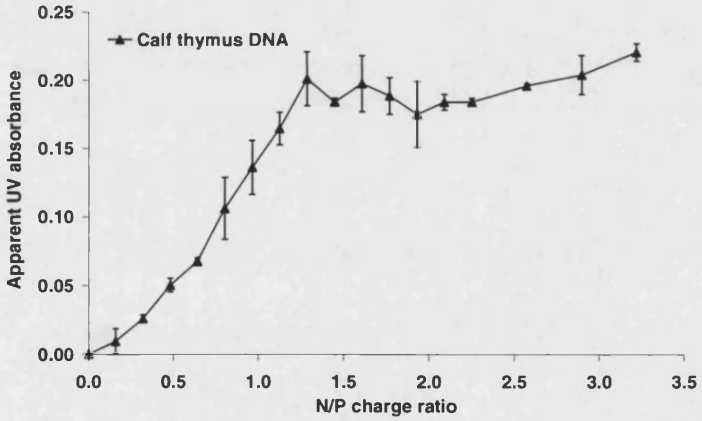

Figure 2.14 CT-DNA condensation studied by light scattering assay (λ = 320 nm) (n = 3, error bars are S.D.), using N^4,N^9-dioleoylspermine

Figure 2.14 also reveals that DNA nanoparticles were formed at similar N/P (1.5-2.0) as shown in the EthBr assay. Vijayanathan *et al.*[150] reported a similar finding that the λ–phage DNA condensed particles (by spermine) were formed in the size range 50-100 nm. In Dunlap *et al.*'s work, another lipospermine (Transfactam) was able to condense pSfiSVneo, pSifiSV19, and pCISfi-γIFN DNA to smaller particle sizes 50-70 nm.[151] The efficient condensation by Transfactam over spermine, resulting in smaller particles sizes (nanoparticles), may also promote more effective transfection via increased cellular uptake.

N^4,N^9-Dioleoylspermine is a better and more efficient DNA condensing agent than spermine. Given this, we extended the confirmatory study on the use of linear vs. circular plasmid DNA, using this molecule. It was found that there is no significant variation in the condensation ability of the studied lipopolyamine on the type of DNA (CT-DNA, pEGFP, and pGL3). These results (Figures 2.15 and 2.16) support the use of a linear DNA (such as CT-DNA) as a replacement for plasmid DNA in the initial DNA condensation studies.

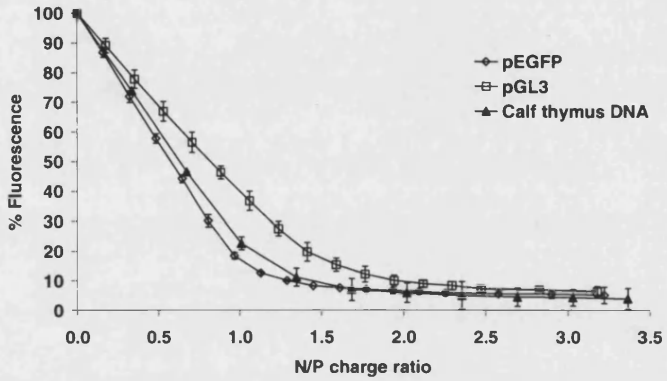

Figure 2.15 pEGFP, pGL3, and CT-DNA condensation studied by EthBr displacement assay (λ_{ex} = 260 nm and λ_{em} = 600 nm) (n = 3, error bars are S.D.), using N^4,N^9-dioleoylspermine

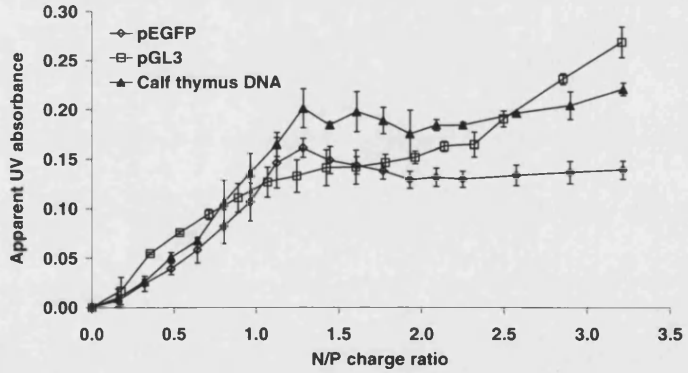

Figure 2.16 pEGFP, pGL3, and CT-DNA condensation studied by light scattering assay (λ = 320 nm) (n = 3, error bars are S.D.), using N^4,N^9-dioleoylspermine

pEGFP and pGL3, carrying marker genes, were used to determine the final result of gene delivery, by measuring the expression of those marker genes. In Figures 2.17 and 2.18 where EthBr and LS data were plotted together on the same graph, N^4,N^9-dioleoylspermine condensed both pEGFP and pGL3 effectively at N/P charge ratio = 1.5-2.0. The plateaus of fluorescence and apparent UV absorbance were found in at the same N/P region. This shows

that both EthBr and LS studies are complimentary to each other, and useful in studies of DNA complexes.

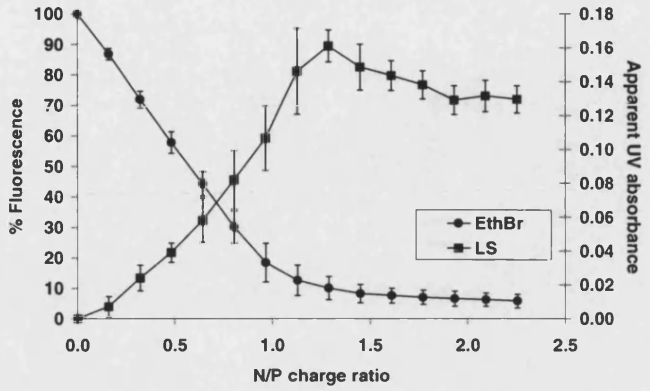

Figure 2.17 pEGFP condensation studied by EthBr assay (λ_{ex} = 260 nm and λ_{em} = 600 nm) and LS assay (λ = 320 nm), using N^4,N^9-dioleoylspermine (n = 3, error bars are S.D.)

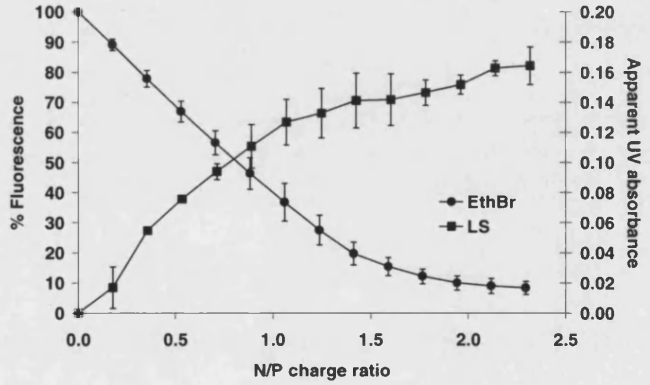

Figure 2.18 pGL3 condensation studied by EthBr assay (λ_{ex} = 260 nm and λ_{em} = 600 nm) and LS assay (λ = 320 nm), using N^4,N^9-dioleoylspermine (n = 3, error bars are S.D.)

N^1-Cholesteryl spermine carbamate-mediated DNA condensation study

N^1-Cholesteryl spermine carbamate is another lipopolyamine synthesised and used in this study. The number of positive charges in this molecule was calculated from pK_a data (10.9, 8.6, 7.3) reported by Blagbrough's research group,[27] to be 2.4 ammonium eq/molecule. This is higher than N^4,N^9-dioleoylspermine (2.0 ammonium eq/molecule).

Figure 2.19 shows the efficient CT-DNA condensation of N^1-cholesteryl spermine, achieving 10% residual fluorescence, and the highest apparent absorbance at about N/P 2.0 (Figure 2.20). The efficiency for gene condensation is slightly lower than N^4,N^9-dioleoylspermine (residual 6%), but much higher than its parent molecule, spermine. The binding of lipophilic

cholesterol to spermine contributes to the improved DNA condensation in this non-viral vector.

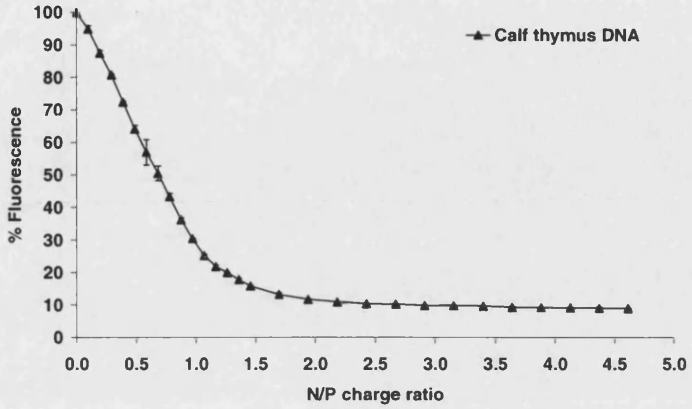

Figure 2.19 CT-DNA condensation studied by EthBr displacement assay (λ_{ex} = 260 nm and λ_{em} = 600 nm) (n = 3, error bars are S.D.), using N^1-cholesteryl spermine carbamate

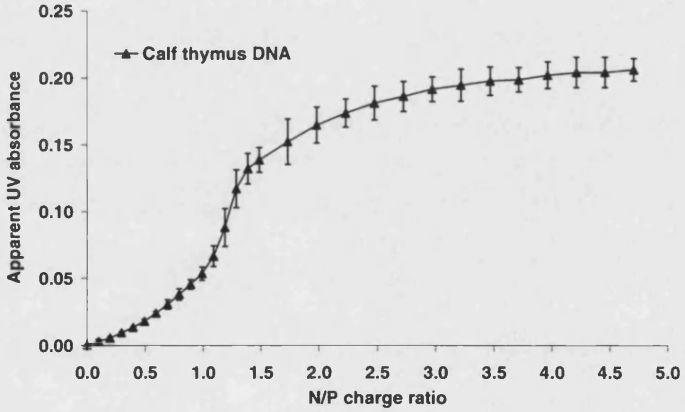

Figure 2.20 CT-DNA condensation studied by light scattering assay (λ = 320 nm) (n = 3, error bars are S.D.), using N^1-cholesteryl spermine carbamate

When comparing the condensation of pEGFP, pGL3, and CT-DNA, there is no significant difference in EthBr (Figure 2.21) and LS data (Figure 2.22) among different types of DNA used. The N/P ratios at which N^1-cholesteryl spermine carbamate achieved its lowest residual fluorescence is the same in all DNAs used in this experiment. EthBr/LS plotted graphs were also drawn for pEGFP and pGL3 condensed with N^1-cholesteryl spermine carbamate. The EthBr (Figure 2.23) and LS assays (Figure 2.24) show the full condensation of plasmids at N/P 2.0. This is in agreement that there is no significant difference in DNA condensation from the type of DNA used in the experiments, which again supports the use of linear CT-DNA in initial DNA condensation studies.

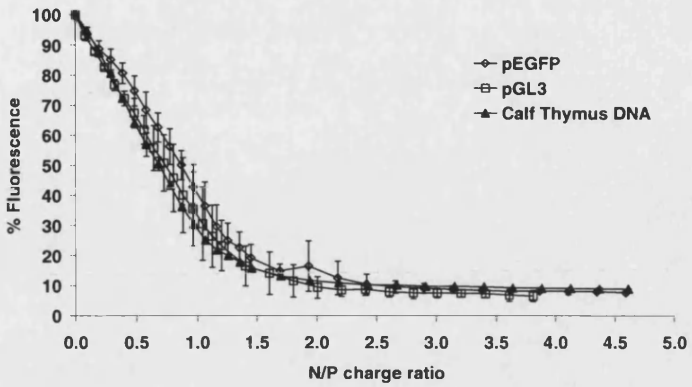

Figure 2.21 pEGFP, pGL3, and CT-DNA condensation studied by EthBr assay (λ_{ex} = 260 nm, λ_{em} = 600 nm) (n = 3, error bars are S.D.), using N^1-cholesteryl spermine carbamate

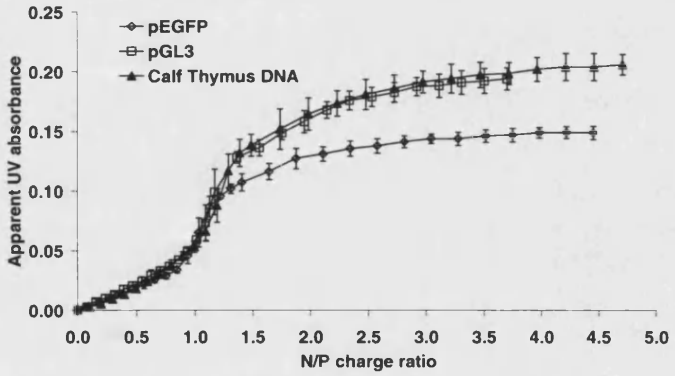

Figure 2.22 pEGFP, pGL3, and CT-DNA condensation studied by light scattering assay (λ = 320 nm) (n = 3, error bars are S.D.), using N^1-cholesteryl spermine carbamate

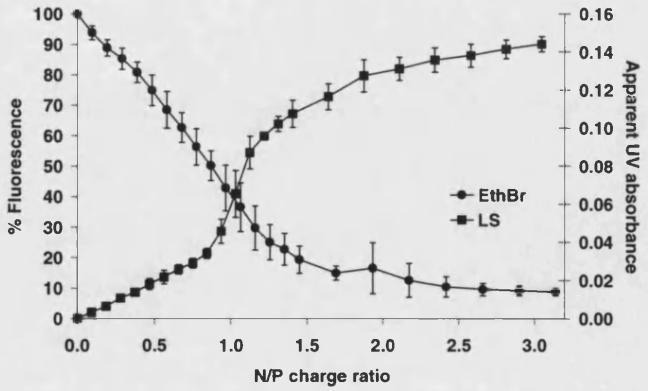

Figure 2.23 pEGFP condensation studied by EthBr assay (λ_{ex} = 260 nm, λ_{em} = 600 nm) and LS assay (λ = 320 nm), using N^1-cholesteryl spermine carbamate (n = 3, error bars are S.D.)

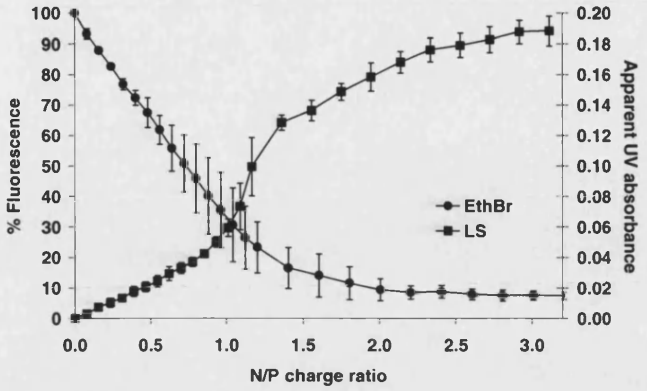

Figure 2.24 pGL3 condensation studied by EthBr displacement (λ_{ex} = 260 nm and λ_{em} = 600 nm) and LS assay (λ = 320 nm), using N^1-cholesteryl spermine carbamate (n = 3, error bars are S.D.)

In Figure 2.25, it was found that N^1-cholesteryl spermine carbamate is less efficient than N^4,N^9-dioleoylspermine in both final residual fluorescence (10 vs. 6 %) and it also reaches the plateau of EthBr assay curves at higher N/P charge ratio (1.5 vs. 2.0). To quantify the difference in DNA condensation of both lipopolyamines, binding constants (K_b) were calculated (as ammonium equivalents) using the estimation method described in the Experimental (Chapter 5).

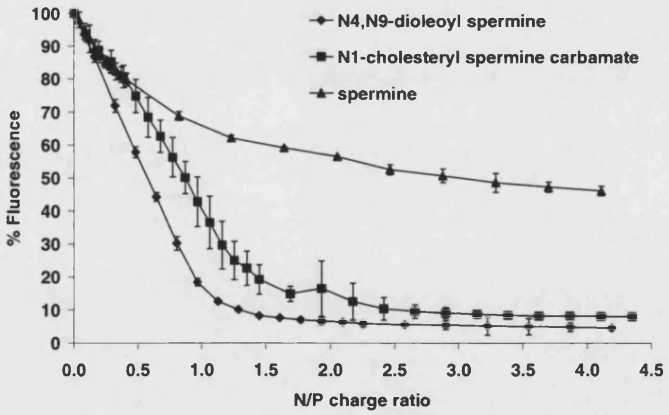

Figure 2.25 Effect of lipid conjugation to spermine, shown by pEGFP condensation - EthBr displacement study (λ_{ex} = 260 nm and λ_{em} = 600 nm) (n = 3, error bars are S.D.)

The binding ability was calculated from the experiment using pEGFP as a model DNA. Calculated K_b are in the order: N^4,N^9-dioleoylspermine (1.1 x 10^7 M^{-1}) > N^1-cholesteryl spermine carbamate (0.7 x 10^7 M^{-1}) > spermine (0.2 x 10^7 M^{-1}). From this binding analysis, N^4,N^9-dioleoylspermine binds to pEGFP more than N^1-cholesteryl spermine carbamate, and

actually in the same magnitude of EthBr ($1.0 \times 10^7 M^{-1}$).[152] This could be due to the difference in both charge number and lipid moiety. We think that the lipid moiety may be more important than the total number of positive charges, given that the higher positively charged compound (N^1-cholesteryl spermine carbamate) showed less efficient DNA packaging properties than N^4,N^9-dioleoylspermine with its 2.0 positive charges.

Transfection of lipoplexes in a primary cell line

From EthBr and LS studies, N^4,N^9-dioleoylspermine and N^1-cholesteryl spermine carbamate are efficient DNA condensing agents. It is important to assess their efficiency in gene delivery. Many previous studies showed that there is no conclusive correlation between DNA condensing ability and *in vitro* transfection, but also many researchers agree that good quality condensed DNA is a prerequisite to successful gene therapy. In this study, pEGFP and pGL3 were used as delivered DNA. Both plasmids carry marker genes, and their gene expression products could be indicators for gene delivery efficiency. pEGFP is a plasmid encoding for enhanced green fluorescent protein (EGFP) which contains a fluorophore detected in successfully transfected cells by FACS (fluorescent-activated cell sorting). pGL3 is a plasmid encoding for firefly luciferase enzyme. This enzyme level was detectable by the addition of its substrate, and any luminescent light produced was measured.

Human primary cell is a cell or cell line taken directly from a human. The cell line is not immortalized, e.g. FEK4 cells used in our studies are from a neonatal foreskin explant.[153] The efficient gene transfer into primary cells is unfortunately still problematic, while these cells are an extremely important model (or target) in gene therapy. Additionally, gene delivery studies in primary cells may also find application in other difficult-to-transfect cell lines, such as stem cells.[154,155]

The commonly used liposomal formulation, Lipofectin (DOTMA/DOPE = 1:1 w/w, Invitrogen, Figure 2.26), was used in this study as the reference transfection. DOTMA functions as a cationic lipid (with one positive charge) and DOPE is added as a helper lipid. DOPE was used to help membrane fusion in cellular processes, especially to promote the endosomal escape of DNA nanoparticles.

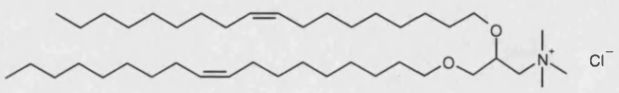

Figure 2.26 DOTMA, a cationic lipid vector in Lipofectin liposomes

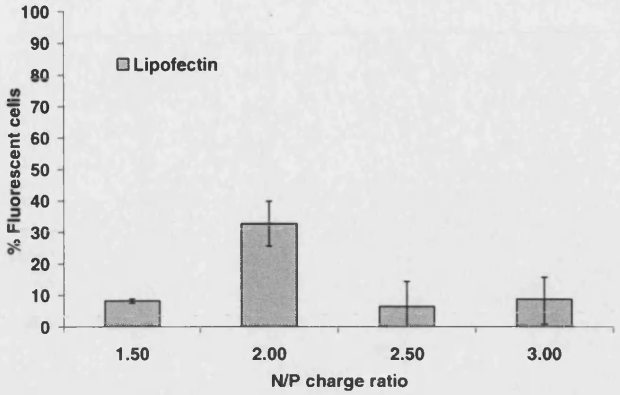

Figure 2.27 EGFP-containing fluorescent cells measured in FEK4 transfected with pEGFP (2 μg/well) using Lipofectin at different N/P charge ratios (λ_{ex} = 488 nm and λ_{em} = 530 nm) (n = 3, error bars are S.D.)

Lipofectin was found to be ineffective in gene transfer in FEK4 cells. The fluorescent cell number (as a percentage) is achieved at 30% at N/P charge ratio 2.0 (Figure 2.27). At other N/P values, the result is as low as 10%. This is not unexpected as FEK4 cell is a difficult-to-transfect cell line. Hamm *et al.*[155] recently reported that liposome-mediated transfection did not satisfactorily deliver genes into human primary cells. Electroporation,[154,155] a direct-to-nucleus gene transfer technique, which bypasses both extracellular and intracellular barriers in gene delivery, was only able to transfect in primary cells with improved efficiencies upto 45%. In Figure 2.27, the optimality of charge ratio is also observed in Lipofectin-mediated transfection.

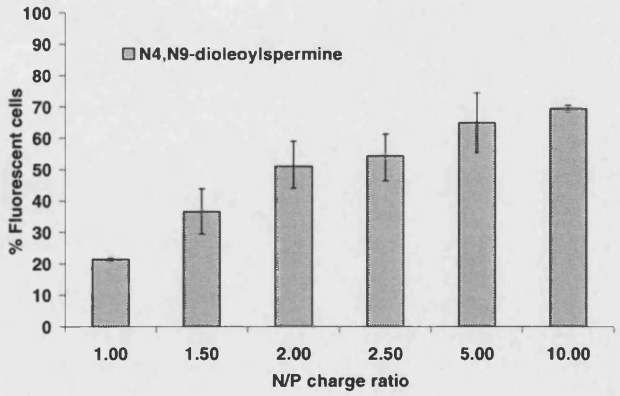

Figure 2.28 EGFP-containing fluorescent cells measured in FEK4 transfected with pEGFP (2 μg/well) using N^4,N^9-dioleoylspermine at different N/P charge ratios (λ_{ex} = 488 nm and λ_{em} = 530 nm) (n = 3, error bars are S.D.)

N^4,N^9-Dioleoylspermine was then tested for transfection at several N/P charge ratios (1.0, 1.5, 2.0, 2.5, 5.0, and 10.0), which N/P ratios were calculated in the same manner as described in the Experimental for the DNA condensation study. Lipoplexes were then formed (after this simple titration) by gentle mixing of plasmid DNA and condensing agent, and regarded as a non-liposome formulation. N/P ratios of Lipofectin (as liposomes) were calculated taking account of the mole ratio of its mixture and positive charge from DOTMA (1 charge/ molecule). FEK4 was used in these experiments at 2.5 x 10^4 cells/well, followed by 4 h incubation with lipoplexes, and gene expression was determined 48 h post-transfection. Figure 2.28 shows the transfection result of pEGFP N^4,N^9-dioleoylspermine complexes, which achieve high transfection efficiency (50-70%) from N/P 2.0. The transfection efficiency remains high until N/P 10.0, where it reaches a plateau.

The optimal charge ratio for FEK4 transfection with pEGFP-N^4,N^9-dioleoylspermine complex starts from 2.0, which corresponds to the optimal DNA condensation N/P ratio. From EthBr assay data, the fluorescence intensity decrease is approaching a plateau from N/P 2.0. From our results, fluorescent cell counts (%) observed in N^4,N^9-dioleoylspermine-mediated transfection are higher than the experiments using Lipofectin, at all N/P ratios. This high transfection may result from our strategy to conjugate C18 oleic acid to spermine, which makes it similar to DOPE, a helper (fusogenic) lipid in Lipofectin formulation.

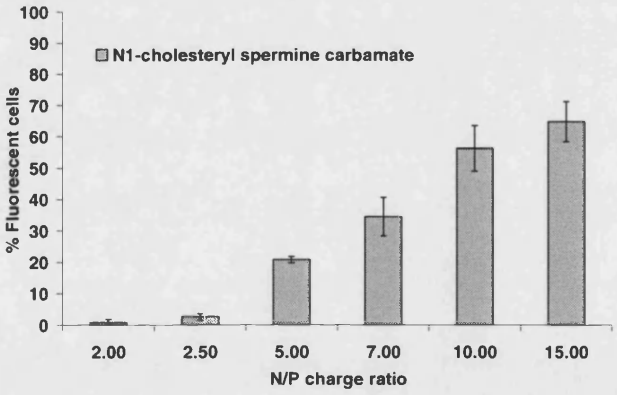

Figure 2.29 EGFP-containing fluorescent cells measured in FEK4 transfected with pEGFP (2 μg/well) using N^1-cholesteryl spermine carbamate at different N/P charge ratios (λ_{ex} = 488 nm and λ_{em} = 530 nm) (n = 3, error bars are S.D.)

N^1-Cholesteryl spermine carbamate was also studied in FEK4 cells and we found a similar high transfection efficiency at 60%, but at higher N/P ratios. Figure 2.29 shows the optimal transfection at N/P 10.0-15.0. We conclude that cholesterol facilitates gene delivery less efficiently than two oleoyl chains on a spermine template.

Unlike immortal cell lines whose passage numbers do not affect their transfectivity, it is recommended to use FEK4 cells only from passage 9-16.[156,157] In our transfection study, different FEK4 passages were used according to the stock availability. Transfection experiments were not necessarily performed using FEK4 from the same passage number. This may raise some concerns over the data analysis from cells at different ages, as their cell's susceptibility to xenobiotics may be different. Transfectivity of FEK4 cells in different passage number with N^4,N^9-dioleoylspermine-pEGFP lipoplexes was studied at N/P ratios 2.0 and 2.5. In Figure 2.30, there is no difference in transfection efficiency using FEK4 from different passages. Thus, passage number does not affect the transfection, as long as it is within the recommended ages.

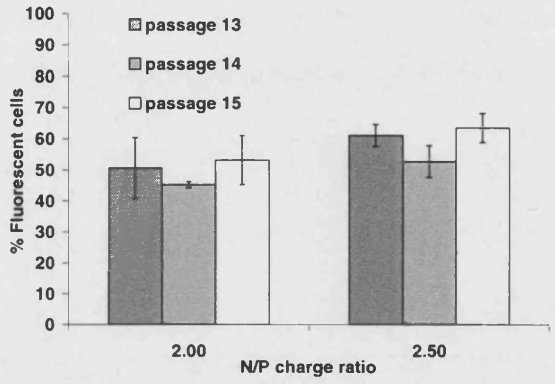

Figure 2.30 Effect of FEK4 passage number in transfection efficiency, using pEGFP at 2 μg/well, complexed with N^4,N^9-dioleoylspermine at N/P charge ratios 2.0 and 2.5 (λ_{ex} = 488 nm and λ_{em} = 530 nm) (n = 3, error bars are S.D.)

In our FEK4 experiments, DNA complexes were prepared by using 2 μg/well DNA, as recommended in the manufacturer's protocol of Lipofectin-mediated transfection (Invitrogen Ltd.). A simple study was performed using two concentrations of pEGFP-N^4,N^9-dioleoylspermine complexes prepared at the N/P ratios 2.0 and 2.5, which offer high transfection levels. At each N/P, lipoplexes formed with pEGFP 1 and 2 μg/well were used in FEK4 transfection. The standard transfection conditions were used in this study. From Figure 2.31, there is no significant difference between the two doses of lipoplexes at both N/P ratios. Recently, Walker *et al.*[158] reported a similar finding that the dilution of pEGFP-lipoplexes (with pUC18, blank plasmid) in COS-7 cells does not compromise transfection efficiency. Their study was different from our experiments, given the DNA plasmid dilution was performed with blank plasmid (similar to diluents in pharmaceutical preparations), and the lipoplex dose remain unchanged. However, their study also supports out conclusion that plasmid DNA dose dilution (either lipoplex or active plasmid) does not alter transfection.

This conclusion has practical advantages in lipoplex preparation, and allows researchers to use less plasmid to minimise cost in studies, and ultimately less DNA condensing agent to minimise toxicity in cells.

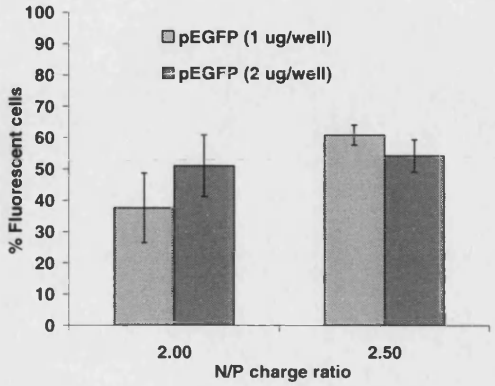

Figure 2.31 Effect of lipoplex dose in FEK4 transfection, with pEGFP at 1 and 2 μg/well, using N^4,N^9-dioleoylspermine at N/P charge ratios 2.0 and 2.5 (λ_{ex} = 488 nm and λ_{em} = 530 nm) (n = 3, error bars are S.D.)

Transfection with pGL3 using Lipofectin and N^4,N^9-dioleoylspermine was studied, using the protocol in the Experimental. Luciferase enzyme, a protein expressed by pGL3, catalyses luciferin oxidation generating oxyluciferin and detectable yellow light (Figure 2.32).[133] The light unit was measured in relative light units (RLU) and normalized by the unit of total cellular protein. Lipofectin enables the high expression of luciferase in FEK4, at N/P 2.0-2.5 (1200-1600 RLU/mg) (Figure 2.33). Lipofectin's optimal N/P charge ratio found in this experiment was similar to the one used in pEGFP transfection (Figure 2.27). However, the efficiency of FEK4 transfection with pGL3 is maintained until N/P 5.0, while pEGFP expression diminished at smaller N/P charge ratios. This suggests that the difference in plasmid construct, such as promoter gene, may lead to different levels of gene expression.

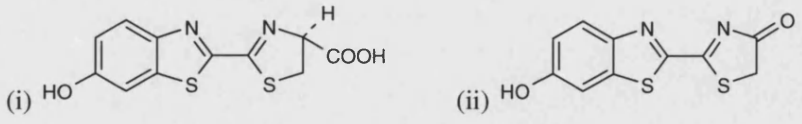

Figure 2.32 Luciferin (substrate of luciferase enzyme) and oxyluciferin (product of the oxidation reaction)

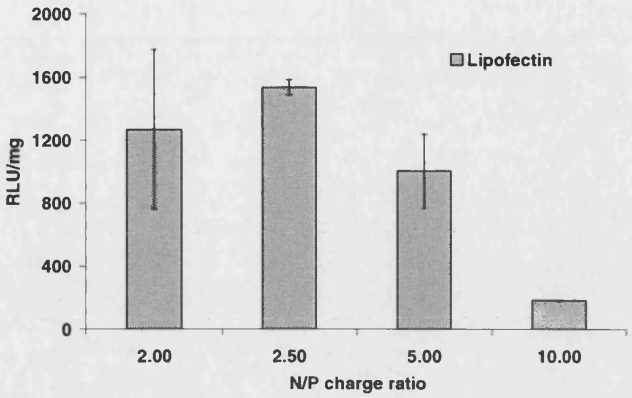

Figure 2.33 FEK4 transfected with pGL3 (2 μg/well) using Lipofectin at different N/P charge ratios, with luminescence measured in RLU/mg of total protein (n = 3, error bars are S.D.)

Luciferase gene transfer experiments were then carried out using N^4,N^9-dioleoylspermine (Figure 2.34). The obtained RLU/mg shows that N/P charge ratio = 2.5 provides a significant high transfection compared to N/P = 5.0. This is in agreement with the results obtained in the expression of pEGFP by N^4,N^9-dioleoylspermine based gene transfer. FEK4 transfection efficiency of pGL3 is comparable to Lipofectin (1200 RLU/mg at N/P 2.5). The loss of superiority of N^4,N^9-dioleoylspermine over Lipofectin may be related to the actual DNA itself, not due to the gene delivery systems. pGL3 is under SV40 promoter and pEGFP has a CMV promoter in its construct. Young *et al.*[159] recently reported that the inclusion of the SV40 promoter/enhancer into plasmids enhance non-viral gene delivery, possibly through the increase of gene uptake by the nucleus. Thus, the observed relative improved transfection of Lipofectin may result from the SV40 promoter sequence in pGL3.

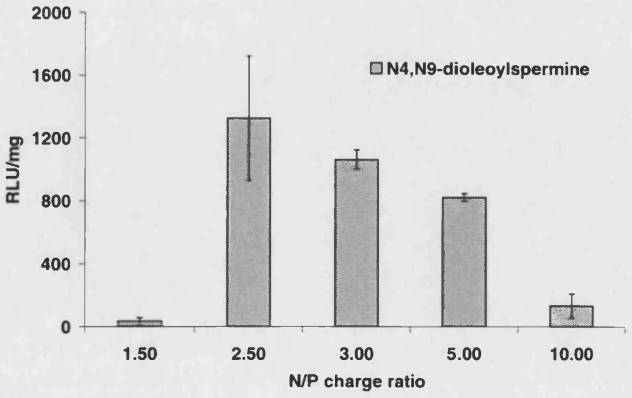

Figure 2.34 FEK4 transfected with pGL3 (2 μg/well) using N^4,N^9-dioleoylspermine at different N/P charge ratios (n = 3, error bars are S.D.)

Transfection of lipoplexes in a carcinoma cell line

Gene therapy is not currently limited to genetic disease treatment where gene delivery in primary cells is important. Cancer gene therapy has been recently developed, aiming to treat cancer by genetic modification of cancer cells to inhibit their growths or increase their susceptibility to other cancer therapies. In our experiments, HeLa cell line is used to understand the DNA delivery mechanism and efficacy in a carcinoma model. HeLa cells are the first continuous cancer cells isolated from the glandular cervical cancer by Gey[159] in 1951. These cells can be cultivated *in vitro*, immortalized, and also have lost their ability of intercellular adhesion.[160,161] Immortalized cell lines are generally easier to transfect than primary cells of the same given tissue origin.[162] A study by Banks *et al.*[163] shows that HeLa cells uptake genes faster than other cells, which contribute to highly efficient gene expression.

Specifically, HtTA-1 is a modified HeLa cell line used in these studies. It incorporates a tetracycline-controlled transactivator (tTA) consisting of the tet repressor fused with the activating domain of virion protein 16 of herpes simplex virus (HSV). This tTA sequence stimulates transcription from a minimal promoter sequence and it is sensitive to the concentration of tetracycline.[164,165] N^4,N^9-Dioleoylspermine and N^1-cholesteryl spermine carbamate were studied for their gene delivery ability in HtTA-1 HeLa, using both pEGFP and pGL3 as reporter genes.

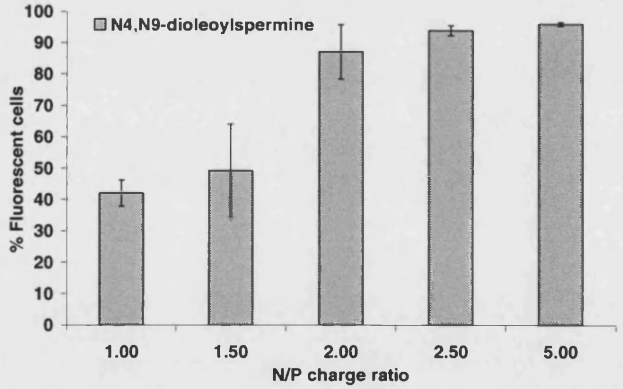

Figure 2.35 EGFP-containing fluorescent cells measured in HtTA-1 HeLa transfected with pEGFP (2 μg/well) using N^4,N^9-dioleoylspermine at different N/P charge ratios (λ_{ex} = 488 nm and λ_{em} = 530 nm) (n = 3, error bars are S.D.)

The graph (Figure 2.35) shows the highest transfection efficacy (90%) in HtTA-1 HeLa cells from N/P 2.0. These results are similar to the previous experiments on FEK4, however the expression levels of pEGFP in HeLa cells continued at higher N/P. The percentage of

fluorescent cells in HeLa cells is significantly higher (2 times) than FEK4 cells at every charge ratio. Similar experiments on pGL3 (Figure 2.36) revealed the optimal charge ratio for N^4,N^9-dioleoylspermine-mediated transfection at 2.0 with very much higher RLU/mg protein than the ones in FEK4 (more than 1000-fold). The high transfection for both FEK4/HeLa and pEGFP/pGL3 is at N/P = 2.0 which could be used as a single N/P charge ratio value for future studies. Additionally, the significantly high expression in HeLa cells will be helpful to understand the intracellular factors contributing to effective gene delivery, in comparison with primary cell lines such as FEK4 cells.

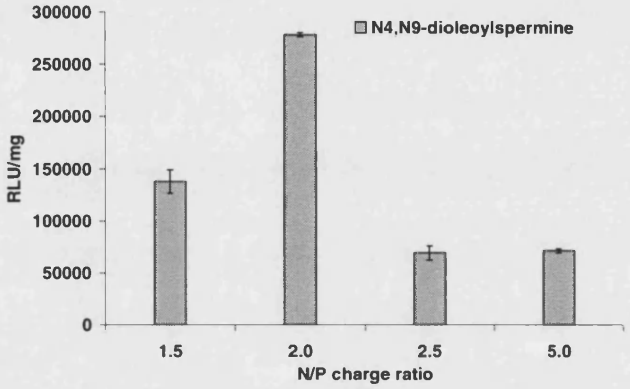

Figure 2.36 EGFP-containing fluorescent cells measured in HtTA-1 HeLa transfected with pGL3 (2 μg/well) using N^4,N^9-dioleoylspermine at different N/P charge ratios (λ_{ex} = 488 nm and λ_{em} = 530 nm) (n = 3, error bars are S.D.)

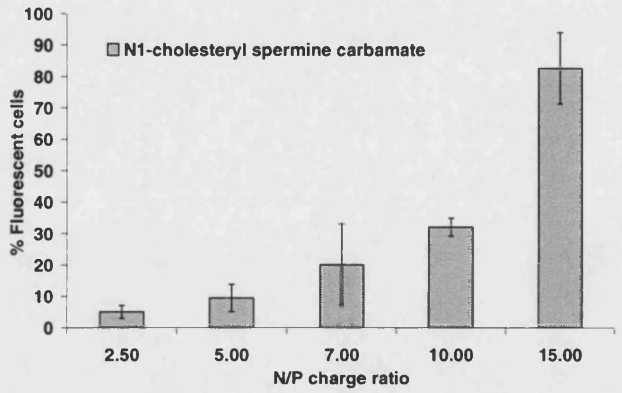

Figure 2.37 EGFP-containing fluorescent cells measured in HtTA-1 HeLa transfected with pEGFP (2 μg/well) using N^1-cholesteryl spermine carbamate at different N/P charge ratios (λ_{ex} = 488 nm and λ_{em} = 530 nm) (n = 3, error bars are S.D.)

Unlike N^4,N^9-dioleoylspermine, in Figure 2.37, N^1-cholesteryl spermine carbamate seems to display lower transfection efficiency, and high transfection was only observed at higher N/P

ratios (N/P 15, with % fluorescent cells = 80%). This suggests that cholesterol facilitates gene delivery less efficiently than two oleoyl chains, which is a similar result to that obtained in our study in FEK4 cells. Given the high efficiency in transfection of the HtTA-1 HeLa cell model, naked DNA (uncomplexed DNA), which though it shows low efficiency in gene delivery is still in some clinical trials, was used in the experiment as a control. Somewhat as expected (Figure 2.38), naked pEGFP and blank media did not show any fluorescent cells. This is probably due to the charge repulsion of negative DNA phosphate and negatively charged cell membrane. Uncomplexed DNA is also more vulnerable to extracellular and intracellular enzymatic degradation, than lipoplexes. This emphasizes the importance of DNA complexation in NVGT.

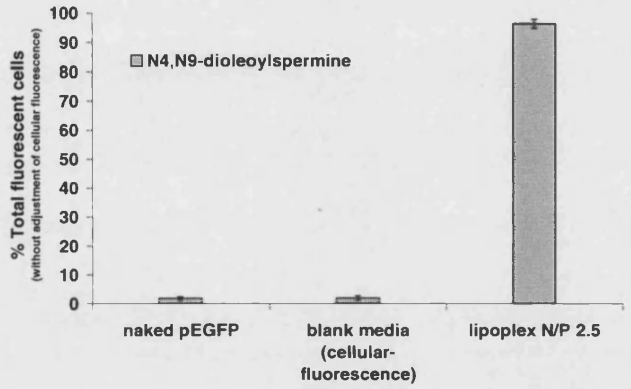

Figure 2.38 EGFP-containing fluorescent cells measured in HtTA-1 HeLa transfected with pEGFP (2 μg/well) without and with N^4,N^9-dioleoylspermine at different N/P charge ratios (λ_{ex} = 488 nm and λ_{em} = 530 nm), compared to blank media (10% FCS EMEM only) (n = 3, error bars are S.D.)

Toxicity study of lipoplex gene delivery

The safety of our synthetic lipopolyamines has been studied using the MTT assay.[136] Soluble tetrazolium salt 3-(4,5-dimethylthiazol-2-yl)-2,5-diphenyltetrazolium bromide (MTT) was added to cells treated with lipopolyamines and their lipoplexes. Only live cells are able to convert MTT into insoluble formazan violet crystals (detectable by UV at 550 nm), as shown in Figure 2.39.

Figure 2.39 MTT assay, a substrate (MTT) was converted into formazan in live cells

IC_{50} (the concentration at which cell viability is 50%)[166] values of N^4,N^9-dioleoylspermine in FEK4 and HtTA-1 HeLa cells were 25 and 30 μg/ml respectively (Figures 2.40 and 2.41), and for the lipoplex were 25 and 31 μg/ml respectively. The results indicate that there is no significant difference in the toxic effects (IC_{50}) of the free lipopolyamine over the lipoplex in the case of both HtTA-1 HeLa and FEK4 cells for the studied lipopolyamines.

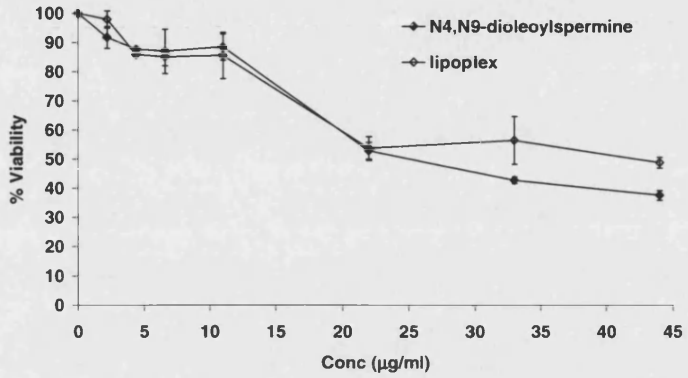

Figure 2.40 Viability of FEK4 cells when exposed to different concentrations of N^4,N^9-dioleoylspermine and lipoplexes (N^4,N^9-dioleoylspermine + pEGFP) in 96-well plates, using the MTT assay (n = 3, error bars are S.D.)

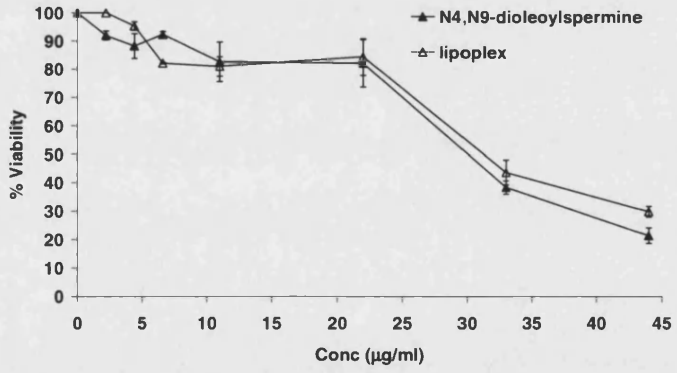

Figure 2.41 Viability of HtTA-1 HeLa cells when exposed to different concentrations of N^4,N^9-dioleoylspermine and lipoplexes (N^4,N^9-dioleoylspermine + pEGFP) in 96-well plates, using the MTT assay (n = 3, error bars are S.D.)

IC_{50} results also revealed that N^4,N^9-dioleoylspermine toxicity in the case of FEK4 cells is not significantly different from that in HtTA-1 HeLa. However, HtTA-1 HeLa is more susceptible to toxicity of lipoplexes than FEK4 at higher concentrations beyond the IC_{50}. For example, the % surviving cells of FEK4 (Figure 2.40) is around 40% while it is 20% for HtTA-1 HeLa (Figure 2.41), when exposed at 40 μg/ml. This could be due to the higher

uptake rate of gene complex in HeLa cells,[163] thus the bioavailable doses of lipopolyamine are also higher in HtTA-1 cells than the ones in FEK4 cells.

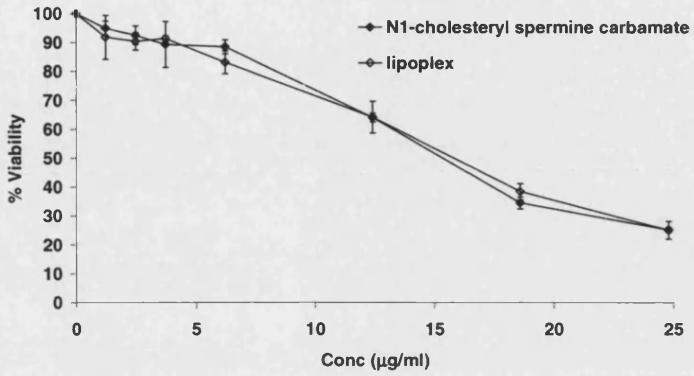

Figure 2.42 Viability of FEK4 cells when exposed to different concentrations of N^1-cholesteryl spermine carbamate and lipoplexes (N^1-cholesteryl spermine carbamate + pEGFP) in 96-well plates, using the MTT assay (n = 3, error bars are S.D.)

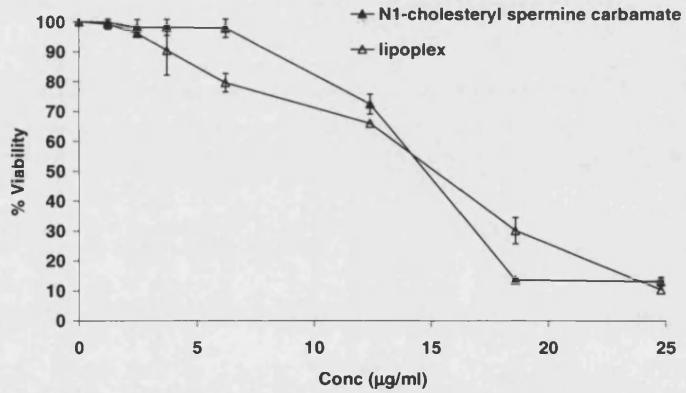

Figure 2.43 Viability of HtTA-1 HeLa cells when exposed to different concentrations of N^1-cholesteryl spermine carbamate and lipoplexes (N^1-cholesteryl spermine carbamate + pEGFP) in 96-well plates, using the MTT assay (n = 3, error bars are S.D.)

In Figures 2.42 and 2.43, IC_{50} values of N^1-cholesteryl spermine carbamate and the lipoplex in FEK4 and HtTA-1 HeLa cells were about 15 µg/ml. The results indicate that there is no significant difference in the toxic effect (IC_{50}) of the free lipopolyamine over the lipoplex in both cell lines. N^1-Cholesteryl spermine carbamate shows equally low toxicity in both FEK4 and HtTA-1 HeLa cell lines, and this lipopolyamine displays higher toxicity than N^4,N^9-dioleoylspermine.

Optimisation of transfection efficiency and toxicity

To optimise the concentration suitable for transfection, IC_{50} values were converted into their equivalent N/P ratios. Figures 2.44 and 2.45 show that the optimal N/P charge ratios for N^4,N^9-dioleoylspermine-mediated transfection are at 2.0-5.0. At this optimal N/P range, N^4,N^9-dioleoylspermine achieves high transfection both FEK4 and HtTA-1 HeLa cells with high survival rates in FEK4 (more than 80%). At higher N/P charge ratios, the lipoplex started to produce toxicity, while the transfection slightly increased.

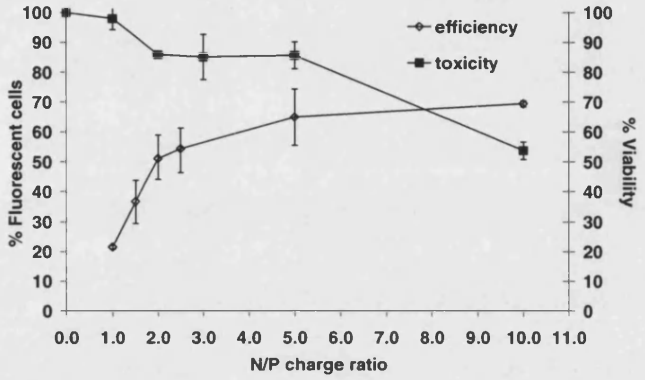

Figure 2.44 Survival of FEK4 cells transfected with pEGFP complexed with N^4,N^9-dioleoylspermine (n = 3, error bars are S.D.)

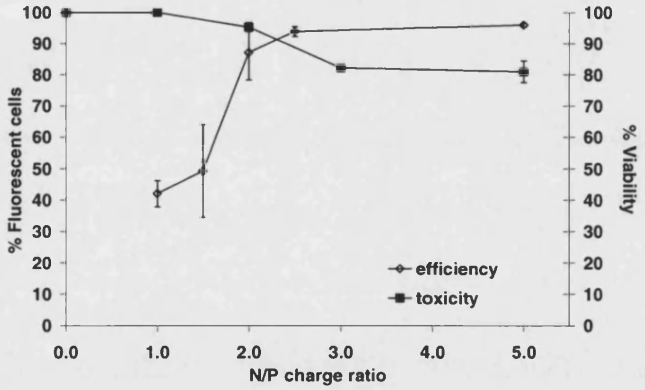

Figure 2.45 Survival of HtTA-1 HeLa cells transfected with pEGFP complexed with N^4,N^9-dioleoylspermine (n = 3, error bars are S.D.)

In Figure 2.46, the enhanced pEGFP delivery by N^1-cholesteryl spermine carbamate at N/P = 10-15 was compromised by its toxicity, for example at N/P 10.0 (60 % efficiency, 60% survival rate), or at N/P 15.0 (70% efficiency, 40% survival rate). A similar finding was found in HtTA-1 HeLa cells (Figure 2.47), high toxicity is coupled with high transfection. This toxicity at high N/P charge ratio may be from the high level of free polycation.[167] From

our results, the optimal transfection using N^1-cholesteryl spermine carbamate is concluded to be at N/P charge ratio 5.0 in both cell lines.

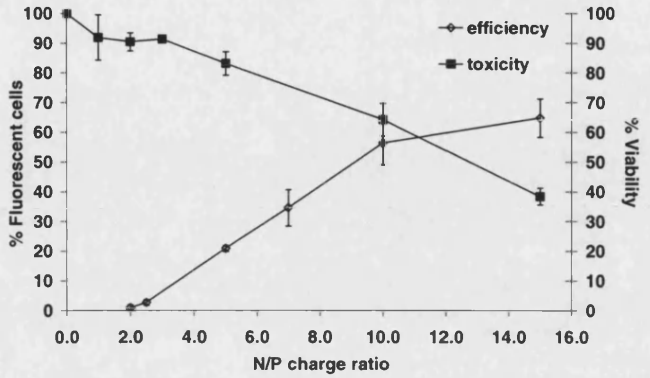

Figure 2.46 Survival of FEK4 cells transfected with pEGFP complexed with N^1-cholesteryl spermine carbamate (n = 3, error bars are S.D.)

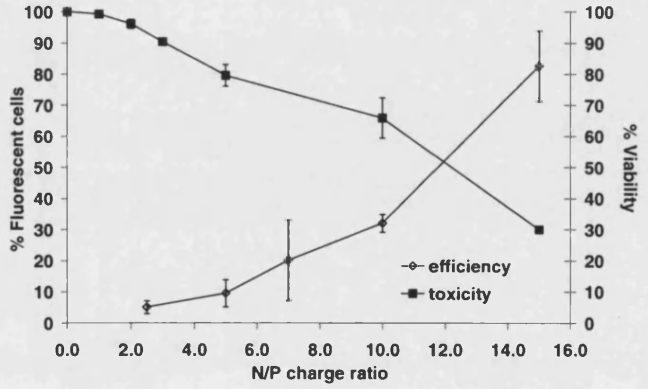

Figure 2.47 Survival of HtTA-1 HeLa cells transfected with pEGFP complexed with N^1-cholesteryl spermine carbamate (n = 3, error bars are S.D.)

In this Chapter, the synthesis of lipopolyamines using spermine conjugated with oleic acid and cholesterol has been discussed, i.e. N^4,N^9-dioleoylspermine and N^1-cholesteryl spermine carbamate. Both molecules are capable of condensing DNA efficiently and much more efficiently than free spermine. The transfection results obtained with our synthetic vectors are higher than those achieved with commercially available and widely used Lipofectin in both primary and carcinoma cells models, while the safety of our vectors has not been compromised at the concentrations used in gene delivery. To understand more about their mechanisms of action, studies on the first step in NVGT (DNA nanoparticle formation) by these vectors are discussed in Chapter 3.

Chapter 3

Fluorescence correlation spectroscopy studies of a single lipopolyamine-DNA nanoparticle

Introduction

DNA binding by lipopolyamines plays an important role in gene delivery success. DNA condensation affords nanoparticles with the appropriate size to enter cells, as well as giving protection from nuclease (DNase), and these are important properties when considering serum stability for *in vivo* applications. Disassociation of DNA from the vector at the right time is crucial, possibly after escaping from the endosome and just before reaching or right after entering the nucleus. However, the mechanism of association and dissociation between these lipopolyamines and DNA are still not well understood.[29,38,86,92]

Fluorescence Correlation Spectroscopy (FCS) is a new technique to study molecular interactions based on fluorescence, combining steady state fluorescence spectroscopy and confocal microscopy. In conventional fluorescence spectroscopy, a relatively large volume of sample is illuminated by an excitation laser. The average fluorescence intensity is recorded with high background noise, leading to limitation in resolution and sensitivity. With the confocal microscopy technology, it is possible to focus sharply a laser beam to excite a very small volume of sample (called the "confocal volume", Figure 3.1) of about 1 femtolitre. This volume is small enough to host only one molecule; hence, FCS is also regarded as a single molecule spectroscopy (SMS). This small volume also eliminates any interference from background signals. A single molecule diffuses through this illuminated volume over time, and give out photons which are recorded by the detection unit. Fluctuations in the detected fluorescence from small fluorescent molecules in this confocal volume are calculated by the autocorrelation function. This autocorrelation function allows faster and slower diffusing particles to be differentiated. This technique was used to study the dynamic processes, on the molecular scale, including DNA nanoparticle formation.[168-173]

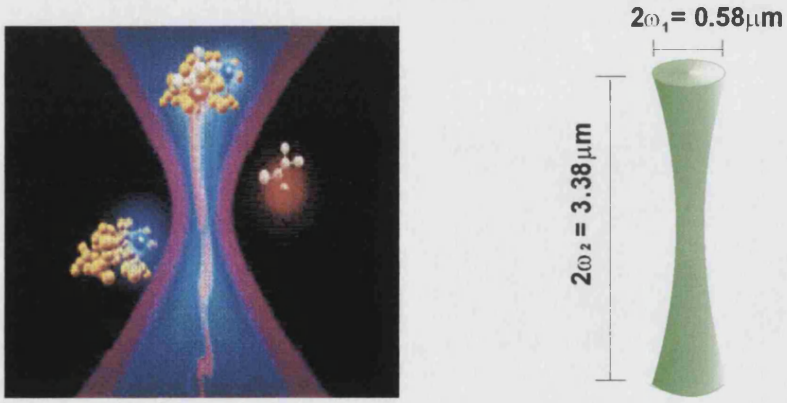

Figure 3.1 Illustration shows a confocal volume in FCS (typical volume is $1x10^{-15}$ litre), which is small enough to host only one molecule. The dimension of the volume element was determined by using standard fluorophores (Rhodamine-6G and Alexa Fluor 488).

Measurement of the confocal volume in FCS

In this experiment, two fluorescent molecules, Rhodamine-6G (R6G, λ_{ex} = 495 nm, λ_{em} = 519 nm) and Alexa Fluor-488 (AF488, λ_{ex} = 525 nm, λ_{em} = 555nm) (Figure 3.2) were chosen to measure the confocal volume in FCS. These fluorophores have high absorption coefficients (R6G = 116,000 $M^{-1}cm^{-1}$, A488 = 71,000 $M^{-1}cm^{-1}$), and less photobleaching which support their use as standard dyes.

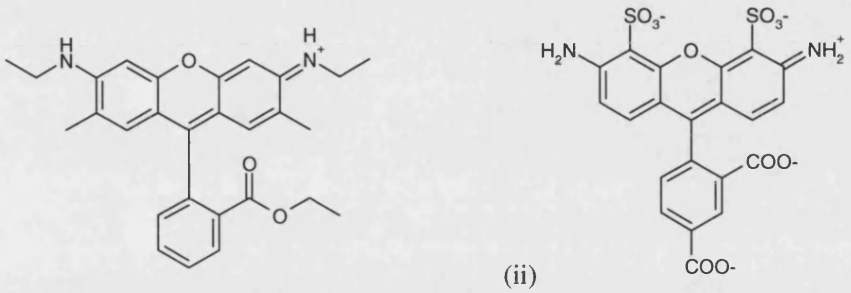

Figure 3.2 Standard fluorophores in FCS's confocal volume determination, (i) Rhodamine-6G and (ii) Alexa Fluor 488

The shape of the confocal volume for calculation purposes was assumed to be a cylinder, based on a special optical situation and this volume (V) is $V = \pi\omega_1^2(2\omega_2)$, given ω_1 and ω_2 are the lateral and axial radii of the detection volume. The fluorescence signal from R6G or AF488 in HEPES buffer was measured by FCS. Diffusion time (τ_D) was determined from the fluctuation caused by the diffusion of these dyes in and out of the confocal volume. From equation (1):-

$$\tau_D = \frac{\omega_1^2}{4D} \qquad (1)$$

Given the standard diffusion coefficient (D) of both dyes is 2.8 x 10^{-10} m^2/s, and. τ_D from experiments, the excitation volume was determined to be about 1 femtolitre (0.9 ± 0.1 femtolitre) regardless of the dye used. The dimensions of the confocal volume in our experiments are: ω_1 = 0.29 ± 0.05 μm, ω_2 = 1.69 ± 0.02 μm, as illustrated in Figure 3.1.

Efficient probe in DNA condensation by FCS

This DNA-intercalation with ethidium bromide (EthBr) study was firstly reported by Webb's research group,[174,175] using the FCS technique. The DNA-binding constant of EthBr and DNA diffusion coefficient using FCS were reported. Kral *et al.*[176,177] recently studied DNA condensation by using EthBr and propidium Iodide (PI) in FCS. The count rate (CR), diffusion time (τ_D), and particle number (PN) observed by FCS at the single molecule level,

and their correlations, can be used to differentiate the nature of DNA/oligonucleotide-polycation interactions.[176-180]

Though EthBr is a commonly used dye in DNA condensation studies, it was found to have effects on DNA structure at high concentration. The helical axis of DNA was dislocated +1.0 A°, and the helix was twisted by 10°, giving rise to an angular unwinding of -26°, and the intercalated base pairs are tilted relative to one another by 8°.[181] Manning's theory of counterion condensation of polyelectrolytes[78] suggested that EthBr intercalation lengthens the DNA by about 0.27 nm.[182] This possible DNA conformational alteration is generally not a concern in steady-state fluorescence spectroscopy with a larger population to be measured, but this is detectable with the high sensitivity of FCS. Additionally, the higher rate of EthBr release from DNA may also lead to a significant reduction in fluorescence, making fluorescence analysis more complex. This in turn leads to the search for new fluorescent dyes which can be used without significant change in DNA conformation, and also possess high absorption coefficients (which allows them to be used at low concentrations), to avoid interference in the DNA condensation behaviour mediated by NVGT vectors.

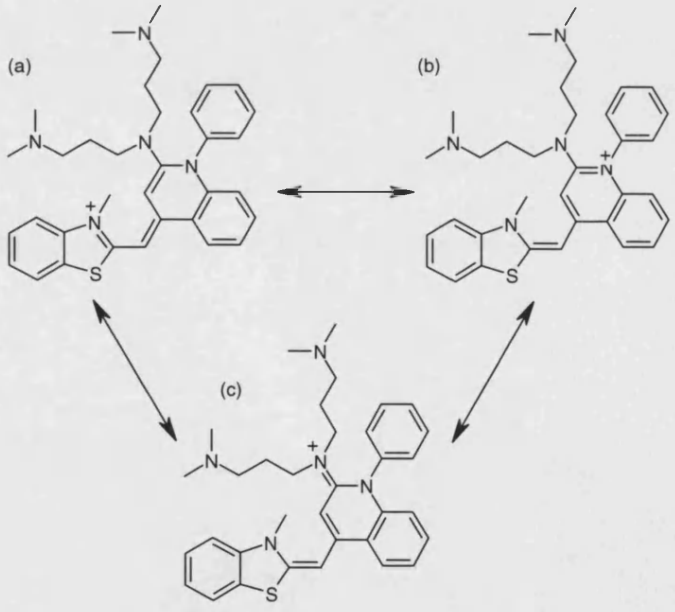

Figure 3.3 PicoGreen® (PG) - an unsymmetrical monomethine cyanine dye containing a polyamine side-chain to improve DNA-binding affinity with three mesomers (a, b, c)

Recently, a new unsymmetrical monomethine cyanine dye, PicoGreen® (PG) (Figure 3.3), was introduced as a patented fluorescent dye from Roth, Haughland and co-workers at

Molecular Probes.[183,184] Its chemical structure was recently reported by Vitzthum and co-workers, confirmed by NMR and MS techniques and named as [2-[*N*-bis-(3-dimethyl-aminopropyl)-amino]-4-[2,3-dihydro-3-methyl-(benzo-1,3-thiazol-2-yl)-methylidene]-1-phenyl-quinolinium]$^+$ (Figure 3.3-a).[185] However, this name could better be (*Chem. Abs.* 9th CI): 2-[bis(3-dimethylaminopropyl)amino]-4-(3-methyl-2(3H)-benzothiazolylidene)methyl-1-phenyl-quinolinium[186] [178918-98-4] and/or 2-[bis-(3-dimethylaminopropyl)amino]-1-phenyl-4(1H)-quinolinylidene)methyl)-3-methyl-benzothiazolium[187] [771577-99-2]. The charge due to quaternization of the aromatic *N*-atoms is delocalized, probably equally well shown residing on the *N*-methyl-benzothiazolium (Figure 3.3a)[187] and on the *N*-phenyl-quinolinium (Figure 3.3b),[186] in a solvent and environment dependent manner. There is also a contribution from the third mesomer, including the lone-pair electrons on the anilino-tertiary amine, as its ammonium ion (Figure 3.3c).[188]

From DNA-intercalation structure-activity relationship considerations, PG carries three positive charges i.e. one on nitrogen in the conjugated, mesomeric heteroaromatic system and two at the 3-dimethylaminopropyl residues. The cationic side chain of PG (compared to EthBr) contributes to higher affinity for dsDNA. Biphasic mode binding was reported for PG interaction with dsDNA. Base-pair intercalation happens at low dye/base-pair ratio, and external binding (minor groove) was found at higher dye/base-pair ratio. At low dye/base-pair ratio, PG shows no base sequence specificity. Zipper *et al.*[185] recently reported that there is no difference in binding on polydA.dT and polydG.dC, using differential absorption spectroscopy at 494 nm, if PG labelling ratio smaller than 100 dye/kbp was used. However, the fluorescence intensities of PG/DNA complexes were related to the DNA sequence at higher ratios.[185] The increase in fluorescence intensity of PG upon binding to DNA is about 1000-fold (absorption coefficient 70,000 $M^{-1}cm^{-1}$) and this makes the background fluorescence from free dye negligible. A small red-shift of the peak absorption (from 498 nm for free dye to 500 nm for the bound dye) was observed for PG.[189] Interestingly, PG binds selectively to ssDNA (low affinity) and dsDNA (high affinity) at 525 nm, unlike EthBr at 610 nm. Thus, the use of PG with EthBr simultaneously at dual wavelength (525 and 610 nm) was recently established as a novel efficient tool to determine the DNA unwinding condition (ss:dsDNA ratio).[190,191] The low affinity of PG for ssDNA helps to ensure that the fluorescence detection mainly arises from dsDNA-PG interactions.

Calf thymus DNA–PicoGreen interaction study

CT-DNA is a linear DNA which minimum kbp = 13 (MW 8,580 MDa). As calculated from: $L = N_{DNA} \times a$, given N_{DNA} is the average number of DNA monomer (base pairs), and a = monomer length (i.e. 0.34 nm for DNA duplex), its contour length is 4.4 μm. PG was used

in our study to monitor CT-DNA. PG intercalation affinity to dsDNA is higher, and it also has a higher absorption coefficient than EthBr. Fluorescence of free PG is low, thus background fluorescence is negligible. In our experiments, fluorescence fluctuation was observed and recorded over the increase of PG concentration (i.e. labelling ratio). Experimental G(τ) functions were satisfactorily fitted to a theoretical diffusion model with a single fluorescent type.

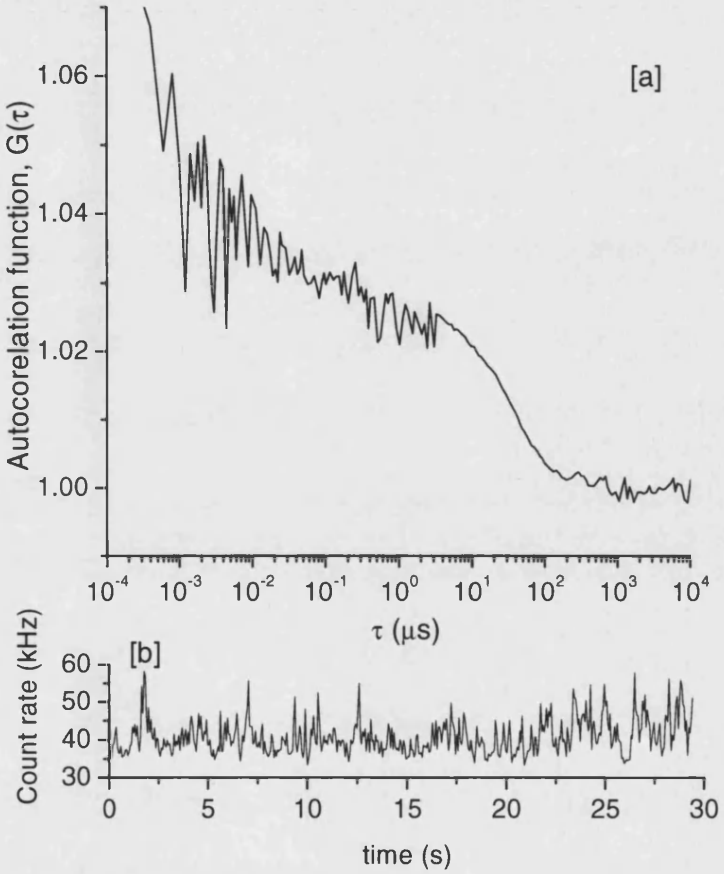

Figure 3.4 Examples of normalized autocorrelation functions, G(τ) [a] and the relative count rates [b] for CT-DNA 1 nM (200 μl) intercalated with PG ($1.1x10^{-6}$ M) 30 μl and $C_{dye}/_{kbp}$ is 13. The nature of multi-labelling DNA (long-chain molecules) causes an overestimation of PN (apparent PN), compared to the PN of singly-labelled small molecules

Typical normalized autocorrelation functions G(τ), are plotted as shown in Figure 3.4. Additionally, the segmental motion of DNA lead to partial detection in the confocal volume, the loop-like structure of DNA chain (not as a stretched chain) would increase the important parameter, Particle Number (PN). PN is defined as the average number of the fluorescent particles in the confocal volume. Thus, more fluorescent events, which increase apparent PN,

would be detected in longer DNA. Consequently, $G(\tau)$ of CT-DNA was determined to be different resulting from the different apparent concentration of DNA, though the real concentration for CT-DNA is 1 nM.

The objective of PG calibration assay is to explore the useful range of DNA labelling ratio by PG. The ideal ratio should give sufficient fluorescence signal with less interference in DNA conformation from intercalating dyes. PG, when intercalating into dsDNA, give fluorescence fluctuation signals directly recorded as "count rate" (CR). From Figure 3.5(i), CR increases in linear relationship with the amount of PG added i.e. dye/kbp ratio at 5-40. More tolerance to the higher labelling ratio is a general trend for mono-intercalating dyes. Therefore, the sensitivity of the nucleic acid labelling dye to the ratio may be primarily dependent on the dissociation constant of its secondary binding mode. The higher the dye dissociation of second binding mode, the greater the useful range of labelling ratio (compared to TOTO-1).[189]

Another two parameters in FCS, diffusion time (τ_D) (Figure 3.5 (ii)) and PN, (Figure 3.5 (iii)) remain constant as initial values at the start of experiments based on the mono-component diffusion model. This suggests that PG has no influence over the hydrodynamic properties of DNA molecules. PG can be used at a very low level (i.e. 5-40 dye molecules/kbp), compared to a similar study using EthBr.[176,177,179] The stability of PG labelled DNA samples is also high, which means that the dilution of sample does not affect the accuracy of the measurement.[189] The stability of the dye-DNA complexes after dilution is also important for a titration study of DNA condensation, which involves the dilution of the sample (i.e. volume addition of DNA condensing agent).

The diffusion coefficients of (PG-labelled) CT-DNA was calculated by considering DNA as a rod-like molecule.[176,177,179] Considering the characteristics of DNA, CT-DNA has a high τ_D which is due to its significantly greater size than circular plasmids; different length DNAs diffuse differently in solution. The previous fluorescence-recovery after photobleaching study (FRAP) using FITC-labelled DNA revealed that D_w (diffusion coefficient in water) was dependent on DNA size, $D_w = 4.9 \times 10^{-10}$ m^2/s x [bp size]$^{-0.72}$ (for 21-6000 bp linear dsDNA). DNA diffusion coefficient decreased by increasing DNA size indicating the complex hydrodynamic properties of DNA with respect to translational diffusion.[192] Similarly, Rigler and co-workers[193] reported that the relative translational diffusion coefficient decreased linearly with the length of double-stranded DNA fragments (at least up to 500 bp) by using fluorescence correlation spectroscopy technique in the study of DNA products formed during PCR. D_w of CT-DNA from calculation (5.3×10^{-13} m^2/s) is similar to

the result as found in FCS experiments ($7x10^{-13}$ m^2/s). Deviation of τ_D found in our FCS experiments and from calculation in CT-DNA may be related to the polydispersity of CT-DNA, which means that different lengths of linear DNA were measured together. However, as the DNA condensation process is regarded as an all-or-none process, it is possible to monitor the nanoparticle formation using CT-DNA.[146,147]

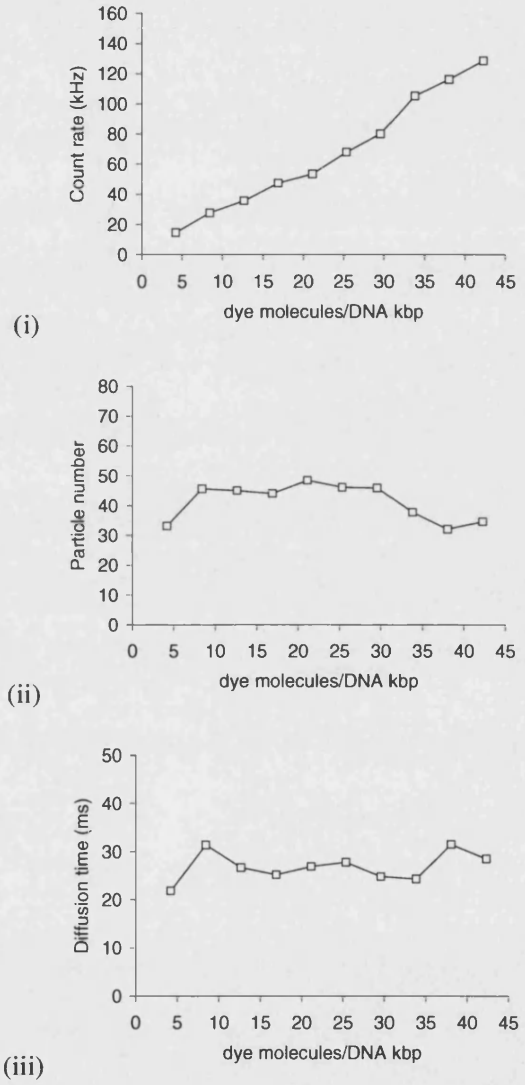

Figure 3.5 PG labelling calibration using CT-DNA. Different volumes of PG (1.1 μM) were added into 200 μl of 1 nM DNA and incubated for 10 min. $G(\tau)$ was recorded at each dye labelling ratio. FCS parameters were calculated and plotted against dye concentration i.e. (i) count rate (CR), (ii) particle number (PN), and (iii) diffusion time (τ_D).

In Figure 3.5, CR increased linearly with dye concentration showing the high efficiency of PG fluorescence on DNA binding, with little effect on DNA hydrodynamic changes from the dye itself. The useful concentration range of PG from the data shown lies within dye molecules/kbp = 5-40.

FCS enables the direct measuring of the average number of fluorescent molecules, the Particle Number (PN), diffusing through the volume element. PN was interpreted from the autocorrelation curve, described as $G(0) = 1+(1/N)$. From Figure 3.5(i), PN calculated from $G(\tau)$ of PG molecules bound to CT-DNA was at 43.1 ± 8.1. This may be explained from the length of DNA, as CT-DNA (contour length = 4.4 μm) is considerably bigger than the confocal element (ω_1 = 0.58 μm, ω_2 = 3.38 μm). In a recent paper,[194] it is proposed that long DNA may have internal conformation diffusion of its chain (segmental motion). This leads to a high number of fluctuations in the fluorescence intensity, i.e. lower $G(\tau)$, especially when considering that the laser focus could excite at least one part of the entire chain, and thus finally leading to a higher PN.

CT-DNA condensation by lipopolyamines

Two lipopolyamines were synthesized and used in these experiments. Both are designed to incorporate a spermine backbone conjugated with a lipophilic moiety i.e. the oleoyl group (amide link) (Figure 3.6(i))[195] and the cholesteryl group (carbamate link) (Figure 3.6(ii)).[69] Both our novel DNA vectors show effective condensation (i.e. yielding 90% fluorescence reduction in the EthBr fluorometric assay at N/P charge ratios as low as 1.5-2.0) and high transfection efficiency.

(i)

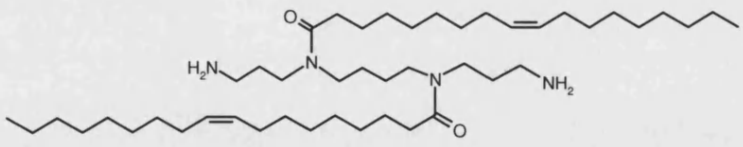

(ii)

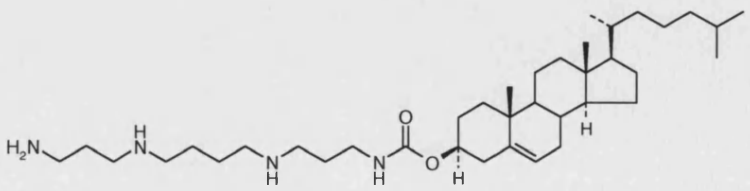

Figure 3.6 (i) N^4,N^9-Dioleoylspermine, (ii) N^1-cholesteryl spermine carbamate

The aim of this study is to understand more of the mechanisms that by which these two vectors interact with DNA, as a single molecule (in this case, specifically regarded as a single nanoparticle) by FCS using PG.

From the calibration curve (Figure 3.5 (i)), optimal dye ratio used for CT-DNA labelling was in the range of 5-40. PG was prepared in 1:200 dilution (according to the manufacturer's protocol), using too much dye would alter the total volume of sample solution. In the DNA condensation experiment, the PG volume added was 30 µl (which is equivalent to dye/kbp ratio = 13). Fluorescence fluctuation was monitored while adding N^4,N^9-dioleoylspermine and N^1-cholesteryl spermine carbamate in solution to a sample containing PG-labelled DNA.

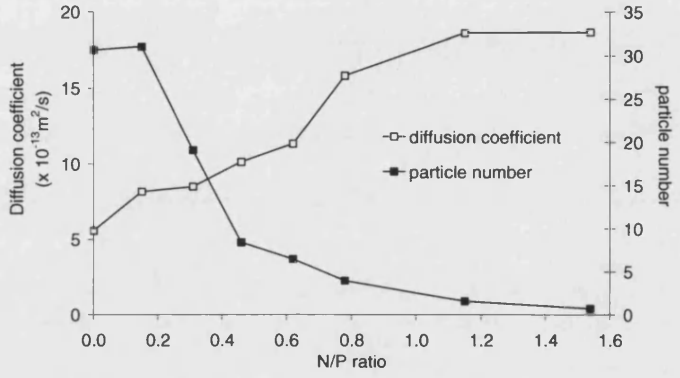

(i)

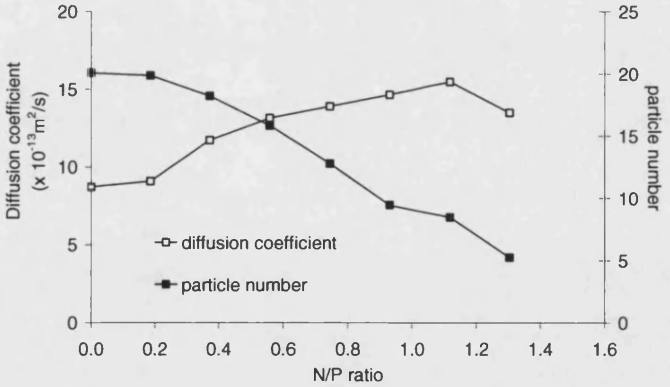

(ii)

Figure 3.7 FCS study of DNA nanoparticle formation: CT-DNA (1 nM, 200 µl) was condensed with lipopolyamines, using PG as a reporter probe.
(i) CT-DNA condensation by N^4,N^9-dioleoylspermine (PG at dye/kbp = 13)
(ii) CT-DNA condensation by N^1-cholesteryl spermine carbamate (PG at dye/kbp = 13)

When the N/P ratio was increased (Figure 3.7), DNA phosphate groups were gradually neutralized by positively charged ammonium groups of N^4,N^9-dioleoylspermine and N^1-cholesteryl spermine carbamate. G(τ) was recorded and FCS parameters (diffusion coefficient and PN) were then calculated throughout the DNA condensation process. The indication for DNA condensation occurrence is the dramatic decrease of τ_D and PN particularly for a system with macromolecules where a single monitored molecule is not small enough to fit in the confocal volume. From Figure 3.7, the diffusion coefficient (D) increased upon the addition of lipopolyamines in both DNA condensation experiments. As faster movement of DNA resulted from condensation, we conclude that smaller (compacted) DNA nanoparticles have been formed. PN also decreased (Figure 3.7) while measured CR remained constant.

Point-like molecule detection in CT-DNA condensation

PN is a direct parameter to prove the number of fluorescent molecules, which here reports on the DNA concentration. In the model with point-like molecules, PN is described by the equation PN = C x V x N_A, where C = molarity of detected molecules (DNA 1 nM), V = confocal volume (1 femtolitre), and $N_A = 6.023 \times 10^{23}$. By using this equation, and as the DNA concentrations used in our experiments were kept constant at 1 nM, the theoretical PN to be achieved is around 0.6. The PN achieved at N/P = 1.0-1.5 for CT-DNA condensed by N^4,N^9-dioleoylspermine, was 0.7. This evidence confirms that DNA was condensed into a point-like molecule by the C18-substituted lipopolyamine, which fulfils the assumptions of FCS and validates the use of FCS as a sensitive method in DNA formulation studies (which is indeed a point-like molecule, when compared to the typical confocal volume). This result is in agreement with other physical studies on DNA particle size, when completely condensed at the nanoscale level. Similar results were also found for DNA condensation with N^1-cholesteryl spermine carbamate, decrease in τ_D and PN. The PN value 5.2 was achieved at N/P = 1.5-2.5 for CT-DNA condensed by N^1-cholesteryl spermine carbamate. From a comparison of these PN results with those obtained with N^4,N^9-dioleoylspermine, we conclude that N^1-cholesteryl spermine carbamate is a poorer DNA condensing agent than N^4,N^9-dioleoylspermine. Additionally, condensation occurred at higher N/P ratios (N/P = 1.5-2.5) than condensation achieved with N^4,N^9-dioleoylspermine (N/P = 1.0-1.5). Considering the positive-charge number of N^4,N^9-dioleoylspermine is less than that of N^1-cholesteryl spermine carbamate (i.e. 2.0 compared to 2.4), we conclude that more efficient DNA condensation is possibly due to the respective regiochemical distribution of these two positive charges together with their lipid moieties (C18 vs cholesterol).

Point-like molecules obtained from CT DNA condensation by N^4,N^9-dioleoylspermine have an average τ_D of 12.0 ms (D = 1.8 x 10^{-12} m^2/s). These nanoparticles diffuse about 3-times faster than free DNA (D = 0.71 x 10^{-12} m^2/s). Similar diffusion behaviour of CT-DNA complexed with N^1-cholesteryl spermine carbamate was also found at 14.0 ms (D = 1.3 x 10^{-12} m^2/s), though the PN has not fulfilled the point-like molecules hypothesis (i.e. not approximating to 0.6). Considering the change in the magnitude of diffusion coefficient (D) between free and condensed DNA, mediated by both our two lipopolyamines and at appropriate N/P ratios to achieve full DNA condensation, provides evidence for the dramatic change that is DNA condensation. Moreover, D is, in general for point-like molecules, a rather insensitive parameter and could incorporate some error (about 10%). On the other hand, PN is much more sensitive, and it accurately shows differences between both condensing agents. Thus, N^4,N^9-dioleoylspermine is a more efficient DNA condensing agent (PN approaching 0.6) than N^1-cholesteryl spermine carbamate.

In the steady state EthBr fluorescence quenching study, it was shown that there is no significant difference found in the condensation of CT-DNA and plasmids. However FCS is a single molecule technique with high sensitivity, it is possible to observe the difference of linear (and big) DNA behaviour and plasmid DNA in a 1 femtolitre confocal volume. We have therefore also studied plasmid DNA nanoparticle formation by FCS/PicoGreen which is discussed in the following section of this Chapter.

Plasmid DNA-PicoGreen labelling study

pGL3 and pEGFP are two circular plasmids used in FCS experiments, which have similar size and contour length. It was expected that the smaller size of both plasmids (compared to CT-DNA) would result in higher diffusion coefficients and lower particle number (PN), when they are detected using FCS and PG.

Table 3.1 Plasmids used in these studies

	pGL3	*pEGFP*
Primary structure	Circular plasmid	
Number of base pairs (kbp)	5.3	4.7
Mean molecular weight (MDa) [a]	3.4	3.0
Contour length (μm) [b]	0.9	0.8

[a] calculated from 330 Da average per nucleotide.[21]

[b] obtained by calculation: $L=N_{DNA} \times a$, given N_{DNA} is the average number of DNA monomer (base pair), and a = monomer length (i.e. 0.34 nm for DNA duplex). Contour length of circular plasmid is calculated by using the half of total DNA length of DNA (kbp).

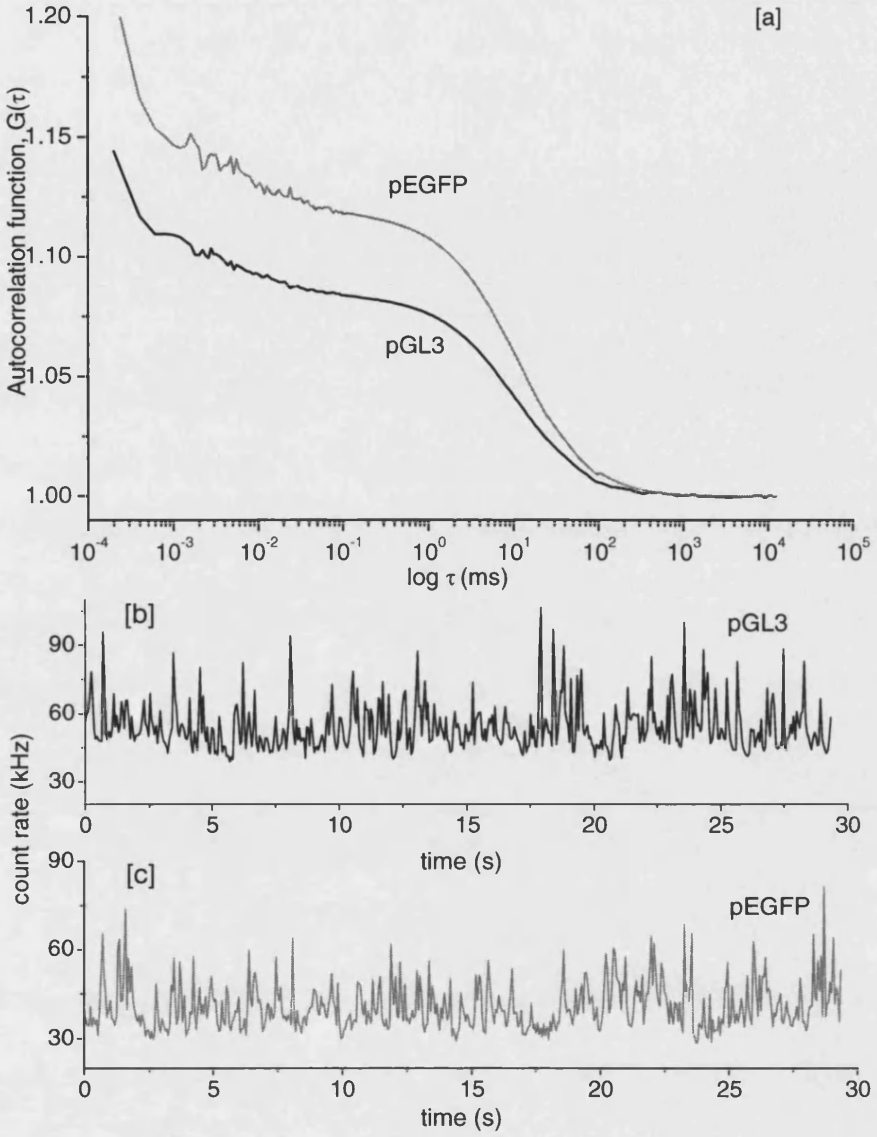

Figure 3.8 Examples of normalized autocorrelation functions, G(τ) [a] and the count rates tracking [b, c] for pGL3 (black line) and pEGFP (grey line) 1 nM (200 µl) intercalated with PG (1.1 µM) 18 µl and pEGFP 1 nM (200 µl) intercalated with PG (1.1 µM) 18 µl $C_{dye}/_{kbp}$ are 18 and 21 respectively.

pGL3 and pEGFP was prepared in HEPES buffer (20 mM NaCl, pH 7.4) in 1 nM concentration and used at 200 µl. Increasing amounts of PG (as a 1.1 µM solution) were added into both plasmids to perform the measurements simulating the different states of PG binding. Experimental G(τ) functions were satisfactorily fitted to a theoretical diffusion model with two-population fluorescent type, which a major population (more than 95%) of

slow diffusion species (D = 10 ms). The other minor component is the fast moving component (D = 0.01 ms). Typical normalized autocorrelation functions G(τ) are plotted in Figure 3.8. The nature of multi-labelling on plasmid DNAs causes an overestimation of PN (apparent PN), similar to that obtained in the experiments with CT-DNA.

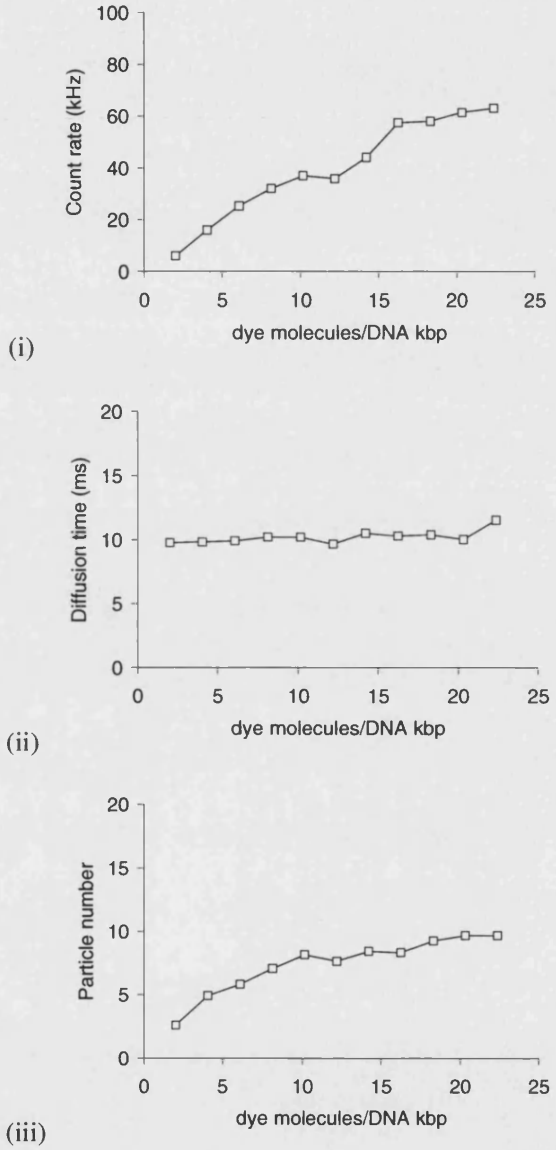

Figure 3.9 PG labelling calibration using pGL3 (□) plasmid. Different volumes of PG (1.1 μM) were added into 1 nM DNA (200 μl) and incubated for 10 min. G(τ) was recorded at each ($C_{dye}/_{kbp}$) ratio. FCS parameters were calculated and plotted against dye concentration i.e. (i) count rate (CR), (ii) diffusion time (τ_D), and (iii) particle number (PN).

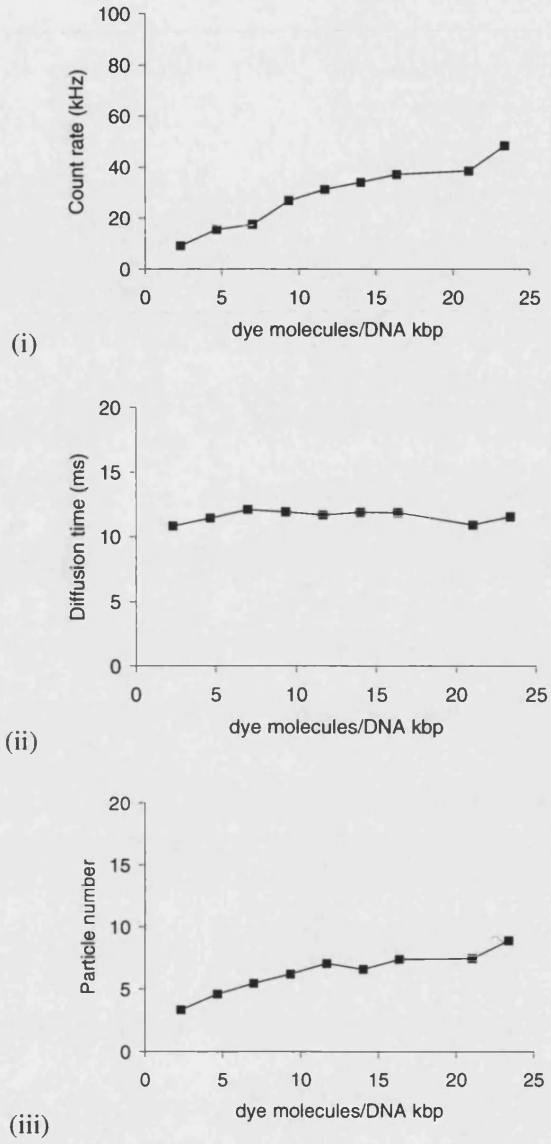

Figure 3.10 PG labelling calibration using pEGFP (■) plasmid. Different volumes of PG (1.1 μM) were added into 1 nM DNA (200 μl) and incubated for 10 min. G(τ) was recorded at each ($C_{dye}/_{kbp}$) ratio. FCS parameters were calculated and plotted against dye concentration i.e. (i) count rate (CR), (ii) diffusion time (τ_D), and (iii) particle number (PN).

From the titration curve of pGL3 (Figure 3.9 (i)) and pEGFP (Figure 3.10 (i)), the useful range of DNA labelling ratio by PG was determined from dye molecule/kbp ratio at 10-25. From Figure 3.9(i) and 3.10(i), CR increases in linear relationship with the amount of PG added i.e. dye/kbp ratio at 10-25. At this range, there is also less interference in DNA conformation. Diffusion times (τ_D) (Figures 3.9 (ii) and 3.10 (ii)) remain essentially constant as initial values at the start of experiments based on the two-component diffusion model.

Particle numbers (PN) (Figures 3.9 (iii) and 3.10 (iii)) increased at the first stage of PG-labelling, and then reached it plateau. The hydrodynamic properties of DNA molecules were not disturbed by the PG labelling. Additionally, PG can be used at a very low level (i.e. 10-25 dye molecules/kbp), compared to the similar study using EthBr which is typically used in an excess concentration (to the number of DNA base-pair equivalents).[176,177,179]

Diffusion behaviour of PG-labelled plasmid DNA

The diffusion coefficients (Figure 3.9 (ii) and 3.10 (ii)) of both pGL3 and pEGFP were calculated by considering DNA as a rod-like molecule.[176,177,179] It was observed that both DNAs diffused at mean diffusion coefficient 1.95×10^{-12} and 2.05×10^{-12} respectively. The circular plasmid shape plays a role to increase diffusion coefficient comparing to previous experiments using linear CT-DNA (7×10^{-13} m^2/s), which is 3-times faster. This diffusion information could further extend to DNA behaviour in cytoplasm and ultimately in the nucleus when dissociated from its lipopolyamine vector.[196] It is also important in NVGT vector design to achieve complexes which diffuse at a favourable rate, aiming to promote mobility and localization to target organelles.

From Figures 3.9 (iii) and 3.10 (iii), PN calculated from $G(\tau)$ of PG molecules bound to pGL3 was similar to that of pEGFP (i.e. 8.7 ± 0.8 and 7.0 ± 1.1 respectively). Considering the confocal element ($\omega_1 = 0.29 \pm 0.01$ μm, $\omega_2 = 1.69 \pm 0.02$ μm), both pGL3 and pEGFP are relatively too big to fit this volume (contour length = 0.9 and 0.8 μm respectively). Both plasmids still fluctuate across the focal volume, thus the effect of multiplied PN was observed.

pGL3 and pEGFP condensation by lipopolyamines

From the calibration curves (Figures 3.9 (i) and 3.10(i)), optimal dye molecule/kbp ratio used for DNA labelling was in the range of 10-25. PG was prepared in 1:200 dilution (according to the manufacturer's protocol), using too much dye would alter the total volume of the sample solution. In the DNA condensation experiment, the PG dilution volume added was kept identical for both pGL3 and pEGFP, at 18 μl (which is equivalent to dye/kbp ratios = 18 and 21 respectively). Two synthetic lipopolyamines were studied in our DNA experiments. The previous EthBr assay (Figure 3.11) shows highly efficient DNA condensation (i.e. much more efficient than spermine) with only 10% residual fluorescence, evidence that DNA is in the condensed state. Fluorescence fluctuation was monitored while adding N^4,N^9-dioleoylspermine and N^1-cholesteryl spermine carbamate in a solution sample containing PG-labelled DNA.

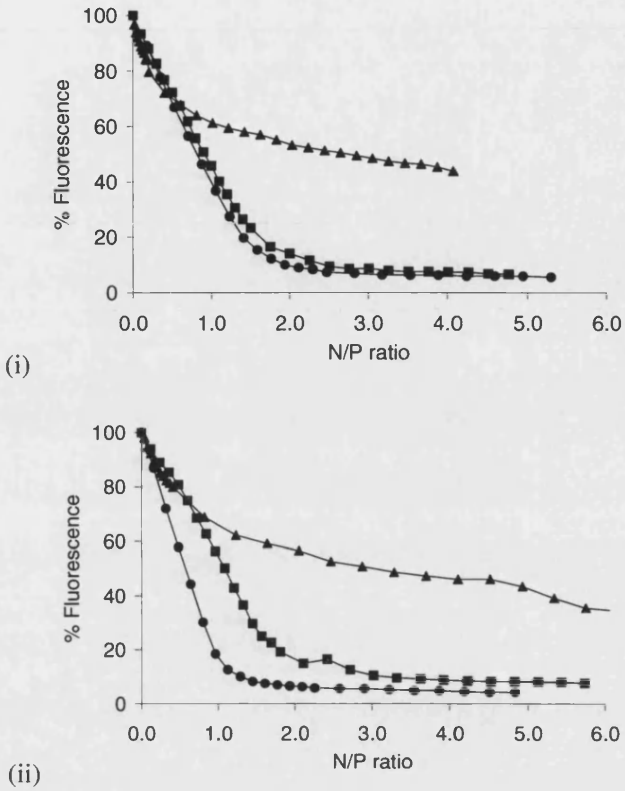

Figure 3.11 DNA condensation study of N^4,N^9-dioleoylspermine (●), N^1-cholesteryl spermine carbamate (■) and spermine (▲) using pGL3 (5.3 kbp, (i)) and pEGFP (4.7 kbp, (ii)) using EthBr displacement assays. EthBr assay shows a decrease of fluorescence intensity (λ_{ex} = 260 nm, and λ_{em} = 600 nm) DNA condensing agent concentration expressed in ammonium/DNA phosphate (N/P) ratios were increased. Both lipopolyamines condense DNA efficiently with 10% residual fluorescence at N/P ratios around 1.5-2.5.

DNA phosphate groups of pGL3 (Figure 3.12) and pEGFP (Figure 3.13) were gradually neutralized by positively charged ammonium groups of N^4,N^9-dioleoylspermine and N^1-cholesteryl spermine carbamate, when the N/P ratio was increased. Throughout the DNA condensation process, G(τ) was recorded and FCS parameters (diffusion coefficient and PN) were then calculated. The indication for DNA condensation occurrence is the dramatic decrease of τ_D and PN particularly for a system with macromolecules where a single monitored molecule is not small enough to fit in the confocal volume. From Figures 3.12 and 13, the diffusion coefficient (D) continuously increased upon the addition of lipopolyamines in both DNA condensation experiments. As faster movement of DNA resulted from condensation, we conclude that smaller (compacted) DNA nanoparticles have been formed. PN also decreased while measured CR remains constant. The CR range was

maintained in the range at 40 - 60 kHz during the DNA condensation, which is a positive indication that PG exhibits high affinity to DNA and was not released from binding to the polynucleotide chain. This lack of PG release confirms that DNA hydrodynamic change is the major contribution to any changes in fluorescence signal found during DNA condensation under the experimental conditions described above.

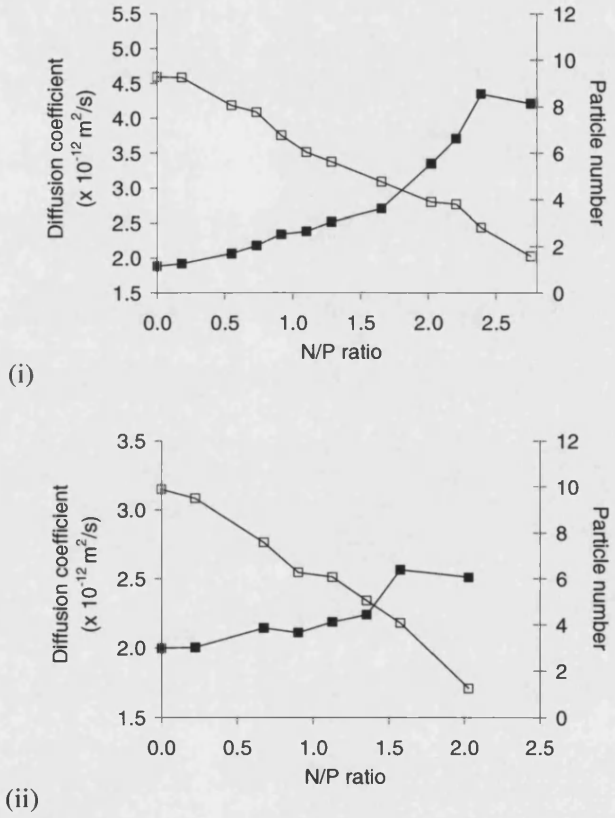

Figure 3.12 FCS study of DNA nanoparticle formation: pGL3 (1 nM, 200 µl) were condensed with lipopolyamines, using PG as a reporter probe. Particle number (□) and diffusion coefficient (■) were measured during the following condensation studies:
(i) pGL3 condensation by N^4,N^9-dioleoylspermine (PG at dye/kbp = 18)
(ii) pGL3 condensation by N^1-cholesteryl spermine carbamate (PG at dye/kbp = 18)

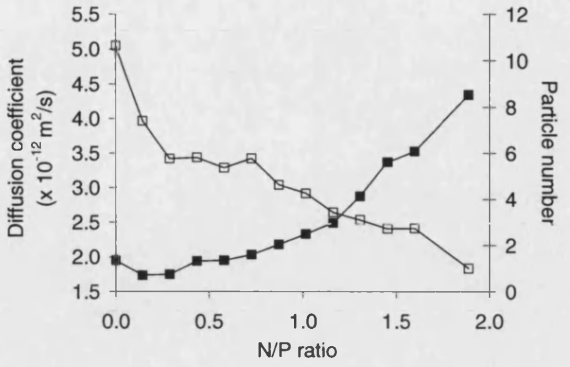

(i)

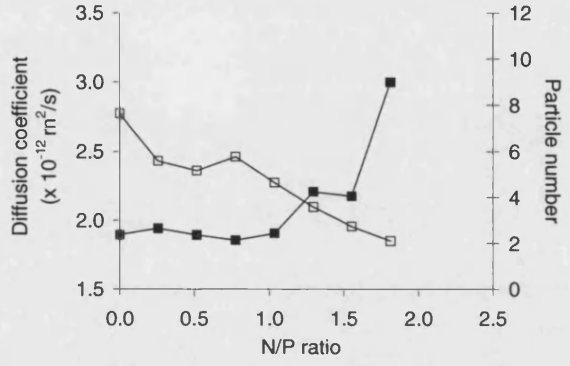

(ii)

Figure 3.13 FCS study of DNA nanoparticle formation: pEGFP (1 nM, 200 µl) were condensed with lipopolyamines, using PG as a reporter probe. Particle number (□) and diffusion coefficient (■) were measured during the following condensation studies:
(ii) pEGFP condensation by N^4,N^9-dioleoylspermine (PG at dye/kbp = 21)
(iv) pEGFP condensation by N^1-cholesteryl spermine carbamate (PG at dye/kbp = 21)

In these studies aiming for point-like molecules, PN is described by PN = C x V x N_A, where C = molarity of detected molecules, V = confocal volume, and $N_A = 6.023 \times 10^{23}$. By using this equation, and as the DNA concentrations used in our experiments were kept constant at 1 nM, the theoretical PN to be achieved is around 0.6. The PN achieved at N/P = 2.0-2.5 for pEGFP, condensed by N^4,N^9-dioleoylspermine was 0.9. From these experimental data, the PN error was calculated as 0.3. Thus the achieved PN = 0.9 is within the experimental error in PN determination.This evidence suggests that pEGFP was condensed into a point-like molecule by the C18-substituted lipopolyamine, which fulfils the assumptions of FCS and validates the use of FCS as a sensitive method in DNA formulation studies (which is indeed a point-like molecule, when compared to the typical confocal volume) (Figure 3.14). As expected, DNA condensation with N^1-cholesteryl spermine carbamate, there was a decrease in τ_D and PN, but the PN values achieved at N/P = 2.0-2.5 for pGL3 and pEGFP, condensed

by N^1-cholesteryl spermine carbamate, were 2.6 and 2.1 respectively. Therefore, N^1-cholesteryl spermine carbamate is a poorer DNA condensing agent than N^4,N^9-dioleoylspermine.

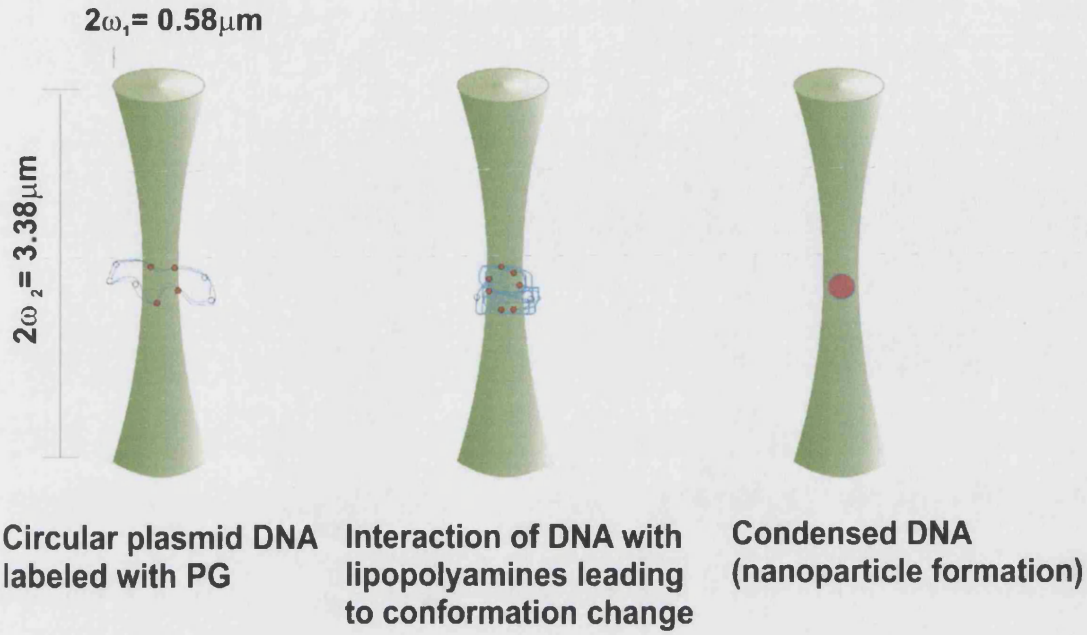

Figure 3.14 Illustration of DNA molecules in the FCS confocal excitation volume (V, green cylindrical volume); V is an approximate cylinder of 1 fl.

Left: a free (no lipopolyamine) plasmid molecule (ribbon) labelled by intercalated PG (both open- and red-circles), but only a fraction of fluorophores (red-circles) lie within the confocal volume, and are therefore excited. PN was found to be higher than real concentration of DNA due to this fluorescence fluctuation.

Middle: Phosphate groups of DNA molecule interacts with lipopolyamines, which alters DNA conformation. Smaller apparent PN was observed, due to smaller size of DNA and higher number of intercalated PG in excitation volume (red-circles).

Right: a lipopolyamine-condensed DNA where all the PG reporter molecules now lie within the confocal volume, and all are therefore excited; this nanometer-sized complex acts as a point-like molecule (a single nanoparticle)

Point-like molecules obtained from pEGFP condensation by N^4,N^9-dioleoylspermine have an average τ_D of 4.7 ms ($D = 4.30 \times 10^{-12}$ m^2/s). These nanoparticles diffuse about 2 times faster than free DNA ($D = 1.95 \times 10^{-12}$ m^2/s). pGL3 condensed by N^4,N^9-dioleoyl-spermine also had a similar average τ_D of 5.8 ms ($D = 4.2 \times 10^{-12}$ m^2/s) at the size of 2 times faster than free pGL3 ($D = 2.05 \times 10^{-12}$ m^2/s). Similar diffusion behaviour of pGL3 and pEGFP complexed with N^1-cholesteryl spermine carbamate was also found at 7.2 ms ($D = 2.9 \times 10^{-12}$

m^2/s) and 7.1 ms ($D = 3.0 \times 10^{-12}$ m^2/s), though the PN has not fulfilled the point-like molecules hypothesis. D values usually have 10% error, PN values are one way to show differences between DNA condensing agents. Thus, N^4,N^9-dioleoylspermine (PN approaching 0.6) is a more efficient DNA condensing agent than N^1-cholesteryl spermine carbamate.

Behaviour of PG during DNA condensation

PicoGreen has been primarily used for DNA quantification with high sensitivity (25 pg/ml dsDNA).[184] It labels nucleic acids uniformly and without any concentration-dependence or artefacts.[189,197] Rapid binding of PG to DNA was also studied by flow cytometry. High-quality burst size distribution histograms of DNA samples were obtained immediately after sample staining, dilution, or mixing. The measured association rates of PicoGreen intercalating into dsDNA were on the order of 10^8 M^{-1} s^{-1}, suggesting a diffusion-controlled process. Re-equilibration can be reached in seconds upon staining, dilution, or mixing, from model simulation. These favourable kinetics also make PG one of the most efficient and versatile DNA probes.[198]

Phenanthridinium dyes, e.g. EthBr, showed monoexponential decays with ssDNA and dsDNA, and with no discrimination between them.[199] Binding of PG to dsDNA preferentially occurs by intercalation between alternating GC base pairs, which was characterized by a monoexponential fluorescence decay rate constant of (0.23 +/- 0.02) ns^{-1}. It was found that binding to the exterior of DNA (the second binding mode of PG) may also efficiently compete with intercalation. Dye molecules in other configurations exhibit fluorescence decay rate constants of about 0.5-0.8 ns^{-1}, and are observed at dye:base-pair ratios larger than 0.30 in CT-DNA. Fluorescence decay is multi-exponential in all types of ssDNA and the dominant mode is intercalation between two different bases (G, T).[191]

In NVGT research, PG was recently used to determine the quantity of free DNA (uncomplexed DNA) to assess the DNA condensation property of gene vectors, e.g. polyamidoamine dendrimer,[200] amine-functionalized carbon nanotube,[201] and protamine sulfate.[202] This is an "indirect" method to measure the DNA condensation. PG was added as a final step, into the DNA complex solutions at different charge ratios. The DNA condensation efficiency at each N/P charge ratio was calculated from the ratio of free DNA over total DNA which is usually expressed in units of percentage. Similarly, the free DNA released from hydrogels of crosslinked polymer oligo(poly(ethylene glycol)fumarate incorporating plasmid DNA (at 37 °C, agitation at 70 rpm, 80-day study), which aid understanding of controlled-released gene delivery.[202]

These indirect DNA condensation (and dissociation) assays[200-203] through free DNA measurement may not sufficiently explain the quality of gene complexes in the (complex) processes of their formation. At the present time, there is only one report on using PG to study DNA condensation directly. The PG dye-exclusion technique was been firstly published to monitor the pCMVlacZ condensation by protamine sulfate.[204] The assay is similar to the EthBr assay,[114] which monitors the steady-state fluorescence measurement of PG-labelled DNA directly. When the DNA is condensed, PG is excluded from the binding site, thus the drop in fluorescence intensity was measured and interpreted as DNA condensation efficiency.[204] This PG exclusion study is done at the high dye/kbp ratio, around 540 i.e. 0.27 μg DNA/μl PG reagent (220 μM). This high loading of PG may affect the DNA structure (e.g. extend the length of DNA etc.) which makes monitoring the process of DNA condensation complicated.[204] However, the photo-physical behaviour of PG bound to DNA chains during DNA condensation process at molecular level is still not known.

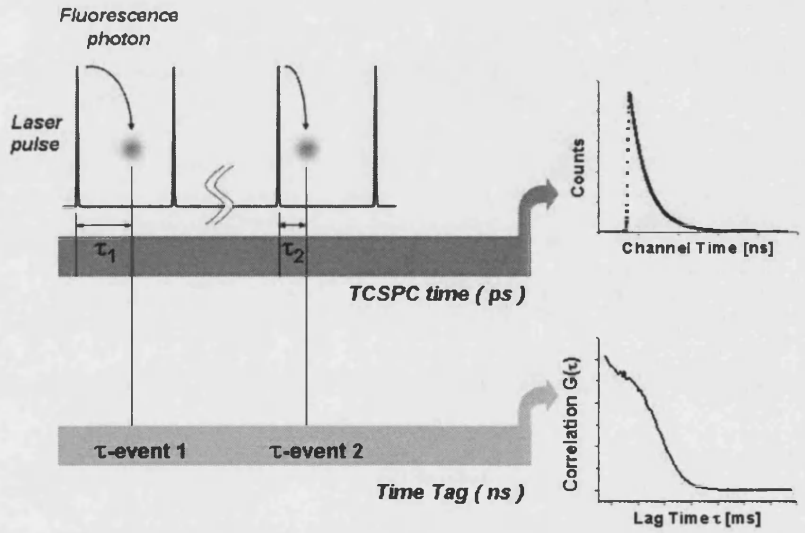

Figure 3.15 Time-tagged time-resolved (TTTR) data acquisition mode enables the monitoring of individual fluorescent photons. The information with time-tagged is converted into autocorrelation function G(τ) of fluorescence intensity. Decay kinetics of different fluorescent species are calculated from TCSPC time. This TR-FCS helps the separation of different fluorescent photons in term of G(τ) and lifetime (τ).

In our studies, we have applied the recently established time-resolved FCS technique (TR-FCS)[205] to monitor the behaviour of PG on DNA at low-labelling ratios (40 dye/kbp) throughout the condensation process. TR-FCS allows the simultaneous monitoring of DNA condensation (through FCS measurement) and PG lifetime (through using the time-resolved

mode). A confocal microscope with (a) pulsed pico-second diode laser excitation, (b) a fast single photon avalanche diode detector, and (c) PicoQuant TimeHarp 200 board was set-up for this experiment. The time-tagged time-resolved (TTTR) mode of TimeHarp was used to capture the fluctuations and the fluorescence decay kinetics of individual photon (Figure 3.15).

PG intercalation in DNA plasmid and its fluorescence decay

PG labelling of plasmid DNA and PG behaviour upon DNA condensation were studied by TR-FCS, using the FCS upgrade set-up. Alexa488 (approx 2 nM) was used to determine the confocal excitation element (V), and found to be $\omega_1 = 0.26 \pm 0.01$ μm, $\omega_2 = 1.87 \pm 0.30$ μm and volume (V) = 0.8 ± 0.1 femtolitre. This is a typical volume for FCS measurement as found in the classical set-up of ConfoCor ® I. Different volume of PG (1.1 μM) in the region of 0-30 dye molecule/kbp was added into pGL3 and pEGFP, left for 10 min to equilibrate before the fluorescence intensity measurement as described in the Experimental.

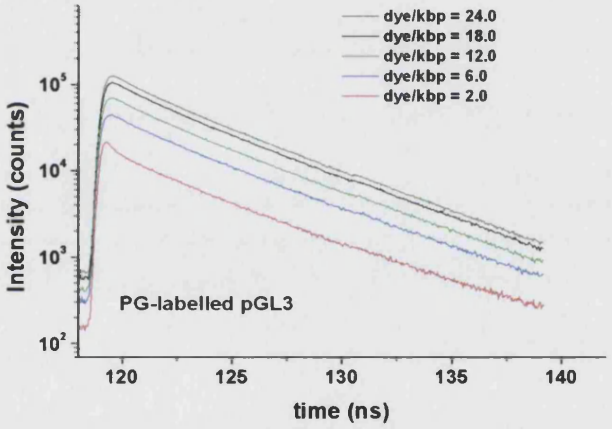

(i)

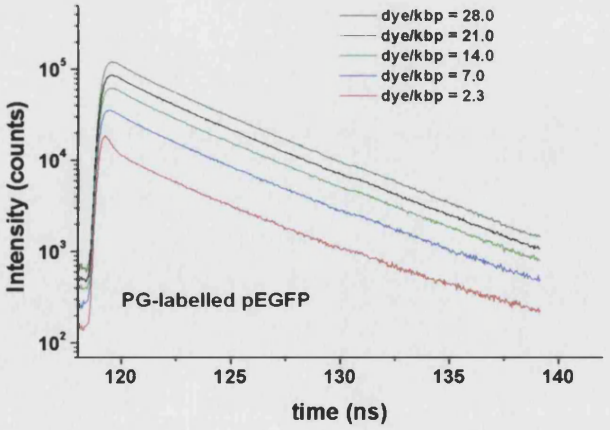

(ii)

Figure 3.16 Fluorescence decay profiles for PG bound to circular plasmid DNA ((i) pGL3 and (ii) pEGFP) obtained from TTTR data acquisition, using TR-FCS setting.

To understand the nature of DNA-binding of PG, fluorescence TTTR data were recorded at different PG dye/kbp ratios using pGL3 and pEGFP. The intensity decay was obtained from TTTR data and fitted by MicroTime200 (Figure 3.16, plotted in OriginPro7.0). The tail fitting was used in this experiment at constant channel time.

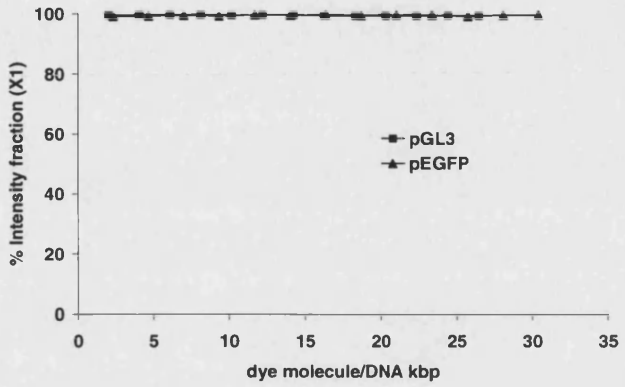

(i)

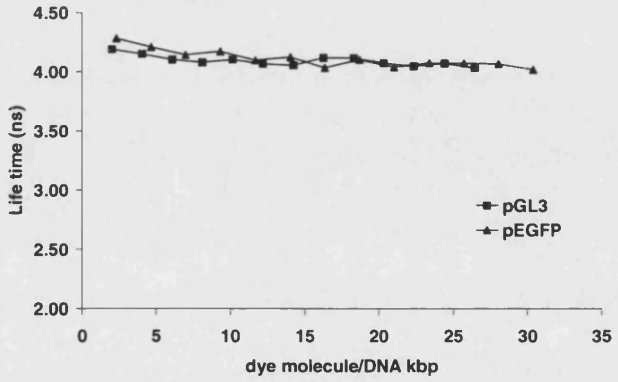

(ii)

Figure 3.17 (i) Major fraction of fluorescent species (97%) and (ii) lifetime of the major fluorescent population over a range of dye labelling ratio. Major fluorescent species of DNA-bound PG shows consistent lifetime, indicating that there is no dye release or dye-environment change.

Fluorescent count data from PG-labelled DNA were best represented by the bi-exponential model, which were better fitted than using the mono-exponential model. From this fitting calculation, there are two populations of DNA-bound PG fluorescent species (a) $\tau = 4.0$ ns (intensity fraction 97%) and (b) $\tau = 1.0$ ns. Considering that the fraction of other PG species (with τ 1.0 ns) is very small, it suggested that τ 4.0 ns species is the major fluorescent PG (Figure 3.17). This is corresponded well to the previous study by fluorescence lifetime measurement with a streak camera, reported by Schweitzer and Scaiano,[191] which also shows

that PG is adequately fitted by monoexponential decays when complexed to dsDNA (but with ± 5% error). In term of model fit, the bi-exponential model has improved χ^2 value over from the mono-exponential model, but the tri-exponential model failed to improve further the χ^2 value. Thus, this model fitting was used throughout our experiments.

From Figure 3.17, it is clear that the majority of PG, in the range of 0-30 dye molecule/kbp, bound to both plasmid DNAs through a single and unified mechanism. PG-labelled DNA showed negative in a circular dichroism study,[199] indicating that the majority of dyes are intercalated between DNA base-pairs. The PG concentration selected in our study is much lower than the saturation of acridine dyes intercalation (i.e. 500 dye/kbp). However, our model also indicates the presence of short-lived PG (1.0 ns), though in very small number. This observation may be related to the higher sensitivity of our confocal microscope in fluorescence detection, compared to the population-based time-resolved study. The constant lifetime of DNA-bound PG at 4.0 ns, also confirms that there is no change in environment surrounding PG intercalating site (which shorten PG lifetime). This ensures that there is no major DNA conformational change due to PG intercalation, which is one of desirable properties of good fluorescent DNA probes.

FCS analysis of intercalated PG on plasmid DNA

In these experiments, the application of time-resolved measurement was used to derive the FCS parameters of DNA-bound PG, hence named TR-FCS. pGL3 and pEGFP plasmids (1 nM in HEPES 20 mM NaCl, pH7.4) were labelled with different concentrations of PG. The FCS parameters of PG on pGL3 and pEGFP were simultaneously analysed using TTTR data and a mathematically-derived filtering technique. From the time-resolved study, it was found that there are two sub-populations with 97% from 4.0 ns species. TR-FCS allows the separation of G(τ) of both species on the basis of decay time difference. However, in our DNA experiments, all detectable fluorescent PG (with any lifetime) are on the same DNA molecule. Thus, the separation of different G(τ) for both species was not able to be performed.

According to G(τ) obtained from TTTR data analysis (Figure 3.18), both PG-labelled plasmids show similarity in the autocorrelation. This similar diffusion coefficient corresponds to their similar size and the structure of pGL3 and pEGFP. Both DNA also show the over-estimated PN rather than the theoretical PN (calculated by the real concentration of DNA used). This is caused by the size of multi-labelled plasmid DNA,

which is too big to fit the confocal volume. This leads to multiplicity of observed PG on a single DNA molecule.

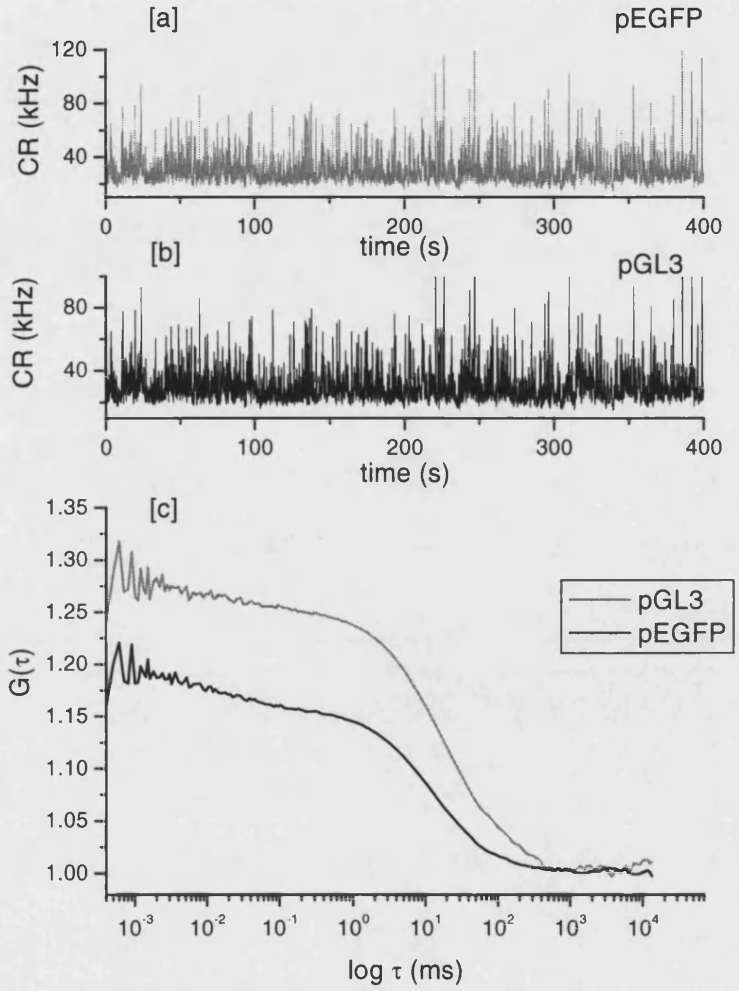

Figure 3.18 Example of CR plot and normalized G(τ) were constructed from TTTR data. The count rates tracking ([a] pEGFP, [b] pGL3) and G(τ) ([c]) for pGL3 1 nM (200 µl) intercalated with PG (1.1 µM) 18 µl (black line) and pEGFP 1 nM (200 µl) intercalated with PG (1.1 µM) 18 µl (grey line), $C_{dye}/_{kbp}$ are 18 and 21 respectively. The nature of multi-labelling DNA (long-chain molecules) causes an overestimation of PN (apparent PN).

FCS parameters (Figures 3.19 and 3.20), calculated from G(τ) (Figure 3.18) and confocal volume obtained from Alexa488 calibration, are complementary to the lifetime information of fluorescent PG. The constant increase of CR when more PG was added confirmed that PG intercalation is the most preferable binding mode in the low-labelling condition (less than 40 kbp). This is important to DNA probe selection which the unity of binding mode may simplify the data interpretation.

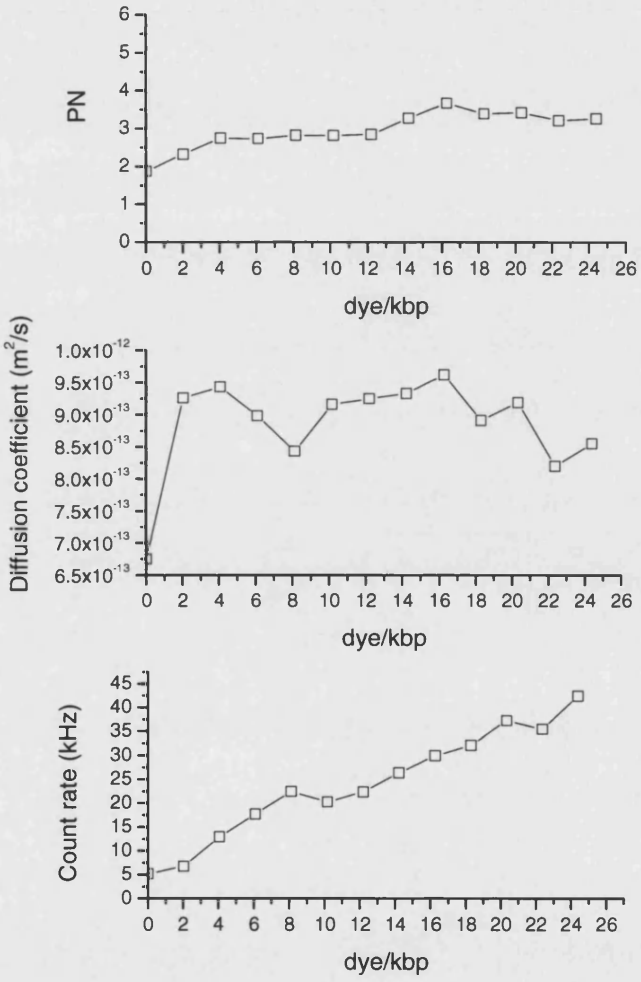

Figure 3.19 FCS parameter in TR-FCS, i.e. PN, CR and diffusion time (or coefficient) of PG-labelled pGL3 (□) was analysed from G(τ). PG was added into DNA solution achieve different dye/kbp ratio.

In Figure 3.19, the constant PN is around 3 and diffusion coefficient is slightly fluctuated in the region of 0.9 x 10^{-12} m^2/s. This suggests that DNA-bound PG molecules does not alter the hydrodynamic property of pGL3 (i.e. not to induce DNA bending or DNA condensation).

PN and diffusion coefficient of labelled pEGFP (Figure 3.20) were found to be constant in the PG titration experiments, which were similar to the ones with pGL3.

Diffusion coefficient of pEGFP(1.3 x 10^{-12} m^2/s) is higher than pGL3 (0.9 x 10^{-12} m^2/s), given its smaller plasmid size. However the PN values of PG-labelled pEGFP were slightly increased and finally get to a constant level. This slight increase of PN did not affect PG fluorescence in DNA, when it is used to monitor the DNA condensation process.

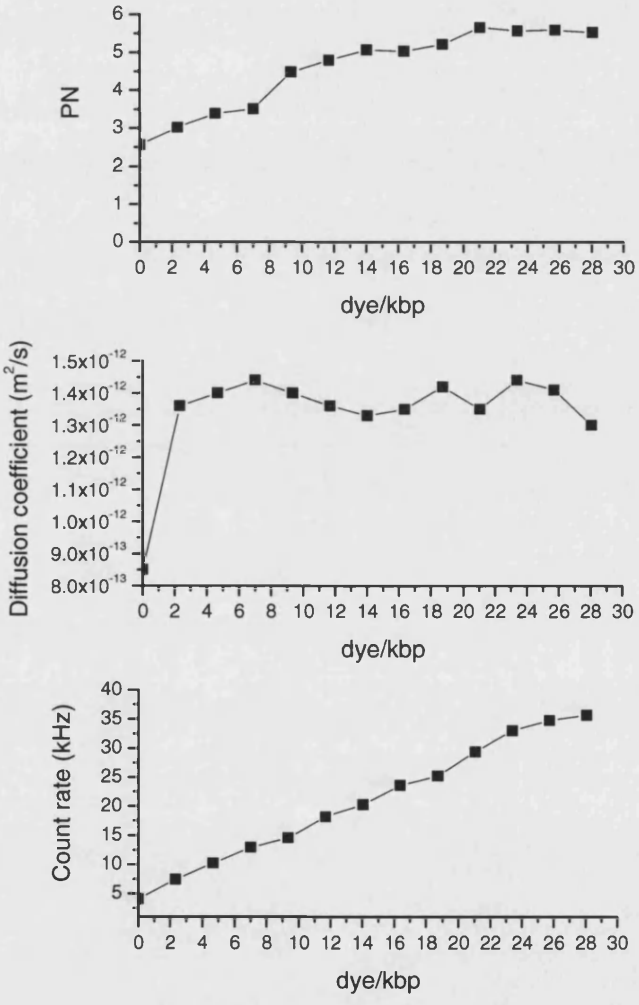

Figure 3.20 FCS parameter in TR-FCS, i.e. PN, CR and diffusion time (or coefficient) of PG-labelled pEGFP (■) was analysed from G(τ). PG was added into DNA solution to achieve different dye/kbp ratio.

FCS analysis of intercalated PG on plasmid DNA through the condensation process

Two lipopolyamines, N^4,N^9-dioleoylspermine (data shown in Figures 3.21 and 3.22) and N^1-cholesteryl spermine carbamate (data shown in Figures 3.23 and 3.24) were used in this study to condense pGL3 and pEGFP. The FCS parameters were obtained from G(τ) (derived from TTTR data).

DNA conformational change toward a condensed DNA was reflected in lower PN values with the increase in N/P. More structured DNA would have less segmental movement, thus reduce the PN value. Based on our classical FCS studies, these two lipopolyamines can achieve the point-like molecule condition (i.e. DNA was seen as one nanoparticle in the confocal volume). Complete DNA condensation was also illustrated by the increase of diffusion coefficient of fluorescent-labelled plasmid.

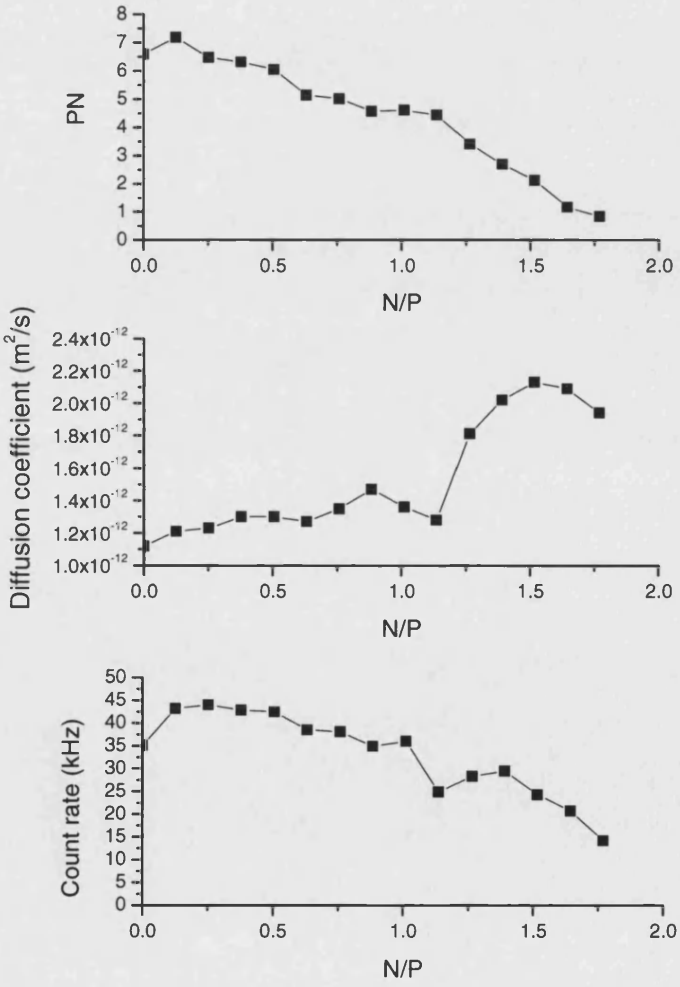

Figure 3.21 FCS parameters derived from TTTR data in TR-FCS, during the condensation process of pGL3 by N^4,N^9-dioleoylspermine, PG used at 18 dye/kbp

In these studies using TR-FCS (Figures 3.21 and 3.22), N^4,N^9-dioleoylspermine condensed pGL3 and pEGFP at N/P = 1.5-2.0. PN measured at the condensation N/P is about 0.9 (theoretical PN = 0.6). From these experimental data, the PN error was calculated as 0.3. Thus the achieved PN = 0.9 is within the experimental error in PN determination.This evidence suggests that pEGFP was condensed into a point-like molecule by this vector. Diffusion coefficient of a DNA nanoparticle is 2.1 x 10^{-12} m^2/s (for pGL3) and 2.5 x 10^{-12} m^2/s (pEGFP), which is approximately 2-times higher than free DNA (1 x 10^{-12} m^2/s). These diffusion coefficients also indicate the formation of compact DNA structured, from the use of N^4,N^9-dioleoylspermine in DNA condensation.

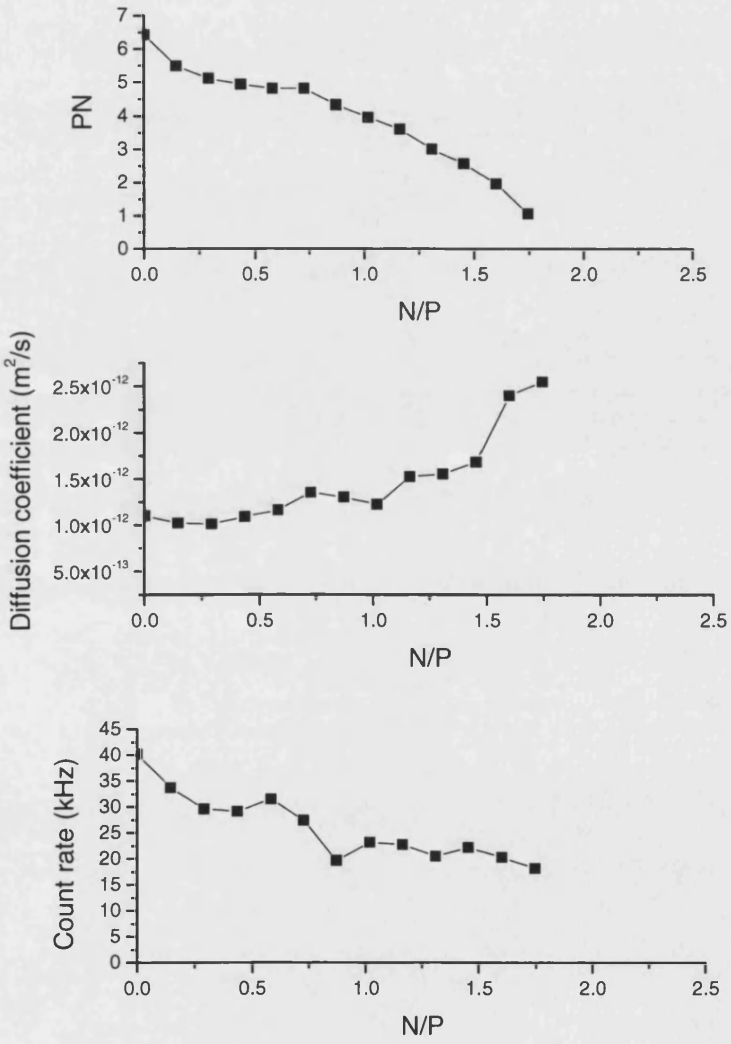

Figure 3.22 FCS parameters derived from TTTR data in TR-FCS, during the condensation process of pEGFP by N^4,N^9-dioleoylspermine, PG used at 21 dye/kbp

Figures 3.23 and 3.24 show the similar results of DNA condensation with N^1-cholesteryl spermine carbamate, there was an increase in diffusion coefficient and a decrease in PN. The PN values achieved at N/P = 1.3-1.5 (pGL3) and 2.5-3.0 (pEGFP). The PN achieved in these TR-FCS experiment was improved from the classical FCS, i.e. 0.3 (pGL3) and 0.5 (pEGFP). Diffusion coefficient of a DNA nanoparticle was 2.4 x 10^{-12} m^2/s (for pGL3) and 2.8 x 10^{-12} m^2/s (pEGFP), which is approximately 2-times higher than free DNA (1 x 10^{-12} m^2/s). The observation of fast-moving particles shows that DNA was packaging into a condensed DNA by N^1-cholesteryl spermine carbamates.

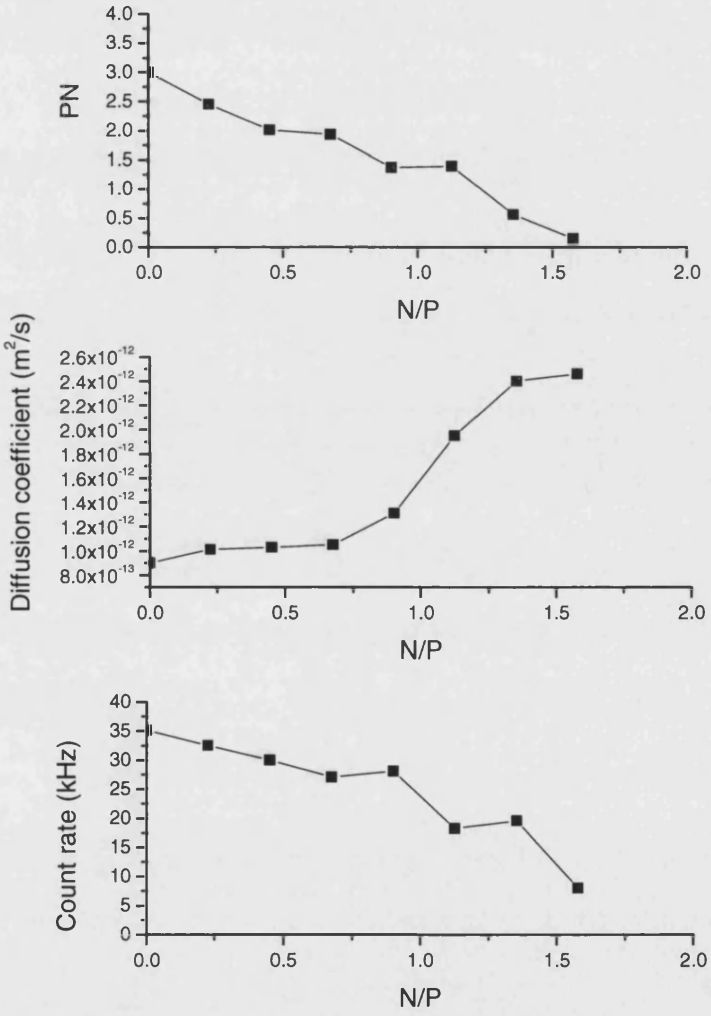

Figure 3.23 FCS parameters derived from TTTR data in TR-FCS, during the condensation process of pGL3 by N^1-cholesteryl spermine carbamate, PG used at 18 dye/kbp

From this TR-FCS, we concluded that both DNA condensing agents: N^4,N^9-dioleoylspermine and N^1-cholesteryl spermine carbamate are highly efficient in DNA packaging. We also

demonstrated that TR-FCS is capable to monitor the DNA condensation, We observed the difference in FCS parameters between TR-FCS and classical FCS. Given all photon events were collected and tagged (for their time of being detected) as an individual data point in TR-FCS, this technique offers more data for analysis. In the classical FCS, all photon data were calculated as a single average value by the correlator (hardware component) in the classical FCS. Thus TR-FCS is a more accurate measurement technique.[205]

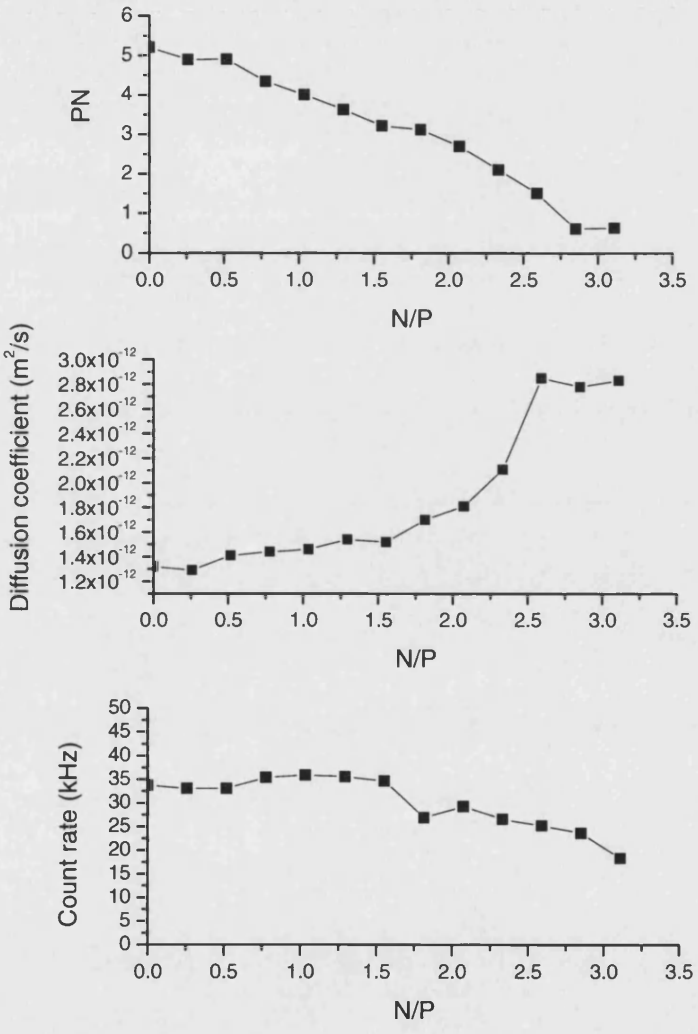

Figure 3.24 FCS parameters derived from TTTR data in TR-FCS, during the condensation process of pEGFP by N^1-cholesteryl spermine carbamate, PG used at 21 dye/kbp

Behaviour of PG on DNA undergoing condensation process

Count rate (CR) is a parameter reporting the fluorescence intensity in the system i.e. intercalated PG. Free form of PG (unbound species) was 1000-times less fluorescent than intercalated PG, thus the signal from PG is wholly from bound dyes. In our decay studies of

DNA-bound PG at different dye/kbp ratios (where there was no DNA condensing agent added), there was no CR decrease found at any labelling ratios. This showed that PG dyes bound to both pGL3 and pEGFP strongly and did not release from the intercalation sites, unless there lipopolyamines were added into DNA solutions.

In the DNA condensation experiments using PG as a probe (Figures 3.21, 3.22, 3.23 and 3.24), the small decrease of fluorescence (0-20 %) was observed reported as CR values during the initial phase of the DNA condensation process. We defined this initial step of the DNA condensation as the stage where there is no significant change in the diffusion coefficient of PG-labelled DNA, but PN change is observable (N/P = 0-1.0).

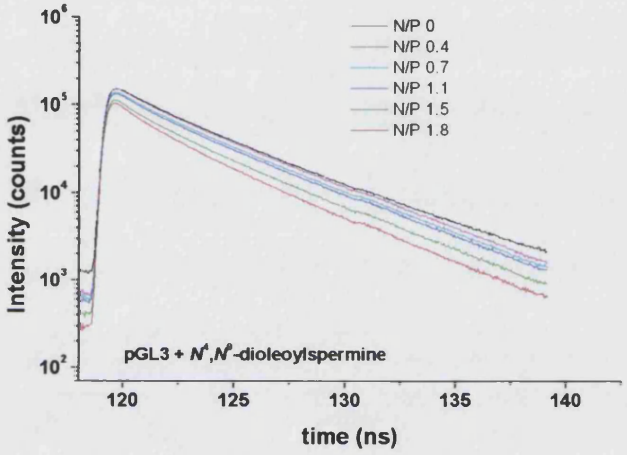

(i)

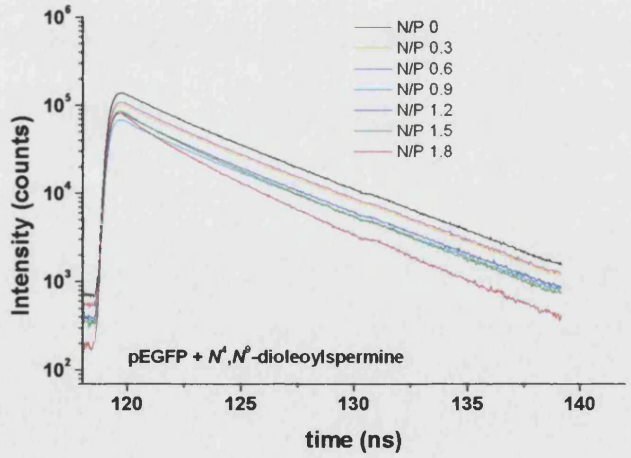

(ii)

Figure 3.25 Fluorescence decay profiles for PG bound to circular plasmid DNA ((i) pGL3 and (ii) pEGFP) obtained from time-tagged time-resolved data acquisition, which undergoes DNA condensation using N^4,N^9-dioleoylspermine

In the next step of DNA condensation (N/P more than 1.0), DNA was further reduced in size. FCS parameter i.e. diffusion coefficient was sharply increased, approximately 2-times, compared to PG-labelled DNA with no lipopolyamines. The degree of CR decrease is also higher in this phase of DNA condensation. We conclude that there is a significant change in the DNA conformation, mediated by N^4,N^9-dioleoylspermine and N^1-cholesteryl spermine carbamate. However, the information from FCS calculation is not sufficient to study the fluorescent signalling behaviour of PG on DNA chains.

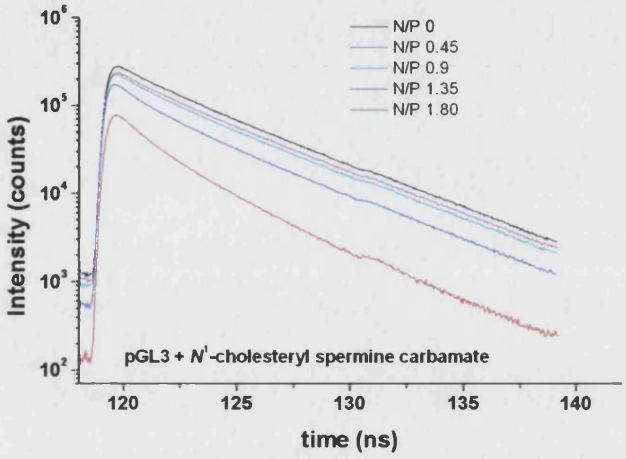

(i)

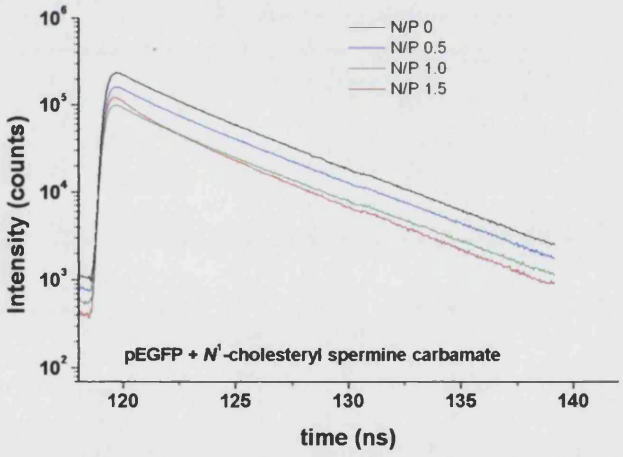

(ii)

Figure 3.26 Fluorescence decay profiles for PG bound to circular plasmid DNA ((i) pGL3 and (ii) pEGFP) obtained from time-tagged time-resolved data acquisition, which undergoes DNA condensation using N^1-cholesteryl spermine carbamate.

In these experiments, TR-FCS offers additional information to explain the behaviour of PG when DNA is in the condensed state. The decay profile of DNA-bound PG was calculated by employing a bi-exponential model. The decay plots are shown in Figures 3.25 and 3.26.

Both DNAs were labelled with PG (1.1 μM) (18 μl). The decay model shows the major population at 4.0 ns with the intensity fraction = 97%.

In Figure 3.27, the major population of fluorescent species in condensed DNA was at 97% consistently through the condensation process, with lifetime at 4.0 ns, which is the same as previously noted in the experiments using uncondensed DNA in Figure 3.17. This emphasizes that most PG molecules remained in the same binding site, and that there was no detectable migration to other binding sites (e.g. minor groove). Lifetime of 4.0 ns dye species was constant in the first stage of DNA condensation (N/P 0-1.0). This showed that there is no change in the environment of intercalation sites. In other words, there is no change in photo-physical properties of intercalated PG due to their surrounding environment.

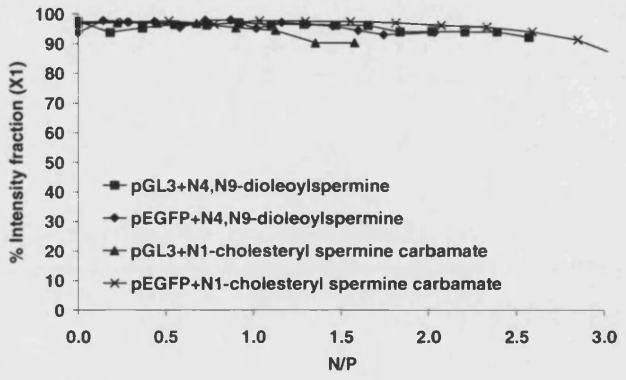

(i)

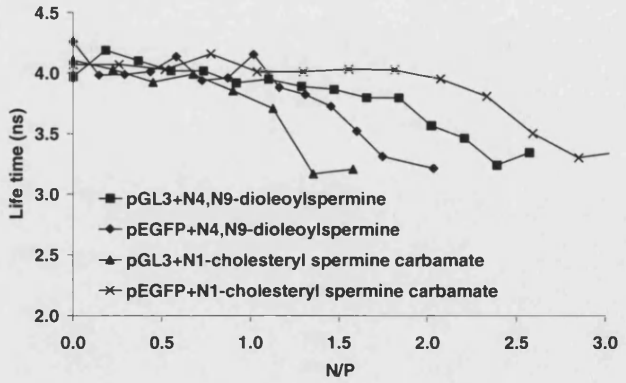

(ii)

Figure 3.27 Major fluorescent species of DNA-bound PG shows there is no intensity fraction of major population (4.0 ns dye species) change during DNA condensation process.

In the DNA condensation where N/P is more than 1.0, the lifetime values found in our experiments started to significantly decrease from 4.0 to 3.0-3.5 ns. We conclude that even though PG molecules were still located in their intercalation binding sites (i.e. τ of the major population of fluorescent species is still around 4.0, and the % of fluorescent species of 1.0 ns was not significantly increased) at this stage, there were some changes in the surrounding environment (which refers to DNA intercalation site) which accelerate the fluorescence loss at a quicker rate (i.e. quenching). This reflected in the decrease of lifetime values. This was probably due to the packing of DNA into nanoparticles, which altered the intercalation sites and the proximity of PG to other quenching agents in the condensed DNA environment, particularly nucleic bases (both purines and pyrimidines).

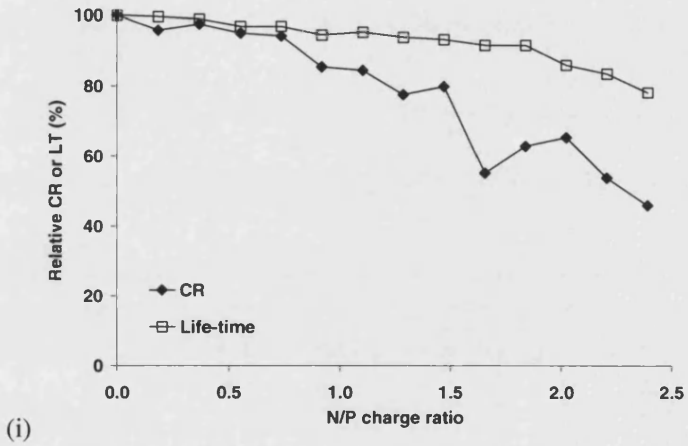

(i)

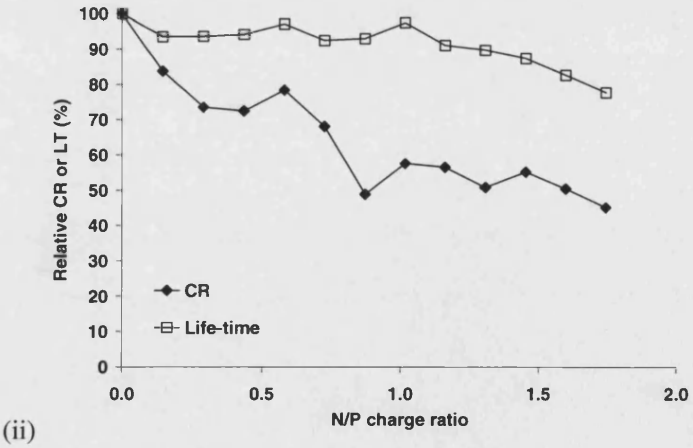

(ii)

Figure 3.28 Lifetime and CR change during DNA condensation process of (i) pGL3 + N^4,N^9-dioleoylspermine, (ii) pEGFP + N^4,N^9-dioleoylspermine

The decrease in lifetime may be related to the migration of PG from one binding mode (intercalation) to another one (e.g. minor groove binding mode), thus the surrounding

environment of PG changed. However, we found that 4.0 ns species are still the major fraction of population (97%) and there is no significant increase in the population of shorter lifetime fluorescent species (1.0 ns). Thus, there is no change or switch of binding mode of PG. The consistent lifetime was observed through the DNA condensation.

To incorporate both FCS information and decay kinetics of PG, both CR and lifetime were normalized in to percentage of the relative fluorescence unit (Figures 3.28 and 3.29) and plotted on the same graph. However, CR and lifetime are the parameters expressed in different units (intensity unit vs time). The conversion of lifetime (time unit) to fluorescence was performed, based on the relationship of fluorescence quantum and lifetime which is described in equation (2) where F_0 = initial fluorescence quantum, F = fluorescence quantum, τ_0 = initial lifetime and τ = lifetime:-

$$\frac{F_o}{F} = \frac{\tau_o}{\tau} \qquad (2)$$

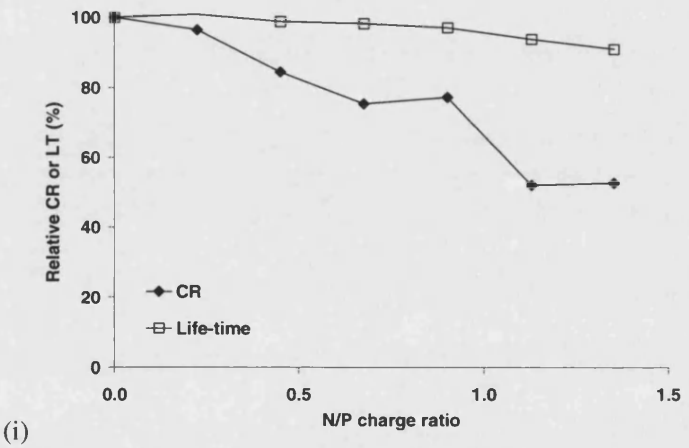

(i)

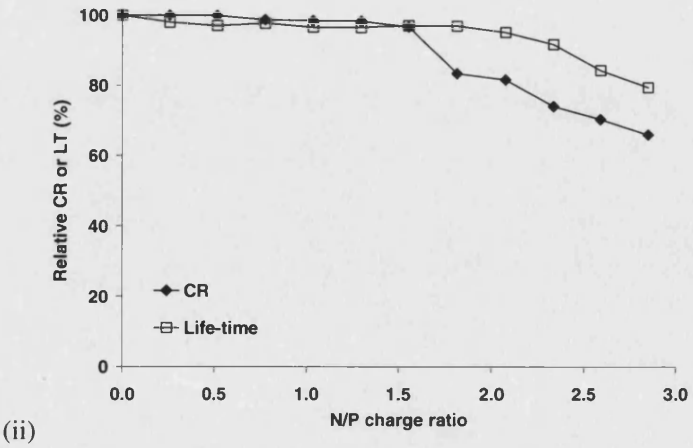

(ii)

Figure 3.29 Lifetime and CR change during DNA condensation process of (i) pGL3 + N^1-cholesteryl spermine carbamate and (ii) pEGFP + N^1-cholesteryl spermine carbamate

In Figures 3.28 and 3.29, the CR values were reported as % relative CR. The CR values represent the total fluorescent intensity detected in the confocal volume. The decrease in CR could be from dye release (physical loss of dye out from DNA, thus total fluorescence intensity dropped) and dye quenching (no physical loss of dye, but shorter lifetime, thus fluorescence intensity dropped). Quenching process is a process which acts on the excited population and thus decreases the mean decay time of the excited state population.

During the first stage of DNA condensation (N/P = 0-1.0), only dye release process leads to the decrease in CR. There is no contribution from dye quenching given there is no change in PG lifetime values. This is supported by the constant life-time (4.0 ns) in this N/P range in Figure 3.27, during the dye release process. Dye release process is a process that some PG molecules are released from the intercalation sites. However, the released PG molecules are so low in fluorescence (lower than the intercalated PG 1000 times) that they are not detectable by TR-FCS, and only the fluorescent species (intercalated PG) were monitored. The conformational change of DNA, when lipopolyamines start to interact and initiate the bending of DNA chains, may induce the release of PG from their binding sites. The similar dye release of DNA intercalators is commonly observed in EthBr.[113] In conclusion, dye release process by itself does not decrease the decay time of intercalated PG.

At N/P charge ratios higher than 1.0, lifetime of fluorescent species started to decrease from 4.0 to 3.0-3.5 ns. Dynamic quenching of PG was then proposed as the principal process leading to fluorescence (CR) loss. According to the equation (2), the shorter lifetime of intercalated PG was in proportional to the decreased CR. In Figures 3.28 and 3.29, the degree of CR decrease was also comparable to the degree of lifetime shortening at this stage of DNA condensation. This supports our proposal that dye quenching is the main source of fluorescence intensity decrease. When considering the FCS parameters, diffusion time of PG-labelled DNA was significantly increased and PN was approaching the theoretical value (PN = 0.6). The formation of DNA nanoparticles may lead to the significant change in the intercalation sites, thus reflecting in the lifetime shortening of DNA-bound PG.

The behaviour of PG on DNA through the DNA condensation was proposed and illustrated in Figure 3.30. PG molecules efficiently intercalated between DNA base-pairs (step I: dye binding) with a single binding mode with 4.0 ns lifetime, and no interference in DNA hydrodynamics. After lipopolyamines were added into DNA, PG molecules were then excluded from DNA in the low level (step II: dye release). It was worthy to note that the fluorescence decrease is not an indicator for the complete DNA nanoparticle formation. DNA was then condensed into a single nanoparticle, resulting in the quenching of PG

fluorescence (step III dye quenching). Dye quenching through the lifetime determination is an effective indicator for the nanoparticle formation detection. In this stage, PN, a reliable parameter for FCS measurement, was also approaching theoretical PN.

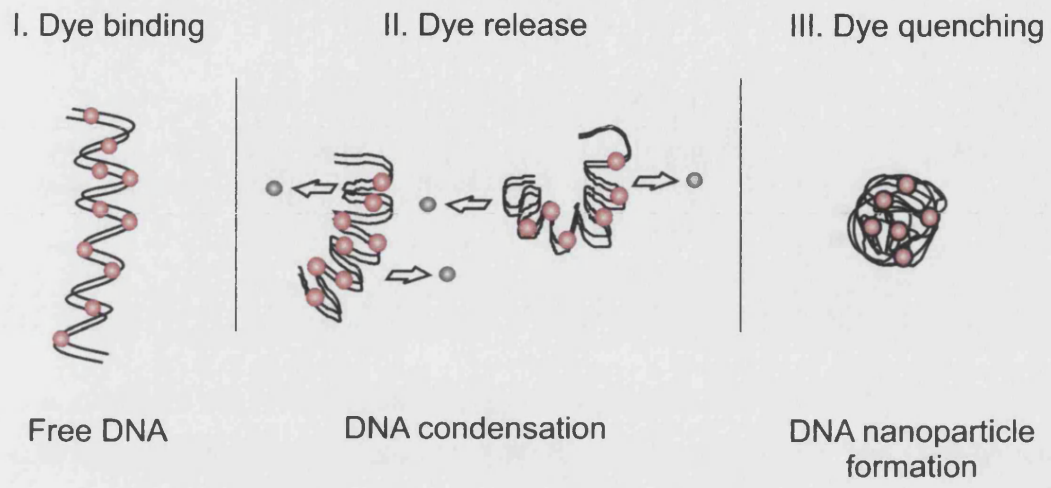

Figure 3.30 PG behaviour through the DNA condensation process

From our studies, the key advantage of using PG in DNA condensation studies is its single mode of binding and high affinity to DNA, compared to other dyes such as EthBr. It can also be used at very low concentrations due to its high absorption coefficient. The fluorescence signal reduction, being observed in the assay, was proved to be from two distinctive mechanism: (i) dyes release and (ii) dyes quenching. Lifetime information of DNA intercalator is also a reliable and helpful parameter in DNA condensation studies, obtained from TR-FCS.

Conclusions

Employing the reported FCS experiments, we were able to monitor lipopolyamine-DNA complex formation at the single molecule level. In comparison to other DNA markers, PG used in our FCS study has several advantages: it does not change the hydrodynamic properties of DNA, and it does not influence the lipopolyamine concentrations necessary for condensation. Additionally, due to its high brightness, PG requires 10-fold lower staining when compared with previously used markers. PG has higher affinity than EthBr and other related dyes for dsDNA, in part, because of the polyamine moiety structural modification which efficiently forms salt bridges with DNA phosphate anions, taken together with DNA intercalation, this is known as biphasic binding. Finally, count rate is practically invariant to

the condensation process, indicating that dye release is not interfering with the condensation process.

As demonstrated using our lipopolyamines, FCS directly visualises the condensation process by tracking changes in diffusion coefficients and particle numbers. In the experiments reported herein, the PN value, which is the most accurate read-out parameter of a FCS experiment, gives quantitative information on the packing density of DNA- lipopolyamine aggregates. Thus, direct information on the quality of condensing molecules can be derived. This analytical platform, FCS provides detailed information and insight about DNA and its interaction with gene carriers, which is crucial to the development of safe and effective non-viral gene delivery vectors.

TR-FCS offers an access to lifetime information which is from TTTR data and analysed simultaneously with FCS analysis. In this study, the upgraded ConfoCor® I and TimeHarp setting was used. pGL3 and pEGFP condensation with N^4,N^9-dioleoylspermine and N^1-cholesteryl spermine carbamate was as a model. We are able to define the fluorescent signalling behaviour of PG through the process from dye binding, dye release and then dye quenching. Dye release was suggested as the indicator for DNA conformational change, but not for the nanoparticle formation. Dye quenching, through the observation of change in lifetime, is a more important event reporting that a single nanoparticles was existed. FCS data derived from TR-FCS is found to be similar and comparable to the classical FCS.

Chapter 4

NVGT mechanistic studies using fluorescent techniques and tools

Introduction

Non-viral gene therapy is a multi-step DNA (as a prodrug) delivery protocol. After DNA condensation, there are several barriers prior to nuclear entry. DNA nanoparticles formed by lipopolyamines must be uptaken into cells, escape from endosomes, traffick to and enter the nucleus for gene expression. Transmembrane delivery is therefore important to the success of gene delivery. Cell membranes are constructed from phospholipid bilayers. The outer membrane contains glycolipids, phophatidylcholine (PC), and sphingomyelin while the inner membrane has phosphatidylethanolamine (PE), phosphatidylserine (PS) and phosphatidylinositol. Cholesterol is found in both the inner and outer layers of the membrane. It rigidifies the membrane and thereby modulates membrane integrity.[106]

Unlike hydrophobic molecules which can cross the membrane by passive diffusion, larger molecules (including DNA nanoparticles) are normally uptaken by ATP-dependent endocytosis.[206] This could be receptor-mediated endocytosis through membrane receptors, e.g. clathrin-coated pits (Figure 4.1). These receptors bind with macromolecules and form clathrin-coated vesicles. The transition of a bud to a vesicle involves membrane fusion, and is associated with GTP-binding protein.[88,106] The clathrin units then dissociate from the vesicle coat. This is the "early endosome" and its membrane composition remains the same as cellular membranes. The "early endosome" further develops to the "late endosome" and fuses with lysosome. At lower pH (5.5), endo-lysosomal vesicle membranes rupture and release the DNA nanoparticles. The receptor recycle rate is about 50% per hour.[106]

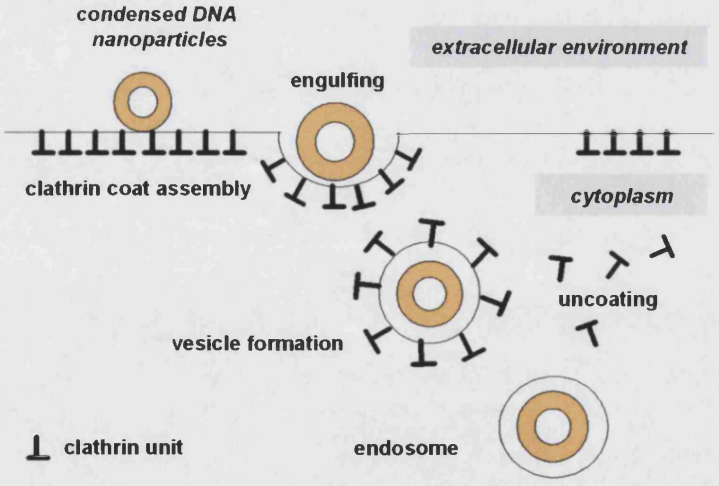

Figure 4.1 Clathrin-mediated endocytosis. The assembly of the clathrin coat introduces curvature into the membrane and then the formation of uniformly sized coated buds (engulfing). Once internalized in to cells, the coat of clathrin-coated vesicles is removed and recycled back to the cell membrane leading to the formation of endosomes.

There was also a recent report on clathrin-independent cellular uptake mode at the membrane sites called caveolae. Caveolae are enriched in lipid (cholesterol and sphingolipids) and have a protein coat (called caveolin). It was found that they could uptake fluids as large vesicles (0.15-5.0 μm).[207,208] Strong evidence has now been established that caveolae are static fixed domains and are not involved in endocytosis (not through endosomes). Their trafficking involves the microtubule network (e.g. kinesin and dyneins) and the association of this pathway to gene delivery is still not well understood.[209] Pathways of internalization of DNA complexed with cationic lipids or polymers by phagocytosis[206] and macropinocytosis[210] have also been reported.

Endocytosis of NVGT lipoplexes

Cellular uptake, especially endocytosis, is important to initiate the gene delivery process in cells. To understand the process of cellular entry of gene complexes, using our synthetic vectors (N^4,N^9-dioleoylspermine and N^1-cholesteryl spermine carbamate, Figure 4.2), both primary (FEK4) and carcinoma cell line (HtTA1 HeLa) models were used in our studies. Commercially available cationic lipid vectors - Lipofectin (DOTMA/DOPE) and Lipofectamine (DOSPA/DOPE) were included as reference lipofection models.

(i)

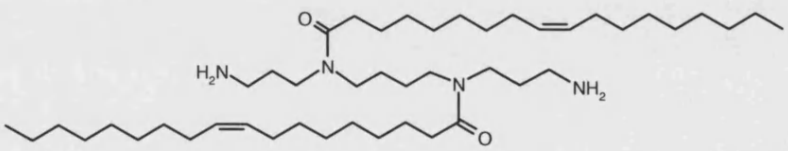

(ii)

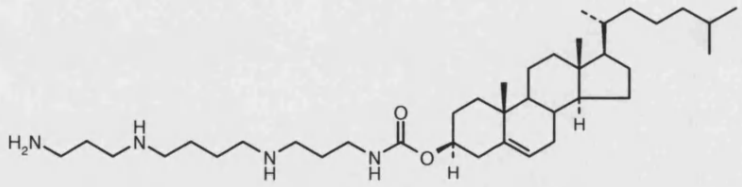

Figure 4.2 (i) N^4,N^9-Dioleoylspermine, (ii) N^1-cholesteryl spermine carbamate

Lucifer yellow carbohydrazide[211] (LY) (Figure 4.3) is used as a non-toxic fluorescent marker for endocytosis (λ_{ex} = 427 and λ_{em} = 535 nm). It is highly soluble in water, lipid-insoluble, and ionised at physiological pH. The two negative charges in the molecule prevent the cross-membrane passage by passive diffusion, and LY enters cells by endocytosis.[211] The effect of temperature on fluid phase endocytosis and the membrane physical state was reported by Wolkers *et al.*[212] using Fourier transform-infrared spectroscopy (FT-IR) and fluorescence anisotropy. The results show that there is a main membrane phase transition at

approximately 8-12 °C. Endocytotic processes are usually blocked at temperatures below 12 °C. For example, LY uptake into pig platelets by fluid phase endocytosis occurs above 15 °C.[212]

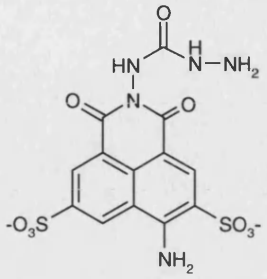

Figure 4.3 Lucifer yellow carbohydrazide (LY) - a marker molecule for endocytosis

The study of cell incubation at 12 °C, where fluid-phase lipid underwent phase transition, was selected for endocytosis investigation in these studies. This low temperature protocol is comparable to other endocytotic studies using endocytosis inhibitors (or ATP depletion agents) such as oligomycin,[213] cytochalasin B.[214] FEK4 and HtTA1 HeLa transfection were performed at selected optimal N/P charge ratios. Cells at 50-70% confluence were exposed for 4 h at 12 °C to pEGFP lipoplexes formed by N^4,N^9-dioleoylspermine or N^1-cholesteryl spermine carbamates. Then the DNA complexes were removed and replaced with regular media according to the cell line. Cells were then incubated at 37 °C for another 44 h. The EGFP expression results were obtained after 48 h post transfection using FACS analysis.

In Figure 4.4, FEK4 cells incubated with lipoplexes of N^4,N^9-dioleoylspermine (N/P 2.5 and 5.0), N^1-cholesteryl spermine carbamate (N/P 5.0), Lipofectin (N/P 2.0), and Lipofectamine (N/P 3.0) show high transfection at 37 °C with high cell survival rate > 80%, as discussed in Chapter 2. When the transfection was carried out at 12 °C, a significant decrease of transfection efficiency was found in the reference lipofection systems, as well as in the experiments using our synthetic vectors. The loss of endocytosis results in less DNA complexes being delivered across the membrane and finally affects gene expression. Matsui *et al.*[210] also show the relationship of cellular entry of lipoplexes and the transfection efficiency in differentiated airway epithelial cells. Cells in the centre part of the well (well-differentiated) which uptake less liposomal complexes (pCMV beta/LipofectACE = 1:5 (w/w)) than poorly-differentiated ones at the edge of the well, displayed a significantly lower transfection result.[210] Figure 4.5 shows that all lipid-based NVGT vectors at 12 °C still retain their ability to deliver DNA into FEK4 when the process of endocytosis was stopped. From these data, we conclude that it is highly possible that endocytosis is not the only route for lipoplexes to gain access to cells. N^4,N^9-Dioleoylspermine at N/P 5.0 shows a

significantly higher relative fluorescent cell percentage than the one at N/P 2.5 (i.e. 30 and 10% respectively). The excess of cationic lipid in the complexation at N/P 5.0 may be related to facilitating the non-endocytosis pathway(s) of cell entry. Even though lipoplexes get into cells mainly by endocytosis, NVGT vectors which are capable of cell entry by multiple routes may help boost the overall level of efficiency in reaching the delivery target.

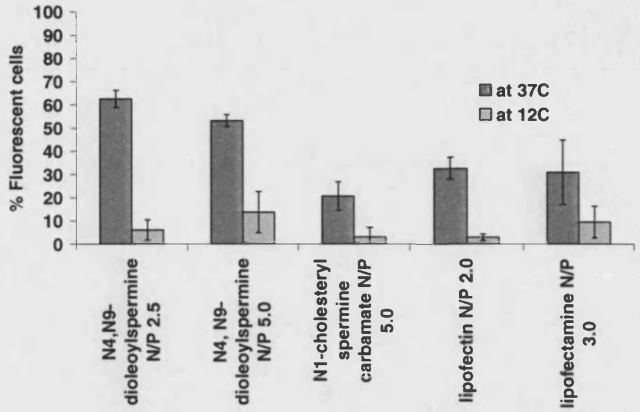

Figure 4.4 Effect of temperature on pEGFP delivery in FEK4 using N^4,N^9-dioleoylspermine, N^1-cholesteryl spermine carbamate, Lipofectin, and Lipofectamine. Endocytosis was found to be the major cellular entry route of DNA nanoparticles. (n = 3, error bars are S.D.)

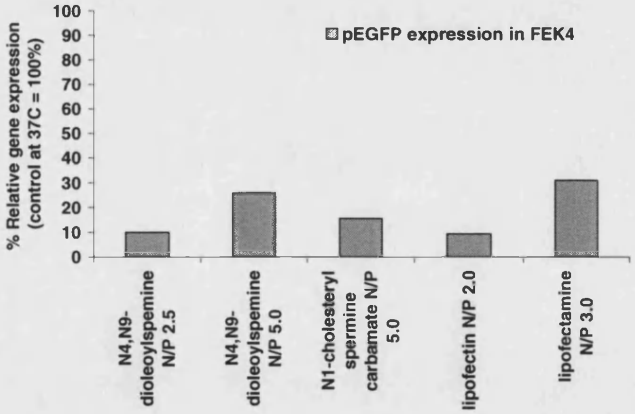

Figure 4.5 Relative gene expression level of pEGFP complexed with N^4,N^9-dioleoylspermine, N^1-cholesteryl spermine carbamate, Lipofectin, and Lipofectamine in FEK4 at 12 °C. (Mean value was used in this graph, considering the gene expression at 37 °C control conditions as 100%)

Similar transfection experiments at low-temperature (12 °C) were also performed in a carcinoma cell model. In Figure 4.6, HtTA1 HeLa cells incubated with lipoplexes of N^4,N^9-dioleoylspermine (N/P 2.5 and 5.0), N^1-cholesteryl spermine carbamate (N/P 5.0), and

Lipofectamine (N/P 3.0) show a significant decrease in transfection at 12 °C, as found in FEK4 cells. In comparison to Figure 4.4, the level of gene expression through the non-endocytotic cellular entry into HtTA1 HeLa cells is slightly lower than in FEK4 cells. This observation is in agreement with the fact that carcinoma cells uptake more DNA complexes than primary cells.[163] Thus, the magnitude of cellular uptake reduction was apparently greater in HeLa cells. Transfection in HtTA1 HeLa (Figure 4.7) also shows a smaller relative fluorescent cell percentage for all studied vectors than in FEK4.

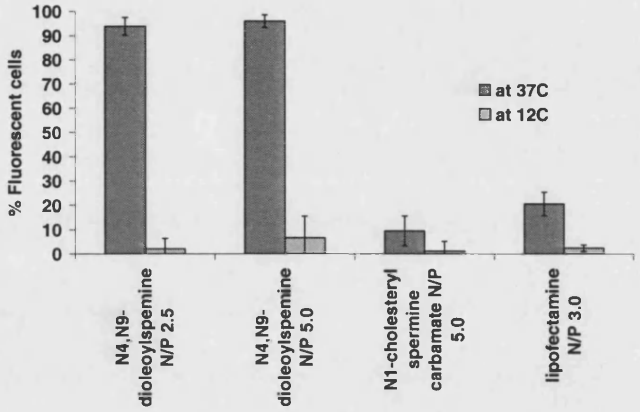

Figure 4.6 Effect of temperature on pEGFP delivery in HtTA1 HeLa cells using N^4,N^9-dioleoylspermine, N^1-cholesteryl spermine carbamate, and Lipofectamine. Endocytosis was found to be the major cellular entry route of DNA nanoparticles. (n = 3, error bars are S.D.)

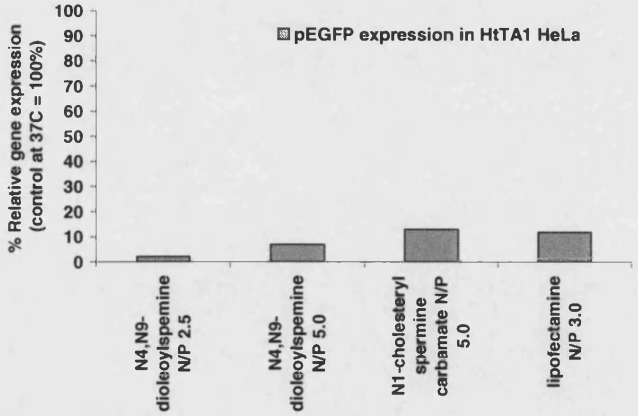

Figure 4.7 Relative gene expression level of pEGFP complexed with N^4,N^9-dioleoylspermine, N^1-cholesteryl spermine carbamate, and Lipofectamine in HtTA1 HeLa cells at 12 °C. (Mean value was used in this graph, considering the gene expression at 37 °C control conditions as 100%)

From these studies, we conclude that endocytosis plays the major role in the cellular uptake of N^4,N^9-dioleoylspermine and N^1-cholesteryl spermine carbamate lipoplexes. However, non-endocytotic cell entry modes also exist and may play roles as auxillary pathways in non-viral gene delivery.

Novel pore-forming NVGT vector

PolyAPS (polyalkylpyridinium salts) (Figure 4.8),[215-217] a marine toxin extracted from *Reniera sarai* was obtained as a gift from Dr. RH Scott (University of Aberdeen, U.K.) and used in our studies. This toxin primarily contains two polymeric 1,3-alkylpyridinium salts of 5.5 and 19 kDa. This compound shows the electrophysiological action in HEK 293 cells (dorsal root ganglion neurons). At high concentration (50 μg/ml), it caused irreversible depolarisation in membrane potential and reduction in input resistance. This increased Ca^{2+} permeability and flux in cells. The effect was less and also was reversible at low dose (50 ng/ml). This unique pore-formation property (membrane permeability alteration) and its poly-positively charged characteristic make polyAPS a good candidate for a gene delivery vector. Transfection of pEGFP and plasmid for human tumour necrosis factor receptor 2 was reported in HEK 293 cells.[218] Stable transfection was achieved with poly-APS although it was less efficient than Lipofectamine.[218] However, apart from this transfection study, there is no published study on the interaction of this polycationic toxin with DNA. Our first study is therefore to explore the effect of its DNA condensation properties, which can lead to a better understanding of its gene delivery mechanism.

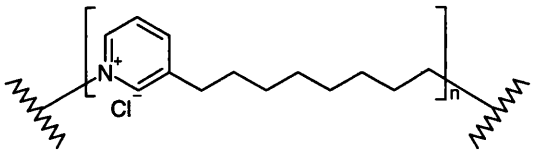

Figure 4.8 Polyalkylpyridinium salt (polyAPS) C8 alkyl chain, existing in two fractions with polymeric units n = 19-29 and n = 99 respectively

Figure 4.9 shows the DNA condensation with poly APS, using different DNA: pEGFP (4.7 kbp), pGL3 (5.3 kbp), and calf thymus DNA (13 kbp). EthBr displacement assay shows the decrease of fluorescence intensity (excitation at 260 nm, emission at 600 nm) when polyAPS concentration (expressed in a mole ratio of ammonium/DNA phosphate (N/P)) was increased. For N/P calculation, the number of positive charges in polyAPS was obtained by counting one positive charge on every monomer unit. All three DNA samples used in our study (pEGFP, pGL3, and CT-DNA) were efficiently (and similarly, see Figure 4.9) condensed by polyAPS with residual fluorescence at 10 % at N/P ratio 3.5-4.0.

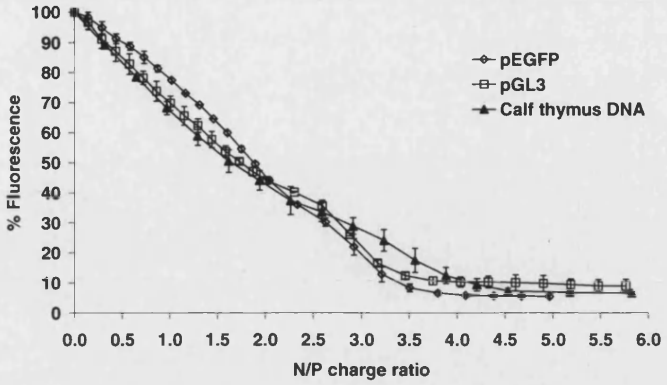

Figure 4.9 pEGFP, pGL3 and CT-DNA condensation study by EthBr displacement assay (λ_{ex} = 260 nm and λ_{em} = 600 nm) (n = 3, S.D. were shown in error bars), using polyalkylpyridinium salt (polyAPS)

Light scattering in Figure 4.10 confirmed that polyAPS-DNA complexes were formed, as the apparent absorbance at 320 nm increases significantly from the DNA only solution. Optimal N/P ratios for DNA condensation for poly-APS were at 3.50-4.00.

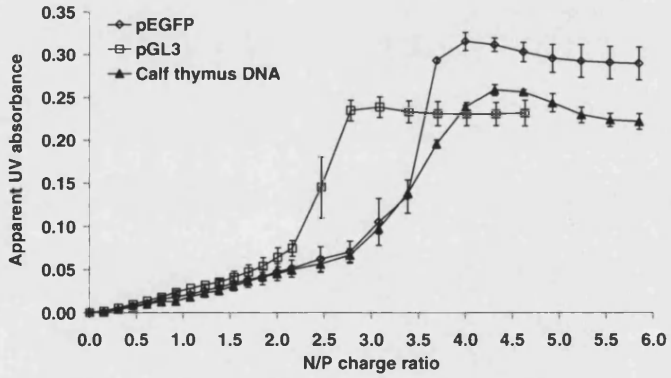

Figure 4.10 pEGFP, pGL3 and CT-DNA condensation study by light scattering assay (λ = 320 nm) (n = 3, S.D. were shown in error bars), using polyalkylpyridinium salt (polyAPS)

In Figure 4.11, the binding ability was calculated from the experiment using pEGFP as a model DNA. Calculated K_b are in the order; N^4,N^9-dioleoylspermine (1.1 x 10^7 M^{-1}) > N^1-cholesteryl spermine carbamate (0.7 x 10^7 M^{-1}) > polyAPS (0.3 x 10^7 M^{-1}). From this binding analysis, both N^4,N^9-dioleoylspermine and N^1-cholesteryl spermine carbamate binds to pEGFP more than polyAPS. The higher affinity to DNA of synthetic lipopolyamines is from the regiochemical distribution of positive charges along the vector molecule (i.e. carbon spacing in lipospermine = 3 or 4, and in polyAPS = 8) and the lipid moiety.

Although the K_b of polyAPS is similar to spermine ($K_b = 0.2 \times 10^7 M^{-1}$), the fluorescent residual of polyAPS-mediated DNA condensation is comparable to the one achieved by our synthetic lipopolyamines. The pyridinium headgroup and its degree of polymerization in polyAPS (n=19-29 and n=99) may contribute to its superior DNA condensation over spermine.

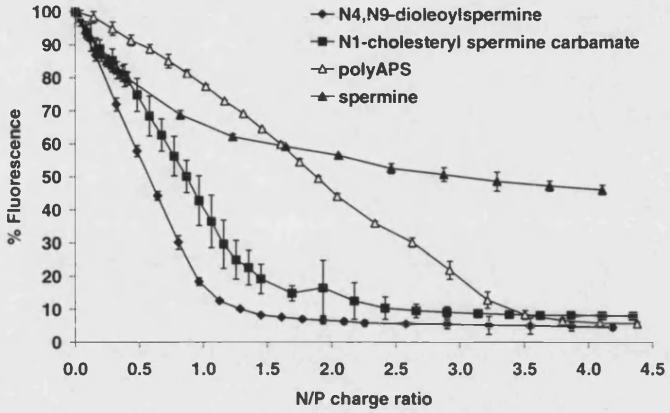

Figure 4.11 pEGFP condensation by polyAPS compared to N^4,N^9-dioleoylspermine, N^1-cholesteryl spermine carbamate and spermine, using EthBr displacement assay (λ_{ex} = 260 nm and λ_{em} = 600 nm) (n = 3, error bars are S.D.)

Given polyAPS is a highly efficient DNA condensing agent; it is possible to develop polyAPS as an NVGT vector. In addition to cell entry facilitation by pore formation, this membrane perturbation could also help in endosomal escape process (i.e. induce pore formation of endosomal membrane), which is one of key barriers in gene delivery. In nature, the pore-formation of polyAPS may act in chemical defence; it may also provide a novel mechanism of natural horizontal genetic material transfer between marine microorganisms. The mechanism by which poly-APS delivers macromolecules into cells and achieves transfection is unknown.[215-217]

Several cell-based membrane leakage assays, which have been used in cell toxicity characterisation, have been re-applied to determine membrane integrity.[214,219] These assays are performed in either a leaking-out or a diffusing-in direction. The first approach involves leaking out of intracellular enzymes (such as luciferase,[214] lactate dehydrogenase[157,214]) and some pre-loaded fluorescent probes help identify the presence of vectors-membrane interaction. Fluorescein *O*-diacetate (FDA) (Figure 4.12),[214,219,220] an acetate ester of fluorescein, was non-fluorescent and readily diffuses through intact cells. FDA undergoes hydrolysis catalysed by cellular esterase into fluorescein (λ_{ex} = 490 nm and λ_{em} = 513 nm),

which is hydrophilic and non-permeant. The cellular retention of fluorescein is compromised in cells with disrupted membrane.

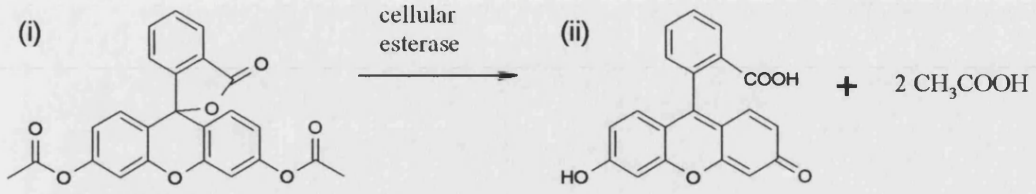

Figure 4.12 Fluorescein *O*-diacetate (FDA) (i) readily diffuses passively across cell membranes when it is hydrolysed to get fluorescein (ii) which is highly fluorescent, polar and non-permeant.

In FDA release experiments of polyAPS in FEK4 (Figure 4.13), M_1 is the population with high FDA-loaded cells in the control group (no polyAPS) in the range of log F_1 (fluorescence intensity in log unit, using F_1 emission filter) at 10^2-10^4. M_2 represents FEK4 cells which released fluorescein out from their cells, showing log F_1 less than 10^3 (mean fluorescence in the control group). The reduction in fluorescence level of M_1 and the increased number of M_2 cells in the population were analysed to determine the level of FDA release.

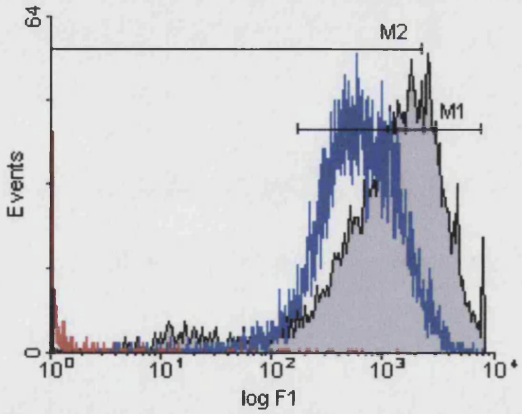

Figure 4.13 Histograms in the FDA release studies of polyAPS (red line = blank group with no FDA, grey shade = control group with FDA only, blue line = polyAPS 1 μg/ml) show sub-population M_1 and M_2 groups of FEK4.

PolyAPS at 1 μg/ml was selected as this concentration shows induce the poration in HEK 293 cells in Scott *et al.*'s studies.[215-217] Histogram of polyAPS-treated cell in blue line shows that FEK4 cells was less fluorescent and number of FDA-released cells were increased,

compared to the control group (grey shade), indicating the change of membrane permeability. From the red-line histogram, the blank sample (without FDA) was found no fluorescence in the log F_1 range used for monitoring, which confirms that there is no interference from intrinsic cellular fluorescence.

Another approach to study the interaction of vector-membrane is the use of non-permeant substances such as fluorescent dyes, fluorescent macromolecules (e.g. FITC-dextran[214,221]) or protein (e.g. HRP - horseradish peroxidase[222]). The magnitude of these substances translocated into intact cells when applying with interested fusogens, was measured to understand the effect to membrane. Propidium iodide (PI) [214,220] is a positively charged probe (Figure 4.14). It free form is low in fluorescence, and does not get into cells with intact membrane. PI is also widely used as a marker used to determine cell death (i.e. detecting the loss of the membrane integrity). Once PI is inside the cells and gets into the nucleus, PI is able to intercalate between nuclear DNA basepair and become fluorescent (λ_{ex} = 493 nm and λ_{em} = 636 nm).

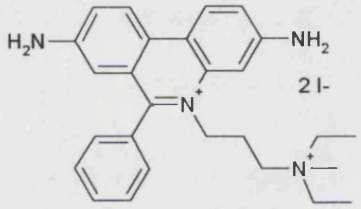

Figure 4.14 Propidium iodide (PI), a non-permeant fluorescent probe, is used for membrane integrity studies. Cells with compromised membrane integrity allow PI uptake

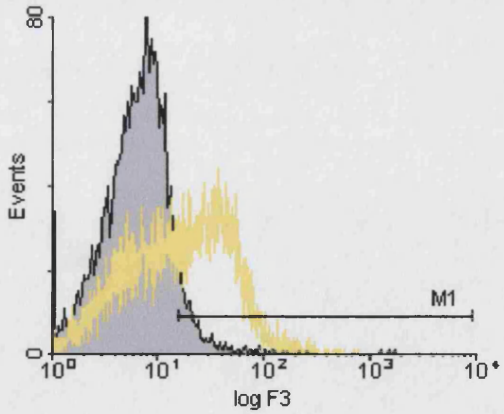

Figure 4.15 Histograms in PI uptake studies (grey shade = control group, yellow line = polyAPS 1 μg/ml) show a sub-population M_1 group of FEK4 used in analysis.

In PI uptake experiments (Figure 4.15), M_1 is the population with PI-uptake cells (PI-loaded only, without lipopolyamines) when log F_3 (fluorescence intensity in log unit, using F_3 emission filter) at more than 10^1. The increase in fluorescence level of M_1 (mean calculated from log F_3 value) and the increased number of M_1 cells in the population were analysed to determine the level of PI uptake. PolyAPS at 1 μg/ml (yellow line in Figure 4.15) shows that the treated cells were more fluorescent and number of PI-uptake cells was slightly increased, compared to the control group (grey shade), indicating the change of membrane permeability.

Results from both experiments (FDA release and PI uptake) are compared and presented in Figure 4.16, which are found to be concordant. Figure 4.16 (left) shows that the % cells with FDA release or PI uptake is 20-30%, compared to polyAPS untreated cells (0%). The mean fluorescence intensity of fluorescein is reduced to 60% of untreated FEK4 cells. Fluorescence intensity of PI is also significantly increased at 2.8-times the control group. This membrane instability result is also in agreement with the electrophysiological studies by Scott and co-workers.[215-217] From our DNA condensation and membrane studies, it is concluded that polyAPS is a novel NVGT vector with high efficiency of DNA condensation and a unique property as a pore former which increase the delivery across cellular membranes.

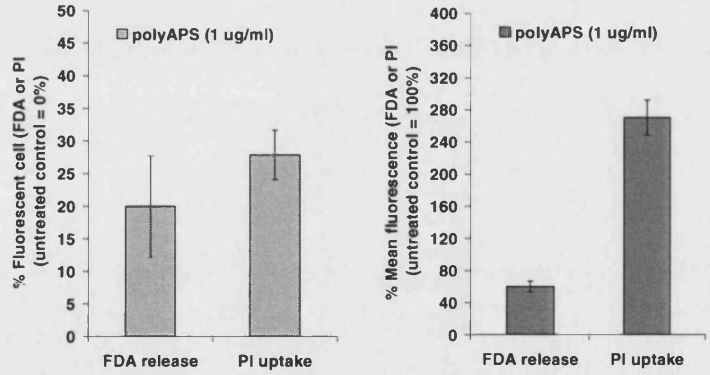

Figure 4.16 PolyAPS in FDA release and PI uptake studies in FEK4 cells (control = polyAPS untreated cells) (n = 3, error bars are S.D.)

Potential membrane fusion/penetration activity of lipopolyamines

From the low-temperature transfection studies (Figures 4.5 and 4.7), non-endocytotic cellular entry pathway are involved in non-viral gene delivery about 5-30%. This leads to our

interests to study if there is any other interaction between synthetic lipopolyamines and cellular membrane. In Figure 4.17, the positive charges of DNA complexes facilitate the electrostatic interaction with negatively charged phospholipids, allowed the cellular uptake. Lipophilic groups in lipopolyamines vector are usually selected or modified from the natural membrane lipids. These lipids may initiate the lipid mixing process in the membrane which alters the orderness of lipids in membrane and the loss of membrane integrity or permeability.[1-4]

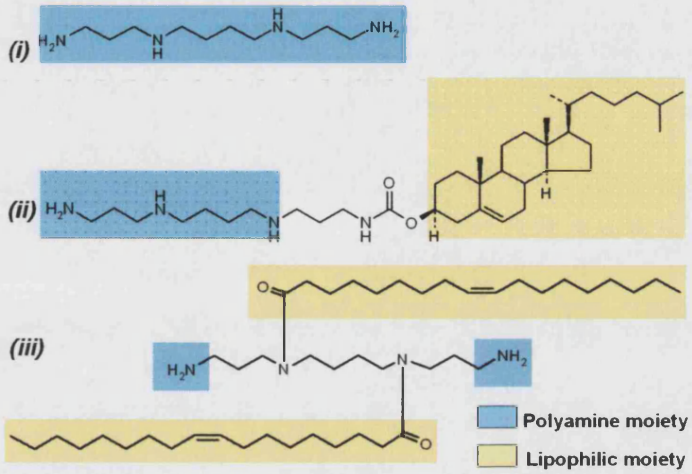

Figure 4.17 Lipopolyamines - N^4,N^9-dioleoylspermine (ii), N^1-cholesteryl spermine carbamate (iii) containing two important parts in NVGT delivery, unlike spermine (i). Polyamine moiety helps in DNA condensation and membrane binding (electrostatic). Lipid moieties (such as steroidal lipid or fatty acids) facilitate the packing and delivery of DNA.

The NVGT process was widely known to be problematic in practice, due to major intracellular barriers in delivery. These barriers include cell entry, endosomal escape (to minimize DNA degradation from endosomal-lysosomal DNase), and nuclear entry. All of these share the common ground as problems involving the interaction of DNA particles with lipid bilayer membranes (i.e. cell membrane, endosomal membrane and nuclear membrane). Thus, the investigation of membrane interaction properties of lipopolyamines would be beneficial better to understand how these DNA carriers deliver DNA into the nucleus. This would help in a design of efficient NVGT vectors which can both effectively condense DNA and interact well with various membranes during the process of DNA delivery.

Membrane fusion modulation by spermine

Membrane fusion process was defined by Meers *et al.*[223] as a process with two steps i.e. (a) aggregation of two vesicles (V_1) to form a dimer (V_2), and (b) fusion of dimer membrane resulting in a fused vesicle (F_2). Fusogen is defined as an agent that affects the overall fusion

rate, through aggregation (C_{11}) or fusion rate (F_{11}), as described in the following process, illustrated in Figure 4.18.

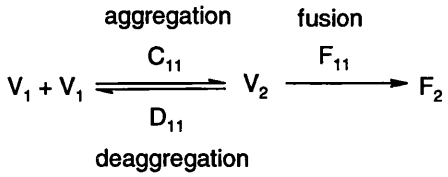

Figure 4.18 Process of spermine-induced membrane fusion

Spermine alone only aggregates, but does not fuses phosphatidate (PA) and PS liposomes. Only in liposomes made from high PE, spermine is able to cause fusion which may be from the fusogenic nature of PE. When used with fusogen like Ca^{2+}, spermine was observed to induce the overall fusion rate of PA liposomes at 70% by promoting higher Ca^{2+} binding. Calcium ions, at optimal concentration, were known to increase C_{11} by the neutralization of surface charge. Unlike spermine, calcium is also able to dehydrate the surface of membranes and the flexibility of bond angles, allowing bilayer shaping in fusion process. This spermine-mediated effect was not detected in PS liposomes. PS has a serine group which minimize the exposure of phosphate group at vesicle surface (i.e. less binding site for spermine), unlike PA. Thus, spermine is regarded as an aggregation promoter, not a fusogen. Nevertheless, a spacing bridge between two vesicles formed by spermine interacted with bilayer phosphate groups, is a first step to membrane fusion.[223] The Gouy (1910)-Chapman (1913)-Stern (1924) theory[224] suggests that surface charge density was reduced when cationic polyamines bind to anionic membrane surfaces. The association of spermine to membrane (PC/PS liposomes)[225] was found at $K_b = 91 \pm 12\ M^{-1}$. This is valid for samples with spermine content lower than half of phospholipids. At the higher concentration of spermine, K_b shifts to higher values. Hydrophobicity is lowered to some extent by the spermine bound to the membrane surface; the effect is common to all position in the chain, indicating that water penetration extends up to the higher hydrophobic region at the centre of the bilayer.

Membrane lipids integrity disturbance by lipid molecules

Most bilayer membranes contain phospholipids (mainly PC and PE at 50 and 20% of total phospholipid mass respectively)[226] and cholesterol, which support their structure. Acyl groups in phospholipid are C14-18 fatty acid, such as palmitic acid, oleic acid etc. Oleic acid is a C18 *cis*-unsaturated fatty acid and widely known as a skin penetration enhancer. Lipid phase separation is expected to be the key mechanism for this membrane activity. The FT-IR technique[227] was employed to determine the change of wavelength number of CH_2 group after the treatment of pig stratum corneum (4 cm^2) and its extract lipids with per-

deuterated oleic acid (30 µl of 300 µg/µl solution) at different temperatures. Oleic acid disorders 6-10 alkyl groups near the polar group of bilayer (highly order region) with no effect on the terminal methyl group. This increases the fraction of lipid in "liquid phase", and creates the permeable interfacial defect (Figure 4.19). The liquid phase was between solid phase membranes, which reduce the diffusional path length/resistance of membrane. The fluorescence anisotropy study[228] in modelled bilayers (human buccal epithelial cells) revealed the similar effect of oleic acid over the lipid packing order. The *trans*-form of oleic acid (elaidic acid) was also able to disrupt membrane, but in less degree than the *cis*-form.[229]

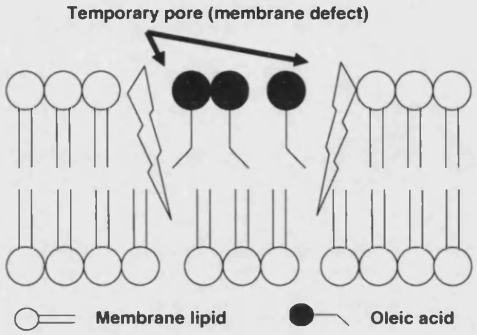

Figure 4.19 Proposed role of C18-oleic acid in membrane disturbance, due to its *cis*-conformation of double bond at C_{9-10}

Membrane studies using FDA were carried out using spermine and oleic acid. Spermine is a poor DNA condensing agent and no reports on the use of spermine as a NVGT vectors were found. In this study, we briefly examined a single concentration of spermine (2 µg/ml). This selected dose is non-toxic, as confirmed by the good quality of cells obtained for FACS analysis. Additionally, in cardiomyocytes (primary cell line from Sprague-Dawley rats), it was reported that spermine at 20 µg/ml or less is not toxic to cells.[230] The selected concentration of spermine (2 µg/ml) is also significantly higher than the previously reported concentration inducing the PA vesicle aggregation (5.5 µM).[223] As expected, spermine (green line in Figure 4.20) showed no membrane disruption at this concentration. This is in agreement with Meers *et al.*'s report that spermine by itself does not fuse the membrane, but only modulates the fusing process.[223]

On the other hand, oleic acid was reported to alter the highest membrane permeability at 0.7 mM (200 µg/ml) in a buccal mucosal cell suspension, using the fluorescence anisotropy technique.[228] In our study, oleic acid was used at 200 µg/ml (in EtOH). From Figure 4.20, oleic acid (red line) showed no membrane effect at this concentration. The difference in our

result from the study of Turunen *et al.*[228] may be from the nature of the cells in culture. The adherent monolayer cell culture of FEK4 (less contact surface area) may require a higher concentration of oleic acid to achieve the membrane effect, than the cell suspension in their study.[228]

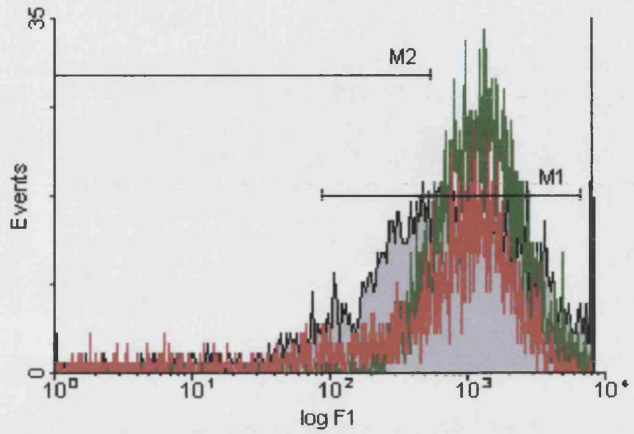

Figure 4.20 Histograms in FDA release studies (grey shade = control group with FDA only, green line = spermine 2 μg/ml, red line = oleic acid 200 μg/ml) show sub-population M_1 and M_2 groups of FEK4.

Dioleoylphosphatidyl ethanolamine (DOPE) (Figure 4.21) is a helper phospholipid frequently used in liposomal NVGT systems.[62,231,232] The presence of phosphatidyl-ethanolamine in the liposomes greatly enhanced fusion whereas the presence of phosphatidyl-choline inhibited fusion. Inclusion of cholesterol (40 mol%) in the liposomes substantially decreased liposomal leakage without impairing fusion.[233]

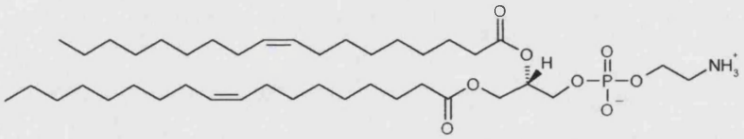

Figure 4.21 DOPE, a helper lipid with two C18-oleoyl chains

Fusogenic lipopolyamines: possible synergistic effects from polyamines and lipid

Lipopolyamines' fusogenic activity has not been widely studied, unlike fusogenic peptides (i.e. polyamine) and fusogenic phospholipids. However, from chemical structure of lipopolyamines, it may be possible to modulate the formation of "salt bridge" of ammonium/guanidinium groups in polyamines and lipid-mediated membrane phase destabilization. Recently, steroid-polyamine conjugates series[74] was studied for haemolytic activity (bovine erythrocyte). The conjugates consist of a hydrophobic, rigid steroid, a

flexible hydrophilic polyamine which can be protonated at physiological pH. From structure-activity-relationship aspect, it was found that the two nitrogen atoms with C4 spacing on polyamine backbone (used at 10-100 μM) are important to higher membrane activity. Examples of hemolytic steroidal-polyamine conjugates[74] are shown in Figure 4.22. The hydrophobic substituent on the steroid side-chain (e.g. propyl group) also enhances membrane fusion. Spermidine was also used as a control, showing no haemolysis, this emphasizes the importance of the lipid moiety in the fusion process.

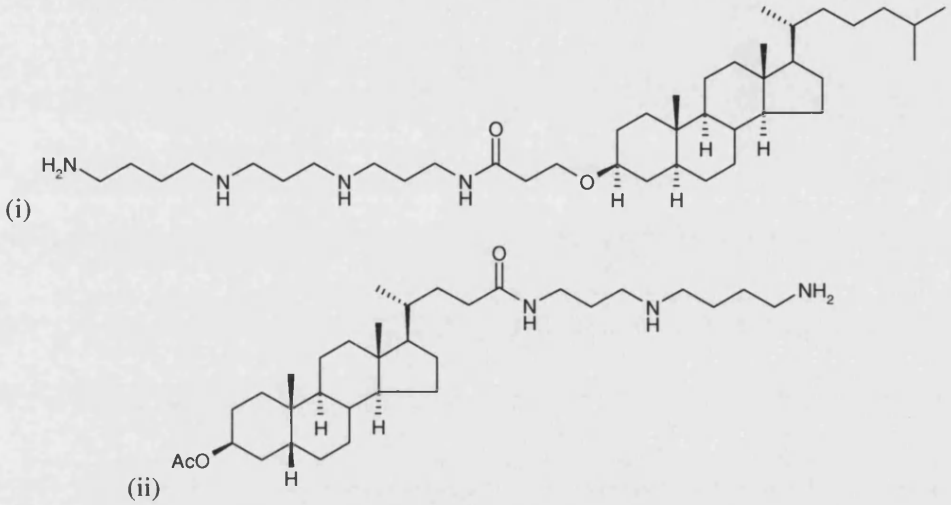

Figure 4.22 Example of hemolytic cholesteryl spermine conjugates[74]

Studies of interaction between lipopolyamines and cellular membrane

Based on our results that N^4,N^9-dioleoylspermine and N^1-cholesteryl spermine carbamate do not only enter cells via an ATP-dependent process (e.g. endocytosis), further studies of both lipopolyamines, at a non-toxic concentration (minimum survival rate 70%), were investigated in an FEK4 model. FEK4 cells were treated with lipopolyamines at different concentrations, following the procedure described in the Experimental. Figure 4.23 is an example of FEK4 cells obtained in FACS samples of N^4,N^9-dioleoylspermine-treated and control. shown in a Dot-plot of light signals from forward-scattered (FSC) and side-scattered (SSC). FSC is a parameter in proportional to cell size, and SSC indicates the cell granularity or internal complexity (typically referred to as cell debris or dead cells). Both groups similarly show good healthy cells (homogenous population). Gating for sub-population (R_1) was consistently applied in all experiments. From this Dot-plot, there is no significant difference in terms of cell morphology and size between FDA-treated and control groups. This ensures that the effects observed in all the following experiments are based on the temporary membrane effect in healthy cells and no artefacts from permanent cellular damage (loss of membrane integrity) are included in this study.

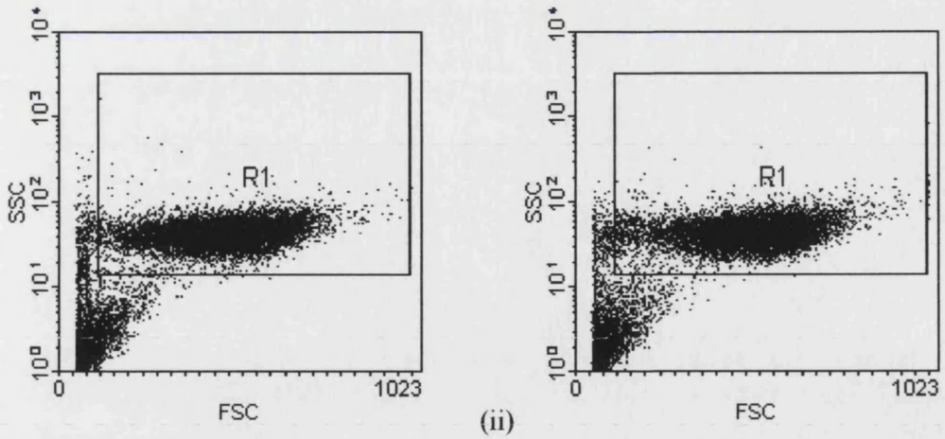

Figure 4.23 Example of a typical Dot-plot diagram of whole FEK4 cells population, (i) negative control group (cells with FDA only) and (ii) sample group (cells with FDA 10 μg/well and treated with N^4,N^9-dioleoylspermine at 11 μg/ml).

The analysis of FDA release was performed by using the same sub-population marking (M1 and M2) as previously described for polyAPS. As an example, in Figure 4.24, N^4,N^9-dioleoylspermine at 11 μg/ml (blue line) shows that the FDA-loaded cells were less fluorescent and the number of FDA-released cells were increased, compared to the control group (grey shade), indicating the change of membrane permeability.

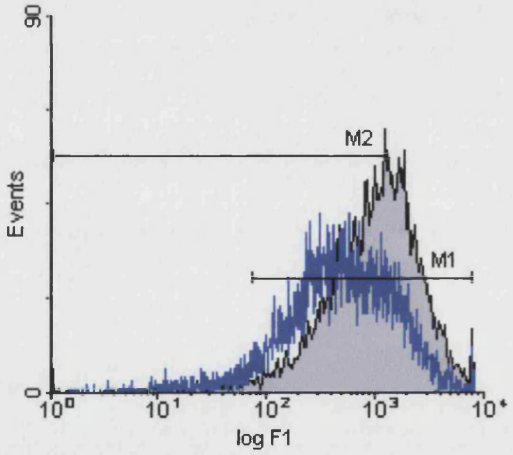

Figure 4.24 Example of typical histograms in FDA release studies (grey shade = control group with FDA only, blue line = N^4,N^9-dioleoylspermine 11 μg/ml) show sub-population M_1 and M_2 groups of FEK4.

In Figure 4.25, the % FDA released cells mediated by N^4,N^9-dioleoylspermine and N^1-cholesteryl spermine carbamate was found to be similar. The level of membrane disturbance

is increased when the vector's concentration is increased. Both vectors showed a comparable effective membrane disturbance (20%) to polyAPS reference at high concentrations. Cells treated with N^1-cholesteryl spermine carbamate displayed slightly higher FDA release.

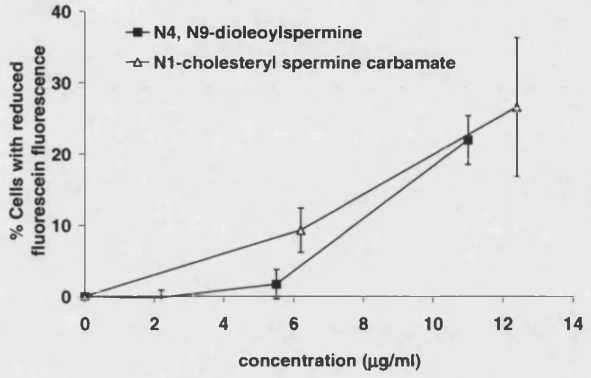

Figure 4.25 Effect of lipopolyamines on fluorescein release in FEK4 cells. FDA (10 µg/well) was pre-loaded for 30 min in FEK4, and N^4,N^9-dioleoylspermine or N^1-cholesteryl spermine carbamate was then added. The M2 population (cells with reduced fluorescence) was measured by FACS and reported as a percentage (M2 = 0% in control cells with no lipopolyamine treatment). (n = 3, error bars are S.D.)

The concentration range of vector used in this experiment is below the level of target (70% survival) and all cells measured are from R_1 (healthy cells). N^4,N^9-Dioleoylspermine at 11 µg/ml (equal to N/P charge ratio = 5.0, for DNA 2 µg/well was used in transfection) shows high FEK4 transfection (70% efficiency) and membrane disturbance (20%). N^1-Cholesteryl spermine carbamate at N/P charge ratio = 12.40 (equal to 12.4 µg/ml) delivers DNA at 60% efficiently and membrane disturbance (25%). Thus, it is highly probable that the increase in membrane interaction of vectors is related to transfection efficiency.

Figure 4.26, the fluorescence intensity of cells (M1), when treated with lipopolyamines, showed a similar decrease in fluorescein intensity in both vectors: N^4,N^9-dioleoylspermine and N^1-cholesteryl spermine carbamate. Cells treated with N^1-cholesteryl spermine carbamate also showed slightly higher FDA-release and lower cellular fluorescein intensity, in the concentration range of vector used in these studies.

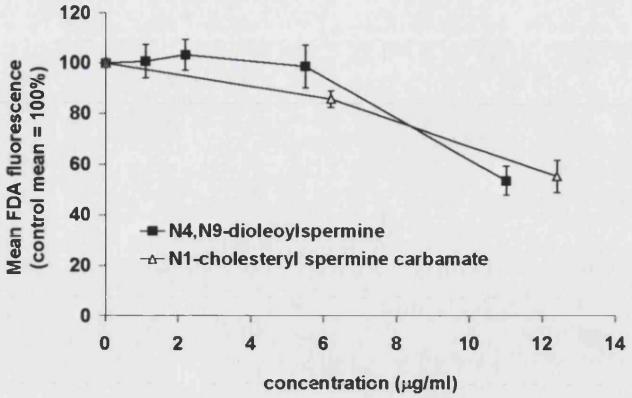

Figure 4.26 Mean fluorescence of FDA-loaded cells (M1) after treatment with N^4,N^9-dioleoylspermine or N^1-cholesteryl spermine carbamate. The M1 population was measured by FACS for its fluorescence intensity. (Mean fluorescence of M1 = 100% in control cells with no lipopolyamine treatment). (n = 3, error bars are S.D.)

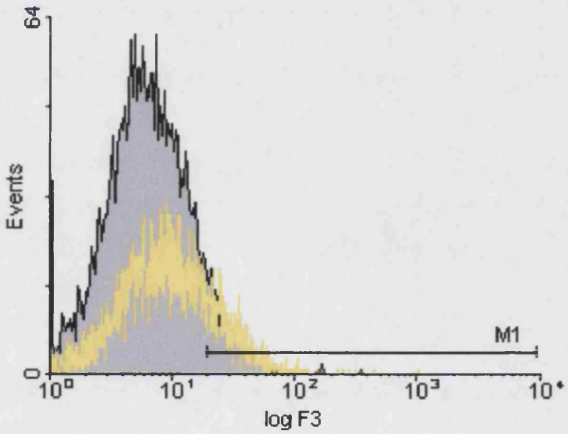

Figure 4.27 Example of typical histograms in PI uptake studies (grey shade = control group, yellow line = N^1-cholesteryl spermine carbamate 12.4 μg/ml) show a sub-population M_1 group of FEK4 used in analysis.

To further understand the membrane effect of lipopolyamines, PI uptake studies were performed. Figure 4.27 is an example of the histograms obtained, N^1-cholesteryl spermine carbamate at 11 μg/ml (yellow line) shows that the treated cells were more fluorescent and the number of PI-uptake cells was slightly increased, compared to the control group (grey shade), indicating the change of membrane permeability. In Figure 4.28, the % PI-uptaken cells mediated by N^4,N^9-dioleoylspermine and N^1-cholesteryl spermine carbamate was found to be different. The level of membrane disturbance is highly increased with the vector's

concentration, in the case of N^1-cholesteryl spermine carbamate. However, both vectors showed less membrane disturbance (less than 10%) than that of polyAPS reference (30%). The similar finding in Figure 4.29 showed that N^4,N^9-dioleoylspermine is less membrane-active than N^1-cholesteryl spermine carbamate at all concentrations used. This difference in membrane activity of both vectors is not highly noticeable in the FDA leakage assay.

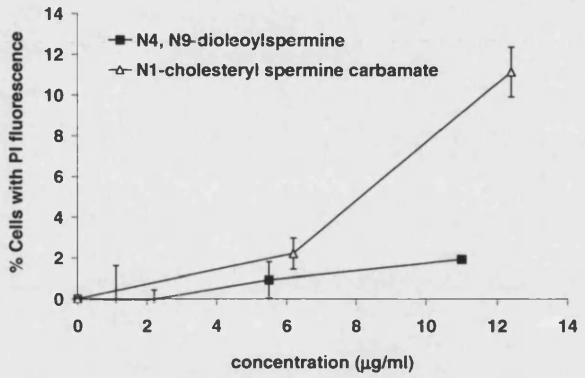

Figure 4.28 Effect of lipopolyamines on PI uptake in FEK4 cells. PI (10 µg/well) was pre-loaded for 30 min in FEK4, and N^4,N^9-dioleoylspermine or N^1-cholesteryl spermine carbamate was then added. The M2 population (cells with reduced fluorescence) was measured by FACS and reported as a percentage (M2 = 0% in control cells with no lipopolyamine treatment). (n = 3, error bars are S.D.)

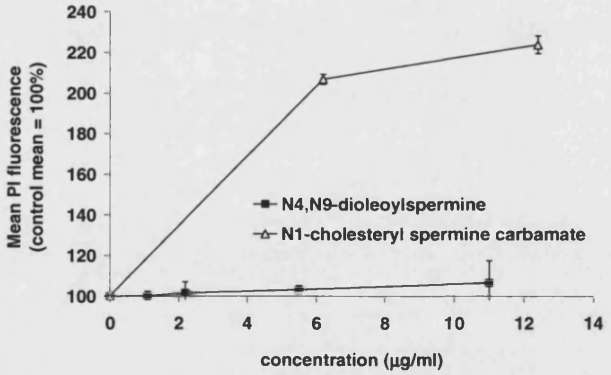

Figure 4.29 Mean fluorescence of cells which uptake PI (M1) after treatment with N^4,N^9-dioleoylspermine and N^1-cholesteryl spermine carbamate. The M1 population was measured by FACS for its fluorescence intensity. (Mean fluorescence of M1 = 100% in control cells with no lipopolyamine treatment). (n = 3, error bars are S.D.)

The difference in FDA release and PI uptake assay may be explained by the nature of the test design and its sensitivity. Ross and co-workers reported that it is recommended to use FDA assay as a first discriminating test, then PI is used as the second test.[234] In our studies, FDA intensity (P1 value, typically in the region of 10^3-10^4) and the number of cells (which release fluorescein, 20-30%) are higher than those of PI (P3 in the region of 10^0-10^1 and % cell with PI at less than 10%). Thus, it is concluded that both N^4,N^9-dioleoylspermine and N^1-cholesteryl spermine carbamate are membrane active (according to the FDA assay) and N^1-cholesteryl spermine carbamate shows superiority in membrane activity. The membrane effect of N^1-cholesteryl spermine carbamate is in agreement with the work of on hemolytic steroidal lipopolyamines by Fujiwara *et al.*[74] In our studies, the selected concentration of N^1-cholesteryl spermine carbamate used is not in the toxic range. So there is no permanent cell break detected as reported in the erythrocyte hemolysis model.[74] However, it is expected that membrane activity of N^1-cholesteryl spermine carbamate must be optimised. As previously discussed in the Chapter 2, N^1-cholesteryl spermine carbamate shows higher toxicity in cells which may also be associated to its higher membrane activity compared to N^4,N^9-dioleoylspermine.

The findings on vector-membrane interaction may be extended to the effects of lipopolyamines on endosomal membranes. The liposomal vesicle leakage assay was used as a model of endosomal escape in a membrane model used by Behr *et al.*[235] Unilamellar liposome (egg phosphatidylcholine (EPC):egg phosphatidylethanolamine (EPE):cholesterol:egg sphingomyelin (ESM) = 10:3:5:2 (mole ratio)) at 100 nm, was loaded with fluorescent dye (calcein, Figure 4.30) to measure membrane fusion activity of fusogenic peptides. However, the FDA release assay we used in our studies is based on the intact cellular membrane, which makes the model more realistic than the liposomal membrane.

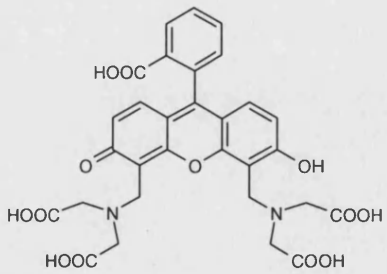

Figure 4.30 Calcein

Even though nuclear membranes[236]also contain double phospholipid layers, they also incorporate more complicated structures than those in cellular and endosomal membranes, such as nuclear pore complex, endoplasmic reticulum network, nuclear lamina proteins.

These proteins and membrane structure are important for a variety of cell functions, including nuclear assembly, replication, transcription, and nuclear integrity. More studies are needed to apply the lipopolyamine-membrane interactions to the nuclear membrane especially any interactions of lipopolyamines and nuclear proteins. This will eventually promote the nuclear entry ability of NVGT vectors.

Fluorescent DNA as a tool in NVGT studies

Fluorescent DNA is a useful probe to gain insight in the NVGT process and barriers, such as cell entry[92,128], intracellular trafficking and nuclear entry.[92,128,129] This information is important to the development of safe and effective gene delivery vectors. In these experiments, pEGFP was covalently labelled with tetramethylrhodamine (TMR) and 5-carboxy-X-rhodamine (CXR) by alkylation to nucleic base (guanine) on DNA double helix. The labelling protocol is described in the Experimental chapter.

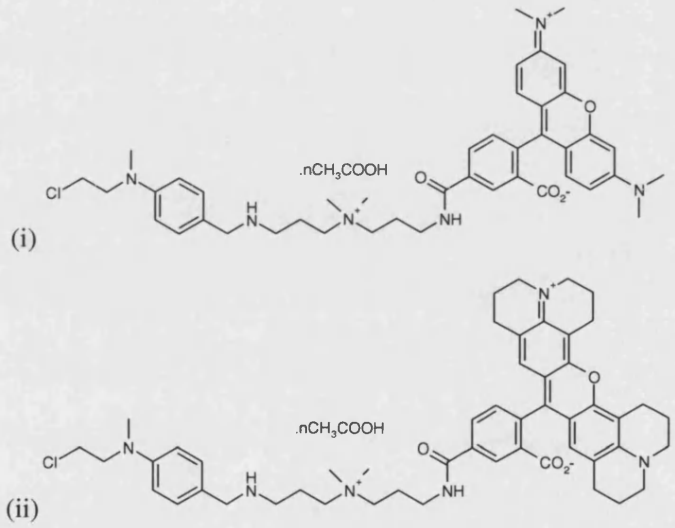

Figure 4.31 (i) Label IT-TM-rhodamine (TMR) and (ii) Label IT CX-rhodamine (CXR)

DNA alkylating reagents shown in Figure 4.31 offer a simple way to label plasmid DNA in one step without using enzyme or radioactive probes. Both molecules (Label IT-TM-rhodamine (TMR) and Label IT CX-rhodamine (CXR)) contain the aromatic nitrogen mustard group which bind covalently to the N^7 of guanine residues in DNA, and different fluorophores allowing the tracking of DNA within cells.[237] The base/dye mole ratio obtained from UV measurement at 260 and 546 nm (for TMR) or 597 nm (for CXR) was approximately 165. Thus, the labelling molecules are present on every 80 base-pairs or calculated as 1% of plasmid bases. The transfection experiments by introducing these

fluorescent plasmids were performed to evaluate the impact of labelled guanine in DNA transcription process and to determine the optimal labelling ratio.

Given the high cost of labelling chemical, DNA (1 µg/well) was used in the smaller amount than the general FEK4 transfection protocol (2 µg/well). In the previous study regarding the dose-response effect of lipoplexes (Chapter 2), the level of gene expression in the low DNA scheme is comparable to the standard amount used. The N/P charge ratio 2.0 was chosen in these studies due to its high transfection efficiency and safety. Non-labelled plasmid (1 µg/well) was used as control at same N/P ratio.

FACS analysis of transfected FEK4 with TMR-pEGFP by N^4,N^9-dioleoylspermine were operated by using dual emission detection i.e. F1 and F2. F1 (530 +/- 15 nm) was able to detect EGFP, a fluorescent protein decoded from pEGFP. F2 (575 +/-15 nm) was able to detect TMR-pEGFP (fluorescent plasmid) at single excitation at 488 nm. Though the λ_{ex} of TMR is at 546 nm, the fluorescence spectrum obtained with this labelled plasmid shows that it is possible to excite TMR at 488 nm to gain emission at 576 nm.

From Table 4.1, it was found that TMR labelled DNA at 1% of plasmid bases appears to have no effect to the transfection level. Both intact pEGFP and TMR-pEGFP reached the similar transfection efficacy at 20%. However, from the F2 measurement, fluorescence intensity at 576 nm (which detect TMR-labelled plasmid) was detected at higher level in FEK4 cells transfected with TMR pEGFP (8% difference). This is an evidence of intracellular delivery of TMR-labelled DNA into FEK4 cells.

Table 4.1 Gene expression and cellular entry level of TMR-pEGFP in FEK4 using N^4,N^9-dioleoylspermine

FEK4 cells sample	F1 %	Transfection efficacy at N/P 2.0 (%)	F2%
TMR-pEGFP 1 µg/well	23.25 %	19.08 %	16.66 %
pEGFP 1 µg/well	22.48 %	18.31 %	8.47 %

Figure 4.32, CXR was used to label pEGFP in FEK4 transfection using N^4,N^9-dioleoylspermine. The result of pEGFP expression in both intact and labelled plasmid was comparable in both N/P charge ratios. Recently Slattum *et al.*'s research group also reported that the covalently labelled plasmids (pCILuc, pEGFP, pEYFP-Nuc) remains expression

competent.[237] Fluorophores and labelling ratio are the key factors contributing to level of gene expression. However, gene expression was still remained in highly labelled (50 label/plasmid), possibly from the transcriptional read-through of the modified bases or repair of modified bases.[237]

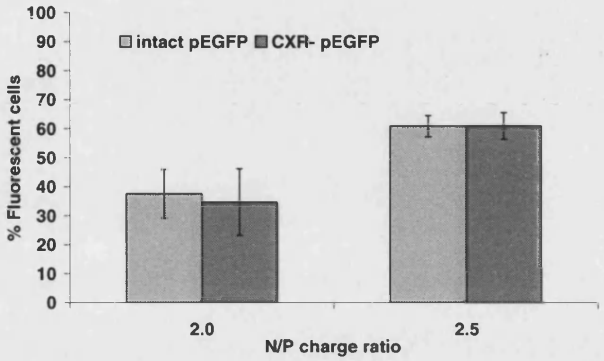

Figure 4.32 Transfection results of intact pEGFP and CXR-labelled pEGFP in FEK4 using N^4,N^9-dioleoylspermine.

It is concluded that covalently fluorescent labelling to DNA provide a safe (non-radiative) and convenient way to probe DNA for NVGT research. It can be used as a tracking tool of DNA in cells. Additionally TMR and CXR labelled DNA can also be used in fluorescent-pair study, or FRET (fluorescence resonance energy transfer). FRET is a technique where the energy change of donor-acceptor is measured. For example, fluorescein (donor, which may be conjugated to gene vectors) was excited at λ_{ex} = 490 nm), it emits the fluorescence (energy) at λ_{em} = 513 nm and this further excite TMR-or CXR-labelled plasmids (acceptor). The fluorescence at their respective emission wavelength is then measured, and it is possible to derive the distance and interactions of donor (vector) and acceptor (DNA) molecule.[195]

Fluorescent lipopolyamine synthesis

From our studies, fatty-acid based lipopolyamine was established as an efficient DNA condensation agent and *in vitro* transfecting reagent. Aiming to maintain the DNA-condensing properties of N^4,N^9-dioleoylspermine, the key structures we incorporated in our fluorescent lipopolyamine are (1) polycation moiety with two primary amine groups maintained at terminal carbon atoms, (3) lipophilic moiety selected from fatty acids with C12-18, and (3) small or no bulky effect from fluorophores. The example of fluorescenct lipopolyamines are shown below (Figure 4.33).

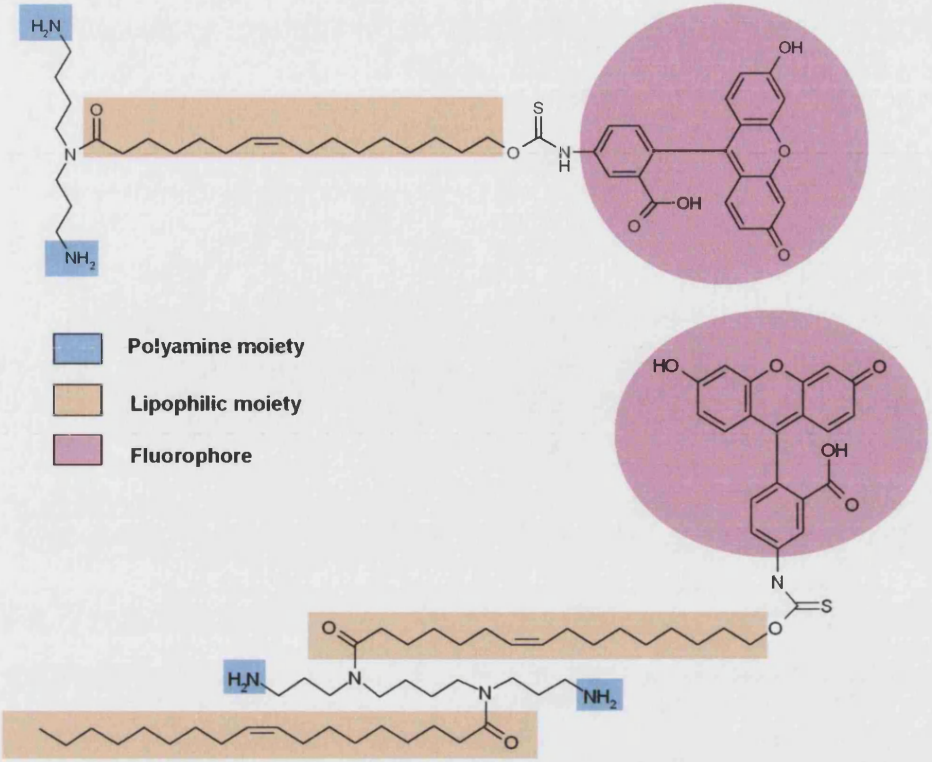

Figure 4.33 Fluorescent lipopolyamines with three major moiety (i) polyamine moiety, (ii) lipophilic moiety, and (iii) fluorophore.

The fluorescent probes derived from lipopolyamines are initially designed by conjugating fluorophores at fatty acid chain position, and not through the conjugation at the polyamine backbone. Unsaturated long-chain fatty acids (to resemble oleoyl chain) with functional group (e.g. OH, NH_2) would be essential in fluorophore conjugation. Our preferable fatty acids should have 12-18 carbons to mimic the fatty acids in cellular membrane phospholipids. For example, 12-hydroxy-(*cis*)-9-octadecenoic acid (ricinoleic acid, Figure 4.34) is commercially available. However, the fluorophore molecule may provide a bulky-group effect to the whole structure so a fatty acid with -OH or -NH_2 at the terminal carbon atom is more preferable. In our synthetic scheme, 16-hydroxy-7-hexadecenoic acid was chosen for the synthesis. It was prepared by the alkaline hydrolysis (saponification) of ambrettolide, as shown in Figure 4.35.

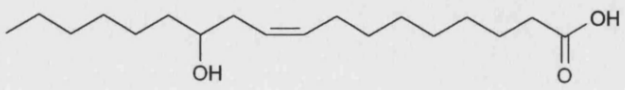

Figure 4.34 Ricinoleic acid

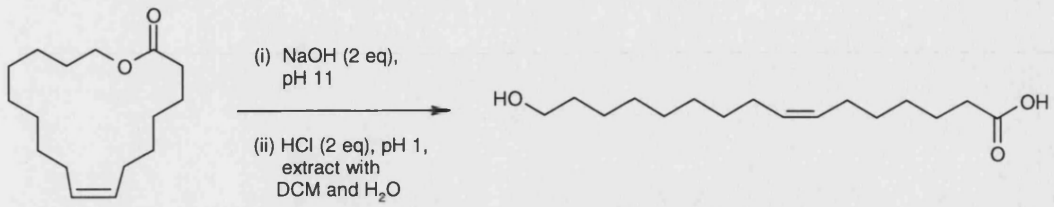

Figure 4.35 Preparation of *Z*-16-hydroxy-7-hexadecenoic acid

Considering the problem with bulky effect from fluorophore, a polyamine conjugate with only one fatty acid chain with fluorophore is most preferable. Giving this, spermidine backbone was chosen in our synthesis, as it provides two primary amine groups and one available secondary amine group for conjugation with a fatty acyl moiety. From chemistry aspects, fluorophores (examples are shown in Figure 4.36) typically contain OH-reactive or NH_2-reactive groups, such as thiocyanate, acid chloride, or otherwise -COOH group which form amide/ester bond using DCC/HoBt as catalysts. However, most fluorophores are big molecules, thus may affect the physico-chemical property of lipopolyamines. A small fluorophore, *N*-methylanthranilic acid (*N*-MANT), was also included in this experiment.

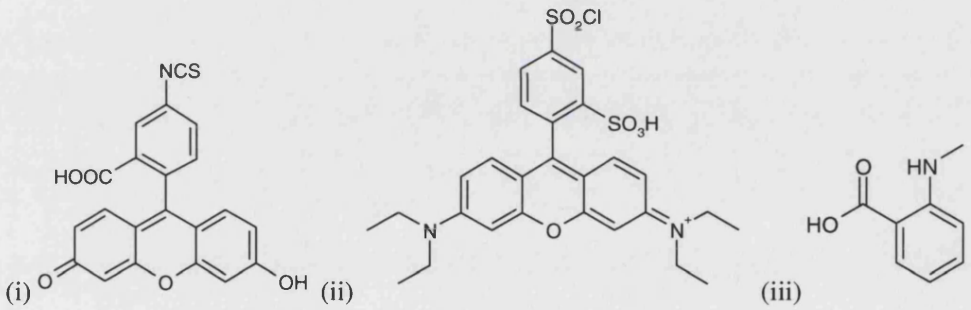

Figure 4.36 (i) Fluorescein isothiocyanate (FITC), (ii) lissamine rhodamine B sulfonyl chloride, and (iii) *N*-methylanthranilic acid (*N*-MANT)

Synthetic procedure of fluorescent lipospermidine

Spermidine was used in this experiment, as it supports our designed fluorescent lipopolyamine. Similar to the synthesis of N^4,N^9-dioleoylspermine (Figure 2.3 in Chapter 2), spermidine was trifluoroacetylated at N^1 and N^9 to yield the di-protected spermidine with one available amino group at N^4. Protected spermidine was then conjugated to *Z*-16-hydroxy-7-hexadecenoic acid, using DCC/HOBt catalysis. In these experiments, FITC and MANT were chosen as fluorophores of choices. The synthetic procedure of N^4-(16-FITC-7-hexadecenoyl)-spermidine is shown in Figure 4.37.

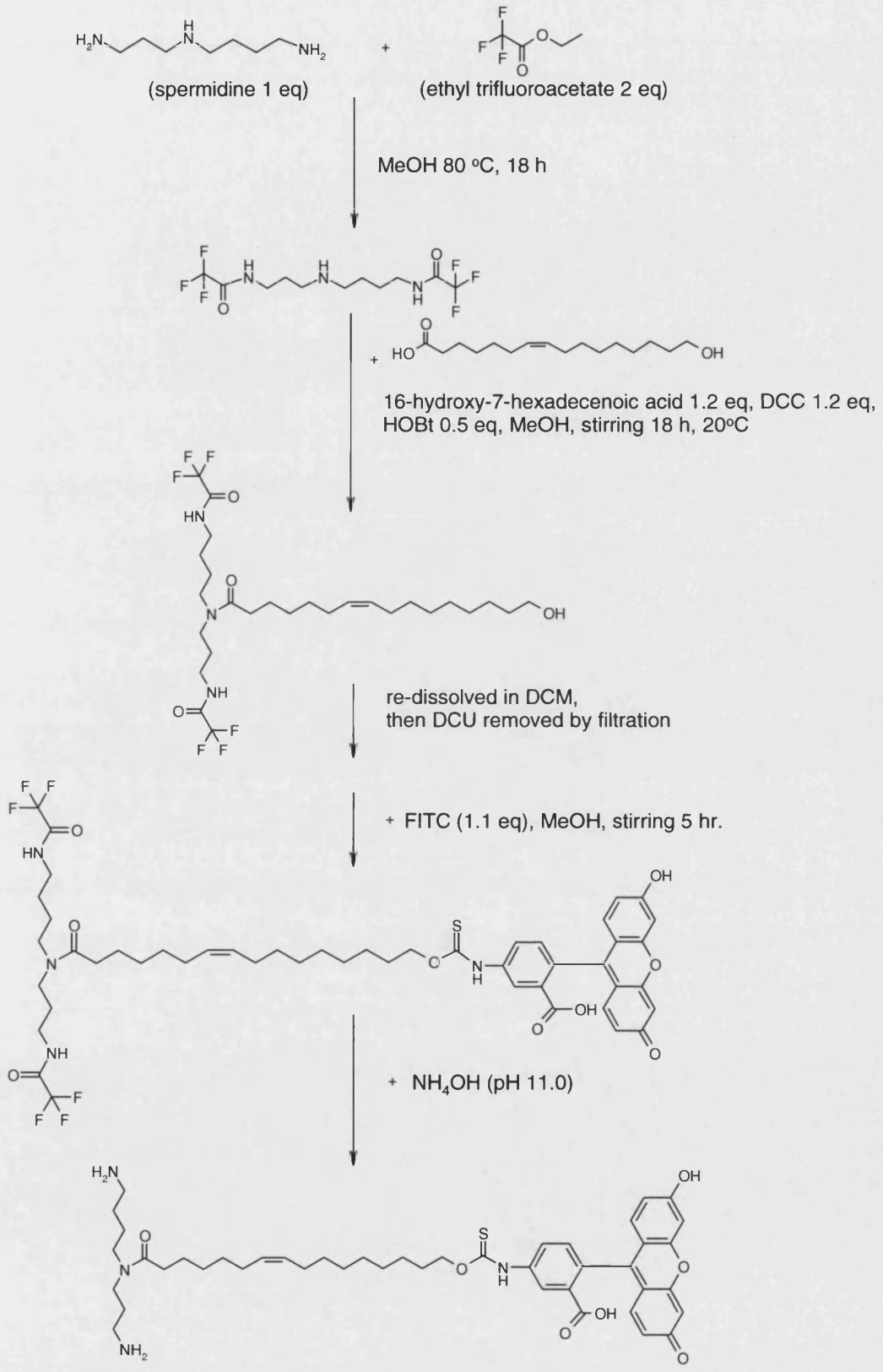

Figure 4.37 Synthesis of N^4-(16-FITC-7-hexadecenoyl) spermidine

N^4-(16-FITC-7-hexadecenoyl)-spermidine obtained from this synthesis show the comparable fluorescence spectra (λ_{ex} = 492 nm, λ_{em} = 516 nm) to its parent fluorophore (FITC, λ_{ex} = 490 nm, λ_{em} = 513 nm) as shown below. This shows the lipospermidine moiety do not affect the fluorescence of FITC, which is a desirable characteristic of fluorescent lipopolyamines.

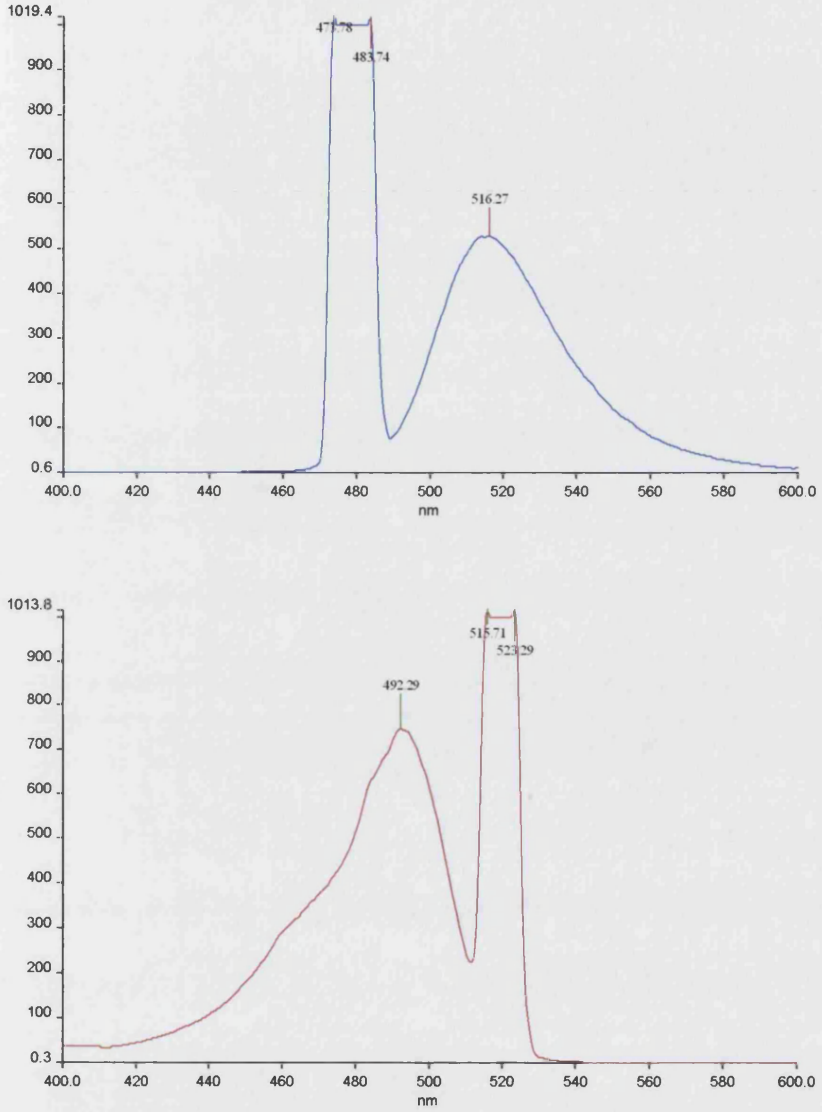

Figure 4.38 Fluorescence spectrum of N^4-(16-FITC-7-hexadecenoyl) spermidine in MeOH; (blue line) emission spectrum (λ_{em} = 516 nm) and excitation spectrum (λ_{ex} = 492 nm) (slit width 5 mm, scan rate 100 nm/min

N^4-(16-MANT-7-hexadecenoeyl) spermidine is another fluorescent lipopolyamine we synthesised. N^1,N^9-Di-trifluoroacetyl-N^4-(16-hydroxy-7-hexadecenoyl)-spermidine was prepared in the same way (Figure 4.38). This protected lipospermidine was then conjugated to MANT using DCC/HOBt as catalysis. The last stage of deprotection was carried out using aq NH_4OH solution (pH 11.0).

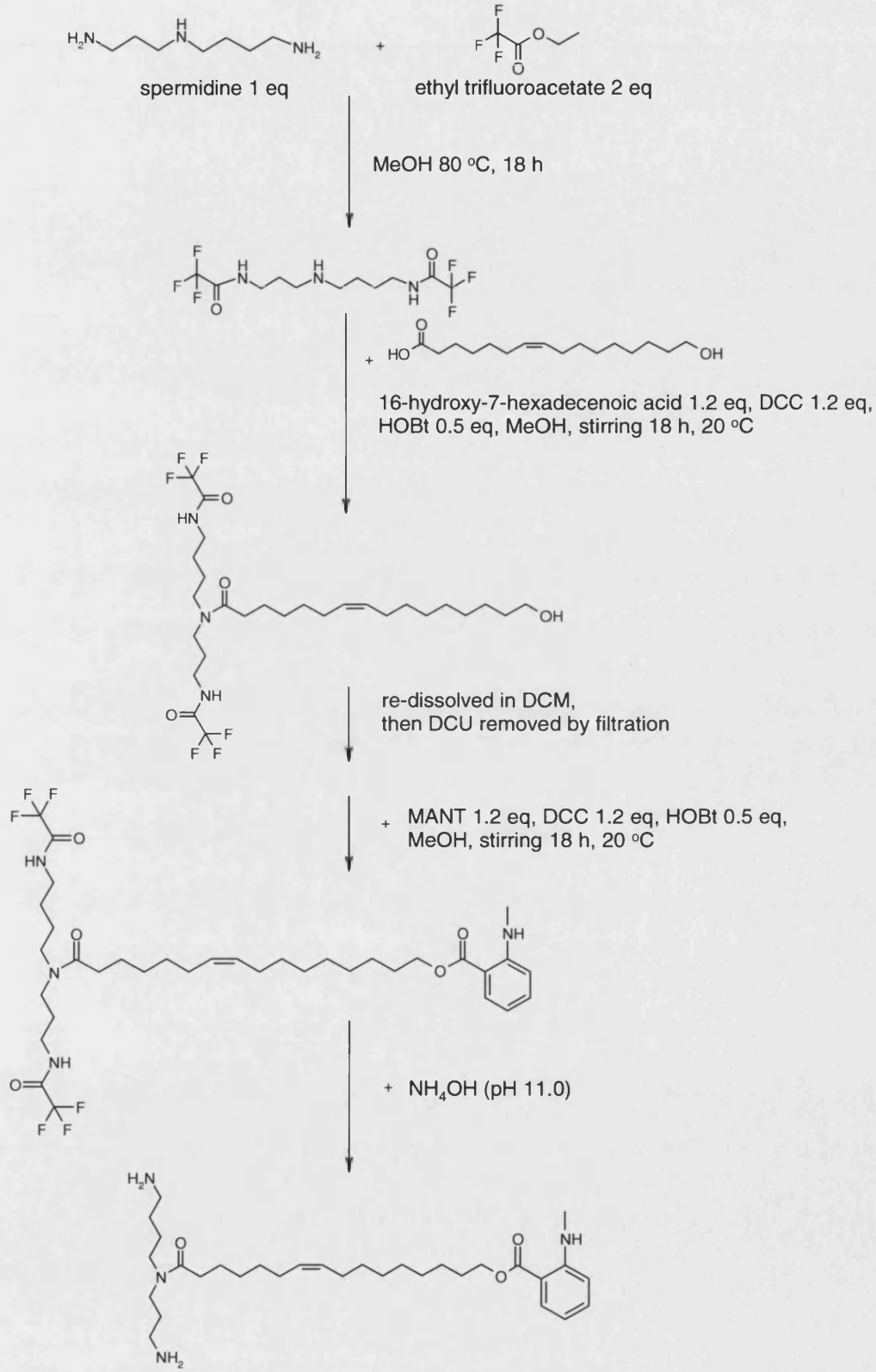

Figure 4.39 Synthesis of N^4-(16-MANT-7-hexadecenoyl)-spermidine

In addition to fluorescent lipospermidines, we also prepared N^1,N^{12}-di-trifluoroacetyl-N^4-oleoylspermine which can be used as a starting lipopolyamine (similar to the starting spermidine in the previous examples in Figures 4.37 and 4.39) to construct fluorescent lipopolyamines.

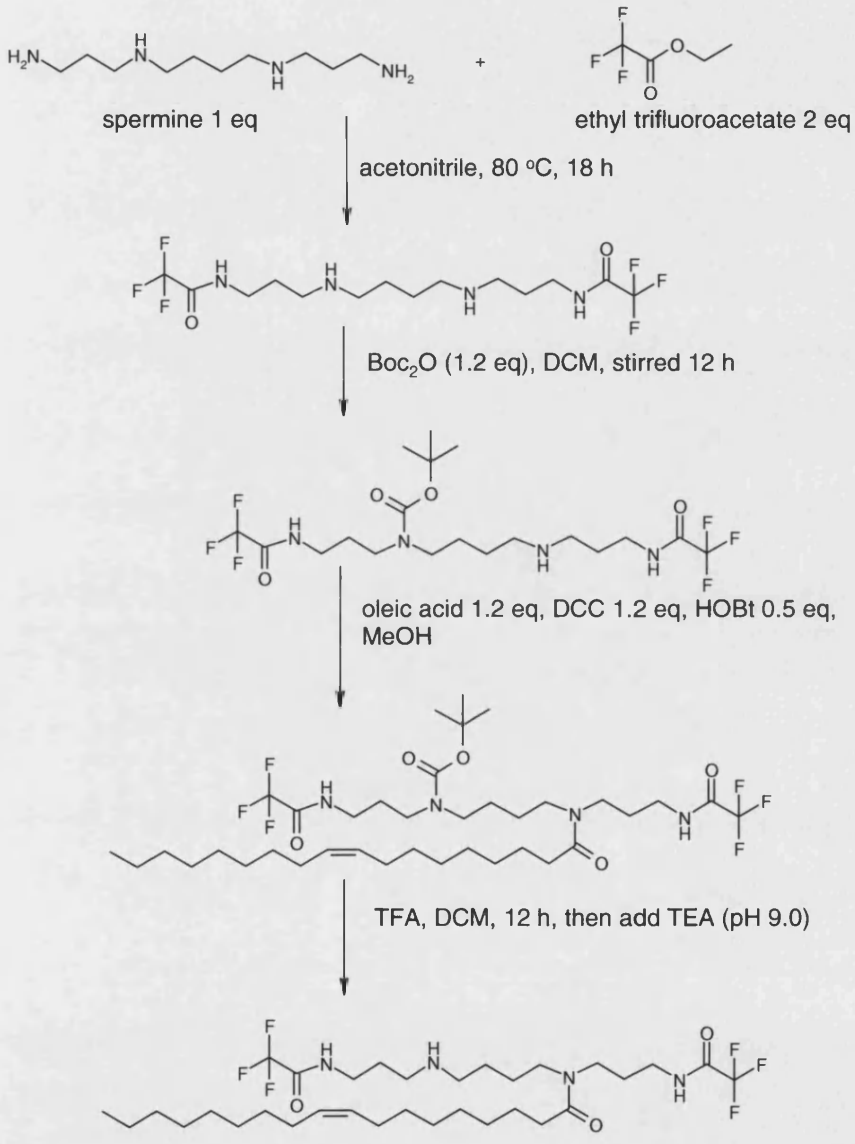

Figure 4.40 Synthesis of N^1,N^{12}-di-trifluoroacetyl-N^4-oleoylspermine

The synthesis involves a two-step orthogonal protection of amino group of spermine. Firstly, spermine was protected by using the selective trifluoroacetylation at N^1 and N^{12}. Diprotected spermine was then protected with Boc (Boc:spermine = 1:1 mole ratio) to yield N^1,N^{12}-di-trifluoroacetyl-N^4-Boc-spermine. This tri-protected spermine was then conjugated to oleic

acid (1 eq of spermine) to yield N^1,N^{12}-di-trifluoroacetyl-N^4-Boc-N^{12}-oleoylspermine. N^1,N^{12}-Di-trifluoroacetyl-N^4-oleoylspermine was obtained by Boc removal. The summary of this synthesis is shown in Figure 4.40.

This mono-oleoyl spermine can be used as the starting chemical to conjugate with Z-16-hydroxy-7-hexadecenoic acid, to obtain the lipospermine with one oleic acyl chain and one hydroxyl fatty acyl chain, with the hydroxyl functional group available for fluorophore conjugation. This probe will resemble N^4,N^9-dioleoylspermine in the aspects of two lipid chains with two terminal primary amino groups. It should occupy a similar 3D shape (isosteric) and possess a similar charge pattern (isoelectronic).

Due to time constraints in the project, the evaluation of DNA condensation of two fluorescent lipopolyamines, N^4-(16-FITC-7-hexadecenoyl)-spermidine and N^4-(16-MANT-7-hexadecenoyl)-spermidine, has not been performed. However, fluorescence techniques are highly sensitive and it is possible to use these probes at low concentrations. These probes may be used as reporting tools in NVGT studies, even if not as a principal DNA delivery agent. In the systems to be studied using these probes, the gene vectors of interest should play the major role in DNA condensation and delivery into cells. Additionally, the transfection experiments were not conducted, as it is not expected that these probes to promote or inhibit the DNA delivery at the low concentration as a reporting probe.

Conclusions

The research described in this thesis covers the chemical, biological, and biophysical studies of lipopolyamines with respect to their applications in NVGT. N^4,N^9-Dioleoylspermine was designed based on tetracationic spermine conjugated to two C18 oleoyl chains which resemble both membrane phospholipids (di-fatty acyl glycerol phosphate) and a synthetic helper lipid (DOPE - dioleoylphosphatidyl-choline). N^1-Cholesteryl spermine carbamate was produced in this work, incorporating cholesterol as the lipophilic moiety. EthBr fluorescence quenching assays were used to assess the DNA condensation ability of these synthetic lipopolyamine vectors. The DNA binding constants of N^4,N^9-dioleoylspermine and N^1-cholesteryl spermine carbamate were similar to EthBr ($K_b = 1 \times 10^7\ M^{-1}$) and 5-times higher than that of (unconjugated) spermine ($K_b = 0.2 \times 10^7\ M^{-1}$). The quality of DNA condensation by these vectors is also significantly improved over that of spermine (90% reduction of fluorescence) at N/P charge ratios 2.0-2.5. Light scattering assays were used to confirm the presence of DNA complexes, apparent absorption being an indication of particle formation.

The gene delivery efficacy of both vectors was studied in primary cells (FEK4) and in a carcinoma (HtTA-1 HeLa) cell culture model. These models represent applications in corrective and cancer gene therapy. In the transfection experiments using plasmid DNA with marker genes (pEGFP and pGL3), both N^4,N^9-dioleoylspermine and N^1-cholesteryl spermine carbamate were shown to be superior to Lipofectin, a common commercially available transfecting cationic lipid. We achieved high levels of transfection in both cell lines routinely reaching 60-90% for transfected cells. These are high efficiency values in primary cell lines. N^1-Cholesteryl spermine carbamate showed higher transfection efficiency at higher N/P ratios than N^4,N^9-dioleoylspermine. The improvement in vectors resulted from the design of molecules incorporating both a polyamine and a lipophilic moiety. Both NVGT vectors showed low toxicity (survival greater than 70%) in the MTT cytotoxicity assay while maintaining their high transfection efficiency. Excess NVGT vectors in DNA complexes are generally known for increased toxicity when used at high N/P charge ratios, such as PEI. The uncomplexed form of our lipopolyamines showed no difference in cellular toxicity, compared to their lipoplexes when used at the same concentration. In conclusion, safe and highly efficient lipopolyamine vectors have been developed for non-viral DNA delivery. In particular, the new non-liposomal system with N^4,N^9-dioleoylspermine has the ability to transfect primary skin cells more efficiently than the commercially available liposomal Lipofectin. Whilst both our non-liposomal lipopolyamines are efficient at transfecting rapidly dividing cancers (HtTA-1 HeLa) cells.

DNA nanoparticle formation, the first important step in NVGT, was studied in detail. In this part of the research project, the DNA condensation process was investigated at a single nanoparticle (equivalent to a single molecule) level by using the technique of fluorescence correlation spectroscopy (FCS). A small fluorescent probe, PicoGreen (PG), was used as a reporter to monitor the interactions between the lipopolyamine and the polynucleotide.

We have studied two circular plasmid DNAs (pEGFP and pGL3) and linear DNA (calf-thymus DNA) using two lipopolyamines. The FCS confocal volume where DNA complexes were detected, was cylindrical in shape and small enough (0.9 ± 0.1 femtolitre) with dimensions ($\omega_1 = 0.29 \pm 0.05$ μm, $\omega_2 = 1.69 \pm 0.02$ μm) which enabled us to detect a single DNA nanoparticle in this study. N^4,N^9-Dioleoylspermine is able to condense DNA into point-like molecules (a fully condensed particle) as shown by determining the particle number (PN) value in both DNA models, but N^1-cholesteryl spermine carbamate showed poorer DNA condensation efficiency at similar N/P charge ratios. Lipid moieties are important to the quality of DNA nanoparticles obtained in the DNA condensation process. The technique of Time-resolved FCS (TR-FCS) was developed to monitor the dynamics of

PG in interactions with DNA duplex. These results support the use of PG as a reliable probe for the nanoparticle formation process. From the decay kinetics of PG, we are able to establish the detailed steps of the fluorescence reporting mechanism of PG during the DNA condensation process. These steps are (i) PG-binding to DNA, (ii) PG release due to DNA-conformational change, and (iii) PG quenching. A reliable and novel PG-based platform to monitor the formation of a single DNA nanoparticle was established and validated, based on our understanding of the behaviour of this fluorescent probe.

Studies of the NVGT process, focusing on the cellular membrane barriers in lipopolyamine-mediated gene delivery, were performed to gain more insight into cell entry, endosomal escape, nuclear entry, and also the cellular toxicity of the vectors. PolyAPS, a polymeric extract from a marine sponge comprising of C8-alkylpyridinium monomer, was studied as a model of a membrane-active NVGT vector. In DNA condensation studies, polyAPS showed the equivalent binding affinity to pEGFP ($K_b = 0.2 \times 10^7\ M^{-1}$) to that of spermine. However, polyAPS efficiently and fully condensed DNA with 10% residual fluorescence unlike spermine (50% residual fluorescence). This is possibly due to the polymeric nature of polyAPS. This novel vector also shows high membrane activity in our studies using fluorescein *O*-diacetate (FDA) release and propidium iodide (PI) uptake assays. PolyAPS highly induced pore formation (20-30% compared to 0% in untreated cells) on the membrane. This leads to the release of hydrophilic fluorescein (a fluorescent product of FDA hydrolysis by cellular esterase) from cells, or the uptake of PI in to cells. The mean fluorescence intensity of fluorescein of polyAPS-treated cells was significantly lower (2 times) from untreated FEK4 cells. In PI studies, the mean fluorescence intensity of PI of polyAPS-treated cells was also higher from the control. The results from both assays indicate the change in membrane permeability caused by polyAPS.

Lipoplexes prepared from our synthetic vectors gain entry into cells mainly by endocytosis (70-90%), thus it is highly possible (30-10%) that both N^4,N^9-dioleoylspermine and N^1-cholesteryl spermine carbamate also interact with membranes by other pathways, possibly involving pore formation. Fluorescent dye transport studies showed that both NVGT vectors are membrane-active, compared to spermine and comparable to polyAPS. N^4,N^9-Dioleoylspermine and N^1-cholesteryl spermine carbamate were found to induce pore formation (10-20% comparing to 0% in untreated cells) in a concentration-dependent manner. More research on the key moiety responsible for membrane-activity may lead the way to the development of membrane-disruptive lipopolyamine vectors, a new sub-class of lipopolyamines. This will ultimately enhance the overall efficiency of this novel NVGT gene delivery system.

To better understand the efficiency of each step in non-viral gene delivery, more novel tracking molecules are needed. Fluorescent lipospermidine probes were therefore designed and synthesized. The aim is to use them as biosensors in gene delivery. Fluorescence techniques can potentially play important roles in all areas of NVGT research. Fluorescent lipopolyamines are tools enabling the intracellular tracking of DNA complexes to reveal (both spectroscopically and microscopically) the key steps and barriers in gene delivery. Additionally, the preparation of fluorescent-labelled DNA was also included in the study, which we established can be used in transfection without compromising its high efficiency in gene expression. Fluorescent labelling of DNA can be used as a complimentary tool with lipopolyamine probes for studies of fluorophore-interactions which represent the interaction of DNA and its cationic carrier. Advanced fluorescent techniques and their combination may be used with these fluorescent tools for future research towards the goals of even more efficient NVGT. Designed small molecule probes will play their part in this. The detail of the Experimental section of this research is to be found in the next Chapter.

Chapter 5

Experimental

General information about materials used in experiments

Equipment used in chemistry experiments

Analytical thin layer chromatography (TLC) was conducted on pre-coated silica gel plates (Merck TLC aluminium sheets silica 60 F_{254}). Chromatograms were visualised with UV light (254 or 366 nm) or stained with ninhydrin (0.3 % w/v solution in methanol (MeOH)). Flash column silica gel was obtained from BDH. Preparative flash column chromatography was performed on columns packed with a slurry of silica gel 60 (35-75 μm), either under gravity or under pressure with an aquarium-type pump.[238] Sand (acid washed) was used to cap the column of silica gel, and pre-washed with the solvent used in each separation system.

Infra-red spectra was recorded as a film (liquid sample), or prepared as a slurry with liquid paraffin (one drop by using a Pasteur pipette) on a NaCl disc, using a Perkin Elmer Spectrum RXI FT-IR spectrophotometer. A JOEL EX400 instrument at 400 MHz was used to record ^{1}H NMR and ^{13}C NMR spectra. Chemical shifts (δ, in parts per million) are measured by reference to tetramethysilane in ^{1}H NMR spectra and solvent signals in ^{13}C NMR spectra. High and low resolution FAB mass spectra (positive ion mode, unless otherwise indicated) were measured on a VG AutoSpec Q spectrometer, using *m*-nitrobenzyl alcohol as the matrix.

Semi-preparative RP-HPLC was performed with a Jasco PU-980 pump with either a Jasco UV-975 detector or a Water 470 scanning fluorescence detector (Millipore), and a printer with chart speed set at 1 cm/min. The stationary phase was a Supelcosil ABZ+ Plus, 5 μm (25 cm x 10 mm) column. LC-MS was performed on a Waters Alliance 2790 LC module connected to a Waters Micromass ZQ (Waters, UK).

The UV spectrophotometer used in particle light-scattering experiments was a Helios UV spectrophotometer. Fluorescence studies were run with Perkin-Elmer Fluorescence Spectrophotometer Model LS50B with a 3 ml glass cuvette (1 cm pathlength), slit width set at 5 nm, with FLWinLab version 2.00 for data processing.

Equipment used in cell biology experiments

A temperature-controlled flask shaker (New Brunswick Scientific, NY, USA) was used to cultivate transformed *E. coli* for plasmid propagation. Centrifuges used in experiments include a Beckmann floor centrifuge model J2-MC (Beckman Coulter, Buckinghamshire, UK), a bench-top centrifuge (MicroCentaur MSE, UK), and a cells centrifuge (Falcon 6/300 MSE Sanyo, UK). Microbial incubation was performed in a temperature-controlled incubator (Heraeus Instrument, UK).

All aseptic techniques for cell culture were carried out in a laminar flow cabinet (Intermed MDH Ltd, UK) designed for vertical re-circulation of air. A temperature-controlled waterbath (Grant, UK) was used to warm the media used in cell biological studies at 37 °C. Cells were cultured in a LEEC PF2 humidified atmosphere at 37 °C with 5% CO_2 95% air (v/v) incubator (Sanyo, Japan). For experiments using low temperature, a refrigerator (Lec, UK) with the temperature controlled at 12 °C was used without CO_2 supply. Cells were visually assessed daily for evidence of microbial contamination under an inverted light microscope (Wilovert, UK).

Biochemical reactions in 96-well plates were generally mixed on a plate shaker (Gyro-Rocker STR9, Bibby, UK) and read using a plate-reader, either a Dynatech MR 5000 with Biolinx assay software or a VERSAmax™ spectrophotometer. Becton Dickinson FACS Vantage dual laser instrument (argon ion laser 488 nm) was used in all FACS experiments. A TD-20/20 luminometer (Turner Designs, USA) was utilised to measure luminescence.

Disposable items in experiments

Sterile 75 ml and 150 ml top tissue culture flasks were obtained from TPP (Trasadingen, Switzerland). Multi-well (6, 12, and 96 wells) plates and 8-chamber cuvettes were obtained from NUNC (Leicestershire, UK). Plastic plates (6 cm diameter), pipettes (5, 10, and 25 ml), pipette tips and Pasteur pipettes were obtained from Fisher (Leicestershire, UK). Cryopreservation ampoules used for storing frozen cells in liquid nitrogen were obtained from Corning Ltd. (Leicestershire, UK). Ultracentrifuge tubes were obtained from Eppendorf Ltd. (Leicestershire, UK). Polypropylene tubes for a luminometer were obtained from Promega (Southampton, UK). Sterile Falcon polypropylene tube (15 and 50 ml) and FACS polystyrene test tubes (12 x 75 mm) were obtained from Falcon (Leicestershire, UK).

Chemicals used

Chemicals used in media preparation were all purchased from Gibco (Paisley, UK). Ambrettolide was a gift from IFF-Benicario, Spain. PicoGreen was obtained from Invitrogen (Paisley, UK). Label IT ® nucleic acid labelling kits were purchased from Mirus (Madison, USA). Luciferase assay kits were purchased from Promega (Southampton, UK). Lipofectin and Lipofectamine were obtained from Invitrogen (Paisley, UK). Other chemicals were purchased from Sigma-Aldrich-Fluka (Dorset, UK). All chemicals were used without further purification. MilliQ water, which was obtained from a MilliQ PF Plus system with ultrafiltration cartridge (Millipore UK, Ltd., Watford, UK), free of DNase and RNase, was used in all biological and HPLC experiments. Unless otherwise specified, distilled water was used in all other experiments. All organic solvents used were of GPR or

HPLC grade and purchased from Fisher (Leicestershire, UK). Solvents were evaporated using a rotary evaporator (Buchi R411, UK) in a temperature-controlled water bath (Buchi B480, UK) under a vacuum system (Vario.PC2001, UK).

Synthesis of N^4,N^9-dioleoylspermine

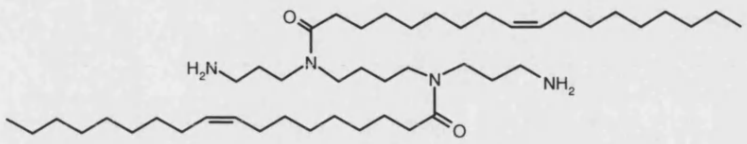

Figure 5.1 N^4,N^9-Dioleoylspermine

Materials

Spermine, ethyl trifluoroacetate, 1,3-dicyclohexylcarbodiimide (DCC), *N*-hydroxy-benzotriazole (HOBt), oleic acid, and ninhydrin for TLC detection were obtained from Sigma-Aldrich (UK). Acetonitrile (MeCN), dichloromethane (DCM), ethyl acetate (EtOAc), absolute ethanol (EtOH), and MeOH were purchased from Fisher Chemicals (UK). Ammonia solution (aq NH_4OH, 33% v/v) was from BDH Laboratory (UK).

Preparation of N^1,N^{12}-di-trifluoroacetylspermine

Spermine 1 g (1 eq, 4.94 mmoles) was dissolved in MeCN (15 ml) and treated with 2 eq ethyl trifluoroacetate dissolved in MeCN (15 ml). The mixture was then stirred and heated under reflux (18 h) at 80 °C. Then, MeCN was removed by evaporation and trifluoroacetylated spermine products were washed twice with EtOAc. A pale-yellow coloured solid (m.p. 195-198 °C) was obtained after removal of all solvents.[137] The obtained sample, when analysed by TLC using MeOH/NH_4OH (4/1 v/v), gave R_f = 0.8 which shows the increased lipophilicity compared to spermine (R_f = 0.1).

Preparation of N^1,N^{12}-di-trifluoroacetyl-N^4,N^9-dioleoyl spermine

Protected spermine was dissolved in DCM (5 ml) and MeOH (as needed to dissolve all the spermine), then oleic acid (2.2 eq), DCC (2.4 eq), and HOBt (1.0 eq) were added. The reaction was carried out at 20 °C with thorough stirring for 18 h. After removal of all the solvents, the tetra-amide was re-dissolved in DCM which allowed DCU to precipitate. The mixture was filtered to obtain a clear yellow solution. The solution showed R_f = 0.8 when analysed by TLC with mobile phase MeOH/NH_4OH (4/1 v/v) against oleic acid (R_f = 0.2). The TLC plate was then observed under UV for C=C double bond of oleic acid, and then derivatised with ninhydrin solution to detect amine groups. The product showed positively with both UV and ninhydrin solution (when heated).

Deprotection of N^1,N^{12}-di-trifluoroacetyl-N^4,N^9-dioleoyl spermine

N^1,N^{12}-Di-trifluoroacetyl-N^4,N^9-dioleoyl spermine was re-dissolved in EtOH (20 ml) and DCM (as needed to dissolve all protected N^4,N^9-dioleoylspermine). Aq NH_4OH was then added into the solution to achieve pH 11.0, and left at 20 °C (18 h) with constant stirring. The final solution was evaporated to remove ammonia and all solvents. Then, the reaction products were redissolved in EtOH. Qualitative detection of N^4,N^9-dioleoylspermine was by using TLC (with $CHCl_3$/MeOH/NH_4OH at 25/10/1 v/v/v) (R_f = 0.24).

Separation of N^4,N^9-dioleoylspermine and other byproducts

The ethanolic solution of N^4,N^9-dioleoylspermine (and other byproducts) was concentrated to 2 ml by evaporation. Separation from unwanted compounds (e.g. oleic acid, DCU etc) was by column chromatographic elution over flash silica gel with $CHCl_3$/MeOH (5/3 v/v) as mobile phase. Then, N^4,N^9-dioleoylspermine was collected by eluting with $CHCl_3$/MeOH/NH_4OH (15/10/1 v/v/v). The obtained N^4,N^9-dioleoylspermine sample from flash column chromatography was homogenous by TLC ($CHCl_3$/MeOH/NH_4OH at 25/10/1 v/v/v) (R_f = 0.24). The obtained yellow oil product displayed FAB^+ m/s 731.7149 Da, $C_{46}H_{91}N_4O_2$ requires 731.7142 $(M+H)^+$. N^4,N^9-Dioleoylspermine: NMR *inter alia* (C^2HCl_3) δ ^{1}H 0.90 (t, 2 x CH_3), 1.24-1.70 (br m, many x CH_2), 2.03 (apparent quartet, 4 x allylic CH_2), 3.24-3.48 (br m, many x NCH_2), 4.55-5.10 (br s, 2 x NH_2), and 5.32-5.41 (m, 2 x CH=CH) ppm, δ ^{13}C 130 (2 x CH=CH) and 173 (2 x CON) ppm.

Fluorescent detection of N^4,N^9-dioleoylspermine

Dansyl chloride and triethylamine (TEA) were obtained from Sigma-Aldrich (UK). N^4,N^9-Dioleoylspermine sample could be derivatized using dansyl chloride as a fluorophore. As a non-specific dansylation process, N^4,N^9-dioleoylspermine solution (0.2 mmoles approximately) was prepared by dissolving in EtOH (2 ml). TEA (1 eq, adjusted to pH 9.0), to prevent the formation of dansylic acid, was added to the polyamine solution and mixed well. DCM containing dansyl chloride (2.2 eq, 5 ml) was added to polyamine solution. The reaction was kept at 70 °C heating oil bath (10 min) or 20 °C in the dark (18 h).[140,239]

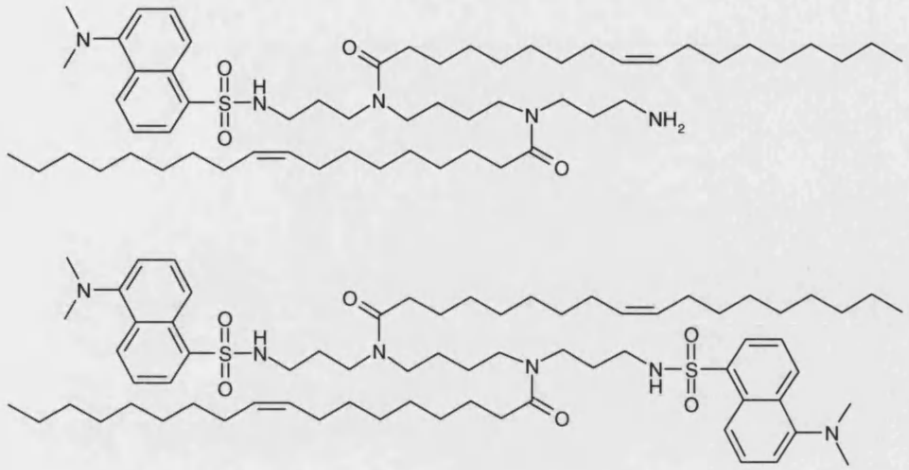

Figure 5.2 Mono-dansylated and di-dansylated products of N^4,N^9-dioleoylspermine

HPLC for dansylated products analysis

Materials and apparatus

HPLC grade MeOH was purchased from Fisher Chemicals. HPLC pump (Jasco PU-980) was used and connected to a fluorimeter detector (Waters 470 scanning fluorescence detector, Millipore) and a printer with chart speed at 1 cm/min. From UV and fluorescence scanning of samples,[240] the detection of samples was performed at λ_{ex} 330 nm, λ_{em} 510 nm (gain x1, attenuation 16).

Method

Based on Escribano's protocol with minor modifications,[140] a reverse-phase HPLC column (Supercosil ABZ+ Plus 5 µm, 150 x 4.4 mm) was used. The injection volume was 20 µl. An isocratic solvent system of MeOH/H_2O (95/5 v/v) at a flow rate of 1.3 ml/min was used for dansylated products resolution. The column was washed using designated solvent for 20 min or until a stable base line was obtained. The fluorescence emission peak was recorded on a chart paper. The first eluted dansylated product had t_R at 11 min. The HPLC was run for 15 min and MeOH (100%) was pumped through the column at 1.3 ml/min for 1 h until all residual samples (typically as a broad peak) are eluted after every injection, for cleaning purposes.

HPLC-MS was also performed to determine the number of dansylated groups on N^4,N^9-dioleoylspermine. Supercosil ABZ+ Plus was used as a stationary phase column and MeOH/H_2O (95/5 v/v, flow rate 1.6 ml/min) were used. Cl^- $(M-H)^-$ m/s 962.74 Da (t_R = 8.24

min), $C_{58}H_{101}N_5O_4S$ requires mass 962 $(M-H)^-$ and 1195.16 Da (t_R = 12.99 min), $C_{70}H_{112}N_6O_6S_2$ requires mass 1195 $(M-H)^-$.

Synthesis of N^1-cholesteryl spermine carbamate

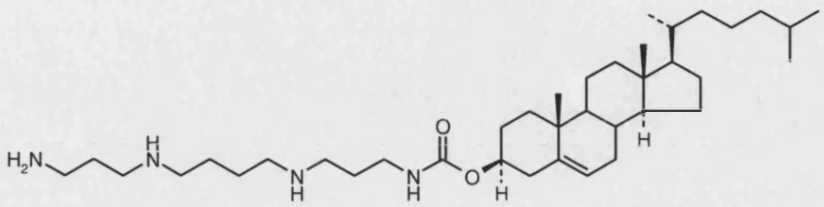

Figure 5.3 N^1-Cholesteryl spermine carbamate

Materials

Spermine, di-tert-butyl-dicarbonate ($(Boc)_2O$), TEA, ethyl trifluoroacetate, and trifluoroacetic acid (TFA) were purchased from Sigma-Aldrich, UK. Cholesteryl chloroformate was purchased from Fluka, UK. All other solvents used were purchased from Fisher, UK.

N^1,N^4,N^9-Tri-Boc protection of spermine

Spermine 1 g (5 mmol) was dissolved in MeOH (70 ml), at -78 °C under anhydrous nitrogen. Ethyl trifluoroacetate (1 eq) was diluted in 10 ml MeOH to have enough volume to add dropwise into spermine solution over 30 min. The the reaction was stirred for another 30 min and the temperature was then raised to 0 °C to obtain N^1-trifluoroacetyl spermine. Di-tert-butyl dicarbonate (excess, 8 eq) was dissolved in MeOH (10 ml), and added dropwise over 3 min. The mixture was stirred continuously at 20 °C for 15 h. The trifluoroacetyl group was then removed by adding aqueous NH_3 (excess) into N^1,N^4,N^9-tri-Boc-N^{12}-trifluoroacetyl spermine solution to achieve pH 11. The reaction was stirred for 18 h. The mixture was concentrated *in vacuo*, and the residue purified over silica gel (DCM/MeOH/NH_3 = 50/10/1 v/v/v) to afford the product as a colourless oil, R_f = 0.6.

Carbamate formation

N^1,N^4,N^9-Tri-Boc-spermine was dissolved in DCM (8 ml) and then TEA (3 eq) was added. Cholesteryl chloroformate (1.2 eq) in 3 ml of DCM (3 ml), was added to the solution over 30 min dropwise at 0 °C under nitrogen. Stirring was continued for 30 min, then the temperature was increased to 20 °C. The reaction was stirred for 12 h, and then the solution was concentrated *in vacuo*. The residue was purified over silica gel (EtOAc/hexane, 4/6 v/v), yielding a foam R_f = 0.44.

Boc removal

To a stirring solution of Boc-protected cholesteryl spermine carbamate dissolved in DCM (180 ml) under nitrogen at 25 °C, TFA (20 ml) was added. After 2 h, the solution was concentrated *in vacuo*. The residue was recrystallized in EtOAc to yield the purified white solid. The product was homogenous on analysis by TLC in DCM/MeOH/NH_3 50/10/1 v/v/v and $R_f = 0.2$. The compound displayed FAB^+ m/s 615.5577 Da, $C_{38}H_{71}N_4O_2$ requires 615.5577 $(M+H)^+$. ^1H and ^{13}C NMR spectroscopic data were all superimposable upon literature values.[69]

Plasmid DNA amplification and purification

Plasmid may be isolated by many methods based on the differential denaturation and reannealing of plasmid DNA and chromosomal DNA. Alkaline lysis is the commonly used technique developed by Birnboim *et al.*[241] and modifications were made to improve its efficiency.[242] Firstly, cell lysis was achieved by treating cells with aq NaOH and SDS (sodium dodecyl sulfate), followed by neutralization with a high concentration of low pH potassium acetate. Bacterial chromosomal DNA and other high molecular weight cellular components were selectively precipitated. The plasmid DNA remains in suspension and was precipitated with isopropanol. The process can be scaled up from small scale called Miniprep (yield less than 20 μg) to larger scale, Maxiprep. The latter provides high yields at 2-5 mg plasmid DNA per 500 ml of culture.[242,243] The DNA obtained can be quantified by employing the maximum UV absorption at 260 nm. This wavelength is an average of the absorption of the individual nucleotides which vary between 256 and 281 nm. The purity of nucleic acids was determined by examining at the maximum wavelength of DNA (260 nm) and protein (280 nm). Ratios of A_{260}/A_{280} between 1.75 and 1.90 were considered as acceptable for quality DNA.[141-143]

Plasmids used in experiments

pEGFP[130] (4.7 kbp) is the plasmid encoding for EGFP, under CMV promoter, obtained from Clontech (Oxford, UK). pGL3 control vector[133] (5.2 kbp), with SV-40 promoter, encoding for modified firefly (*Photinus pyralis*) luciferase, was purchased from Promega (Southampton, UK).

Media used in JM109 culture

LB broth base powder, producing a media formulation (%w/v): 1% tryptone (pancreatic digest of casein), 0.5% yeast extract, and 1% NaCl), was used in LB broth and agar preparation. LB broth was prepared in a bottle by dissolving LB broth base powder (5 g) in MilliQ water (200 ml). LB agar was prepared from LB broth base powder (12.5 g), agar (7.5

g), and MilliQ water (500 ml). Both LB agar and broth media were autoclaved (121 °C, 15 lb/inch^2) for 30 min before use. After leaving LB agar and broth were cooled down to 40 °C, ampicillin solution (0.1 g/ml in MilliQ water, 500 µl) was added in both LB media (500 ml) and swirled to attain a homogenous solution. LB broth can be kept at 20 °C with a closed cap for one month. For LB agar, media (10 ml) was poured in a 6 cm plate, using aseptic techniques. LB agar plate was then left for 45 min until cooler. It was then incubated for 20 min in a hot room (37 °C) upside down until dry. The solidified agar plate was kept in a cold room (4 °C) for use within 3 months of preparation.

E. coli JM 109 transformation and plasmid propagation

Competent *E. coli* JM109 cells high efficiency (10^8 cfu/µg) were purchased from Promega (Oxford, UK) and used for the propagation of all plasmids. The heat shock technique was employed to transform the bacteria. Competent cells were taken from a freezer (-70 °C), and warmed on ice until thawed. Temperature was kept at 4 °C. Then, cell suspension (100 µl) was transferred into cryotubes (1.5 ml). Plasmid solution (1 µg/ml, 10 µl) was added into separate cryotubes containing competent cells and left on ice for 30 min. The tubes were transferred to a water bath (43 °C) for exactly 45 s, and placed on ice for 2 min. LB (800 µl) was then added into cryotubes and the cell suspension was transferred to a 50 ml Falcon tube. The tube with transformed *E. coli* was finally put on the shaker at 37 °C, 300 rpm for 1.5 h.

Transformed cell suspension (200 µl) was inoculated on a plate with LB-ampicillin agar, and kept upside down for 18 h in an incubator (37 °C). Colonies of *E. coli* carrying the appropriate plasmid (i.e. ampicillin-resistant gene), which were able to grow on the plate, were used for inoculation. A single *E. coli* colony was transferred into 2 ml LB broth containing ampicillin (100 µg/ml) in a 50 ml Falcon tube. The starter culture was incubated for 8 h on a shaker at 37 °C, 300 rpm. The culture was then scaled up by adding the starter culture (2 ml) into a flask containing LB broth (250 ml) with ampicillin (100 µg/ml). The final culture flask was incubated on a shaker at 37 °C, 300 rpm for 18 h.

Plasmid isolation and purification

The plasmid was isolated and the cell lysate purification protocol was based on the modified alkaline lysis method.[242] Maxiprep plasmid purification kit, purchased from Qiagen (West Sussex, UK) was used in the experiment. The anion-exchange resin for DNA purification was employed in this protocol for higher purity of DNA obtained. Positively charged diethylaminoethanol (DEAE) resin was used to separate negatively charged phosphate groups of DNA, by properly adjusting the NaCl concentration of the elution media. The

range of 1.2-1.6 M NaCl solution was used to elute DNA, and separate the plasmid from other contaminants, especially RNA.

Bacterial culture (250 ml) was transferred into a plastic bottle and cells were harvested by centrifugation at 6000 rpm, 4 °C for 15 min in a Beckmann floor centrifuge, using a rotor JA-10. Ice-cooled P1 buffer (50 mM Tris-Cl, 10 mM EDTA, 100 μg/ml RNase A, pH 8.0) (10 ml) was added into the bottle to fully resuspend pelleted cells. P2 lysis buffer (200 mM NaOH, 1% w/v sodium dodecyl sulfate) (10 ml) was then added into the cell suspension. The tube was then inverted gently 4 times and incubated at 20 °C for 5 min. Ice-cooled P3 neutralisation buffer (3.0 M potassium acetate, pH 5.5) was added into the lysate and the mixture was inverted gently 4 times. The lysate was poured into the barrel of the QIAfilter cartridge and incubated for 10 min, with the outlet nozzle closed.

Buffer QBT (750 mM NaCl, 50 mM 3-[*N*-morpholino]propanesulfonic acid (MOPS), 15% v/v isopropanol, 0.15 %v/v Triton ® X-100) (4 ml) was used to equilibrate the HiSpeed Maxi Tip (a syringe column with a filtration unit). The column was allowed to empty by gravity flow. The outlet nozzle cap of the cartridge was removed and the plunger was gently inserted into the cartridge. The filtrate was collected into the Maxi Tip and allowed to filter through the resin. Buffer QC (1.0 M NaCl, 50 mM MOPS, 15% v/v isopropanol, pH 7.0) (60 ml) was added to wash the tip. DNA was entrapped in the resin and all flushed solution from filtration was discarded. DNA was eluted from the resin by adding buffer QF (1.25 M NaCl, 50 mM Tris-Cl, 15% v/v isopropanol, pH 8.5) (15 ml) into the tip. The eluted solution was kept in a 50 ml Falcon tube. Isopropanol (10.5 ml) was added and mixed well to precipitate the DNA solution. The resultant mixture was then incubated at 20 °C for 5 min. During incubation, QIA precipitator tip (DNA collection unit) was attached to the nozzle of a 30 ml syringe from which a plunger was removed. The precipitated DNA was added into the precipitator unit, and the plunger was inserted into the syringe using constant pressure. DNA was entrapped in the precipitator unit and all the flushed solution from the filtration was discarded. Then, the tip and plunger were removed from the syringe. After that, the tip was connected to the syringe nozzle and 70% EtOH (2 ml) was added into the syringe. EtOH was pushed by inserting the plunger to the unit with constant pressure, to wash the precipitated DNA. Then, DNA was dried by removing the plunger from syringe and pushing air through the precipitator 2-3 times. The precipitated DNA remained on a tip was further left dried by air on absorbent paper.

Buffer TE (10 mM Tris-Cl, 1 mM EDTA, pH 8.0) (1 ml) was added into the new 5 ml syringe of which the nozzle was connected to the precipitator tip. The plunger was pushed

gently into the syringe barrel. The obtained solution was collected in an ultracentrifuge tube (1.5 ml). Then, the tip and plunger were removed from the syringe. The obtained solution was then added into the same syringe with a tip connected, to elute the remaining DNA on the tip for the second time. The final DNA solution was kept at -20 °C, for further purity and quantification.

DNA sample purity and quantification

Plasmid DNA sample (5 µl) was diluted to 1 ml with TE buffer, in a microcuvette. The absorbance was measured at 260 nm (A_{260}) and 280 nm (A_{280}) on a GeneQuan II spectrophotometer. TE buffer (5 µl diluted to 1 ml in water) was used as a standard reference. The calculation for DNA concentration was determined by the dilution factor (20 times) and conversion factor (for dsDNA, 50 µg/ml/A_{260} unit), using the equation:-

$$DNA\ (\mu g / ml) = A_{260} \times 1000 \qquad (1)$$

The absorbance at 260 and at 280 nm was converted into ratios:-

$$Ratio = \frac{A_{260}}{A_{280}} \qquad (2)$$

Ratios of A_{260}/A_{280} obtained from this protocol were checked to ensure that they conformed to the acceptable ratio for quality DNA (between 1.75 and 1.90).[141-143]

Study of lipopolyamine-mediated DNA condensation by ethidium bromide fluorescence quenching assay

DNA condensing agents, both polyamines and synthetic lipopolyamines, were used in these Ethidium bromide (EthBr) experiments to determine their ability in DNA binding and packing.[114] In general, the solutions of condensing agents were prepared in 2 different strengths, which allow the incremental volume to be added between 2-5 µl during the whole experiments. At the higher charge ratio,[15,69] the more concentrated solution was used in the experiments to maintain the total volume of sample solution (which therefore minimised any change in DNA concentration in the measured sample).

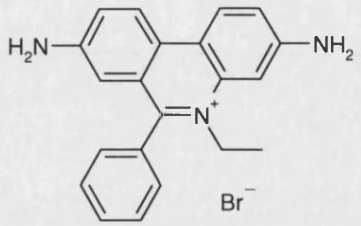

Figure 5.4 Ethidium bromide

Polyamine solutions

Spermine solutions were prepared using MilliQ water, at 0.02 and 0.2 μg/μl.

Lipopolyamine solutions

N^4,N^9-Dioleoylspermine was prepared in a solution (2 μg/μl) using absolute EtOH as solvent. The working solution at 0.25 and 0.5 μg/μl was prepared by diluting the ethanolic stock solution with MilliQ water. N^1-Cholesteryl spermine carbamate was dissolved in MilliQ water to prepare solutions at 0.1 and 0.25 μg/μl.

DNA used in experiments

Plasmid DNAs (pEGFP and pGL3) were prepared using MaxiPrep, as noted in the section of plasmid preparation. Calf thymus DNA (CT-DNA) was purchased from Sigma-Aldrich (UK). All DNA solutions were diluted using TE buffer and their concentrations were measured by using a GeneQuant II spectrophotometer. The standard DNA solutions for experiments were made at 1 μg/μl.

Buffers used in EthBr quenching experiments

HEPES buffer was made of 2 mM HEPES, 20 mM NaCl, 10 μM EDTA, and MilliQ water. Final pH was adjusted to 7.4 with aq NaOH solution. The HEPES buffer was filtered through a 0.45 μm membrane prior to use.

Charge ratio calculations

The composition of DNA complexes is related to the net charge of the system and expressed as "N/P charge ratio"(N/P = ammonium/phosphate), using this equation:-

$$N/P = \frac{ammonium\ equivalents\ of\ the\ cationic\ component}{phosphate\ equivalents\ of\ the\ DNA\ used} \qquad (3)$$

Ammonium equivalents of the cationic component were determined from the protonation degree (from the pK_a of each amino group). In HEPES pH 7.4, spermine (pK_a = 10.9, 10.1,

8.9, 8.1) carries 3.8 ammonium eq/mole. N^4,N^9-Dioleoylspermine carries 2.0 ammonium eq/mole (pK_a = 10.9, 10.1) and N^1-cholesteryl spermine carbamate (pK_a = 10.9, 8.6, 7.3) provides 2.4 ammonium eq/mole. The charge number was calculated by using the rearranged Henderson-Hasselbach equation (equation (4)). The number of phosphate eq was derived from the concentration of DNA measured at 260 nm.

$$number\ of\ ammonium\ eq\ per\ molecule = \sum_{i=1}^{n} \frac{1}{1+10^{(7.4-pKa_i)}} \qquad (4)$$

Fluorescence measurement

The fluorescence measurement was performed at λ_{ex} = 260 nm (excitation through DNA bases), λ_{em} = 600 nm, using 1 cm pathlength, 3 ml glass cuvette. DNA (1 μg/μl, 6 μl) was added into HEPES buffer (3 ml) in a glass cuvette stirred with a micro-flea. Fluorescence measurement was performed and regarded as a blank. Immediately prior to analysis, EthBr solution (3 μl, 0.5 μg/μl) was added to the DNA solution, stirred for 1 min to equilibrate the binding process, before the measurement. Aliquots (4 μl) of polyamines or lipopolyamine solutions were added to the stirring DNA solution and the fluorescence measured after 1 min equilibration for each incremental volume of DNA condensing agents. The emission intensity was reported as the percentage of maximum fluorescence (100%) when DNA was fully intercalated by EthBr without the DNA binding agents and corrected for the background fluorescence of total EthBr in buffer solution. Fluorescence percentage was plotted against N/P charge ratio to obtain the EthBr assay curves for each DNA and DNA condensing agents used in the experiments.

For the comparison of indirect excitation with the classical EthBr assay, the DNA condensation assay was also performed using the direct excitation of EthBr at λ_{ex} = 546 nm, λ_{em} = 600 nm. Only pEGFP condensation by spermine was analysed using this method. The study on effect of DNA type in DNA condensations was studied using different DNAs which are pEGFP, pGL3, and CT-DNA. The EthBr assay protocol as described previously was employed. The % fluorescence was plotted against N/P charge ratios to compare their EthBr fluorescence quenching profile.

Binding constant estimation

From the EthBr assay curves for each DNA and DNA condensing agent used in the experiments, the binding constants of DNA condensing agent (vector) to DNA can be estimated and compared by the loss of EthBr fluorescence as a function of DNA condensing agent concentration.

Cain[244] established the binding equations of DNA vectors and EthBr binding to DNA as described:-

$$[\text{DNA}] + [\text{vector}] \rightleftharpoons [\text{DNA-vector}] \quad (5)$$

$$[\text{DNA}] + [\text{EthBr}] \rightleftharpoons [\text{DNA-EthBr}] \quad (6)$$

From $K_b(vector) = \frac{[DNA-vector]}{[DNA]\times[vector]}$ and $K_b(EthBr) = \frac{[DNA-EthBr]}{[DNA]\times[EthBr]}$

a combined equation was expressed as:-

$$K_b(vector) = \frac{[DNA-vector]\times[EthBr]\times K_b(EthBr)}{[vector]\times[DNA-EthBr]}$$

Morgan[152] previously reported the binding constant of EthBr or K_b (EthBr) as to 10^7 M^{-1}, and EthBr was used at 3.8 μM in all experiments. At 50% residual fluorescence, the ratio of [DNA-vector] over [DNA-EthBr] is 1. Given DNA used in the experiments was constant at 6 μM (calculated as mononucleotide concentration), [vector] is equal to N/P multiplied by [DNA]. Given this, K_b (as ammonium eq) is finally described as the following equation, in units of M^{-1}:-

$$K_b(vector) = \frac{3.8\times10^7}{(N/P)\times6} \quad (7)$$

Light scattering study of lipopolyamine-DNA complex

DNA condensing agents both polyamines and lipopolyamines were used to form DNA complexes, and UV absorbance was measured at 320 nm, as there is absorption interference from free DNA. DNA complexes formed in a sample gave scattering of light, and "apparent" UV absorbance was increased (i.e. decreased light transmission output).[69]

Polyamine solutions

Spermine solutions were prepared using MilliQ water, in 0.2 and 2.0 μg/μl.

Lipopolyamine solutions

N^4,N^9-Dioleoylspermine was prepared into a solution (2 μg/μl) using absolute EtOH as solvent. N^1-Cholesteryl spermine carbamate was dissolved in MilliQ water to prepare solutions at 1.0 and 2.5 μg/μl.

DNA used in experiments

Plasmid DNAs (pEGFP and pGL3) were prepared by MaxiPrep, as noted in the section of plasmid preparation. Calf thymus DNA was purchased from Sigma-Aldrich (UK). All DNA solutions were diluted using TE buffer and their concentrations were measured by using a GeneQuant II spectrophotometer. The standard DNA solutions for experiments were prepared at 1 μg/μl.

Buffers used in experiments

HEPES buffer was made of 2 mM HEPES, 20 mM NaCl, 10 μM EDTA, and MilliQ water. Finally, the pH was adjusted to 7.4 with aq NaOH solution. The HEPES buffer was filtered through a 0.45 μm membrane prior to use.

UV absorbance measurement

The UV measurement was performed at λ_{ex} = 320 nm, using 1 cm pathlength, 3 ml glass cuvette. DNA (1 μg/μl, 60 μl) was added into HEPES buffer (2.94 ml) in a glass cuvette stirred with a micro-flea. UV measurement of this DNA-buffer solution was performed and adjusted to zero. Aliquots (4 μl) of polyamine or lipopolyamines were added to the stirring DNA solution and A_{320} was measured after 1 min equilibration for each incremental volume of DNA condensing agents. The absorbance values were then plotted against N/P ratios. In the study on effect of DNA type in DNA condensation, different DNAs (pEGFP, pGL3, and CT-DNA) were used in the study. Apparent UV absorbance was plotted against N/P charge ratios to compare their UV apparent absorption profile.

Human skin fibroblast (FEK4) transfection

FEK4 cell line was used as a model for human primary cells (mortal cell line). FEK4 is a normal human primary skin fibroblast cells derived from a foreskin explant.[153] FEK4 cells were kindly provided by Professor R.M. Tyrell, Department of Pharmacy and Pharmacology, University of Bath, UK.

Media and buffer used in cell culture

Cells were cultured in Earle's Minimal Essential Medium (EMEM) supplemented with foetal calf serum (FCS) 15% (15% FCS EMEM). Each 500 ml media contains 50 ml EMEM (10x), 13.5 ml $NaHCO_3$ (7.5%), 5 ml L-glutamine (200 mM), 25000 IU penicillin G, 25000 µg streptomycin, 15% FCS in autoclaved MilliQ water (354 ml). FCS, prior to use, was heat-inactivated by putting in the water bath at 56 °C and incubated for 45 min. Phosphate buffered saline (PBS) solution was used in all experiments to wash cells, and contains 0.01 M phosphate buffer, 0.0027 M KCl, and 0.137 M NaCl, pH 7.4, at 25 °C in autoclaved MilliQ water. Trypsin was diluted to a working concentration at 0.25% v/v with PBS.

Cell culture

A monolayer of FEK4 cells, at a density of 1 x 10^6 cells, was grown in a 150 ml flask with 25 ml of 15% FCS EMEM. The culture was incubated at 37 °C, 5% CO_2. The skin fibroblasts were passaged twice a week by trypsinization and used between passages 9 and 16.[156]

Trypsinisation technique for subculturing of cell line

The monolayers of cells in a 150 ml flask were rinsed with PBS (10 ml/flask) twice and buffer removed by aspiration, then trypsin (0.25%, 3 ml/flask) was added. The flask was incubated at 37 °C, 5% CO_2 for 10 min, for trypsinisation reaction. The trypsinised cells were checked with a microscope to ensure 80% cell detachment, and 15% FCS EMEM was added to stop trypsinisation. The cell suspension was then transferred to a 50 ml Falcon tube. The cells suspension with known concentration was added to a new flask for next passage at 1 x 10^6 cells/flask. When the cells reach passage 17, they were discarded.

Estimation of the cell numbers

A viable count was employed using a haematocytometer slide to determine the concentration of cells in a sample. Stained cell suspension was prepared by mixing trypsinised cells (50 µl) with nigrosin (50 µl). A cover slip was put over the raised sides of glass chambers (top and bottom) on a haematocytometer slide (0.1 mm). The cell sample (20 µl) was loaded into each etched glass chamber from the edge of the cover slip until the whole chamber was fully loaded. The slide was then placed under an inverted light microscope. Viable cells were detected using a bright halo light around their cell membrane, whereas dead cells were permeabilised by the dye and stained black. The viable cell numbers in the four squares surrounding the central square were counted. The same procedure was repeated for the other side of the haemocytometer chamber. The viable cell concentration in the original suspension was derived using the equation:-

$$cell\ number\ (cells/ml) = \frac{total\ cell\ counts\ in\ 4\ squares}{2} \times 10^4 \quad (8)$$

DNA complexing

pEGFP and pGL3 were prepared according to the MaxiPrep plasmid amplification and purification protocol. For each well, solutions A (DNA solution) and B (DNA condensing agents) were prepared. Solution A was obtained by diluting DNA (2 μg) into Opti-MEM medium (serum-free EMEM media, 100 μl) in a sterile 1.5 ml microcentrifuge tube, gently mixed using a vortex (2 s) and incubated for 30 min at 20 °C. The transfection agents studied in FEK4 transfection include: Lipofectin (DOTMA/DOPE, 1:1 w/w), Lipofectamine (DOSPA/DOPE, 3:1 w/w), N^4,N^9-dioleoylspermine, and N^1-cholesteryl spermine carbamate, each added at different volumes into Opti-MEM medium (100 μl) to achieve the desired N/P charge ratio, as described in the N/P determination section of the EthBr assay.[15] For liposomal transfection agents, DOTMA carries 1 ammonium eq/mole and DOSPA carries 4 ammonium eq/mole. The obtained solution was briefly vortexed (2 s) and allowed to stand at 20 °C for 30 min. Solutions A and B together with a bench top vortex (2 s), were then incubated at 20 °C for 20 min for complete DNA complexing.[245]

The relationship of lipoplex concentration and transfection efficiency was also studied. pEGFP (1 μg/well) complexed with N^4,N^9-dioleoylspermine at N/P charge ratios 2.0 and 2.5, was used in the transfection and compared to lipoplexes formed with pEGFP (2 μg/ml). The transfection protocol is described in the next section.

Transfection of adherent cells

In a 6-wells or 35 mm tissue culture plate, 2.5 x 10^4 cells were seeded in 4 ml of 15% FCS EMEM. The cells were incubated at 37 °C, 5% CO_2 in a CO_2 incubator for 48 h, until the cells were 50-70% confluent. Prior to transfection, cells were washed with PBS (2 ml/well) twice and Opti-MEM medium (1 ml/well) once. Serum-free Opti-MEM media (800 μl) and DNA complex solution (200 μl) were added to each well. For control wells, the DNA complex was replaced by Opti-MEM media at the same volume. The transfection process was allowed for 4 h in a 37 °C, 5% CO_2 incubator. After the incubation, the DNA-containing medium was replaced with 2 ml of 15% FCS EMEM, then the transfected cells were incubated at 37 °C, 5% CO_2 for another 44 h.[245] Sample preparation and transfection efficiency determination are based on the gene expression marker used in the delivered plasmid DNA. pEGFP expression assay was carried out by fluorescent-activated cell sorting (FACS), while firefly luciferase production from pGL3 transfected cells was determined by luminometry.

In the study on transfectivity of FEK4 cells from different passage numbers, FEK4 from passages 13, 14, and 15 were chosen. Transfection of pEGFP was performed using N^4,N^9-dioleoylspermine at N/P charge ratios 2.0 and 2.5. The transfection protocol was used as described previously.

HtTA-1 HeLa cells transfection

Human cervix carcinoma, HeLa derivative and transformed cell line (HtTA-1) was used as a model for carcinoma cells (an immortal cell line). The HtTA-1 cells being stably transfected with a tetracycline-controlled transactivator (tTA) consisting of the tet repressor fused with the activating domain of virion protein 16 of the herpes simplex virus (HSV). HtTA-1 cells were kindly provided by Professor R.M. Tyrell, Department of Pharmacy and Pharmacology, University of Bath, UK.

Media and buffer used in cell culture

Cells were cultured in Earle's Minimal Essential Medium (EMEM) supplemented with foetal calf serum (FCS) 15% (15% FCS EMEM). Each 500 ml media contains 50 ml EMEM (10x), 13.5 ml $NaHCO_3$ (7.5%), 5 ml L-glutamine (200 mM), 25000 IU penicillin G, 25000 µg streptomycin, 10% FCS in autoclaved MilliQ water (354 ml). FCS, prior to use, was heat-inactivated in a water bath at 56 °C and incubated for 45 min. PBS solution was used in all experiments to wash the cells.

Cell culture

HtTA-1 HeLa cells, at a density of 1 x 10^6 cells, were grown in a 150 ml flask with 25 ml of 10% FCS EMEM.[161,164,165,246] The culture was incubated at 37 °C, 5% CO_2. The cells were passaged every 3 days. Trypsinised cells were added to the next passage at 1 x 10^6 cells/flask. Trypsinisation procedures were carried out using the same protocol for FEK4 subculturing.

DNA complexing

pEGFP and pGL3 were prepared according to the Maxiprep protocol. For each well, prepared the solution A by diluting DNA (2 µg) into Opti-MEM medium (serum-free media,100 µl). The transfection agents studied in FEK4 transfection include Lipofectin (DOTMA/DOPE, 1:1 w/w), Lipofectamine (DOSPA/DOPE, 3:1 w/w), N^4,N^9-dioleoylspermine, and N^1-cholesteryl spermine carbamate each added at different volumes into Opti-MEM medium (100 µl) to achieve the desired N/P charge ratio, as described in the N/P calculation section of the EthBr assay protocol. Solution B was vortexed for 2 s and left

at 20 °C for 30 min. Mixed solutions A and B were then vortexed together (2 s), incubated at 20 °C for 20 min for complete DNA complexing.[245]

The study using naked (uncomplexed) DNA was also performed to assess if there was any transfection efficiency from this naked DNA system compared to lipoplexes. In each well treated with naked DNA, pEGFP 2 μg/well was prepared by adding pEGFP (2 μg) in a microcentrifuge tube and adjusted with Opti-MEM media to 200 μl. The same transfection protocol as described in the next section was used.

Transfection

In a 6-wells or 35 mm tissue culture plate, 2.5 x 10^4 cells were seeded in 4 ml of 10% FCS EMEM. The cells were incubated at 37 °C, 5% CO_2 in a CO_2 incubator about 24 h, until the cells were 50-70% confluent. The transfection protocol used was the same as in FEK4 cell transfection.[245] The 48 h post-transfection samples were analysed using FACS (for EGFP) or using a luminometer (for luciferase levels).

Fluorescent-activated cell sorting experiments

The fluorescent-activated cell sorting (FACS) technique was used to determine the fluorescent molecules (or biomolecules) inside the studied cells. In this study, FACS technique was used in pEGFP gene expression and membrane integrity (dye loading) study. Becton Dickinson FACS Vantage dual laser instrument (argon ion laser 488 nm, excitation) was used in all experiments. Filter lens (F) for emission detection was chosen based on the fluorophore. EGFP and fluorescein diacetate (FDA) were detected by F1 (λ_{em} = 530 ± 15 nm), while propidium iodide (PI) was monitored by F3 (λ_{em} = 670 nm and higher).

Preparation of cell samples for FACS analysis

The 6-wells plate cells (either transfected or dye-loaded cells) were harvested by washing with PBS (1 ml/well, twice) and trypsinisation (trypsin 0.25%, 0.5 ml/well) for 5 min. Cell detachment (80%) was then confirmed by light microscopy. The collected trypsinised cells were transferred to a FACS tube filled with 2 ml of 15% FCS EMEM. The suspension was centrifuged at 1000 rpm, 20 °C for 5 min, and the supernatant was decanted. The pellet was resuspended in PBS (1 ml/tube) for further centrifugation at 1000 rpm, 20 °C for 5 min. Cell suspension for FACS analysis was obtained by dissolving the pellet in 500 μl PBS/tube. A sample with untreated cells was used as a control in the measurement.

Data analysis

CELLQuest v.1.0 was used for cytometry data acquisition. Either CELLQuest v.1.0 or WinMDI was used to analyse FACS data. Only a subset of the data obtained from healthy cells data (major population) was analysed through a gate setting. This gating was determined from the dot plots between forward-scattered light (FSC) and side-scattered light (SSC). FSC is a parameter proportional to cell size and SSC indicates the cell granularity or internal complexity. In the histogram of events at different fluorescence intensity control group, the fluorescence intensity range (M_1) was set as a constant range throughout the experiments. For EGFP detection, the % fluorescence cells sorting events in the established range (M_1) was reported with the correction of the background fluorescence of the control sample. The detail on data analysis for FDA and PI assay are described in their respective experimental parts.

Bioluminescence assay of luciferase

Luciferase assay kit from Promega was used to evaluate pGL3 transfection in FEK4 and HtTA-1 HeLa cells. The luciferase activity was reported in RLU (relative luminescence units) and was normalised for the amount of cellular protein, which was analysed using the Bradford assay.

Cell lysates preparation

15% FCS EMEM media was removed from a 6-wells plate containing transfected FEK4 or HtTA-1 HeLa cells with pGL3. The attached cells were rinsed with PBS (1 ml/well). The equilibrated 1X reporter lysis buffer at 20 °C (250 µl/well) was added to cover the cells thoroughly. The culture plate was rocked on a shaker for 20 min at 20 °C. The 6-well plate with lysed cells was put in a freezer (-70 °C) for 20 min, and then taken out to settle at 20 °C, for complete lysis. The attached cells were scraped from the well using a scraper, then transferred to microcentrifuge tubes (1.5 ml size) and placed on ice. The tubes were vortexed for 10-15 s and centrifuged at 12,000 x g for 2 min (at 4 °C). The supernatant was collected in a new tube and stored at -70 °C for luminometric analysis.[133,247]

Luminescence analysis

Luciferase assay reagent (100 µl/tube), which contains luciferin as a substrate and coenzyme A as a catalyst, was dispensed into a luminometer tube. The luminometer was programmed at 2 s measurement delay and 10 s measurement read. The cell lysate obtained was added into a luminometer tube containing assay reagent. The solution tube was vortexed for 2 s and then immediately placed in the luminometer for reading records, using a tube filled with only assay reagent as a control.[247] The RLU obtained was calculated in RLU/protein (mg).

Protein assay (Bradford's assay)

A protein calculation standard curve was prepared by a Bradford reaction of standard bovine serum albumin (BSA) at different amounts. BSA (1 mg/ml) at 0, 1, 2, 3, 4, 5, 6, and 7 μg was added to each standard well in a 96-well plate. Then, Bradford reagent (Brilliant BlueG in phosphoric acid and MeOH) (250 μl) was added into each BSA concentration. Autoclaved MilliQ water was added to make 260 μl volume in total. The cell lysate samples (5 μl), Bradford reagent (250 μl), and autoclaved water (5 μl) were added into the sample wells. The plate with standard and sample mixtures was rocked for 30 s and incubated at 20 °C for 5 min which allows protein-dye complex to be formed. The absorbance of each well was recorded by a 96-well plate reader at 595 nm.[248] The standard curve was plotted and protein amounts in the cell lysates were calculated using Biolinx software.

Toxicity assessment of DNA condensing agents by MTT assay

MTT assay is a colorimetric assay to evaluate the ability of viable cells to covert a soluble tetrazolium salt [3-(4,5-dimethylthiazol-2-yl)-2,5-diphenyltetrazolium bromide, (MTT)] into an insoluble formazan crystal. This assay is used to determine the cytotoxic effects of lipopolyamines and lipoplexes (pEGFP complexes).

Lipopolyamine solutions

N^4,N^9-Dioleoylspermine was prepared in a solution (2 μg/μl) using absolute EtOH as solvent. The stock solution was diluted with MilliQ water to obtain a solution (1 μg/μl). N^1-Cholesteryl spermine carbamate was dissolved in MilliQ water to prepare a solution at 1.0 μg/μl. The stock solution was used at different volumes, to achieve the various concentrations, and diluted with Opti-MEM to a total volume of 100 μl/well.

Lipoplex solutions

N^4,N^9-Dioleoyl spermine and N^1-cholesteryl spermine carbamate were complexed with pEGFP (0.2 μg/well) to achieve the different N/P ratios (range from 0-20), by preparing solutions A and B in the similar way as the transfection protocol. For each well, solution A was prepared by dilution of pEGFP (0.2 μg) in Opti-MEM medium(50 μl), then the solution was vortexed (2 s) and left at 20 °C for 30 min. DNA condensing agents (N^4,N^9-dioleoyl spermine and N^1-cholesteryl spermine carbamate) were added into Opti-MEM media (50 μl/well) to attain solution B at the desired N/P ratios. Solution B was then vortexed (2 s) and left at 20 °C for 30 min. Solutions A and B were mixed and vortexed together (2 s), and then incubated at 20 °C for 20 min for complete DNA complexing.

Cell culture and sample loading

FEK4 and HtTA-1 HeLa cells were seeded in 96-well plates at 8000 cells/well and incubated for 24 h at 37 °C in 5% CO_2, to achieve 50% confluence. Lipopolyamine or lipoplex solutions at different concentrations (100 μl) were loaded into each well (n = 3 wells/sample). In the study of lipopolyamine toxicity, Opti-MEM (100 μl) was used as a control. DNA solution (100 μl) (pEGFP 0.2 μg in Opti-MEM, without DNA condensing agents) was used as a control for the study of lipoplex toxicity. The plate was then incubated at 37 °C in 5% CO_2 for 4 h. After cells were exposed with lipopolyamine and lipoplex for 4 h, medium was aspirated out and replaced with 15% FCS EMEM (for FEK4) or 10% FCS EMEM (for HtTA-1 HeLa) (100 μl). The plate was put back in an incubator 37 °C in 5% CO_2 for a further 39 h. After incubation, sterile filtered MTT solution (5 μg/μl) (10 μl) was added into each well and the 96-well plate was further incubated at 37 °C in 5% CO_2 for 5 h.

UV measurement of MTT product

After incubation (total time 48 h), the media and the unreacted dye were aspirated and the formed blue formazan crystals were dissolved in 200 μl/well of dimethyl sulfoxide (DMSO), and the blue solutions was pipetted up and down to ensure the complete dissolution of crystalline product. The produced colour was measured using a plate-reader at λ = 550 nm. The % viability[41] was calculated by the following equation:-

$$\% \ cell \ viability = \left(\frac{A_{550} sample}{A_{550} control} \right) \times 100 \qquad (9)$$

General information on FCS experiments

PicoGreen concentration determination

PicoGreen (PG) is patented, and its concentration was not provided by Molecular Probes (USA). Diluted PG solution absorbance was measured with a UV spectrophotometer at 500 nm. The molar concentration was then calculated by using the molar absorptivity from the literature (70,000 M^{-1} cm^{-1} at 500 nm).[185] The PG solution supplied by Molecular Probes was found to be 220 μM and therefore its 1/200 dilution (i.e. at the recommended dilution by the company) is 1.1 μM.

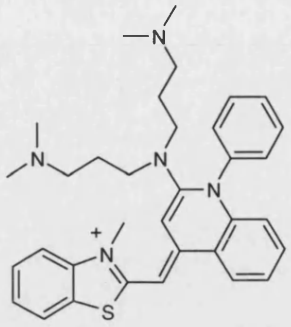

Figure 5.5 PicoGreen

DNA sample preparation and quantification

pGL3 DNA (5.3 kbp) was purchased from Promega UK. and pEGFP (4.7 kbp), obtained from Clontech. Both plasmids were amplified and purified by MaxiPrep kit (Qiagen UK.) and confirmed by gel electrophoresis for these experiments. Calf thymus DNA (minimum size 13 kbp) was purchased from Sigma-Aldrich (UK). Each DNA sample was dissolved in HEPES buffer and stored at –80 °C. For quantification of DNA, a 5 µl sample was diluted to 1 ml with water and the UV absorbance measured at 260 nm and 280 nm on a GeneQuan II spectrophotometer. TE buffer (5 µl diluted to 1 ml in water) was used as a standard reference. The A260/A280 ratio was calculated to analyze the purity of the DNA.[141,142]

ConfoCor instrument setup

FCS was performed on a ConfoCor®1 (Carl Zeiss Jena, Germany). ConfoCor1 is a PC-controlled fluorescence correlation-adapted AXIOVERT 135 TV microscope, equipped with an x-y-z adjustable pinhole, avalanche Photodiode SPCM-200-PQ, ALV-hardware correlator and CCD camera. The Ar^+-laser beam (excitation wavelength 514 nm, excitation intensity: 1 mW) was focused by using a water-immersion microscope objective at an open focal light cell. The same objective, a dichroic mirror, proper bandpass filters, and a pinhole in the image space block collected fluorescent light. The volume of the confocal excitation element, calibrated with Alexa488 or Rhodamine6G, was determined to be about 1 femtolitre (0.9 ± 0.1 femtolitre).

Studies of DNA binding of PicoGreen using FCS

A DNA sample for measurement (1 nM DNA, 200 µl) was loaded into one of an 8-chamber cover glasses (NUNC®) with the glass bottom facing the ConfoCor water-immersion microscope objective. A small volume of PG (1:200 v/v dilution in HEPES buffer) was added stepwise into the DNA solution and incubated for 10 min before recording the fluctuation signal (30 s/time, 20 times/measurement). A calibration curve of DNA

intercalation by PG was then prepared to determine the optimal dye/kbp ratio for FCS experiment.

Studies of lipopolyamine-mediated DNA condensation using FCS

A DNA sample for measurement (1 nM DNA, 200 µl) was loaded into one of an 8-chamber cover glasses, followed by the addition of PG at the optimal dye/kbp ratio. After 10 min incubation, the DNA solution was titrated by DNA condensing agents. FCS reading was also recorded (30 s/time, 20 times/measurement).

FCS data analysis

FCS analysis was processed using the ConfoCor® II software. The fluorescence intensity signal I(t) fluctuating around a temporal average [$I(t) = < I(t) > + \delta I(t)$] was processed with a digital hardware correlator interface yielding the normalized autocorrelation function or G(τ). This function is expressed as:-

$$G(\tau) = \frac{\langle I(t) * I(t+\tau) \rangle}{\langle I(t) \rangle^2} \tag{10}$$

Assuming small point-like non-interacting molecules freely diffusing in a space much larger than the detection volume, showing up only triplet state dynamics, $G(\tau)$ takes the form:-

$$G(\tau) = 1 + \left(1 - T + Te^{-\tau/\tau_{tr}}\right)\left(\frac{1}{PN[1-T]}\right)\left(\frac{1}{1+(\tau/\tau_D)}\right)\left(\frac{1}{1+(\tau/\tau_D)(\omega_1/\omega_2)^2}\right)^{1/2} \tag{11}$$

where T is a triplet fraction, τ_{tr} is a triplet decay time, PN is the apparent particle number, τ_D is a diffusion time, and ω_1 and ω_2 are the lateral and axial radii of detection volume. The shape of the confocal volume for calculation purposes was assumed to be a cylinder, based on a special optical situation where the pinhole diameter and/or the objective lens were adjusted, and this volume (V) is $V = \pi\omega_1^2(2\omega_2)$. The derivation of equations for the applied models makes use of the natural laws applied in classical methods of perturbation kinetics as the only difference is in the source of fluctuations. The parameters τ_D and PN are related with macroscopic values of concentration c, and the rate of diffusion, called the diffusion constant[179] or diffusion coefficient (D)[170] via:-

$$\tau_D = \frac{\omega_1^2}{4D} \tag{12}$$

and $$PN = c\pi\omega_1^2 \tag{13}$$

The diffusion coefficient (D) for spherically symmetric molecules is related to the hydrodynamic radius r_h via the Einstein-Stokes equation:-

$$D = \frac{\omega_1^2}{4\tau_D} = \frac{k_B T}{6\pi\eta r_h} \tag{14}$$

where k_B is the Boltzmann constant, here T is thermodynamic temperature, η is dynamic viscosity, and r_h is hydrodynamic radius. The hydrodynamic radius can be calculated from molecular mass M using:-

$$r_h = \sqrt[3]{\frac{3M}{4\pi\rho N_A}} \tag{15}$$

where ρ is the mean density of the molecule and N_A is Avogadro's number.

The translational diffusion coefficient (D) depends largely on the shape of the molecule. For rod-like molecules, such as a DNA, D can be estimated as:-

$$D = \frac{Ak_B T}{3\pi\eta L} \tag{16}$$

where L corresponds to the length of the rod (for a DNA it is the rise per base-pair (0.34 nm) multiplied by the number of base-pairs), d is a diameter of the rod (2.38 nm for DNA), and A represents a correction factor:-

$$A = \ln(L/d) + 0.312 + 0.565/(L/d) - 0.1/(L/d)^2 \tag{17}$$

This shows that the diffusion coefficient (D) of a 1000 bp DNA is approximately 5-times smaller and τ_D 5-times larger for a rod-like shaped molecule than for a spherical one.

Time-resolved fluorescence correlation spectroscopy

ConfoCor and Time-correlated single photon counting (TCSPC) apparatus setup[205]

FCS was performed on a ConfoCor®1 (Carl Zeiss Jena, Germany). ConfoCor1 is a PC-controlled fluorescence correlation-adapted AXIOVERT 135 TV microscope, equipped with an x-y-z adjustable pinhole, avalanche Photodiode SPCM-200-PQ, ALV-hardware correlator, and CCD camera.

PicoQuant laser-head emitting beam (excitation wavelength 470 nm, excitation intensity: 0.97 mW, repetition rate: 40 MHz) was focused by a water-immersion microscope objective at an open focal light cell. Pinhole adjustment was performed by using Alexa488 (100 nM) (20 µl) dissolved in MQ water (500 µl). The same objective, a dichroic mirror, proper bandpass filters, and a pinhole in the image space-block collected fluorescent light. This laser head was driven from a single PDL800-D driver, which provides electrical pulses synchronous with light pulses (SYNC signal) necessary for TCSPC data acquisition.

For TR-FCS measurement, the SPCM-200-PQ was replaced by a Perkin-Elmer SPCM-AQR-13-FC single photon avalanche diode (SPAD), to allow the fast electrical response to photon impact required by time-correlated single photon counting (TCSPC). The FWHM of the final instrument response function (IRF) is 450 ps. PicoQuant TimeHarp 200 TCSPC board with dedicated software (MicroTime200) was placed in a PCI slot of a separated PC with fast processor, from the hardware autocorrelator PC. The SPAD output was fed directly to the Time-Harp's START input through a 20 dB inline rf attenuator.

Alexa488, at concentration approximately 0.4 nM, was added into one chamber of an 8-chambers cuvette to determine the volume of the confocal excitation element. As typically observed in classical FCS, excitation volume was determined to be about 1 femtolitre (0.9 ± 0.1 femtolitre).

TCSPC acquisition analysis

PG calibration assay and DNA condensation were performed using the same protocol as the classical FCS. The data acquisition mode is called time-tagged time-resolved (TTTR) mode. The photon events were recorded individually without on-line data reduction (which was typically performed by the autocorrelator). Three pieces of information were gathered for all photons and stored as one photo record: (a) timing between the excitation pulse and

fluorescence photon detection (35 ps resolution), (b) coarsely tagged-timing (100 ns resolution) in relation to the start time of experiment, and (c) routing bits which were generated simultaneously to identify the actual detector channel.

Multiple-exponential decay model was used to derive the lifetime of each fluorescent species being monitored. TTTR data were processed by using MicroTime200 software. The decay is expressed as:-

$$I(t) = \sum_{i=1}^{n} \alpha_i * exp(-t / \tau_i) \tag{18}$$

where $I(t)$ = intensity of fluorescence at time t, α_i = amplitude of the components at time zero, n = number of lifetimes, and τ_i = lifetime (the average amount of time a fluorophore remains in the excited state following excitation). The decay kinetic was calculated using tail-fitting mode with constant range of channel time. Decay model was fit-tested by using F-statistics, and calculated χ^2 should be around 1.0.

Fractional intensities, a value to indicate the fraction of fluorescent species with different lifetimes, were obtained by amplitude-weighted formula and Σf_i was normalized to unity:-

$$f_i = \frac{\alpha_i \tau_i}{\sum_{i=1}^{n} \alpha_i \tau_i} \tag{19}$$

For double-exponential decay, average lifetime ($\bar{\tau}$) was expressed as:-

$$\bar{\tau} = \frac{\alpha_1 \tau_1^{\,2} + \alpha_2 \tau_2^{\,2}}{\alpha_1 \tau_1 + \alpha_2 \tau_2} = f_1 \alpha_1 + f_2 \alpha_2 \tag{20}$$

FCS data analysis

FCS analysis was processed using the time-tagged TTTR data. Time-gating is employed to reject scattered light or background noise. Statistical filters are derived from the difference of fluorescent species "decay curves".[249] The fluorescence intensity signal I(t) fluctuating around a temporal average [$I(t) = < I(t) > + \delta I(t)$] was processed through filters to yield the normalized autocorrelation function, G(τ). Other FCS parameters were calculated in a similar manner as the classical FCS.

FEK4 and HtTA-1 HeLa transfection at 12 °C

Transfection protocols used were modified from the standard transfection at 37 °C. The processes of endocytosis are temperature dependent as temperature affects both rate of ligand binding and mobility of ligand-receptor complexes in membranes. Endocytosis processes are usually blocked at temperatures below 12 °C. This transfection experiment at low temperature was chosen to study the effect of ATP-dependent processes in gene delivery. Lipopolyamines and liposomal NVGT vectors (Lipofectin and Lipofectamine) were used in these pEGFP delivery experiments.

Buffer medium used during the 12 °C incubation

HEPES-NaCl buffer is a NaCl-based extracellular solution used in all incubations at 12 °C. This buffer was prepared from 130 mM NaCl, 3.0 mM KCl, 2.0 mM $CaCl_2$, 0.6 mM $MgCl_2$, 1.0 mM $NaHCO_3$, 10.0 mM HEPES, and 5.0 mM glucose in autoclaved MilliQ water. The pH and osmolarity of extracellular solutions were adjusted to 7.4 and 310-320 mOsmol/l with aq NaOH and sucrose respectively.

DNA complexing

DNA complex solution for each well was prepared from solution A and solution B. For solution A, pEGFP (2 μg/well) was diluted to 100 μl with Opti-MEM medium (serum-free media). Solution B was prepared from various DNA condensing agents: N^4,N^9-dioleoylspermine, N^1-cholesteryl spermine carbamate, Lipofectin, and Lipofectamine, which were diluted to 100 μl with Opti-MEM medium. Each solution was vortexed (2 s) and left at 20 °C for 30 min. Solutions A and B were then mixed together by vortexing (2 s), and then incubated at 20 °C for 20 min for complete DNA complexing.

Transfection

In 6-well tissue culture plates, FEK4 or HtTA-1 (2.5×10^4 cells/ml) were seeded in 15% FCS EMEM (4 ml, for FEK4) or 10% FCS EMEM (4 ml, for HtTA-1) respectively. The cells were incubated at 37 °C with 5% CO_2 in an incubator for 24 h, until the cells were 50 – 70% confluent. Media was then removed and cells were washed with PBS (2 ml/well) twice and HEPES-NaCl buffer (1 ml/well) once. Ice cool HEPES-NaCl buffer was then added (800 μl/well). The 6-well plates were pre-cooled by placing in a temperature-controlled refrigerator for 10 min before the transfection. The DNA complexes solution (200 μl/well) was then added, and cells were incubated at 12 °C in the refrigerator for 4 h. After the incubation, the DNA-containing medium was replaced with 15% FCS EMEM (2 ml, for FEK4) or 10% FCS EMEM (2 ml, for HtTA-1), then the transfected cells were incubated at

37 °C, 5% CO_2 for another 44 h. The 48 h post-transfection samples were analysed using FACS for EGFP level.

DNA condensation studies of polyalkylpyridinium salt

Materials

Polyalkylpyridinium salt (PolyAPS) solutions (0.1 and 0.25 μg/μl) were prepared in MilliQ water. Plasmid DNAs (pEGFP and pGL3) were prepared using MaxiPrep, as noted in the section on plasmid preparation. Calf thymus DNA was purchased from Sigma-Aldrich (UK). All DNA solutions were diluted using TE buffer and their concentrations were measured by using a GeneQuant II spectrophotometer. The standard DNA solution for experiments was 1 μg/μl.

N/P charge ratio was calculated using equation (3). PolyAPS (pyridinium) carries 1 ammonium eq/monomer. The number of phosphates was derived from the concentration of DNA measured at 260 nm.

Buffers used in experiments

HEPES buffer was made of 2 mM HEPES, 20 mM NaCl, 10 μM EDTA, and MilliQ water. The final pH was adjusted to 7.4 with aq NaOH solution. The HEPES buffer was filtered through a 0.45 μm membrane prior to use.

Fluorescence measurement

The fluorescence measurement was performed at λ_{ex} = 260 nm (excitation through DNA bases), λ_{em} = 600 nm, using 1 cm pathlength, 3 ml glass cuvette. DNA (1 μg/μl, 6 μl) was added into HEPES buffer (3 ml) in a glass cuvette stirred with a micro-flea. Fluorescence measurement was performed as a blank. Immediately prior to analysis, EthBr solution (3 μl, 0.5 μg/μl) was added to the DNA solution, stirred for 1 min to equilibrate the binding before measurement. Aliquots of polyAPS solutions were added to the stirred DNA solution and the fluorescence measured after 1 min equilibration for each incremental volume of DNA condensing agents. EthBr fluorescence quenching was plotted as explained in the previous Experimental - DNA condensation studies using lipopolyamines. Binding constant estimation was calculated for its approximate value using equation (7).

Light scattering study of DNA complexed with polyAPS

Polyamine solutions

Polyalkylpyridinium salt (PolyAPS) solutions (1.0 and 2.5 μg/μl) were prepared in MilliQ water.

DNA used in experiments

Plasmid DNAs (pEGFP and pGL3) were prepared by MaxiPrep, as noted in the section on plasmid preparation. Calf thymus DNA was purchased from Sigma-Aldrich (UK). All DNA solutions were diluted using TE buffer and their concentrations were measured by using GeneQuant II spectrophotometer. The standard DNA solutions for experiments were made at 1 μg/μl.

Buffers used in experiments

HEPES buffer was made of 2 mM HEPES, 20 mM NaCl, 10 μM EDTA and MilliQ water. The final pH was adjusted to 7.4 with aq NaOH solution. The HEPES buffer was filtered through a 0.45 μm membrane prior to use.

UV absorbance measurement

The UV measurement was performed at λ_{ex} = 320 nm, using 1 cm pathlength, 3 ml glass cuvette. DNA (1 μg/μl, 60 μl) was added into HEPES buffer (2.94 ml) in a glass cuvette stirred with a micro-flea. UV measurement of this DNA-buffer solution was performed and adjusted to zero. Aliquots (4 μl) of polyamine or lipopolyamine solutions were added to the stirring DNA solution and A_{320} was measured after 1 min equilibration for each incremental volume of DNA condensing agent. The absorbance values were then plotted against N/P ratios.

Fluorescein *O*-diacetate release assay of polyAPS

Fluorescein *O*-diacetate (FDA) is a non-fluorescent dye which readily diffuses through intact cells. FDA undergoes hydrolysis by cellular esterase into fluorescein which is hydrophilic and non-permeant. The cellular retention of FDA is compromised in cells with disrupted membrane. Lipopolyamines and pore-forming PolyAPS were studied using this FDA assay, to determine their interaction with membranes which may play important roles in facilitating gene delivery. The primary cell line, FEK4 was chosen as a model for the membrane integrity study.

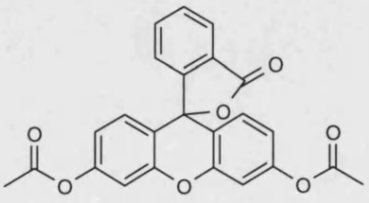

Figure 5.6 Fluorescein-*O*-diacetate

PolyAPS solution

Polyalkylpyridinium salt (PolyAPS) solution (0.2 μg/μl) was prepared in MilliQ water. This compound with known pore-forming activity was used as a positive control in the experiments.[215-217]

Cell culture and sample loading

FEK4 cells (1 x 10^5 cells/well) were seeded in 6-well plates and 15% FCS EMEM media (4 ml) was added. The cell cultures were incubated at 37 °C, 5% CO_2 for 24 h, to obtain 70% confluence. Opti-MEM without PR is a media formulation containing minimum essential amino acids, but without serum and no added phenol red (PR), was only used. This was the media used in the dye loading stage. 15% FCS EMEM media was aspirated out and replaced with Opti-MEM without PR (799 μl/well) and FDA solution (in DMSO, 10 μg/μl) was added at 1 μl/well. The blank well was filled with only Opti-MEM without PR (800 μl). The 6-well plates were then rocked for 1 min to ensure thorough mixing. Then the plates with FDA-loaded cells were incubated at 37 °C, 5% CO_2 for 30 min.

After FDA was fully uptaken into cells, a stock solution of PolyAPS (5 μl) was added to obtain a final concentration of 1 μg/μl, and the total volume was also adjusted to 1 ml with Opti-MEM without PR. For negative control wells, only Opti-MEM without PR (200 μl) was added. The 6-well plates were then rocked for 1 min to ensure thorough mixing. The plates were incubated for another 30 min, and the total time of incubation is 1 h.

FACS analysis of samples

After incubation, cell samples were prepared by following the protocol described in the FACS experimental section. The samples were analysed by FACS using an F1 filter, compared to the control.

Data analysis

CELLQuest v.1.0 was used for cytometry data acquisition. Either CELLQuest v.1.0 or WinMDI was used to analyse FACS data. Only a subset of healthy cells data (major population) was analysed through a gate setting. In the histogram of events at different fluorescence intensity control group, the highly FDA fluorescence intensity range (M_1) was set as a constant range throughout the experiments. Mean intensity of fluorescent cells (M_1) in each sample (F_{sample}) was compared to the mean fluorescence of control tubes ($F_{control}$). The relative FDA fluorescence in percentage was calculated from the equation:-

$$FDA\ fluorescence\ (\%) = \left(\frac{F_{sample}}{F_{control}} \right) \times 100 \qquad (21)$$

The % fluorescent cells in the established range (M_2) was reported. The M_2 sub-population is a group of cells with fluorescent intensity less the mean value of M_1 population, which represents cells with fluorescein leakage.

$$Fluorescent\ cells\ (FDA\ release)\ (\%) = \%M2_{sample} - \%M2_{control} \qquad (22)$$

Propidium iodide uptake assay of polyAPS

Propidium iodide (PI) is a fluorescent dye which intercalates between nucleic bases of nuclear DNA. Due to its hydrophilicity, PI is not able to diffuse through intact cell membranes. The cellular uptake of PI is compromised in cells with disrupted membranes. Lipopolyamines and pore-forming PolyAPS were studied using this PI assay, to determine their interaction with membranes which may play important roles in facilitating gene delivery. The primary cell line, FEK4 was chosen as a model for the membrane integrity study.

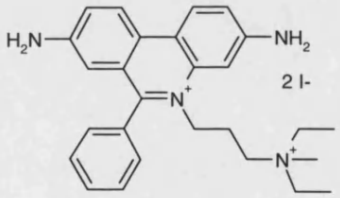

Figure 5.7 Propidium iodide

PolyAPS solution

PolyAPS solution (0.2 μg/μl) was prepared in MilliQ water. This compound with known pore-forming activity was used as a positive control in the experiments.[215-217]

Cell culture and sample loading

FEK4 cells (1 x 10^5 cells/well) were seeded in 6-well plates and 15% FCS EMEM media (4 ml) was added. The cell cultures were incubated at 37 °C, 5% CO_2 for 24 h, to obtain 70% confluence. Similar to the FDA release assay, only Opti-MEM without PR was used to avoid any interference from PR. 15% FCS EMEM media was aspirated out and replaced with Opti-MEM without PR (900 μl/well) and PI solution (in MilliQ water, 10 μg/μl) was added at 2 μl/well. The blank well was filled with only Opti-MEM without PR (1 ml).

A stock solution of polyAPS (5 µl) was added to obtain the final concentration of 1 µg/µl, and the total volume was also adjusted to 1 ml with Opti-MEM without PR. For control wells, there is no polyAPS added and .the total volume was also adjusted to 1 ml with Opti-MEM without PR. The 6-well plates were then rocked for 1 min to ensure thorough mixing. Then the plates with PI-loaded cells were incubated at 37 °C, 5% CO_2 for 60 min.

FACS analysis of samples

After incubation, cell samples were prepared by following the protocol described in the FACS experimental section. The samples were analysed by FACS using an F3 filter, compared to control cells and polyAPS-added cells.

Data analysis

CELLQuest v.1.0 was used for cytometry data acquisition. Either CELLQuest v.1.0 or WinMDI was used to analyse FACS data. Only a subset of healthy cells data (major population) was analysed through a gate setting. In the histogram of events at different fluorescence intensity control group, the PI fluorescence intensity range (M_1) was set as a constant range throughout the experiments. The number of positive cells and their fluorescence intensity were analysed, by removing the background fluorescence from control samples (PI-only treated cells). The mean intensity of fluorescent cells in each sample (F_{sample}) was compared to the mean fluorescence of control tubes ($F_{control}$). The relative PI fluorescence in percentage was calculated from the equation:-

$$PI\ fluorescence\ (\%) = \left(\frac{F_{sample}}{F_{control}}\right) \times 100 \qquad (23)$$

The % fluorescent cells in the established range (M_1) was also reported, which represents cells which uptake PI.

$$Fluorescent\ cells\ (PI\ uptake)\ (\%) = \%M1_{sample} - \%M1_{control} \qquad (24)$$

Membrane integrity study of spermine and oleic acid

Spermine solution was prepared in MilliQ water at 1 µg/µl. Spermine was used at 2 µl/well to achieve the final concentration of 2 µg/ml. Oleic acid solution was prepared in absolute EtOH at 10 µg/µl and used at 20 µl/well, to achieve the final concentration 200 µg/ml. FDA release and PI uptake assays were performed, by employing the same protocol as described in the section of polyAPS-membrane interaction study. In both FDA and PI assays, spermine and oleic acid solutions were added at different volume to achieve the desired

concentration, and the total volume was adjusted to 1 ml/well with Opti-MEM without PR. The procedure on FACS analysis and data treatment was the same as previously described in the section of polyAPS's membrane study.

Membrane integrity study of synthetic lipopolyamines

N^4,N^9-Dioleoylspermine was prepared in a solution (2 μg/μl) using absolute EtOH as the solvent. The stock solution was diluted with MilliQ water to obtain a solution (1 μg/μl). N^1-Cholesteryl spermine carbamate was dissolved in MilliQ water to prepare a 1.0 μg/μl. solution. FDA release and PI uptake assays were performed, by employing the same protocol as described in the section of polyAPS-membrane interaction study. In both FDA and PI assays, lipopolyamine solutions were added at different volume to achieve the desired concentration, and the total volume was adjusted to 1 ml/well with Opti-MEM without PR. The concentration of lipopolyamines used in the studies is in the range of 0-13 μg/ml. The procedure on FACS analysis and data treatment was the same as previously described in the section of polyAPS's membrane study.

Fluorescent labelling of plasmid DNA

Fluorescent probes based on DNA alkylating agents (Label IT ®) were utilised to label plasmid DNA for same transfection studies. This method provides higher efficiency in labelling than the enzymatic process using "labelled nucleotide" (i.e. nick translation). The DNA was covalently labelled at guanine nucleotide bases, thus it is suitable to use as a probe or marker in transfection studies. Label IT® nucleic acid labelling kits, i.e. tetramethyl-rhodamine (TMR), MIR 4125 (λ_{ex} 546 nm, λ_{em} 576 nm) and 5-carboxy-X-rhodamine (CXR), MIR3125 (λ_{ex} 576 nm, λ_{em} 597 nm) were used to label both pGL3 and pEGFP.

Labelling reaction

Reconstitution solution (DMSO, 25 μl) was added into labelling reagent pellet (in an ultracentrifuge tube) to obtain the final labelling reagent. This reagent was thoroughly mixed by vigorous pipetting up and down. The labelling reaction was performed by adding MilliQ water (35 μl), 10x labelling buffer A (200 mM MOPS, pH 7.5, 5 μl), plasmid DNA (1 mg/ml, 5 μl) and labelling reagent (5 μl) into a microcentrifuge tube, then incubated at 37 °C for 1 h. The reaction mixture should be quickly vortexed (2 s) after 30 min of incubation to minimise the effect of evaporation and change in concentration. Unreacted labelling reagent was removed from the labelled plasmid by EtOH precipitation.[250]

Labelled DNA purification by EtOH precipitation

NaCl solution (3M, 5 µl) and ice cold 100% EtOH (100 µl) were added to the reaction (50 µl), mixed and placed in a -20 °C (or colder) freezer for 15 min. The reaction microcentrifuge tube was centrifuged at full speed (13000 rpm) for 30 min to obtain the pellet of labelled DNA. The pellet was carefully collected by EtOH removal, and washed with 70% EtOH (30 µl) without disturbing the pellet. The labelled DNA was centrifuged at full speed (13000 rpm, 10 min) and all traces of EtOH were removed with a micropipette. TE buffer (50 µl) was added to redissolve the labelled DNA.[250] The final DNA solution was stored at -20 °C until use.

Labelling ratio determination

Labelled DNA was measured for UV absorbance at λ 260 nm (A_{260}) and at λ_{ex} of labelling agents (A_{dye}) respectively in a microcuvette (1.5 ml). As dyes used in the experiment may also absorb UV at 260 nm, the corrected A_{260} value ($A_{DNA\ base}$) must be obtained by using the dyes' correction factor (C.F.) and the following equation:-

$$A_{DNA\ base} = A_{260} - (A_{dye} \times C.F._{\cdot 260}) \tag{25}$$

given $C.F._{\cdot 260}$ for TMR and CXR is 0.27 and 0 (negligible) respectively. The labelling ratio, expressed in dye/kbp, was calculated from the equation:-

$$dye/kbp = \left(\frac{A_{dye}}{A_{DNA\ base} \times \varepsilon_{dye}} \right) \times (1.32 \times 10^7) \tag{26}$$

given $\varepsilon_{dye\ (TMR)}$ and $\varepsilon_{dye\ (CXR)}$ are 100,000 and 82,000 $M^{-1}cm^{-1}$ respectively.[250]

Human skin fibroblast (FEK4) cells transfection with labelled DNA

Transfection protocols used were the same as described earlier. Fluorescent tagged plasmids were used to determine their ability in transfection efficacy and applicability as NVGT probes.

Fluorescent DNA

pEGFP was labelled with TMR and CXR Label IT® as mentioned in the DNA labelling section, using the DNA/dye reagent volume ratio = 1:1. Non-labelled plasmids were used as controls at the same N/P ratio.

DNA complexing

For each well, solution A was prepared by diluting fluorescent plasmid DNA (1 μg/well) into 100 μl Opti-MEM medium, then the solution was vortexed (2 s) and left at 20 °C for 30 min. N^4,N^9-Dioleoylspermine was added at different volumes into 100 μl Opti-MEM medium to achieve the desired N/P ratio, vortexed (2 s) and left at 20 °C for 30 min. Solutions A and B were then vortexed together for 2 s, and then incubated at 20 °C for 20 min for complete DNA complexing.[245]

Transfection

In 6-well or 35 mm tissue culture plates, 2.5 x 10^4 cells were seeded in 4 ml of 15% FCS EMEM (for FEK4). The cells were incubated at 37 °C, 5% CO_2 in a CO_2 incubator about 24 h, until the cells were 50-70% confluent. The 48 h post-transfection samples were analysed by FACS (for EGFP) or using a luminometer (for luciferase levels).

Synthesis of fluorescent lipospermidine

Materials

Spermidine, Boc_2O, TEA, ethyl trifluoroacetate, *N*-methylanthranilic acid (MANT), and fluorescein isothiocyanate (FITC) were purchased from Sigma-Aldrich, UK. Ambrettolide was given as a gift from IFF, Spain. All other solvents used were from Fisher, UK.

Preparation of 16-hydroxy-7-hexadecenoic acid

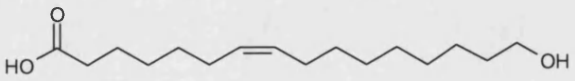

Figure 5.8 16-Hydroxy-7-hexadecenoic acid

Ambrettolide (1 eq, 1 g) was dissolved in MeOH (10 ml). NaOH (2 eq, 317 mg) was dissolved in MeOH (50 ml) and the solution was heated if necessary to ensure full solubility. This methanolic NaOH solution was added to the ambrettolide solution and the mixture (pH 11) was stirred (2 h) at 20 °C. The reaction solution was then put in an ice bath, and adjusted to pH 1.0 (HCl) to convert the product salt into the desired protonated carboxylic acid alcohol. The solution was extracted using DCM (3 x 40 ml). The DCM layer (lower layer) was collected and concentrated *in vacuo*. The sample, when analysed by TLC using EtOAc/hexane (4/6 v/v), give a single spot $R_f = 0.4$ by UV. An additional signal at 3417 cm^{-1} was found in the IR spectrum, indicating the presence of an alcohol functional group. The obtained colourless oil product displayed FAB$^-$ m/s 269.2 Da, $C_{16}H_{30}O_3$ requires 269 $(M-H)^-$. Mass peak at 252.4 (starting material lactone) was not found in the mass spectrum.

Preparation of N^1,N^9-di-trifluoroacetylspermidine

Spermidine 1 g (1 eq, 6.88 mmoles) was dissolved in MeOH (15 ml) and treated with 2 eq ethyl trifluoroacetate dissolved in MeOH (15 ml). The mixture was then stirred (18 h) at 20 °C. Then, MeOH was removed *in vacuo* and a colourless oil was obtained.[137] TLC analysis using DCM/MeOH/NH_3 (25/10/1 v/v/v), R_f = 0.14, showing the increased lipophilicity compared to spermidine which was immobile and stayed at the baseline. FAB^+ m/s 338.1 Da, $C_{11}H_{17}F_6N_3O_2$ requires 338 $(M+H)^+$.

Preparation of N^1,N^9-di-trifluoroacetyl-N^4-(16-hydroxy-7-hexadecenoyl)-spermidine

N^1,N^9-Di-trifluoroacetylspermidine (1 eq, 450 mg) was dissolved in DCM (5 ml) and MeOH (as needed to dissolve the starting material), then 16-hydroxy-7-hexadecenoic acid (1.2 eq), DCC (1.2 eq), and HOBt (0.5 eq) were added. The reaction was carried out at 20 °C with thorough stirring for 18 h. After concentration *in vacuo*, the tri-amide was re-dissolved in DCM so that DCU was precipitated. The mixture was filtered to obtain a clear yellow solution, which was concentrated *in vacuo*. The residue was purified by flash silica gel column chromatography, using DCM/MeOH/NH_3 (60/10/1 v/v/v). The fraction with TLC R_f = 0.50 DCM/MeOH/NH_3 (60/10/1 v/v/v) was collected. The obtained yellow oil product (540 mg, 69% yield) displayed FAB^+ m/s 590.0 Da, $C_{27}H_{45}F_6N_3O_4$ requires 590 $(M+H)^+$.

Attempted preparation of N^4-(16-FITC-7-hexadecenoyl)-spermidine

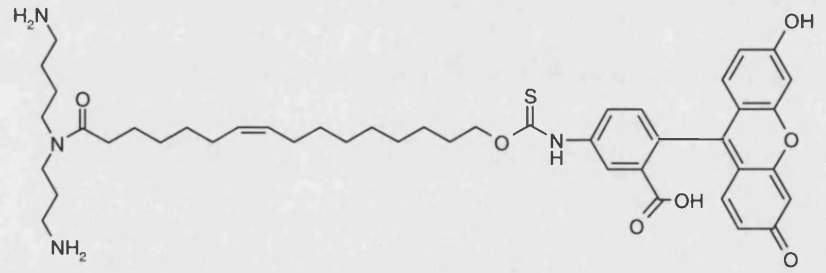

Figure 5.9 N^4-(16-FITC-7-hexadecenoyl)-spermidine

N^1,N^9-Di-trifluoroacetyl-N^4-(16-hydroxy-7-hexadecenoyl)-spermidine (1 eq, 100 mg) was dissolved in anhydrous DMSO (10 ml). FITC (1.1 eq, 72 mg) was added, and stirred at 20 °C (2 h) in the dark. Aq NH_4OH was then added to pH 11.0, and stirred at 20 °C (36 h) in the dark. The solution was then concentrated *in vacuo*. The residue was redissolved in MeOH and purified by flash silica gel column chromatography, using DCM/MeOH (25/10 v/v). The fraction with R_f = 0.33 on TLC in DCM/MeOH (25/10 v/v) was collected. The obtained brown solid product (56 mg, 42% yield) displayed FAB^+ m/s 827.4 Da $(M+K)^+$ (?) and 865.3 Da $(M-H+2K)^+$ (?), and $C_{44}H_{59}N_4O_7S$ requires 787 $(M+H)^+$. In the MS spectral

data, the observed $(M+K)^+$ and $(M-H+2K)^+$ were found at 10% relative intensity each with more 2 H^+ than the calculated mass. This may be from the replacement of $^1H^+$ with $^2H^+$ or ^{12}C with ^{13}C.

Preparation of N^4-(16-MANT-7-hexadecenoyl)-spermidine

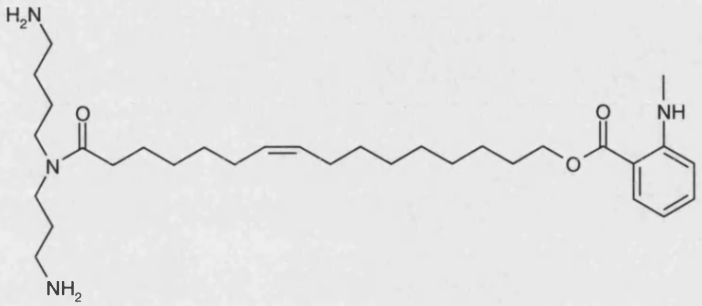

Figure 5.10 N^4-(16-MANT-7-hexadecenoyl)-spermidine

N^1,N^9-Di-trifluoroacetyl-N^4-(16-hydroxy-7-hexadecenoyl)-spermidine (1 eq, 100 mg) was dissolved in MeOH (10 ml). MANT (1.2 eq, 31 mg), DCC (1.2 eq, 206 mg), and HOBt (0.5 eq, 135 mg) were added to the solution, and stirred for 18 h at 20 °C in the dark. Directly, the two trifluoroacetyl protecting groups were removed by treatment with aq NH_4OH (to pH 11.0), and stirred at 20 °C (36 h) in the dark. The solution was then concentrated *in vacuo*. The residue was redissolved in MeOH and purified by flash silica gel column chromatography, using DCM/MeOH (25/10 v/v). The fraction with R_f = 0.43 on TLC in DCM/MeOH/NH_3 (25/10/1 v/v/v) mobile phase was collected, which showed two close spots. HPLC-Fluorescence detection (Supercosil ABZ+ Plus) eluting with MeOH/H_2O 80/20 (v/v) (1 ml/min) was used to resolve this mixed fraction. A single peak (λ_{ex} 368 nm, λ_{em} 437 nm) was eluted with t_R 2 min (no starting material MANT peak at t_R 4.2 min was found). N^4-(16-MANT-7-hexadecenoyl)-spermidine: NMR *inter alia* ($C^2H_3O^2H$) δ ^1H 1.24-1.70 (br m, many x CH_2), 1.99 (apparent quartet, 2 x allylic CH_2), 3.28-3.56 (br m, 2 x NCH_2 and OCH_2), 5.37-5.42 (m, CH=CH), and 7.29-7.78 (m, 4 x CH aromatic) ppm. The FAB mass spectral data showed the MANT fatty acid ester, but also spermidine, and no mass ion for the desired product was observed.

Synthesis of N^1,N^{12}-di-trifluoroacetyl-N^4-oleoylspermine

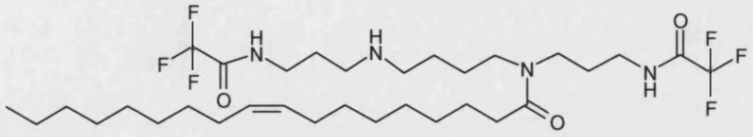

Figure 5.11 N^1,N^{12}-Di-trifluoroacetyl-N^4-oleoylspermine

Materials

Spermine, ethyl trifluoroacetate, DCC, HOBt, oleic acid, TFA, and ninhydrin for TLC detection were obtained from Sigma-Aldrich (UK). MeCN, DCM, EtOAc, and MeOH were purchased from Fisher Chemicals. Ammonia solution (aq NH_4OH, 33% v/v) was from BDH Laboratory (UK).

Preparation of N^1,N^{12}-di-trifluoroacetylspermine

Spermine 1 g (1 eq, 4.94 mmoles) was dissolved in MeCN (15 ml) and treated with 2 eq ethyl trifluoroacetate dissolved in MeCN (15 ml). The mixture was then stirred and heated under reflux (18 h) at 80 °C. Then, MeCN was removed by evaporation *in vacuo* and trifluoroacetylated spermine products were washed twice with EtOAc. A pale-yellow coloured solid (m.p. 195-198 °C) was obtained after concentration *in vacuo*.[137] The obtained sample, when analysed by TLC using MeOH/NH_4OH (4/1 v/v), gave $R_f = 0.8$ showed increased lipophilicity compared to spermine ($R_f = 0.1$).

Preparation of N^1,N^{12}-di-trifluoroacetyl-N^4-Boc-spermine

Di-tert-butyl dicarbonate (1.2 eq, in 10 ml MeOH) was added to N^1,N^{12}-ditrifluoroacetyl spermine (440 mg, 1 eq) dropwise over 3 min. The mixture was stirred at 20 °C for 4 h. MeOH was then evaporated *in vacuo* and the residue was purified by silica-gel chromatography using DCM/MeOH/NH_3 (75/10/1 v/v/v) ($R_f = 0.7$) to afford the desired orthogonally protected spermine (410 mg, 74% yield).

Preparation of N^1,N^{12}-di-trifluoroacetyl-N^4-Boc-N^9-oleoylspermine

N^1,N^{12}-Di-trifluoroacetyl-N^4-Boc-spermine (1 eq, 84 mg) was dissolved in MeOH (10 ml). Oleic acid (1.2 eq, 54 mg), DCC (1.2 eq, 40 mg), and HOBt (0.5 eq, 25 mg) were added to the solution, and stirred for 18 h at 20 °C. The solution was concentrated *in vacuo*, and redissolved in DCM (10 ml). The precipitate of DCU was removed by filtration to yield a yellow solution which was taken directly into the final deprotection step.

Boc removal

To a stirred solution of N^1,N^{12}-di-trifluoroacetyl-N^4-Boc-N^9-oleoylspermine in DCM (180 ml) under nitrogen at 25 °C, TFA (20 ml) was added. After 2 h, the solution was concentrated *in vacuo*. The residue was purified by silica-gel chromatography using DCM/MeOH/NH_3 (60/10/1 v/v/v). The yellow semi-solid product was analysed by TLC in DCM/MeOH/NH_3 60/10/1 v/v/v and $R_f = 0.5$. The desired product (40 mg, 36% yield) N^1,N^{12}-di-trifluoroacetyl-N^4-Boc-N^9-oleoylspermine displayed FAB^- m/s 656.3 Da, $C_{32}H_{56}F_6N_4O_3$ $(M-H)^-$ requires mass 657.

References

1. Watson, J. D.; Crick, F. H. C. A structure of deoxyribose nucleic acid. *Nature* **1953,** *171*, 737-738.

2. Romano, G.; Pacilio, C.; Giordano, A. Gene transfer technology in therapy: Current applications and future goals. *Stem Cells* **1999,** *17*, 191-202.

3. Kouraklis, G. Progress in cancer gene therapy. *Acta Oncol.* **1999,** *38*, 675-683.

4. Sandhu, J. S.; Keating, A.; Hozumi, N. Human gene therapy. *Crit. Rev. Biotechnol.* **1997,** *17*, 307-326.

5. Pandha, H. S.; Martin, L. A.; Rigg, A. S.; Ross, P.; Dalgleish, A. G. Gene therapy: Recent progress in the clinical oncology arena. *Curr. Opin. Mol. Ther.* **2000,** *2*, 362-375.

6. Brooks, G. *Gene therapy : The use of DNA as a drug;* Pharmaceutical Press: 2002.

7. Kirn, D.; Niculescu-Duvaz, I.; Hallden, G.; Springer, C. J. The emerging fields of suicide gene therapy and virotherapy. *Trends Mol. Med.* **2002,** *8*, S68-S73.

8. http://www.wiley.com/legacy/wileychi/genmed/clinical/, accessed on Aug 28, 2005.

9. Jimenez-Sanchez, G.; Childs, B.; Valle, D. Human disease genes. *Nature* **2001,** *409*, 853-855.

10. Crystal, R. G. Transfer of genes to humans - Early lessons and obstacles to success. *Science* **1995,** *270*, 404-410.

11. El Aneed, A. An overview of current delivery systems in cancer gene therapy. *J. Control. Release* **2004,** *94*, 1-14.

12. Dobbelstein, M. Viruses in therapy - Royal road or dead end? *Virus Res.* **2003,** *92*, 219-221.

13. Walther, W.; Stein, U. Viral vectors for gene transfer - a review of their use in the treatment of human diseases. *Drugs* **2000,** *60*, 249-271.

14. Verma, I. M.; Somia, N. Gene therapy - Promises, problems and prospects. *Nature* **1997,** *389*, 239-242.

15. Felgner, P. L.; Barenholz, Y.; Behr, J. P.; Cheng, S. H.; Cullis, P.; Huang, L.; Jessee, J. A.; Seymour, L.; Szoka, F.; Thierry, A. R.; Wagner, E.; Wu, G. Nomenclature for synthetic gene delivery systems. *Hum. Gene Ther.* **1997,** *8*, 511-512.

16. Hagstrom, J. E. Plasmid-based gene delivery to target tissues in vivo: The intravascular approach. *Curr. Opin. Mol. Ther.* **2003,** *5*, 338-344.

17. Nishitani, M. A.; Sakai, T.; Kanayama, H. O.; Himeno, K.; Kagawa, S. Cytokine gene therapy for cancer with naked DNA. *Molecular Urology* **2000,** *4*, 47-50.

18. Mehier-Humbert, S.; Guy, R. H. Physical methods for gene transfer: Improving the kinetics of gene delivery into cells. *Adv. Drug Deliv. Rev.* **2005,** *57*, 733-753.

19. Cullis, P. M.; Green, R. E.; Merson-Davies, L.; Travis, N. Probing the mechanism of transport and compartmentalisation of polyamines in mammalian cells. *Chem. Biol.* **1999,** *6*, 717-729.

20. Melnikova, Y. S.; Lindman, B. pH-controlled DNA condensation in the presence of dodecyldimethylamine oxide. *Langmuir* **2000,** *16*, 5871-5878.

21. Rungsardthong, U.; Ehtezazi, T.; Bailey, L.; Armes, S. P.; Garnett, M. C.; Stolnik, S. Effect of polymer ionization on the interaction with DNA in nonviral gene delivery systems. *Biomacromolecules* **2003,** *4*, 683-690.

22. Delcros, J. G.; Sturkenboom, M. C.; Basu, H. S.; Shafer, R. H.; Szollosi, J.; Feuerstein, B. G.; Marton, L. J. Differential effects of spermine and its analogues on the structures of polynucleotides complexed with ethidium bromide. *Biochem. J.* **1993,** *291*, 269-274.

23. Vijayanathan, V.; Thomas, T.; Thomas, T. J. DNA nanoparticles and development of DNA delivery vehicles for gene therapy. *Biochemistry* **2002,** *41*, 14085-14094.

24. Feuerstein, B. G.; Williams, L. D.; Basu, H. S.; Marton, L. J. Implications and concepts of polyamine-nucleic acid interactions. *J. Cell. Biochem.* **1991,** *46*, 37-47.

25. Bloomfield, V. A. DNA condensation. *Curr. Opin. Struct. Biol.* **1996,** *6*, 334-341.

26. Geall, A. J.; Al-Hadithi, D.; Blagbrough, I. S. Spermine and thermine conjugates of cholic acid condense DNA, but lithocholic acid polyamine conjugates do so more efficiently. *Chem. Commun.* **1998,** 2035-2036.

27. Geall, A. J.; Eaton, M. A. W.; Baker, T. S.; Catterall, C. F.; Blagbrough, I. S. The regiochemical distribution of positive charges along cholesterol polyamine carbamates plays significant roles in modulating DNA binding affinity and lipofection. *FEBS Lett.* **1999,** *459*, 337-342.

28. Bloomfield, V. A. DNA condensation by multivalent cations. *Biopolymers* **1997,** *44*, 269-282.

29. Blagbrough, I. S.; Geall, A. J.; Neal, A. P. Polyamines and novel polyamine conjugates interact with DNA in ways that can be exploited in non-viral gene therapy. *Biochem. Soc. Trans.* **2003,** *31*, 397-406.

30. Hsiang, M. W.; Cole, R. D. Structure of Histone H1-DNA Complex - Effect of Histone H-1 on DNA Condensation. *Proc. Natl. Acad. Sci. U. S. A.* **1977,** *74*, 4852-4856.

31. Berg, J. M.; Tymoczko, J. L.; Stryer, L. *Biochemistry;* 4 ed.; 1995.

32. Balicki, D.; Reisfeld, R. A.; Pertl, U.; Beutler, E.; Lode, H. N. Histone H2A-mediated transient cytokine gene delivery induces efficient antitumor responses in murine neuroblastoma. *Proc. Natl. Acad. Sci. U. S. A.* **2000,** *97*, 11500-11504.

33. Balicki, D.; Putnam, C. D.; Scaria, P. V.; Beutler, E. Structure and function correlation in histone H2A peptide-mediated gene transfer. *Proc. Natl. Acad. Sci. U. S. A* **2002,** *99*, 7467-7471.

34. Lucius, H.; Haberland, A.; Zaitsev, S.; Dalluge, R.; Schneider, M.; Bottger, M. Structure of transfection-active histone H1/DNA complexes. *Mol. Biol. Rep.* **2001,** *28*, 157-165.

35. Boussif, O.; Lezoualc'h, F.; Zanta, M. A.; Mergny, M. D.; Scherman, D.; Demeneix, B.; Behr, J. P. A versatile vector for gene and oligonucleotide transfer into cells in culture and in vivo: polyethylenimine. *Proc. Natl. Acad. Sci. U. S. A* **1995,** *92*, 7297-7301.

36. Remy, J. S.; Abdallah, B.; Zanta, M. A.; Boussif, O.; Behr, J. P.; Demeneix, B. Gene transfer with lipospermines and polyethylenimines. *Adv. Drug Deliv. Rev.* **1998,** *30*, 85-95.

37. Wagner, E. Strategies to improve DNA polyplexes for in vivo gene transfer: Will "artificial viruses" be the answer? *Pharm. Res.* **2004,** *21*, 8-14.

38. Godbey, W. T.; Wu, K. K.; Mikos, A. G. Tracking the intracellular path of poly(ethylenimine)/DNA complexes for gene delivery. *Proc. Natl. Acad. Sci. U. S. A.* **1999,** *96*, 5177-5181.

39. Clamme, J. P.; Krishnamoorthy, G.; Mely, Y. Intracellular dynamics of the gene delivery vehicle polyethylenimine during transfection: investigation by two- photon fluorescence correlation spectroscopy. *Biochim. Biophys. Acta-Biomembr.* **2003,** *1617*, 52-61.

40. Godbey, W. T.; Wu, K. K.; Mikos, A. G. Poly(ethylenimine) and its role in gene delivery. *J. Control. Release* **1999,** *60*, 149-160.

41. Fischer, D.; Bieber, T.; Li, Y. X.; Elsasser, H. P.; Kissel, T. A novel non-viral vector for DNA delivery based on low molecular weight, branched polyethylenimine: Effect of molecular weight on transfection efficiency and cytotoxicity. *Pharm. Res.* **1999,** *16*, 1273-1279.

42. Dash, P. R.; Toncheva, V.; Schacht, E.; Seymour, L. W. Synthetic polymers for vectorial delivery of DNA: characterisation of polymer-DNA complexes by photon correlation spectroscopy and stability to nuclease degradation and disruption by polyanions in vitro. *J. Control. Release* **1997,** *48*, 269-276.

43. Mannisto, M.; Vanderkerken, S.; Toncheva, V.; Elomaa, M.; Ruponen, M.; Schacht, E.; Urtti, A. Structure-activity relationships of poly(L-lysines): effects of pegylation and molecular shape on physicochemical and biological properties in gene delivery. *J. Control. Release* **2002,** *83*, 169-182.

44. Pouton, C. W.; Lucas, P.; Thomas, B. J.; Uduehi, A. N.; Milroy, D. A.; Moss, S. H. Polycation-DNA complexes for gene delivery: a comparison of the biopharmaceutical properties of cationic polypeptides and cationic lipids. *J. Control Release* **1998,** *53*, 289-299.

45. Ramsay, E.; Hadgraft, J.; Birchall, J.; Gumbleton, M. Examination of the biophysical interaction between plasmid DNA and the polycations, polylysine and polyornithine, as a basis for their differential gene transfection in-vitro. *Int. J. Pharm.* **2000,** *210*, 97-107.

46. Futaki, S.; Ohashi, W.; Suzuki, T.; Niwa, M.; Tanaka, S.; Ueda, K.; Harashima, H.; Sugiura, Y. Stearylated arginine-rich peptides: A new class of transfection systems. *Bioconjug. Chem.* **2001,** *12*, 1005-1011.

47. Mitchell, D. J.; Kim, D. T.; Steinman, L.; Fathman, C. G.; Rothbard, J. B. Polyarginine enters cells more efficiently than other polycationic homopolymers. *J. Pept. Res.* **2000,** *56*, 318-325.

48. Wender, P. A.; Mitchell, D. J.; Pattabiraman, K.; Pelkey, E. T.; Steinman, L.; Rothbard, J. B. The design, synthesis, and evaluation of molecules that enable or enhance cellular uptake: Peptoid molecular transporters. *Proc. Natl. Acad. Sci. U. S. A.* **2000,** *97*, 13003-13008.

49. Pichon, C.; Goncalves, C.; Midoux, P. Histidine-rich peptides and polymers for nucleic acids delivery. *Adv. Drug Deliv. Rev.* **2001,** *53*, 75-94.

50. Pack, D. W.; Putnam, D.; Langer, R. Design of imidazole-containing endosomolytic biopolymers for gene delivery. *Biotechnol. Bioeng.* **2000,** *67*, 217-223.

51. Ishii, T.; Okahata, Y.; Sato, T. Mechanism of cell transfection with plasmid/chitosan complexes. *Biochim. Biophys. Acta-Biomembr.* **2001,** *1514*, 51-64.

52. Sato, T.; Ishii, T.; Okahata, Y. In vitro gene delivery mediated by chitosan. Effect of pH, serum, and molecular mass of chitosan on the transfection efficiency. *Biomaterials* **2001,** *22*, 2075-2080.

53. Corsi, K.; Chellat, F.; Yahia, L.; Fernandes, J. C. Mesenchymal stem cells, MG63 and HEK293 transfection using chitosan-DNA nanoparticles. *Biomaterials* **2003,** *24*, 1255-1264.

54. Reineke, T. M.; Davis, M. E. Structural effects of carbohydrate-containing polycations on gene delivery. 1. Carbohydrate size and its distance from charge centers. *Bioconjug. Chem.* **2003,** *14*, 247-254.

55. Reineke, T. M.; Davis, M. E. Structural effects of carbohydrate-containing polycations on gene delivery. 2. Charge center type. *Bioconjug. Chem.* **2003,** *14*, 255-261.

56. Popielarski, S. R.; Mishra, S.; Davis, M. E. Structural effects of carbohydrate-containing polycations on gene delivery. 3. Cyclodextrin type and functionalization. *Bioconjug. Chem.* **2003,** *14*, 672-678.

57. Felgner, P. L.; Sridhar, C. N.; Wheeler, C. J.; Felgner, J. Enhanced gene delivery and mechanism studies with a novel series of cationic lipid formulations. *J. Cell. Biochem.* **1993,** 206.

58. Tranchant, I.; Thompson, B.; Nicolazzi, C.; Mignet, N.; Scherman, D. Physicochemical optimisation of plasmid delivery by cationic lipids. *J. Gene Med.* **2004,** *6*, S24-S35.

59. de Lima, M. C. P.; Neves, S.; Filipe, A.; Duzgunes, N.; Simoes, S. Cationic liposomes for gene delivery: From biophysics to biological applications. *Curr. Med. Chem.* **2003,** *10*, 1221-1231.

60. Felgner, P. L.; Gadek, T. R.; Holm, M.; Roman, R.; Chan, H. W.; Wenz, M.; Northrop, J. P.; Ringold, G. M.; Danielsen, M. Lipofection - a highly efficient, lipid-

mediated DNA- transfection procedure. *Proc. Natl. Acad. Sci. U. S. A.* **1987,** *84*, 7413-7417.

61. Tseng, W. C.; Huang, L. Liposome-based gene therapy. *Pharm. Sci. Technol. Today* **1998,** *1*, 206-213.

62. Farhood, H.; Serbina, N.; Huang, L. The role of dioleoyl phosphatidylethanolamine in cationic liposome mediated gene transfer. *Biochim. Biophys. Acta* **1995,** *1235*, 289-295.

63. Gao, X.; Huang, L. A novel cationic liposome reagent for rfficient transfection of mammalian-cells. *Biochem. Biophys. Res. Commun.* **1991,** *179*, 280-285.

64. Li, S.; Gao, X. A.; Son, K. G.; Sorgi, F.; Hofland, H.; Huang, L. DC-Chol lipid system in gene transfer. *J. Control. Release* **1996,** *39*, 373-381.

65. VanDerWoude, I.; Wagenaar, A.; Meekel, A. A. P.; TerBeest, M. B. A.; Ruiters, M. H. J.; Engberts, J. B. F. N.; Hoekstra, D. Novel pyridinium surfactants for efficient, nontoxic in vitro gene delivery. *Proc. Natl. Acad. Sci. U. S. A.* **1997,** *94*, 1160-1165.

66. Behr, J. P.; Demeneix, B.; Loeffler, J. P.; Perez-Mutul, J. Efficient gene transfer into mammalian primary endocrine cells with lipopolyamine-coated DNA. *Proc. Natl. Acad. Sci. U. S. A.* **1989,** *86*, 6982-6986.

67. Byk, G.; Dubertret, C.; Escriou, V.; Frederic, M.; Jaslin, G.; Rangara, R.; Pitard, B.; Crouzet, J.; Wils, P.; Schwartz, B.; Scherman, D. Synthesis, activity, and structure--activity relationship studies of novel cationic lipids for DNA transfer. *J. Med. Chem.* **1998,** *41*, 224-235.

68. Buchberger, B.; Fernholz, E.; v.d.Eltz, H.; Hinzepeter, M. DOSPER liposomal transfection reagent: A reagent with unique transfection properties. *Biochem. Inform.* **1996,** *98*, 27-29.

69. Geall, A. J.; Taylor, R. J.; Earll, M. E.; Eaton, M. A. W.; Blagbrough, I. S. Synthesis of cholesteryl polyamine carbamates: pKa studies and condensation of calf thymus DNA. *Bioconjug. Chem.* **2000,** *11*, 314-326.

70. Gaucheron, J.; Santaella, C.; Vierling, P. Highly fluorinated lipospermines for gene transfer: Synthesis and evaluation of their in vitro transfection efficiency. *Bioconjug. Chem.* **2001,** *12*, 114-128.

71. Lee, E. R.; Marshall, J.; Siegel, C. S.; Jiang, C. W.; Yew, N. S.; Nichols, M. R.; Nietupski, J. B.; Ziegler, R. J.; Lane, M. B.; Wang, K. X.; Wan, N. C.; Scheule, R. K.; Harris, D. J.; Smith, A. E.; Cheng, S. H. Detailed analysis of structures and formulations of cationic lipids for efficient gene transfer to the lung. *Hum. Gene Ther.* **1996,** *7*, 1701-1717.

72. Oudrhiri, N.; Vigneron, J. P.; Peuchmaur, M.; Leclerc, T.; Lehn, J. M.; Lehn, P. Gene transfer by guanidinium-cholesterol cationic lipids into airway epithelial cells in vitro and in vivo. *Proc. Natl. Acad. Sci. U. S. A.* **1997,** *94*, 1651-1656.

73. Pitard, B.; Oudrhiri, N.; Vigneron, J. P.; Hauchecorne, M.; Aguerre, O.; Toury, R.; Airiau, M.; Ramasawmy, R.; Scherman, D.; Crouzet, J.; Lehn, J. M.; Lehn, P. Structural characteristics of supramolecular assemblies formed by guanidinium-cholesterol reagents for gene transfection. *Proc. Natl. Acad. Sci. U. S. A.* **1999,** *96*, 2621-2626.

74. Fujiwara, T.; Hirashima, N.; Hasegawa, S.; Nakanishi, M.; Ohwada, T. Space-filling effects in membrane disruption by cationic amphiphiles. *Bioorg. Med. Chem.* **2001,** *9*, 1013-1024.

75. Geall, A. J.; Blagbrough, I. S. Homologation of polyamines in the rapid synthesis of lipospermine conjugates and related lipoplexes. *Tetrahedron* **2000,** *56*, 2449-2460.

76. Geall, A. J.; Al Hadithi, D.; Blagbrough, I. S. Efficient calf thymus DNA condensation upon binding with novel bile acid polyamine amides. *Bioconjug. Chem.* **2002,** *13*, 481-490.

77. Belmont, P.; Aissaoui, A.; Hauchecorne, M.; Oudrhiri, N.; Petit, L.; Vigneron, J. P.; Lehn, J. M.; Lehn, P. Aminoglycoside-derived cationic lipids as efficient vectors for gene transfection in vitro and in vivo. *J. Gene Med.* **2002,** *4*, 517-526.

78. Manning, G. S. Molecular theory of polyelectrolyte solutions with applications to electrostatic properties of polynucleotides. *Q. Rev. Biophys.* **1978,** *11*, 179-246.

79. Golan, R.; Pietrasanta, L. I.; Hsieh, W.; Hansma, H. G. DNA toroids: stages in condensation. *Biochemistry* **1999,** *38*, 14069-14076.

80. Lambert, O.; Letellier, L.; Gelbart, W. M.; Rigaud, J. L. DNA delivery by phage as a strategy for encapsulating toroidal condensates of arbitrary size into liposomes. *Proc. Natl. Acad. Sci. U. S. A.* **2000,** *97*, 7248-7253.

81. Yoshikawa, Y.; Yoshikawa, K.; Kanbe, T. Formation of a giant toroid from long duplex DNA. *Langmuir* **1999,** *15*, 4085-4088.

82. Hud, N. V.; Downing, K. H. Cryoelectron microscopy of lambda phage DNA condensates in vitreous ice: The fine structure of DNA toroids. *Proc. Natl. Acad. Sci. U. S. A.* **2001,** *98*, 14925-14930.

83. Shen, M. R.; Downing, K. H.; Balhorn, R.; Hud, N. V. Nucleation of DNA condensation by static loops: Formation of DNA toroids with reduced dimensions. *J. Am. Chem. Soc.* **2000,** *122*, 4833-4834.

84. Bloomfield, V. A. Condensation of DNA by multivalent cations - Considerations on mechanism. *Biopolymers* **1991,** *31*, 1471-1481.

85. Noguchi, H.; Yoshikawa, K. Folding path in a semiflexible homopolymer chain: A Brownian dynamics simulation. *J. Chem. Phys.* **2000,** *113*, 854-862.

86. Wiethoff, C. M.; Middaugh, C. R. Barriers to nonviral gene delivery. *J. Pharm. Sci.* **2003,** *92*, 203-217.

87. Friend, D. S.; Papahadjopoulos, D.; Debs, R. J. Endocytosis and intracellular processing accompanying transfection mediated by cationic liposomes. *Biochim. Biophys. Acta* **1996,** *1278*, 41-50.

88. Zuhorn, I. S.; Kalicharan, R.; Hoekstra, D. Lipoplex-mediated transfection of mammalian cells occurs through the cholesterol-dependent clathrin-mediated pathway of endocytosis. *J. Biol. Chem.* **2002,** *277*, 18021-18028.

89. Singh, A. K.; Kasinath, B. S.; Lewis, E. J. Interaction of polycations with cell-surface negative charges of epithelial-cells. *Biochim. Biophys. Acta* **1992,** *1120*, 337-342.

90. Zauner, W.; Farrow, N. A.; Haines, A. M. R. In vitro uptake of polystyrene microspheres: effect of particle size, cell line and cell density. *J. Control. Release* **2001,** *71*, 39-51.

91. Remy-Kristensen, A.; Clamme, J. P.; Vuilleumier, C.; Kuhry, J. G.; Mely, Y. Role of endocytosis in the transfection of L929 fibroblasts by polyethylenimine/DNA complexes. *Biochim. Biophys. Acta* **2001,** *1514*, 21-32.

92. Zabner, J.; Fasbender, A. J.; Moninger, T.; Poellinger, K. A.; Welsh, M. J. Cellular and molecular barriers to gene transfer by a cationic lipid. *J. Biol. Chem.* **1995,** *270*, 18997-19007.

93. Wagner, E.; Curiel, D.; Cotten, M. Delivery of drugs, proteins and genes into cells using transferrin as a ligand for receptor-mediated endocytosis. *Adv. Drug Deliv. Rev.* **1994,** *14*, 113-135.

94. Akinc, A.; Langer, R. Measuring the pH environment of DNA delivered using nonviral vectors: Implications for lysosomal trafficking. *Biotechnol. Bioeng.* **2002,** *78*, 503-508.

95. Cho, Y. W.; Kim, J. D.; Park, K. Polycation gene delivery systems: Escape from endosomes to cytosol. *J. Pharm. Pharmacol.* **2003,** *55*, 721-734.

96. Langner, M. The intracellular fate of non-viral DNA carriers. *Cell Mol. Biol. Lett.* **2000,** *5*, 295-313.

97. Hafez, I. M.; Maurer, N.; Cullis, P. R. On the mechanism whereby cationic lipids promote intracellular delivery of polynucleic acids. *Gene Ther.* **2001,** *8*, 1188-1196.

98. Zelphati, O.; Szoka, F. C., Jr. Mechanism of oligonucleotide release from cationic liposomes. *Proc. Natl. Acad. Sci. U. S. A.* **1996,** *93*, 11493-11498.

99. Fields, B. N.; Knipe, D. M.; Howley, P. M. *Fields Virology;* third ed.; 1996.

100. Lee, H.; Jeong, J. H.; Park, T. G. PEG grafted polylysine with fusogenic peptide for gene delivery: high transfection efficiency with low cytotoxicity. *J. Control. Release* **2002,** *79*, 283-291.

101. Martin, I.; Ruysschaert, J. M. Common properties of fusion peptides from diverse systems. *Biosci. Rep.* **2000,** *20*, 483-500.

102. Li, W. J.; Nicol, F.; Szoka, F. C. GALA: a designed synthetic pH-responsive amphipathic peptide with applications in drug and gene delivery. *Adv. Drug Deliv. Rev.* **2004,** *56*, 967-985.

103. Wyman, T. B.; Nicol, F.; Zelphati, O.; Scaria, P. V.; Plank, C.; Szoka, F. C., Jr. Design, synthesis, and characterization of a cationic peptide that binds to nucleic acids and permeabilizes bilayers. *Biochemistry* **1997,** *36*, 3008-3017.

104. Zhang, X. H.; Collins, L.; Fabre, J. W. A powerful cooperative interaction between a fusogenic peptide and lipofectamine for the enhancement of receptor-targeted, non-viral gene delivery via integrin receptors. *J. Gene Med.* **2001,** *3*, 560-568.

105. Lechardeur, D.; Sohn, K. J.; Haardt, M.; Joshi, P. B.; Monck, M.; Graham, R. W.; Beatty, B.; Squire, J.; O'Brodovich, H.; Lukacs, G. L. Metabolic instability of

plasmid DNA in the cytosol: a potential barrier to gene transfer. *Gene Ther.* **1999,** *6*, 482-497.

106. Cooper, G. M. The Cell, A Molecular Approach. 2nd ed.; 2000; pp 315-327.

107. Zanta, M. A.; Belguise-Valladier, P.; Behr, J. P. Gene delivery: A single nuclear localization signal peptide is sufficient to carry DNA to the cell nucleus. *Proc. Natl. Acad. Sci. U. S. A.* **1999,** *96*, 91-96.

108. Tachibana, R.; Harashima, H.; Ide, N.; Ukitsu, S.; Ohta, Y.; Suzuki, N.; Kikuchi, H.; Shinohara, Y.; Kiwada, H. Quantitative analysis of correlation between number of nuclear plasmids and gene expression activity after transfection with cationic liposomes. *Pharm. Res.* **2002,** *19*, 377-381.

109. Xu, Y. H.; Szoka, F. C. Mechanism of DNA release from cationic liposome/DNA complexes used in cell transfection. *Biochemistry* **1996,** *35*, 5616-5623.

110. Pollard, H.; Remy, J. S.; Loussouarn, G.; Demolombe, S.; Behr, J. P.; Escande, D. Polyethylenimine but not cationic lipids promotes transgene delivery to the nucleus in mammalian cells. *J. Biol. Chem.* **1998,** *273*, 7507-7511.

111. Tachibana, R.; Harashima, H.; Shinohara, Y.; Kiwada, H. Quantitative studies on the nuclear transport of plasmid DNA and gene expression employing nonviral vectors. *Adv. Drug Deliv. Rev.* **2001,** *52*, 219-226.

112. Harrington, K. J.; Linardakis, E.; Vile, R. G. Transcriptional control: An essential component of cancer gene therapy strategies? *Adv. Drug Deliv. Rev.* **2000,** *44*, 167-184.

113. LePecq, J. B.; Paoletti, C. A fluorescent complex between ethidium bromide and nucleic acids. Physical-chemical characterization. *J. Mol. Biol.* **1967,** *27*, 87-106.

114. Geall, A. J.; Blagbrough, I. S. Rapid and sensitive ethidium bromide fluorescence quenching assay of polyamine conjugate-DNA interactions for the analysis of lipoplex formation in gene therapy. *J. Pharm. Biomed. Anal.* **2000,** *22*, 849-859.

115. Gershon, H.; Ghirlando, R.; Guttman, S. B.; Minsky, A. Mode of formation and structural features of DNA-cationic liposome complexes used for transfection. *Biochemistry* **1993,** *32*, 7143-7151.

116. Read, M. L.; Etrych, T.; Ulbrich, K.; Seymour, L. W. Characterisation of the binding interaction between poly(L-lysine) and DNA using the fluorescamine assay in the preparation of non-viral gene delivery vectors. *FEBS Lett.* **1999,** *461*, 96-100.

117. Bode, J.; Willmitzer Application of fluorescamine to the study of protein-DNA interactions. *Nucleic Acids Res.* **1975,** *2*, 1951-1965.

118. Itaka, K.; Harada, A.; Nakamura, K.; Kawaguchi, H.; Kataoka, K. Evaluation by fluorescence resonance energy transfer of the stability of nonviral gene delivery vectors under physiological conditions. *Biomacromolecules* **2002,** *3*, 841-845.

119. Neal, A. P.; Blagbrough, I. S. Design and synthesis of fluorescent cholesterol and lithocholic acid polyamine conjugates. *Abstr. Pap. Am. Chem. Soc.* **2001,** *221*, 332-MEDI.

120. Neal, A. P.; Blagbrough, I. S. Fluorescent steroidal lipopolyamine conjugates for monitoring gene delivery. *Abstr. Pap. Am. Chem. Soc.* **2001,** *221*, 352-MEDI.

121. Byk, G.; Scherman, D. Genetic chemistry: Tools for gene therapy coming from unexpected directions. *Drug Dev. Res.* **2000,** *50*, 566-572.

122. Byk, G.; Wetzer, B.; Frederic, M.; Dubertret, C.; Pitard, B.; Jaslin, G.; Scherman, D. Reduction-sensitive lipopolyamines as a novel nonviral gene delivery system for modulated release of DNA with improved transgene expression. *J. Med. Chem.* **2000,** *43*, 4377-4387.

123. Uyechi, L. S.; Gagne, L.; Thurston, G.; Szoka, F. C. Mechanism of lipoplex gene delivery in mouse lung: Binding and internalization of fluorescent lipid and DNA components. *Gene Ther.* **2001,** *8*, 828-836.

124. Naylor, B. L.; Picardo, M.; Homan, R.; Pownall, H. J. Effects of fluorophore structure and hydrophobicity on the uptake and metabolism of fluorescent lipid analogs. *Chem. Phys. Lipids* **1991,** *58*, 111-119.

125. Bolton, P. H.; Kearns, D. R. Spectroscopic properties of ethidium monoazide: a fluorescent photoaffinity label for nucleic acids. *Nucleic Acids Res.* **1978,** *5*, 4891-4903.

126. Neves, C.; Byk, G.; Escriou, V.; Bussone, F.; Scherman, D.; Wils, P. Novel method for covalent fluorescent labeling of plasmid DNA that maintains structural integrity of the plasmid. *Bioconjug. Chem.* **2000,** *11*, 51-55.

127. Keller, G. H.; Huang, D. P.; Manak, M. M. Labeling of DNA probes with a photoactivatable hapten. *Anal. Biochem.* **1989,** *177*, 392-395.

128. Yoshinaga, T.; Yasuda, K.; Ogawa, Y.; Takakura, Y. Efficient uptake and rapid degradation of plasmid DNA by murine dendritic cells via a specific mechanism. *Biochemical and biophysical research communications* **2002,** *299*, 389-394.

129. Byrnes, C. K.; Nass, P. H.; Shim, J.; Duncan, M. D.; Lacy, B.; Harmon, J. W. Novel nuclear shuttle peptide to increase transfection efficiency in esophageal mucosal cells. *J. Gastrointest. Surg.* **2002,** *6*, 37-42.

130. Cormack, B. P.; Valdivia, R. H.; Falkow, S. FACS-optimized mutants of the green fluorescent protein (GFP). *Gene* **1996,** *173*, 33-38.

131. Gross, L. A.; Baird, G. S.; Hoffman, R. C.; Baldridge, K. K.; Tsien, R. Y. The structure of the chromophore within DsRed, a red fluorescent protein from coral. *Proc. Natl. Acad. Sci. U. S. A.* **2000,** *97*, 11990-11995.

132. Nolan, G. P.; Fiering, S.; Nicolas, J. F.; Herzenberg, L. A. Fluorescence-activated cell analysis and sorting of viable mammalian-cells based on beta-D-galactosidase activity after transduction of *Escherichia coli* Lacz. *Proc. Natl. Acad. Sci. U. S. A.* **1988,** *85*, 2603-2607.

133. Deluca, M.; McElory, W. D. Purification and properties of firefly luciferase. *Methods Enzymol.* **1978,** *57*, 3-15.

134. Geoffrey, M. C. *The cell, a molecular approach;* 2nd ed.; 2000.

135. Boesze-Battaglia, K.; Schimmel, R. J. Cell membrane lipid composition and distribution: Implications for cell function and lessons learned from photoreceptors and platelets. *J. Exp. Biol.* **1997,** *200*, 2927-2936.

136. Mosmann, T. Rapid colorimetric assay for cellular growth and survival - Application to proliferation and cytotoxicity assays. *J. Immunol. Methods* **1983,** *65*, 55-63.

137. Osullivan, M. C.; Dalrymple, D. M. A one-step procedure for the selective trifluoroacetylation of primary amino-groups of polyamines. *Tetrahedron Lett.* **1995,** *36*, 3451-3452.

138. Ronsin, G.; Perrin, C.; Guedat, P.; Kremer, A.; Camilleri, P.; Kirby, A. J. Novel spermine-based cationic gemini surfactants for gene delivery. *Chem. Commun.* **2001,** 2234-2235.

139. Kirby, A. J.; Camilleri, P.; Engberts, J. B.; Feiters, M. C.; Nolte, R. J.; Soderman, O.; Bergsma, M.; Bell, P. C.; Fielden, M. L.; Garcia Rodriguez, C. L.; Guedat, P.; Kremer, A.; McGregor, C.; Perrin, C.; Ronsin, G.; van Eijk, M. C. Gemini surfactants: new synthetic vectors for gene transfection. *Angew. Chem. Int. Ed Engl.* **2003,** *42*, 1448-1457.

140. Escribano, M. I.; Legaz, M. E. High-performance liquid-chromatography of the dansyl derivatives of putrescine, spermidine, and spermine. *Plant Physiol.* **1988,** *87*, 519-522.

141. Manchester, K. L. Value of A260/A280 ratios for measurement of purity of nucleic acids. *Biotechniques* **1995,** *19*, 208-210.

142. Manchester, K. L. Use of UV methods for measurement of protein and nucleic acid concentrations. *Biotechniques* **1996,** *20*, 968-970.

143. Rapley, R. Spectrophotometric Analysis of Nucleic Acids. In *The Nucleic Acid Protocol Handbook*, first ed.; Humana Press: 2000; pp 57-60.

144. Hsieh, H. P.; Muller, J. G.; Burrows, C. J. Synthesis and DNA-binding properties of C3-substituted, C-12-substituted, and C24-substituted amino-steroids serived from bile-acids. *Bioorg. Med. Chem.* **1995,** *3*, 823-838.

145. Deng, H.; Bloomfield, V. A.; Benevides, J. M.; Thomas, G. J. Structural basis of polyamine-DNA recognition: spermidine and spermine interactions with genomic B-DNAs of different GC content probed by Raman spectroscopy. *Nucleic Acids Res.* **2000,** *28*, 3379-3385.

146. Yoshikawa, K.; Yoshikawa, Y.; Kanbe, T. All-or-none folding transition in giant mammalian DNA. *Chem. Phys. Lett.* **2002,** *354*, 354-359.

147. Kleideiter, G.; Nordmeier, E. Poly(ethylene glycol)-induced DNA condensation in aqueous/methanol containing low-molecular-weight electrolyte solutions Part II. Comparison between experiment and theory. *Polymer* **1999,** *40*, 4025-4033.

148. Wilson, R. W.; Bloomfield, V. A. Counterion-induced condesation of deoxyribonucleic acid. a light-scattering study. *Biochemistry* **1979,** *18*, 2192-2196.

149. Basu, H. S.; Marton, L. J. The interaction of spermine and pentamines with DNA. *Biochem. J.* **1987,** *244*, 243-246.

150. Vijayanathan, V.; Thomas, T.; Shirahata, A.; Thomas, T. J. DNA condensation by polyamines: a laser light scattering study of structural effects. *Biochemistry* **2001,** *40*, 13644-13651.

151. Dunlap, D. D.; Maggi, A.; Soria, M. R.; Monaco, L. Nanoscopic structure of DNA condensed for gene delivery. *Nucleic Acids Res.* **1997,** *25*, 3095-3101.

152. Morgan, A. R.; Lee, J. S.; Pulleyblank, D. E.; Murray, N. L.; Evans, D. H. Ethidium fluorescence assays .1. Physicochemical studies. *Nucleic Acids Res.* **1979,** *7*, 547-569.

153. Tyrrell, R. M.; Pidoux, M. Quantitative differences in host-cell reactivation of ultraviolet-damaged virus in human-skin fibroblasts and epidermal-keratinocytes cultured from the same foreskin biopsy. *Cancer Res.* **1986,** *46*, 2665-2669.

154. Gresch, O.; Engel, F. B.; Nesic, D.; Tran, T. T.; England, H. M.; Hickman, E. S.; Korner, I.; Gan, L.; Chen, S.; Castro-Obregon, S.; Hammermann, R.; Wolf, J.; Muller-Hartmann, H.; Nix, M.; Siebenkotten, G.; Kraus, G.; Lun, K. New non-viral method for gene transfer into primary cells. *Methods* **2004,** *33*, 151-163.

155. Hamm, A.; Krott, N.; Breibach, I.; Blindt, R.; Bosserhoff, A. K. Efficient transfection method for primary cells. *Tissue Eng.* **2002,** *8*, 235-245.

156. Vile, G. F.; Tyrrell, R. M. Oxidative stress resulting from ultraviolet-A irradiation of human skin fibroblasts leads to a heme oxygenase-dependent increase in ferritin. *J. Biol. Chem.* **1993,** *268*, 14678-14681.

157. Vile, G. F.; Basu-Modak, S.; Waltner, C.; Tyrrell, R. M. Heme oxygenase 1 mediates an adaptive response to oxidative stress in human skin fibroblasts. *Proc. Natl. Acad. Sci. U. S. A* **1994,** *91*, 2607-2610.

158. Walker, W. E.; Porteous, D. J.; Boyd, A. C. The effects of plasmid copy number and sequence context upon transfection efficiency. *J. Control. Release* **2004,** *94*, 245-252.

159. Young, J. L.; Benoit, J. N.; Dean, D. A. Effect of a DNA nuclear targeting sequence on gene transfer and expression of plasmids in the intact vasculature. *Gene Ther.* **2003,** *10*, 1465-1470.

160. Masters, J. R. HeLa cells 50 years on: the good, the bad and the ugly. *Nat. Rev. Cancer* **2002,** *2*, 315-319.

161. Stoffler, H. E.; Honnert, U.; Bauer, C. A.; Hofer, D.; Schwarz, H.; Muller, R. T.; Drenckhahn, D.; Bahler, M. Targeting of the myosin-I myr 3 to intercellular adherens type junctions induced by dominant active Cdc42 in HeLa cells. *J. Cell Sci.* **1998,** *111*, 2779-2788.

162. Boussif, O.; Zanta, M. A.; Behr, J. P. Optimized galenics improve in vitro gene transfer with cationic molecules up to 1000-fold. *Gene Ther.* **1996,** *3*, 1074-1080.

163. Banks, G. A.; Roselli, R. J.; Chen, R.; Giorgio, T. D. A model for the analysis of nonviral gene therapy. *Gene Ther.* **2003,** *10*, 1766-1775.

164. Ryter, S.; Kvam, E.; Richman, L.; Hartmann, F.; Tyrrell, R. M. A chromatographic assay for heme oxygenase activity in cultured human cells: Application to artificial heme oxygenase overexpression. *Free Radic. Biol. Med.* **1998,** *24*, 959-971.

165. Gossen, M.; Bujard, H. Tight control of gene-expression in mammalian-cells by tetracycline-responsive promoters. *Proc. Natl. Acad. Sci. U. S. A.* **1992,** *89*, 5547-5551.

166. Kunath, K.; von Harpe, A.; Fischer, D.; Peterson, H.; Bickel, U.; Voigt, K.; Kissel, T. Low-molecular-weight polyethylenimine as a non-viral vector for DNA delivery: Comparison of physicochemical properties, transfection efficiency and in vivo distribution with high-molecular-weight polyethylenimine. *J. Control. Release* **2003,** *89*, 113-125.

167. Clamme, J. P.; Azoulay, J.; Mely, Y. Monitoring of the formation and dissociation of polyethylenimine/DNA complexes by two photon fluorescence correlation spectroscopy. *Biophys. J.* **2003,** *84*, 1960-1968.

168. *Fluorescence correlation spectroscopy: Theory and applications;* 1 ed.; Springer-Verlag, Berlin: 2001.

169. Brock, R. Fluorescence correlation spectroscopy in cell biology. In *Fluorescence methods and applications: Advanced methods and their applications to membranes, proteins, DNA, and cells*, Hof, M., Hutterer, R., Fidler, V., Eds.; Springer: 2004; pp 245-262.

170. Eigen, M.; Rigler, R. Sorting single molecules: application to diagnostics and evolutionary biotechnology. *Proc. Natl. Acad. Sci. U. S. A* **1994,** *91*, 5740-5747.

171. Enderlein, J. Single molecule spectroscopy: Basics and applications. In *Fluorescence methods and applications: Advanced methods and their applications to membranes, proteins, DNA, and cells*, Hof, M., Hutterer, R., Filder, V., Eds.; Springer: 2004; pp 104-122.

172. Thompson, N. L. Fluorescence correlation spectroscopy. In *Topics in fluorescence spectroscopy*, Lakowicz, J. R., Ed.; New York Kluwer Academic Publishers: 1991; p 337.

173. Walter, N. G.; Schwille, P.; Eigen, M. Fluorescence correlation analysis of probe diffusion simplifies quantitative pathogen detection by PCR. *Proc. Natl. Acad. Sci. U. S. A* **1996,** *93*, 12805-12810.

174. Magde, D.; Webb, W. W.; Elson, E. Thermodynamic fluctuations in a reacting system - Measurement by fluorescence correlation spectroscopy. *Phys. Rev. Lett.* **1972,** *29*, 705-708.

175. Magde, D.; Elson, E. L.; Webb, W. W. Fluorescence correlation spectroscopy .2. experimental realization. *Biopolymers* **1974,** *13*, 29-61.

176. Kral, T.; Hof, M.; Langner, M. The effect of spermine on plasmid condensation and dye release observed by fluorescence correlation spectroscopy. *Biol. Chem.* **2002,** *383*, 331-335.

177. Kral, T.; Langner, M.; Benes, M.; Baczynska, D.; Ugorski, M.; Hof, M. The application of fluorescence correlation spectroscopy in detecting DNA condensation. *Biophys. Chem.* **2002,** *95*, 135-144.

178. Jurkiewicz, P.; Okruszek, A.; Hof, M.; Langner, M. Associating oligonucleotides with positively charged liposomes. *Cell Mol. Biol. Lett.* **2003,** *8*, 77-84.

179. Kral, T.; Hof, M.; Jurkiewicz, P.; Langner, M. Fluorescence correlation spectroscopy (FCS) as a tool to study DNA condensation with hexadecyltrimethylammonium bromide (HTAB). *Cell Mol. Biol. Lett.* **2002,** *7*, 203-211.

180. Van Rompaey, E.; Engelborghs, Y.; Sanders, N.; De Smedt, S. C.; Demeester, J. Interactions between oligonucleotides and cationic polymers investigated by fluorescence correlation spectroscopy. *Pharm. Res.* **2001,** *18*, 928-936.

181. Sobell, H. M.; Tsai, C. C.; Jain, S. C.; Gilbert, S. G. Visualization of drug-nucleic acid interactions at atomic resolution. III. Unifying structural concepts in understanding drug-DNA interactions and their broader implications in understanding protein-DNA interactions. *J. Mol. Biol.* **1977,** *114*, 333-365.

182. Nordmeier, E. Absorption-spectroscopy and dynamic and static light- scattering-studies of ethidium-bromide binding to calf thymus DNA - Implications for outside binding and intercalation. *J. Phys. Chem.* **1992,** *96*, 6045-6055.

183. Millard, P. J.; Roth, B. L.; Thi, H. P. T.; Yue, S. T.; Haugland, R. P. Development of the FUN-1 family of fluorescent probes for vacuole labeling and viability testing of yeasts. *Appl. Environ. Microbiol.* **1997,** *63*, 2897-2905.

184. Singer, V. L.; Jones, L. J.; Yue, S. T.; Haugland, R. P. Characterization of PicoGreen reagent and development of a fluorescence-based solution assay for double-stranded DNA quantitation. *Anal. Biochem.* **1997,** *249*, 228-238.

185. Zipper, H.; Brunner, H.; Bernhagen, J.; Vitzthum, F. Investigations on DNA intercalation and surface binding by SYBR Green I, its structure determination and methodological implications. *Nucleic Acids Res.* **2004,** *32*, art-e103.

186. Eriksson, M.; Karlsson, H. J.; Westman, G.; Akerman, B. Groove-binding unsymmetrical cyanine dyes for staining of DNA: Dissociation rates in free solution and electrophoresis gels. *Nucleic Acids Res.* **2003,** *31*, 6235-6242.

187. Petty, J. T.; Bordelon, J. A.; Robertson, M. E. Thermodynamic characterization of the association of cyanine dyes with DNA. *J. Phys. Chem. B* **2000,** *104*, 7221-7227.

188. Zipper, H.; Buta, C.; Lammle, K.; Brunner, H.; Bernhagen, J.; Vitzthum, F. Mechanisms underlying the impact of humic acids on DNA quantification by SYBR Green I and consequences for the analysis of soils and aquatic sediments. *Nucleic Acids Res.* **2003,** *31*, art-e39.

189. Yan, X. M.; Grace, W. K.; Yoshida, T. M.; Habbersett, R. C.; Velappan, N.; Jett, J. H.; Keller, R. A.; Marrone, B. L. Characteristics of different nucleic acid staining dyes for DNA fragment sizing by flow cytometry. *Anal. Chem.* **1999,** *71*, 5470-5480.

190. Beach, L.; Schweitzer, C.; Scaiano, J. C. Direct determination of single-to-double stranded DNA ratio in solution using steady-state fluorescence measurements. *Org. Biomol. Chem.* **2003,** *1*, 450-451.

191. Schweitzer, C.; Scaiano, J. C. Selective binding and local photophysics of the fluorescent cyanine dye PicoGreen in double-stranded and single-stranded DNA. *Phys. Chem. Chem. Phys.* **2003,** *5*, 4911-4917.

192. Lukacs, G. L.; Haggie, P.; Seksek, O.; Lechardeur, D.; Freedman, N.; Verkman, A. S. Size-dependent DNA mobility in cytoplasm and nucleus. *J. Biol. Chem.* **2000,** *275*, 1625-1629.

193. Bjorling, S.; Kinjo, M.; Foldes-Papp, Z.; Hagman, E.; Thyberg, P.; Rigler, R. Fluorescence correlation spectroscopy of enzymatic DNA polymerization. *Biochemistry* **1998,** *37*, 12971-12978.

194. Lumma, D.; Keller, S.; Vilgis, T.; Radler, J. O. Dynamics of large semiflexible chains probed by fluorescence correlation spectroscopy. *Phys. Rev. Lett.* **2003,** *90*, 218301(1)-218301(4).

195. Adjimatera, N.; Neal, A. P.; Blagbrough, I. S. Fluorescence techniques in non-viral gene therapy. In *Fluorescence spectroscopy in biology: Advanced methods and their applications to membranes, proteins, DNA, and cells*, Hof, M., Hutterer, R., Fidler, V., Eds.; Springer: 2005; pp 201-228.

196. De Smedt, S. C.; Remaut, K.; Lucas, B.; Braeckmans, K.; Sanders, N. N.; Demeester, J. Studying biophysical barriers to DNA delivery by advanced light microscopy. *Adv. Drug Deliv. Rev.* **2005,** *57*, 191-210.

197. Kral, T.; Widerak, K.; Langner, M.; Hof, M. Propidium iodide and PicoGreen as dyes for the DNA fluorescence correlation spectroscopy measurements. *J. Fluorescence* **2005,** *15*, 179-183.

198. Yan, X. M.; Habbersett, R. C.; Yoshida, T. M.; Nolan, J. P.; Jett, J. H.; Marrone, B. L. Probing the kinetics of SYTOX orange stain binding to double- stranded DNA with implications for DNA analysis. *Anal. Chem.* **2005,** *77*, 3554-3562.

199. Cosa, G.; Focsaneanu, K. S.; Mclean, J. R. N.; McNamee, J. P.; Scaiano, J. C. Photophysical properties of fluorescent DNA-dyes bound to single- and double-stranded DNA in aqueous buffered solution. *Photochem. Photobiol.* **2001,** *73*, 585-599.

200. Choi, J. S.; Nam, K.; Park, J.; Kim, J. B.; Lee, J. K.; Park, J. Enhanced transfection efficiency of PAMAM dendrimer by surface modification with L-arginine. *J. Control. Release* **2004,** *99*, 445-456.

201. Singh, R.; Pantarotto, D.; McCarthy, D.; Chaloin, O.; Hoebeke, J.; Partidos, C. D.; Briand, J. P.; Prato, M.; Bianco, A.; Kostarelos, K. Binding and condensation of plasmid DNA onto functionalized carbon nanotubes: Toward the construction of nanotube-based gene delivery vectors. *J. Am. Chem. Soc.* **2005,** *127*, 4388-4396.

202. Tsai, J. T.; Furstoss, K. J.; Michnick, T.; Sloane, D. L.; Paul, R. W. Quantitative physical characterization of lipid-polycation-DNA lipopolyplexes. *Biotechnol. Appl. Biochem.* **2002,** *36*, 13-20.

203. Kasper, F. K.; Seidlits, S. K.; Tang, A.; Crowther, R. S.; Carney, D. H.; Barry, M. A.; Mikos, A. G. In vitro release of plasmid DNA from oligo(poly(ethylene glycol) fumarate) hydrogels. *J. Control. Release* **2005,** *104*, 521-539.

204. Welz, C.; Fahr, A. Spectroscopic methods for characterization of nonviral gene delivery systems from a pharmaceutical point of view. *Appl. Spectrosc. Rev.* **2001,** *36*, 333-397.

205. Benda, A.; Hof, M.; Wahl, M.; Patting, M.; Erdmann, R.; Kapusta, P. TCSPC upgrade of a confocal FCS microscope. *Rev. Sci. Instrum.* **2005,** *76*.

206. LabatMoleur, F.; Steffan, A. M.; Brisson, C.; Perron, H.; Feugeas, O.; Furstenberger, P.; Oberling, F.; Brambilla, E.; Behr, J. P. An electron microscopy study into the mechanism of gene transfer with lipopolyamines. *Gene Ther.* **1996,** *3*, 1010-1017.

207. Rejman, J.; Bragonzi, A.; Conese, M. Role of clathrin- and caveolae-mediated endocytosis in gene transfer mediated by lipo- and polyplexes. *Mol. Ther.* **2005,** *12*, 468-474.

208. Schnitzer, J. E. Caveolae: from basic trafficking mechanisms to targeting transcytosis for tissue-specific drug and gene delivery in vivo. *Adv. Drug Deliv. Rev.* **2001,** *49*, 265-280.

209. Thomsen, P.; Roepstorff, K.; Stahlhut, M.; van Deurs, B. Caveolae are highly immobile plasma membrane microdomains, which are not involved in constitutive endocytic trafficking. *Mol. Biol. Cell* **2002,** *13*, 238-250.

210. Matsui, H.; Johnson, L. G.; Randell, S. H.; Boucher, R. C. Loss of binding and entry of liposome-DNA complexes decreases transfection efficiency in differentiated airway epithelial cells. *J. Biol. Chem.* **1997,** *272*, 1117-1126.

211. Stewart, W. W. Lucifer Dyes - Highly fluorescent dyes for biological tracing. *Nature* **1981,** *292*, 17-21.

212. Wolkers, W. F.; Looper, S. A.; Fontanilla, R. A.; Tsvetkova, N. M.; Tablin, F.; Crowe, J. H. Temperature dependence of fluid phase endocytosis coincides with membrane properties of pig platelets. *Biochim. Biophys. Acta-Biomembr.* **2003,** *1612*, 154-163.

213. Zhong, J. L.; Yiakouvaki, A.; Holley, P.; Tyrrell, R. M.; Pourzand, C. Susceptibility of skin cells to UVA-induced necrotic cell death reflects the intracellular level of labile iron. *J. Invest. Dermatol.* **2004,** *123*, 771-780.

214. Hong, S.; Bielinska, A. U.; Mecke, A.; Keszler, B.; Beals, J. L.; Shi, X.; Balogh, L.; Orr, B. G.; Baker, J. R., Jr.; Banaszak Holl, M. M. Interaction of poly(amidoamine) dendrimers with supported lipid bilayers and cells: Hole formation and the relation to transport. *Bioconjug. Chem.* **2004,** *15*, 774-782.

215. McClelland, D.; Evans, R. M.; Abidin, I.; Sharma, S.; Choudhry, F. Z.; Jaspars, M.; Sepcic, K.; Scott, R. H. Irreversible and reversible pore formation by polymeric alkylpyridinium salts (poly-APS) from the sponge Reniera sarai. *Br. J. Pharmacol.* **2003,** *139*, 1399-1408.

216. Tucker, S. J.; McClelland, D.; Jaspars, M.; Sepcic, K.; MacEwan, D. J.; Scott, R. H. The influence of alkyl pyridinium sponge toxins on membrane properties, cytotoxicity, transfection and protein expression in mammalian cells. *Biochim. Biophys. Acta-Biomembr.* **2003,** *1614*, 171-181.

217. Scott, R. H.; Whyment, A. D.; Foster, A.; Gordon, K. H.; Milne, B. F.; Jaspars, M. Analysis of the structure and electrophysiological actions of halitoxins: 1,3 alkyl-pyridinium salts from Callyspongia ridleyi. *J. Membr. Biol.* **2000,** *176*, 119-131.

218. Tucker, S. J.; McClelland, D.; Jaspars, M.; Sepcic, K.; MacEwan, D. J.; Scott, R. H. The influence of alkyl pyridinium sponge toxins on membrane properties, cytotoxicity, transfection and protein expression in mammalian cells. *Biochim. Biophys. Acta-Biomembr.* **2003,** *1614*, 171-181.

219. Larsson, P.; Andersson, E.; Johansson, U.; Ollinger, K.; Rosdahl, I. Ultraviolet A and B affect human melanocytes and keratinocytes differently. A study of oxidative alterations and apoptosis. *Exp. Dermatol.* **2005,** *14*, 117-123.

220. Umebayashi, Y.; Miyamoto, Y.; Wakita, M.; Kobayashi, A.; Nishisaka, T. Elevation of plasma membrane permeability on laser irradiation of extracellular latex particles. *J. Biochem. (Tokyo)* **2003,** *134*, 219-224.

221. Warren, G.; Davoust, J.; Cockcroft, A. Recycling of transferrin receptors in A431 cells is inhibited during mitosis. *EMBO J.* **1984,** *3*, 2217-2225.

222. Berlin, R. D.; Oliver, J. M.; Walter, R. J. Surface functions during Mitosis I: Phagocytosis, pinocytosis and mobility of surface-bound Con A. *Cell* **1978,** *15*, 327-341.

223. Meers, P.; Hong, K.; Bentz, J.; Papahadjopoulos, D. Spermine as a modulator of membrane-fusion - Interactions with acidic phospholipids. *Biochemistry* **1986,** *25*, 3109-3118.

224. Chung, L.; Kaloyanides, G.; McDaniel, R.; McLaughlin, A.; McLaughlin, S. Interaction of gentamicin and spermine with bilayer membranes containing negatively charged phospholipids. *Biochemistry* **1985,** *24*, 442-452.

225. Momo, F.; Wisniewska, A.; Stevanato, R. EPR study of spermine interaction with multilamellar phosphatidylcholine liposomes. *Biochim. Biophys. Acta-Biomembr.* **1995,** *1240*, 89-94.

226. Henneberry, A. L.; Wright, M. M.; McMaster, C. R. The major sites of cellular phospholipid synthesis and molecular determinants of fatty acid and lipid head group specificity. *Mol. Biol. Cell* **2002,** *13*, 3148-3161.

227. Ongpipattanakul, B.; Burnette, R. R.; Potts, R. O.; Francoeur, M. L. Evidence that oleic acid exists in a separate phase within stratum corneum lipids. *Pharm. Res.* **1991,** *8*, 350-354.

228. Turunen, T. M.; Urtti, A.; Paronen, P.; Audus, K. L.; Rytting, J. H. Effect of some penetration enhancers on epithelial membrane lipid domains: evidence from fluorescence spectroscopy studies. *Pharm. Res.* **1994,** *11*, 288-294.

229. Evrard, D.; Touitou, E.; Kolusheva, S.; Fishov, Y.; Jelinek, R. A new colorimetric assay for studying and rapid screening of membrane penetration enhancers. *Pharm. Res.* **2001,** *18*, 943-949.

230. Tipnis, U. R.; He, G. Y. Mechanism of polyamine toxicity in cultured cardiac myocytes. *Toxicol. in Vitro* **1998,** *12*, 233-+.

231. ElOuahabi, A.; Thiry, M.; Pector, V.; Fuks, R.; Ruysschaert, J. M.; Vandenbranden, M. The role of endosome destabilizing activity in the gene transfer process mediated by cationic lipids. *Febs Letters* **1997,** *414*, 187-192.

232. Pantazatos, S. P.; MacDonald, R. C. Real-time observation of lipoplex formation and interaction with anionic bilayer vesicles. *J. Membr. Biol.* **2003,** *191*, 99-112.

233. Connor, J.; Yatvin, M. B.; Huang, L. pH-sensitive liposomes: acid-induced liposome fusion. *Proc. Natl. Acad. Sci. U. S. A* **1984,** *81*, 1715-1718.

234. Ross, D. D.; Joneckis, C. C.; Ordonez, J. V.; Sisk, A. M.; Wu, R. K.; Hamburger, A. W.; Nora, R. E. Estimation of cell-survival by flow cytometric quantification of fluorescein diacetate propidium iodide viable cell number. *Cancer Res.* **1989,** *49*, 3776-3782.

235. Kichler, A.; Mechtler, K.; Behr, J. P.; Wagner, E. Influence of membrane-active peptides on lipospermine/DNA complex mediated gene transfer. *Bioconjug. Chem.* **1997,** *8*, 213-221.

236. Holaska, J. M.; Wilson, K. L.; Mansharamani, M. The nuclear envelope, lamins and nuclear assembly. *Curr. Opin. Cell Biol.* **2002,** *14*, 357-364.

237. Slattum, P. S.; Loomis, A. G.; Machnik, K. J.; Watt, M. A.; Duzeski, J. L.; Budker, V. G.; Wolff, J. A.; Hagstrom, J. E. Efficient in vitro and in vivo expression of covalently modified plasmid DNA. *Mol. Ther.* **2003,** *8*, 255-263.

238. Still, W. C.; Kahn, M.; Mitra, A. Rapid Chromatographic Technique for Preparative Separations with Moderate Resolution. *J. Org. Chem.* **1978,** *43*, 2923-2925.

239. Abdel-Monem, M. M.; Ohno, K. Polyamine metabolism I: Synthesis of dansyl derivatives of N-(monoaminoalkyl)- and N-(polyaminoalkyl)acetamides and elucidation in urine of a cancer patient. *J. Pharm. Sci.* **1977,** *66*, 1089-1094.

240. Hawel, L.; Byus, C. V. A streamlined method for the isolation and quantitation of nanomole levels of exported polyamines in cell culture media. *Anal. Biochem.* **2002,** *311*, 127-132.

241. Birnboim, H. C.; Doly, J. A rapid alkaline extraction procedure for screening recombinant plasmid DNA. *Nucleic Acids Res.* **1979,** *7*, 1513-1523.

242. Sambrook, J.; Frisch, E. F.; Maniatis, T. Plasmid vectors. In *Molecular Cloning : a Laboratory Manual*, 1st ed.; Cold Spring Harbor Laboratory Press: 1989; p 1.21-1.38.

243. Rapley, R. Extraction and Purification of Plasmid DNA. In *The Nucleic Acid Protocol Handbook*, 1st ed.; Humana Press: 2000; pp 327-331.

244. Cain, B. F.; Baguley, B. C.; Denny, W. A. Potenial antitumor agents. 28. Deoxyribonucleic acid polyintercalating agents. *J. Med. Chem.* **1978,** *21*, 658-668.

245. Invitrogen Ltd. Lipofectin technical document, 2001.

246. Muller, R. T.; Honnert, U.; Reinhard, J.; Bahler, M. The rat myosin myr 5 is a GTPase-activating protein for Rho in vivo: Essential role of arginine 1695. *Mol. Biol. Cell* **1997,** *8*, 2039-2053.

247. Promega Corporation. Luciferase assay system (Technical bulletin no.281), 2002.

248. Sigma Aldrich Corporation, Bradford reagent technical bulletin (B 6916), 2001.

249. Bohmer, M.; Wahl, M.; Rahn, H. J.; Erdmann, R.; Enderlein, J. Time-resolved fluorescence correlation spectroscopy. *Chem. Phys. Lett.* **2002,** *353*, 439-445.

250. Mirus Ltd., Label IT Nucleic acid labeling kits - Frequently asked questions, 2002.

Appendix

List of Publications

1. O. A. A. Ahmed, **N. Adjimatera**, C. Pourzand, and I. S. Blagbrough, *N^4,N^9-Dioleoyl Spermine is a Novel Non-Viral Lipopolyamine Vector for Plasmid DNA Formulation*, Pharmaceutical Research, 2005, 22, 972-80.

2. **N. Adjimatera**, A. P. Neal, and I. S. Blagbrough. *Chapter 12: Fluorescence Techniques in Non-Viral Gene Therapy.* In M. Hof, R. Hutterer, and V. Fidler (eds), *Fluorescence Spectroscopy in Biology: Advanced Methods and Their Applications to Membranes, Proteins, DNA and Cells* (Springer Series on Fluorescence Spectroscopy Volume 3), Springer, 2005, 201-228.

3. I. S. Blagbrough, **N. Adjimatera**, O. A. A. Ahmed, A. P. Neal and C. Pourzand, *Chapter 16: Spermine and Lipopolyamines as Gene Delivery Agent.* In: D. J. Beadle, I. R. Mellor and P. N. R. Usherwood (eds), *Neurotox'03: Neurotoxicological Targets from Functional Genomics and Proteomics*, Society of Chemical Industry, 2004, 147-159.

List of Presentations

1. *Analysis of Single Lipopolyamine-DNA Nanocomplex Formation in Non-viral Gene Therapy by Fluorescence Correlation Spectroscopy using PicoGreen* **(ORAL)** British Pharmaceutical Conference (BPC2005), Royal Pharmaceutical Society of Great Britain, Manchester, UK, 2005.

2. *Synthesis and Biological Testing of N^2,N^3-Dioleoylspermine – a Nanopharmaceutical for DNA Condensation and Plasmid Delivery* **(POSTER)** British Pharmaceutical Conference (BPC2005), Royal Pharmaceutical Society of Great Britain, Manchester, UK, 2005.

3. *Monitoring Single Lipopolyamine-DNA Nanoparticle Formation in Non-Viral Gene Therapy By Fluorescence Correlation Spectroscopy Using Picogreen* **(POSTER)** 9th International Conference on Methods and Applications of Fluorescence (MAF9), Portugal, 2005.

4. *Fluorescent Lipopolyamines: a New Class of Molecular Probes in Non-Viral Gene Therapy* **(POSTER)** 9th International Conference on Methods and Applications of Fluorescence (MAF9), Portugal, 2005.

5. *Sensing DNA Nanocomplex Delivery by Fluorescent Probes* **(ORAL)** 229th National Meeting, American Chemical Society (229th ACS), San Diego/US, 2005.

6. *Monitoring Formulation and Intracellular Delivery of Plasmids by Lipopolyamines* **(ORAL)** 229th National Meeting, American Chemical Society (229th ACS), San Diego/US, 2005.

7. *Synthesis and Biological Testing of N^2,N^3-Dioleoylspermine – a Nanopharmaceutical for DNA Condensation and Plasmid Delivery* **(POSTER)** 229th American Chemical Society National Meeting (229th ACS), San Diego/US, March 2005.

8. *Fluorescent Lipopolyamines: a New Class of Molecular Probes in Non-Viral Gene Therapy* **(POSTER)** British Pharmaceutical Conference, Royal Pharmaceutical Society of Great Britain (BPC2004), Manchester, UK, 2004.

9. *Fluorescence Correlation Spectroscopy of Spermine-DNA Interactions –Nanostructure and Physical Supramolecular Chemistry of DNA Condensation* **(POSTER)** International Conference on Supramolecular Science & Technology (ISS&T2004), Czech Republic, Sept 2004. (Published in *Chem Listy* 98, supplement, 2004, pp s22-s23)

10. *Molecular Modelling of DNA-Ethidium Bromide Weak Interactions –DNA Bending by Polyamines Leading to Self Assembly of Nanoparticles* **(POSTER)** International Conference on Supramolecular Science & Technology, Czech Republic (ISS&T2004), Sept 2004. (Published in *Chem Listy* 98, supplement, 2004, pp s23-s24)

11. *Synthesis and Biological Testing of N^2,N^3-Dioleoylspermine – a Nanopharmaceutical for DNA Condensation and Plasmid Delivery* **(POSTER)** International Conference on Supramolecular Science & Technology, Czech Republic (ISS&T2004), Sept 2004. (Published in *Chem Listy* 98, supplement, 2004, pp s24-s25)

12. *Fluorescence Techniques in Non-Viral Gene Therapy: Using Spermine and Lipopolyamines as DNA Delivery Agents* **(POSTER)** 8th International Conference on Methods and Applications of Fluorescence (MAF8), Czech Republic, 2003.

Pharmaceutical Research, Vol. 22, No. 6, June 2005 (© 2005)
DOI: 10.1007/s11095-005-4592-1

Research Paper

N^4,N^9-Dioleoyl Spermine Is a Novel Nonviral Lipopolyamine Vector for Plasmid DNA Formulation

Osama A. A. Ahmed,[1] Noppadon Adjimatera,[1] Charareh Pourzand,[1] and Ian S. Blagbrough[1,2]

Received November 28, 2004; accepted February 15, 2005

Purpose. To study the effect of synthesized N^4,N^9-dioleoyl spermine on DNA condensation and then measure its transfection efficiency in cell culture.
Methods. The lipopolyamine was synthesized from the naturally occurring polyamine spermine. The ability of this novel compound to condense DNA was studied using ethidium bromide fluorescence quenching and light scattering assays. Transfection efficiency was studied in primary skin cells (FEK4) and in an immortalized cancer cell line (HtTA), and compared with the commercially available transfection formulations Lipofectin and Lipofectamine.
Results. The synthesized N^4,N^9-dioleoyl spermine formula is efficient at condensing calf thymus and circular plasmid DNA and effectively transfects both primary skin cells and cancer cell lines at low charge ratios of (+/− ammonium/phosphate) 2.5.
Conclusions. N^4,N^9-Dioleoyl spermine condenses DNA and achieves high transfection levels in cultured cells.

KEY WORDS: FEK4; gene delivery; lipopolyamine; N^4,N^9-dioleoyl spermine; transfection.

INTRODUCTION

It is widely believed that gene therapy will become an efficient medicine for the treatment of diseases such as cancer, cystic fibrosis and for vaccination. The essential requirements for gene delivery are the transport of DNA through the cell membrane and ultimately to the nucleus. The design of an efficient formula for the delivery of genetic material requires a detailed understanding of the mechanism of gene delivery to the nucleus. Different strategies have been used for the delivery of genetic material into target cells, classified as viral or non-viral delivery systems (1–3). Viral delivery systems depend on the development of genetically-modified viruses to utilize their capability of efficiently delivering DNA into cells without their pathogenic characteristics (3). Although high efficiency is achieved by viral vectors, there are concerns about their use which include: a limit in the size of the DNA delivered (the "payload"), endogenous viral recombination, unexpected anti-vector immune response, and oncogene activation (4–7). Since the design and formulation of Lipofectin by Felgner and co-workers, reported in 1987 (8), the focus on nonviral vectors for DNA delivery has shown a remarkable increase worldwide (9–15).

Efficient nonviral formulation should be able to deliver safely the required DNA across the various cellular barriers to the nucleus. These barriers that hinder the delivery of DNA to its physical site of action (the nucleus) have been summarized in Fig. 1. They include complex formation between the DNA and cationic lipid or polymer that leads to condensation of DNA into nanoparticles. Cell-membrane entry is thought to be mediated by cationic substances, which interact with the DNA payload, and can then cause adsorptive endocytosis and internalization of the complex. Also, the lipid moiety in cationic lipids interacts with the phospholipid bilayer of the cell membrane that facilitates cell entry. The internalized material is fused with early endosome. That leads to sorting to the late endosomal compartment, at this stage the DNA complex should escape the endosomal vesicle before the later stage of the lysosome where the DNA will be degraded. After endosomal escape, the DNA (either complexed or dissociated from the condensing agent) should find its way to the nucleus and cross the nuclear membrane which is thought to occur through the nuclear pore complex (NPC) or by direct association with the chromatin during mitosis. After nuclear entry, the payload DNA should successfully be able to give the desired protein through the processes of transcription and translation.

For drug formulators, it is difficult to deliver a drug molecule of 3.3 kDa molecular weight carrying 10 negative charges, but in the case of the (prodrug) DNA, a 5 kbp

[1] Department of Pharmacy and Pharmacology, University of Bath, Bath BA2 7AY, United Kingdom.
[2] To whom correspondence should be addressed. (e-mail: prsisb@bath.ac.uk)

ABBREVIATIONS: DCC, dicyclohexylcarbodiimide; DOGS, dioctadecylamidoglycylspermine; DOSPER, 1,3-dioleoyloxy-2-(6-carboxyspermine; EGFP, enhanced green fluorescent protein; EMEM, Earle's minimal essential medium; EthBr, ethidium bromide; FCS, fetal calf serum; HOBt, hydroxybenzotriazole; NPC, nuclear pore complex; PEI, polyethylenimine; PLL, poly-L-lysine.

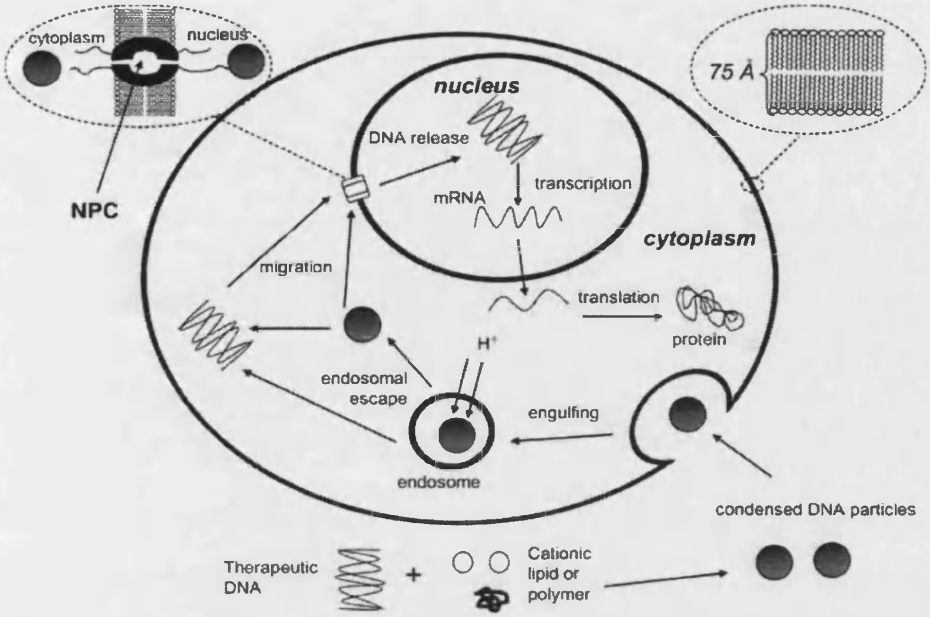

Fig. 1. Steps in the process of nonviral gene therapy by endocytosis showing the barriers for DNA nanoparticles, from the formation of the DNA-polycation complex (condensed DNA particles) to protein synthesis.

plasmid has a molecular weight of about 3.3 megadaltons and carries 10,000 negative charges. So the first key step in gene formulation is DNA condensation into a nanoparticle form through masking the negative charges of the phosphate backbone which causes alleviation of charge repulsion between remote phosphates on the DNA helix leading to collapse into a more compact structure (2,16). The importance of DNA condensation is attributed to the correlation of the transfection efficiency with the formation of DNA nanoparticles that are essential for the delivery of DNA through the cell membrane (16–20).

Cationic lipids are considered to be the major gene carriers among the non-viral delivery systems. They have the ability to condense DNA into particles that can be readily endocytosed by cultured cells, and facilitate endosomal escape leading to efficient delivery to the nucleus (21). They can be classified as liposomal and non-liposomal nonviral delivery vectors. Liposomal delivery vectors usually contain two types of lipids, a cationic lipid (positively charged amphiphile) for DNA condensation and cellular membrane interaction, and a neutral helper lipid (phospholipid), most use dioleoylphosphatidyl-ethanolamine (DOPE) (Fig. 2) to increase transfection efficiency as it has a membrane fusion promoting ability (8,22,23). Nonliposomal cationic-lipid delivery vectors combine both the characteristics of cationic and helper lipids.

The synthesis of the lipopolyamine dioctadecylamidoglycylspermine (DOGS) by Behr and co-workers (24) as a promising transfecting agent, encouraged several laboratories to focus on the synthesis of novel cationic lipids based on the naturally occurring polyamine spermine, for example, RPR120535 (25) and 1,3-dioleoyloxy-2-(6-carboxyspermine) DOSPER (26) (Fig. 2). The design of a novel lipopolyamine formula for DNA condensation and cellular delivery relies on previous and continuing studies of the structure-activity relationships of DNA binding and condensation by polyamines (16,27–30). Although lipopolyamines are less efficient in comparison with viral vectors, their promising lower toxicity than viral vectors ensures a continuous effort to design novel lipopolyamines with improved transfection efficiency. In this study, we synthesized and formulated a novel lipospermine in which the tetra-amine spermine (the cationic moiety) and dioleoyl chains (the lipophilic moiety) that is reported to improve the transfection efficiency by fusion with cellular membrane (31). These unsaturated chains are linked by amide bonds at the secondary amino groups of spermine to form N^4,N^9-dioleoyl spermine (commercially available as LipoGen) (32). These amide linkers have the advantages of being both biodegradable and less toxic than the ether bonds in DOTMA (33,34). The ability of this synthetic lipopolyamine to condense DNA was studied using ethidium bromide (EthBr) fluorescence quenching and light scattering assays. Transfection efficiency was studied in an immortalized cancer cell line (HtTA), and in primary skin cells (FEK4) for the first time. The difficulties found in efficiently transfecting primary cell lines were largely overcome with this nonliposomal formulation comprising a vector with two covalently bound oleoyl chains. The results are compared with two commercially available (liposomal) transfection formulations, Lipofectin® and Lipofectamine that incorporate such oleoyl or oleyl (C18) chains.

MATERIALS AND METHODS

Materials

Chemicals, including polyamines spermine, polyethylenimine (PEI), and poly-L-lysine (PLL), reagents, solvents, buffers, and DNA were routinely purchased from Sigma-Aldrich, UK, except where indicated. Lipofectin and Lipo-

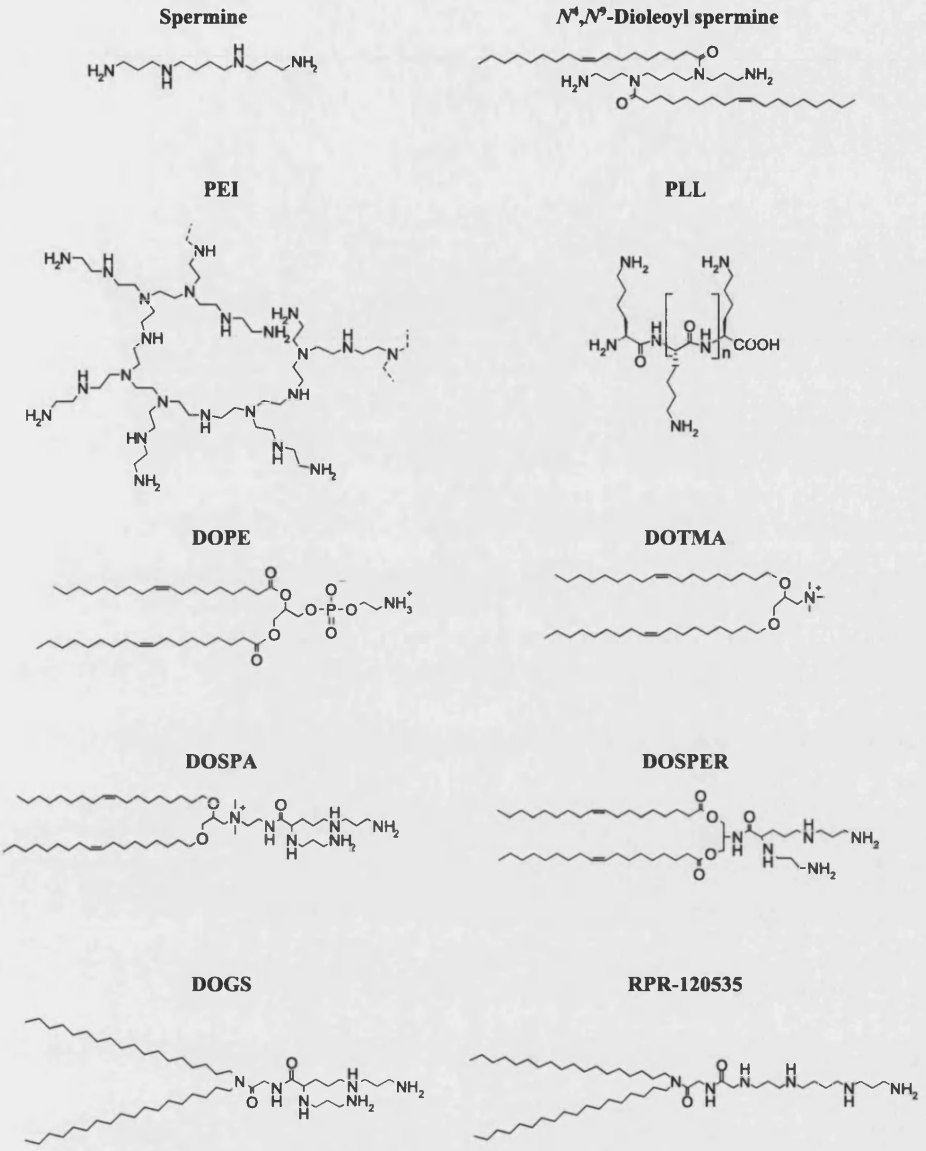

Fig. 2. Chemical structures of spermine, PEI, PLL, DOPE, DOTMA, and spermine based lipopolyamines.

fectamine reagents from Invitrogen (Life Technologies Gibco BRL) and cell cultures materials from Life Technologies (Paisley, Scotland).

Synthesis of N^4,N^9-Dioleoyl Spermine

Spermine was used as the starting material for the synthesis process (35), outlined in Fig. 3. Spermine was protected on the primary amino functional groups with ethyl trifluoroacetate (2.2 eq) in methanol and the reaction mixture was stirred for 18 h at 25°C. The solvent was evaporated to dryness *in vacuo* to form N^1,N^{12}-ditrifluoroacetyl-1,12-diamino-4,9-diazadodecane. Dicyclohexylcarbodiimide (DCC, 2.5 eq), 1-hydroxybenzotriazole (HOBt, 0.2 eq) and oleic acid (2.2 eq) were added to the diprotected spermine solution in CH_2Cl_2 and methanol (1:1). The solution was stirred for 18 h at 25°C. The solvent was evaporated to dryness *in vacuo*. The residue was dissolved in CH_2Cl_2 and the solution filtered and evaporated to dryness *in vacuo* to form N^4,N^9-dioleoyl-N^1,N^{12}-ditrifluoroacetyl-1,12-diamino-4,9-diazadodecane. For the removal of the di-trifluoroacetyl groups, the tetra-amide was dissolved in methanol and the pH of the solution was increased by saturating with ammonia gas, then it was left (18 h) and evaporated to dryness *in vacuo* to give a residue which was purified over silica gel (CH_2Cl_2-MeOH 5:3 v/v, then CH_2Cl_2-MeOH-conc. aq. NH_3 25:10:1 v/v/v) to afford N^4,N^9-dioleoyl spermine R_f 0.3 (CH_2Cl_2-MeOH-conc. aq. NH_3 25:10:1 v/v/v).

Amplification and Purification of Plasmid DNA (pEGFP)

DNA plasmid encoding enhanced green fluorescent protein (pEGFP) purchased from Clontech was transformed into *Escherichia coli* JM 109 bacterial strain (Promega). The

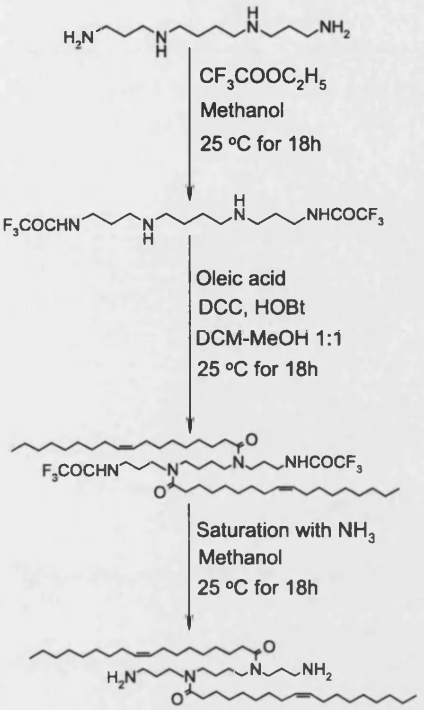

Fig. 3. Synthesis of N^4,N^9-dioleoyl spermine.

transformed cells were grown in larger quantities of Luria-Bertani (LB) broth supplemented with 125 mg/L ampicillin. pEGFP plasmid was produced in large-scale using HiSpeed plasmid purification Maxi kit (Qiagen) according to the manufacturers protocol. DNA yields and purity were determined spectroscopically (OD_{260}/OD_{280} = 1.80 to 1.90 OD, optical density) and by agarose gel (1% agarose) analysis.

Ethidium Bromide Fluorescence Quenching Assay

Each concentration of the DNA stock solutions (approximately 1 μg/μl, 1 ml) was determined spectroscopically (Milton Roy Spectronic 601 spectrometer, 1 cm path length, 3 ml cuvette) (2) and 6 μg (approximately 6 μl) of DNA was diluted to 3 ml with buffer (20 mM NaCl, 2 mM HEPES, 10 μM EDTA, pH 7.4) in a glass cuvette stirred with a micro-flea. Immediately prior to analysis, EthBr solution (3 μl, 0.5 mg/ml) was added to the stirring solution and allowed to equilibrate for 10 min. Separately for each polyamine or lipopolyamine (spermine, poly-L-lysine (average molecular weight 9600 Da, PLL 9.6k), polyethylenimine (average molecular weight 2000 Da, PEI 2K), N^4,N^9-dioleoyl spermine, Lipofectin, and Lipofectamine) aliquots (5 μl, according to the ammonium/phosphate (+/−) charge ratio required) were then added to the stirring solution and the fluorescence measured after 1 min equilibration using Perkin-Elmer LS 50B luminescent spectrometer (λ_{excit} = 260 nm and λ_{emiss} = 600 nm with slit width 5 nm) while stirring using an electronic stirrer (Rank Bros. Ltd.) (36). The total polyamine solution added to the DNA solution did not exceed 5% of the total volume of the solution, so no correction was made for sample dilution. The fluorescence was expressed as the percentage of the maximum fluorescence when EthBr was bound to the DNA in the absence of competition for binding and was corrected for background fluorescence of free EthBr in solution.

Light Scattering Assay

DNA (60 μg, 60 μl of 1 mg/ml solution) was diluted to 3 ml with HEPES buffer (2 mM HEPES, 20 mM NaCl, 10 μM EDTA, pH 7.4) in a cuvette with a micro-flea, and the concentration determined spectroscopically (Milton Roy Spectronic 601 spectrometer, 1 cm path length, 3 ml cuvette). Then aliquots (5 μl, according to the ammonium/phosphate (+/−) charge ratio) of the tested polyamines were then added to the stirring solution and the absorbance (light scattering) at 320 nm was measured after 1 min stirring to allow the mixture to reach equilibrium. The increase in absorbance due to the scattered light was expressed as the percentage of relative maximum apparent absorbance (% rel. max. app. abs.) due to light scattering of the bound polyamine with DNA.

Cell Culture and Transfection Experiments

Two cell lines were used in the transfection experiment, a human primary skin fibroblast cells FEK4 (37) derived from a foreskin explant and a human cervix carcinoma, HeLa derivative and transformed cell line (HtTA). The HtTA cells being stably transfected with a tetracycline-controlled transactivator (tTA) consisting of the tet repressor fused with the activating domain of virion protein 16 of the herpes simplex virus (HSV). Cells were cultured in Earle's minimal essential medium (EMEM) supplemented with foetal calf serum (FCS) 15% in the case of FEK4 and 10% in the case of HtTA cells, penicillin and streptomycin (50 IU/ml each), glutamine (2 mM), and sodium bicarbonate (0.2%).

For the transfection (gene delivery) and the resultant gene activity (transfection efficiency), FEK4 and HtTA cells were seeded at 1×10^5 cell/well in 6 well plates in 4 ml EMEM media with FCS for 24 h to reach a plate confluency of 50–60% on the day of transfection. The complex was prepared by mixing 2 μg of pEGFP with the cationic liposomes or lipopolyamine in Opti-MEM (serum free media, Gibco BRL) according to the charge ratio at room temperature for 30 min and then incubated with the cells for 4 h at 37°C in 5% CO_2. Then the cells were washed and cultured for further 44 h in growth medium at 37°C in 5% CO_2 before the assay.

Levels of enhanced green fluorescent protein (EGFP positive cells) in the transfected cells were detected and corrected for background fluorescence of the control cells using a fluorescence activated cell sorting (FACS) machine (Becton Dickinson FACS Vantage dual Laser Instrument, argon ion laser 488 nm). The transfection efficiency was calculated based on the percentage of the cells that expressed EGFP (positive cells) in the total number of cells.

Cytotoxicity (MTT) Assay of the Formed Lipoplexes

FEK4 and HtTA cells were seeded in 96 well plates at 8000 cell/well and incubated for 24 h at 37°C in 5% CO_2. N^4,N^9-Dioleoyl spermine complexed with pEGFP was added in the same way as the transfection protocol. After incubation for 44 h, the media was replaced with 90 μl of fresh media and

10 µl of sterile filtered MTT solution (Sigma-Aldrich, UK) (5 mg/ml) to reach a final concentration of 0.5 mg/ml. Then the plates were incubated for a further 4 h at 37°C in an atmosphere of 5% v/v CO_2. After incubation, the media and the unreacted dye were aspirated and the formed blue formazan crystals were dissolved in 200 µl/well of dimethyl sulfoxide (DMSO). The produced color was measured using a plate-reader (VERSAmax) at wavelength 570 nm. The % viability related to control wells containing cells without DNA and/or polymer and is calculated by (test absorbance/control absorbance) × 100 (38). The same protocol was applied in case of the commercially available reagents Lipofectin and Lipofectamine.

RESULTS

Synthesis of N^4, N^9-Dioleoyl Spermine

The synthesized N^4,N^9-dioleoyl spermine (Fig. 3) was homogenous on silica gel thin-layer chromatography and was fully characterized by ^{1}H-NMR (at 400 MHz) and ^{13}C-NMR and high-resolution accurate mass spectroscopy.

Ethidium Bromide Fluorescence Quenching Assay

To study the ability of N^4,N^9-dioleoyl spermine to condense calf thymus DNA and pEGFP as well as compared this effect with the effect of different known polycations spermine, PLL (39) and PEI (40) (Fig. 2) to condense DNA. Figure 4 shows the ability of the studied polyamines to displace EthBr from DNA. The binding ability was in the order PEI 2K > N^4,N^9-dioleoyl spermine > PLL 9.6K > spermine according to the charge ratio. The charge ratio was calculated according to the ammonium/phosphate (+/−) ratio for: spermine, 202.35 g/mole with four nitrogen atoms that can be protonated; PLL 9.6K, one positive charge/lysine monomer; N^4,N^9-dioleoyl spermine, with two positive charges. In the case of PEI 2K the charge ratio was calculated as 25% of the amino groups in the polymer that can be protonated, assuming that 43.1 g/mol is the repeating unit of PEI that contains one nitrogen atom (41,42). It seems to be that there is no agreement in the literature for the calculation of the PEI/DNA ratio. Although it is calculated as PEI nitrogen/DNA phosphate (40) not as charge ratio, it is reported that every third atom of PEI polymer is a protonatable nitrogen (40), but one in five of the protonatable nitrogens in PEI are protonated at pH 7 (43). However, Wagner (11) reported that one of every seven nitrogens within PEI polymer is protonated at pH 7. The polycations (PEI 2K and PLL 9.6K) are known for their ability to condense DNA efficiently at a relatively low charge ratio compared to spermine. On the other hand, the results revealed that N^4,N^9-dioleoyl spermine is able to condense DNA at a lower charge ratio than PLL 9.6K and spermine (Fig. 4), and produces a 50% fluorescence decrease at charge ratio 0.52. Also, Fig. 5 shows DNA condensation ability of N^4,N^9-dioleoyl spermine in comparison with the commercially available, cationic lipid, liposomal formulations Lipofectin and Lipofectamine. All three cationic lipid formulations have the ability to condense completely DNA through the displacement of EthBr leading to fluorescence quenching. At lower charge ratios N^4,N^9-dioleoyl spermine has better ability to suppress the fluorescence than Lipofectin and Lipofectamine. On studying the effect of N^4,N^9-dioleoyl spermine on the type of DNA (calf thymus DNA, and plasmid pEGFP), it was found that there is no significant variation in the condensation ability of the studied lipopolyamine on the type of DNA.

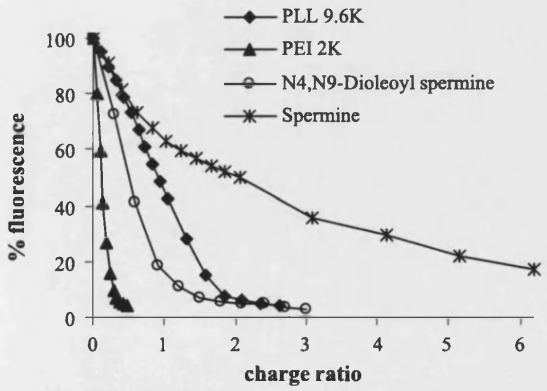

Fig. 4. Plot of EthBr displacement assay of calf thymus DNA complexed with PLL 9.6K, PEI 2K, N^4,N^9-dioleoyl spermine, and spermine.

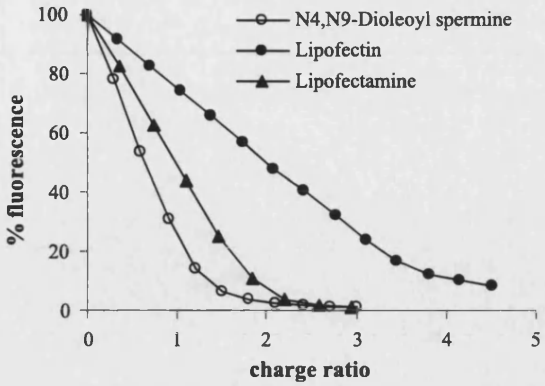

Fig. 5. Plot of EthBr displacement assay of calf thymus DNA complexed with N^4,N^9-dioleoyl spermine, Lipofectin, and Lipofectamine.

Light Scattering Assay

This experiment has been carried out to investigate the condensation of DNA by polyamines and the formation of particles (44). The apparent UV absorbance at 320 nm (where there is no DNA absorbance above 300 nm) was measured (28,45,46) showing light scattering. The results from Fig. 6 indicated the formation of particles upon interaction of spermine, PLL 9.6K and PEI 2K. In addition, Fig. 7 shows that the light scattering due to particle formation increases with the increase in the displaced EthBr and reaches the maximum at approximately the same charge ratio at which there is a maximum EthBr displacement, although the concentration of DNA used in light scattering experiments is ten times the concentration used in fluorescence quenching experiments which is related to the lack of sensitivity of light scattering experiment in comparison with fluorescence assay. Also, from light scattering results, there is a decrease in the % relative maximal apparent absorbance (% rel. max. app. abs.) after reaching the maximum absor-

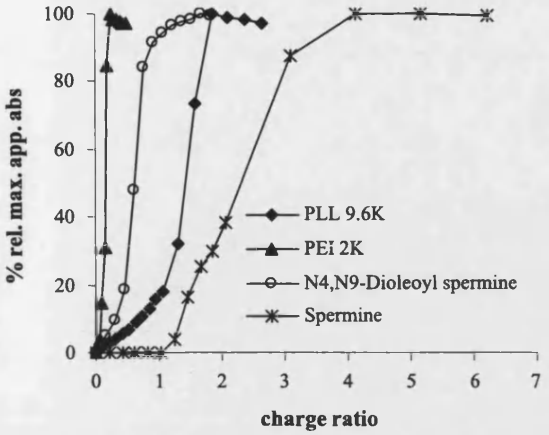

Fig. 6. Light scattering assay (% relative maximum apparent absorbance at λ = 320 nm) of calf thymus DNA complexed with PLL 9.6K, PEI 2K, N^4,N^9-dioleoyl spermine and spermine.

bance, which could be attributed to the formation of polyamine-DNA aggregates as reported by Gosule and Schellman (47).

Transfection Experiments

The transfection efficiency of pEGFP into FEK4 primary cell line and the cancer HtTA cells was studied using N^4,N^9-dioleoyl spermine and the commercially available reagents (Lipofectin and Lipofectamine). The transfection results of pEGFP into FEK4 indicated higher transfection ability of N^4,N^9-dioleoyl spermine (75%) and Lipofectamine (66%) formulations over Lipofectin (18%); there is no significant difference in the transfection activity between N^4,N^9-dioleoyl spermine and Lipofectamine (Fig. 8). On the other hand, both N^4,N^9-dioleoyl spermine and Lipofectamine formulations show a similar transfection activity in HtTA cells (about 70%), higher than Lipofectin (58%). N^4,N^9-Dioleoyl spermine transfects the cells best at charge ratio (+/−) 2.5 (5.54 μg/ml), Lipofectin at charge ratio 0.6 (5.0 μg/ml), while Lipofectamine transfect both cell lines at charge ratio 3.7 (10.0 μg/ml).

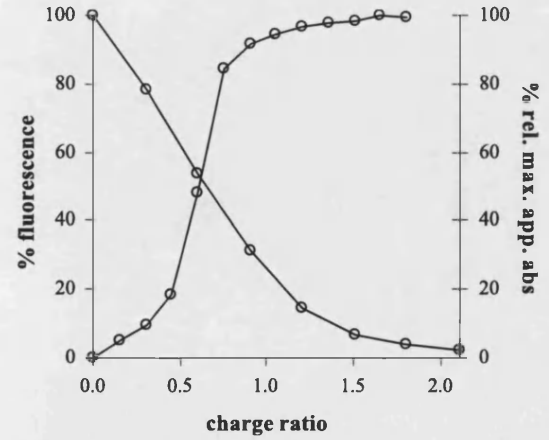

Fig. 7. Comparison of EthBr displacement and light scattering assays of calf thymus DNA with N^4,N^9-dioleoyl spermine.

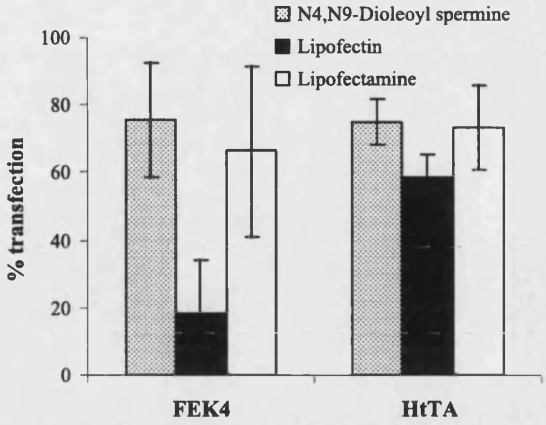

Fig. 8. Lipofection of FEK4 and HtTA cells transfected with pEGFP complexed with N^4,N^9-dioleoyl spermine, Lipofectin or Lipofectamine (at their respective N/P ratios for best transfection). The data represent 3 different experiments (3 replicates each) and the error bars represent the standard deviation.

In Vitro Cytotoxicity

The cytotoxicity of N^4,N^9-dioleoyl spermine was studied in FEK4 and HtTA cells using MTT assay (48) (Fig. 9). The IC_{50} (the concentration at which cell growth is inhibited by 50%) (42) values for the free polycation in FEK4 and HtTA

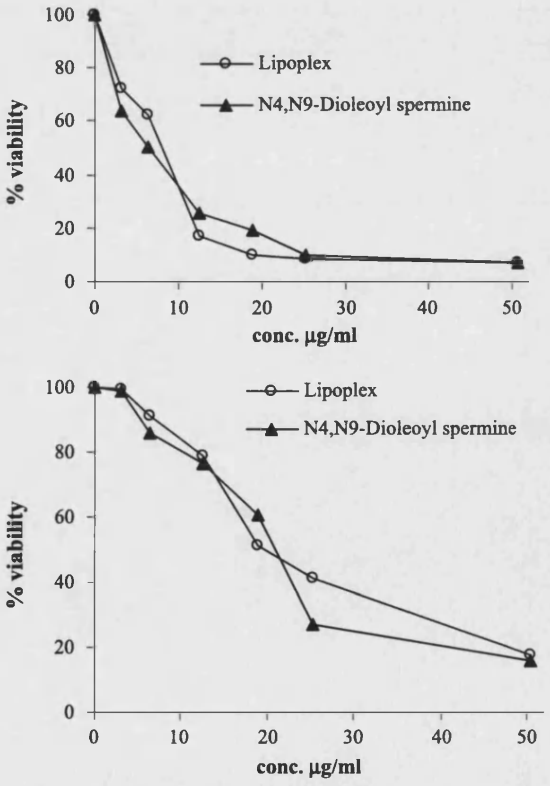

Fig. 9. Viability of HtTA cells (above) and FEK4 primary skin cells (below) after application of different concentrations of N^4,N^9-dioleoyl spermine either free or complexed with pEGFP.

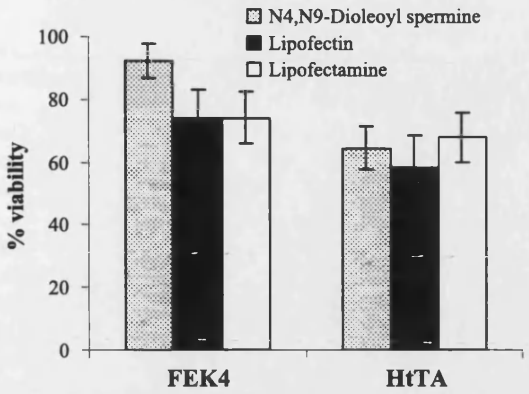

Fig. 10. Cytotoxicity effect of pEGFP (2 μg/ml) complexed with either N^4,N^9-dioleoyl spermine (5.54 μg/ml), Lipofectin (5 μg/ml) or Lipofectamine (10 μg/ml) in FEK4 and HtTA cells.

cells were 20.47 and 6.31 μg/ml respectively, and for the lipoplex were 19.82 and 8.35 μg/ml respectively. The results indicate that there is no significant difference in the toxic effect (IC_{50}) of the free polycation over the lipoplex in the case of HtTA cells and FEK4 cells for the studied lipopolyamines. N^4,N^9-Dioleoyl spermine show a significant difference in the % viability comparing to either Lipofectin and Lipofectamine in the primary skin cell line FEK4, but there is no difference in the case of the cancer cell line HtTA (Fig. 10). These results also revealed that N^4,N^9-dioleoyl spermine toxicity is higher (lower concentrations) in the case of HtTA cells more than with the primary cell line FEK4 which could be attributed to the ease of transfection of immortalized cancer cell lines over primary cell lines.

DISCUSSION

Non-viral delivery systems can be defined to include the use of plasmid DNA alone (so-called naked DNA) (49,50) as well as DNA complexed to synthetic carriers such as cationic lipids (51–54) or polymers (55). The use of an efficient carrier for nucleic acid delivery is considered to be a determinant factor for the successful application of gene therapy (56). This carrier is responsible for the complex process of gene delivery to the nucleus (57).

Ethidium bromide (EthBr) (2,7-diamino-10-ethyl-9-phenylphenanthridinium bromide, Fig. 11) is a cationic dye that displays a marked increase in the fluorescence upon binding with DNA and RNA through the intercalation between the EthBr phenanthridinium-moiety and adjacent base-pairs of DNA sequences (36,58). Within the prerequisites for delivery of DNA across intact cytoplasmic membrane are condensation and masking the negative charge of the phosphate backbone. Condensation of DNA occurs when about 90% of the charge on DNA is neutralized (16,47).

The ability of the cationic lipid N^4,N^9-dioleoyl spermine to compact DNA more efficiently than both spermine and the powerful condensing agent PLL a cationic polymer (9), (Fig. 4) shows the importance of the lipid moiety we have bound to the cationic polyamine in order to achieve improvements in its ability to condense DNA, cellular entry, and lowering the toxicity of the polyamine conjugate (11,59,60).

The formation of N^4,N^9-dioleoyl spermine-DNA lipoplex at lower charge ratio decreases the toxicity of the DNA delivering lipopolyamine. As the mammalian cell membrane is a semipermeable membrane formed of phospholipids bilayer that allows the transport of macromolecules by endocytosis, neutralization of the negative charges on the DNA by polycations will improve the delivery of DNA through the cell membrane because of the presence of negative charges on both DNA and cell membrane. Also, the positively charged lipid complex will mediate transfection by fusion with cell membranes (60,61). It was found that both the number of positive charges and their distribution on the surface of the molecule have profound effects on DNA condensation (28,62,63).

In addition, in a study on the transfection activity of cholesterol carbamate cationic lipids (28), Blagbrough and co-workers reported that the carbamate with a spermine polyamine moiety has the highest transfection activity with its ability to condense DNA efficiently. Our findings are in agreement with the literature, the cationic liposomal formulation Lipofectin, with its cationic moiety DOTMA containing one positively charged quaternary ammonium group, has lower ability to displace the EthBr from DNA than Lipofectamine formulation that contains DOSPA (Fig. 2) with its four positively charged nitrogens (15) and N^4,N^9-dioleoyl spermine with its two positively charged nitrogens. The higher ability of N^4,N^9-dioleoyl spermine (two positive charges) over Lipofectamine (four positive charges) in DNA condensation, though N^4,N^9-dioleoyl spermine has a lower number of positive charges/molecule, may be attributed to the distribution of the positive charges on the molecule allowing a higher affinity of the vector for DNA and leading to the efficient displacement of EthBr. Another variable is the liposomal formulation of Lipofectamine compared to the non-liposomal formulation of N^4,N^9-dioleoyl spermine.

The helper lipid DOPE which is the second component of the cationic liposomes is used to increase the transfection activity of the cationic liposome through its ability to destabilize lipid bilayers leading to endosomal destabilization with subsequent increase in the total cellular uptake of the delivered DNA (23,64). Lipospermines (Fig. 2) with their cationic headgroup sometimes form micelles (in the absence of DNA) rather than the bilayer produced by the small cationic quaternary ammonium headgroup of DOTMA (Lipofectin formulation) (43,65). N^4,N^9-Dioleoyl spermine combines in its structure the two oleoyl chains that have the characteristics of the fusogenic lipid DOPE and the cationic polyamine spermine (Fig. 2). Thus, DNA is condensed by the

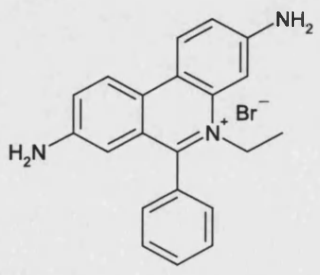

Fig. 11. Structure of ethidium bromide.

two primary amines and coated by the dioleoyl lipophilic moiety. The DNA condensation results of N^4,N^9-dioleoyl spermine (Fig. 5) show a higher efficiency than either liposomal formulation. The transfection results reveal higher transfection ability (levels of expression) of N^4,N^9-dioleoyl spermine compared to Lipofectin (Fig. 8) in FEK4 and HtTA cells. These results indicate the roles of both number and distribution of positive charges along the polyamine backbone on the ability of the compound to condense DNA. On the other hand, there is no significant difference in the transfection activity between N^4,N^9-dioleoyl spermine and Lipofectamine in both FEK4 and HtTA cell lines, which indicates the importance of lipid coating over the DNA molecule on both the condensation and cellular delivery of DNA in case of the liposomal and non liposomal formulations (65). N^4,N^9-Dioleoyl spermine achieved high levels of transfection in both a cancer cell line and a primary skin cell line (73%), which indicates the ability of this vector to deliver DNA. Cell viability results revealed improved FEK4 viability more than the cancer cells HtTA (Fig. 9). Also, N^4,N^9-dioleoyl spermine showed a significant improvement in primary FEK4 cell viability over the liposomal formulatios (Fig. 10), but no significant difference in HtTA cells. Previous studies on Lipofectin and Lipofectamine on different cell lines showed the cytotoxic effects of these liposomal formulations (66–70). In conclusion, a lipopolyamine vector has been developed for DNA delivery. This new non-liposomal formulation has the ability to transfect primary skin cells more efficiently than the commercially available liposomal Lipofectin formulation.

ACKNOWLEDGMENTS

We acknowledge the financial support of the Egyptian Government studentship to O.A.A. A. and Universities U.K. for an ORS award to N. A. We are grateful to Prof R.M. Tyrrell (University of Bath) for FEK4 and HtTA cell lines.

REFERENCES

1. T. Friedmann and R. Roblin. Gene therapy for human genetic disease? *Science* **175**:949–955 (1972).
2. P. L. Felgner, Y. Barenholz, J. P. Behr, S. H. Cheng, P. Cullis, L. Huang, J. A. Jessee, L. Seymour, F. Szoka, A. R. Thierry, E. Wagner, and G. Wu. Nomenclature for synthetic gene delivery systems. *Hum. Gene Ther.* **8**:511–512 (1997).
3. I. M. Verma and N. Somia. Gene therapy—promises, problems and prospects. *Nature* **389**:239–242 (1997).
4. D. Barr, J. Tubb, D. Ferguson, A. Scaria, A. Lieber, C. Wilson, J. Perkins, and M. A. Kay. Strain related variations in adenovirally mediated transgene expression from mouse hepatocytes *in-vivo*—comparisons between immunocompetent and immunodeficient inbred strains. *Gene Ther.* **2**:151–155 (1995).
5. J. M. Bishop. The molecular-genetics of cancer. *Science* **235**:305–311 (1987).
6. R. E. Donahue, S. W. Kessler, D. Bodine, K. Mcdonagh, C. Dunbar, S. Goodman, B. Agricola, E. Byrne, M. Raffeld, R. Moen, J. Bacher, K. M. Zsebo, and A. W. Nienhuis. Helper virus-induced T-cell lymphoma in nonhuman-primates after retroviral mediated gene-transfer. *J. Exp. Med.* 176:1125– 1135 (1992).
7. S. J. Russell, A. Brandenburger, C. L. Flemming, M. K. L. Collins, and J. Rommelaere. Transformation-dependent expression of interleukin genes delivered by a recombinant parvovirus. *J. Virol.* **66**:2821–2828 (1992).
8. P. L. Felgner, T. R. Gadek, M. Holm, R. Roman, H. W. Chan, M. Wenz, J. P. Northrop, G. M. Ringold, and M. Danielsen. Lipofection—a highly efficient, lipid-mediated DNA- transfection procedure. *Proc. Natl. Acad. Sci. USA* **84**:7413–7417 (1987).
9. S. C. De Smedt, J. Demeester, and W. E. Hennink. Cationic polymer based gene delivery systems. *Pharm. Res.* **17**:113–126 (2000).
10. A. Noguchi, N. Hirashima, and M. Nakanishi. Cationic cholesterol promotes gene transfection using the nuclear localization signal in protamine. *Pharm. Res.* **19**:933–938 (2002).
11. E. Wagner. Strategies to improve DNA polyplexes for *in vivo* gene transfer: will "artificial viruses" be the answer? *Pharm. Res.* **21**:8–14 (2004).
12. S. A. Cryan and C. M. O'Driscoll. Mechanistic studies on nonviral gene delivery to the intestine using *in vitro* differentiated cell culture models and an *in vivo* rat intestinal loop. *Pharm. Res.* **20**:569–575 (2003).
13. C. M. Wiethoff and R. Middaugh. Barriers to nonviral gene delivery. *J. Pharm. Sci.* **92**:203–217 (2003).
14. J. P. Behr. Gene-transfer with synthetic cationic amphiphiles—prospects for gene therapy. *Bioconjug. Chem.* **5**:382–389 (1994).
15. J. S. Remy, C. Sirlin, P. Vierling, and J. P. Behr. Gene-transfer with a series of lipophilic DNA-binding molecules. *Bioconjug. Chem.* **5**:647–654 (1994).
16. V. A. Bloomfield. DNA condensation by multivalent cations. *Biopolymers* **44**:269–282 (1997).
17. T. Blessing, J. S. Remy, and J. P. Behr. Monomolecular collapse of plasmid DNA into stable virus-like particles. *Proc. Natl. Acad. Sci. USA* **95**:1427–1431 (1998).
18. W. J. Montigny, C. R. Houchens, S. Illenye, J. Gilbert, E. Coonrod, Y. C. Chang, and N. H. Heintz. Condensation by DNA looping facilitates transfer of large DNA molecules into mammalian cells. *Nucleic Acids Res.* **29**:1982–1988 (2001).
19. J. O. Radler, I. Koltover, T. Salditt, and C. R. Safinya. Structure of DNA-cationic liposome complexes: DNA intercalation in multilamellar membranes in distinct interhelical packing regimes. *Science* **275**:810–814 (1997).
20. T. Niidome, N. Ohmori, A. Ichinose, A. Wada, H. Mihara, T. Hirayama, and H. Aoyagi. Binding of cationic alpha-helical peptides to plasmid DNA and their gene transfer abilities into cells. *J. Biol. Chem.* **272**:15307–15312 (1997).
21. P. L. Felgner, C. N. Sridhar, C. J. Wheeler, and J. Felgner. Enhanced gene delivery and mechanism studies with a novel series of cationic lipid formulations. *J Cell Biochem.* 206 (1993).
22. W. C. Tseng and L. Huang. Liposome-based gene therapy. *Pharm. Sci. Technol. Today* **1**:206–213 (1998).
23. H. Farhood, N. Serbina, and L. Huang. The role of dioleoyl phosphatidylethanolamine in cationic liposome-mediated gene-transfer. *Biochim. Biophys. Acta, Biomembr.* **1235**:289–295 (1995).
24. J. P. Behr, B. Demeneix, J. P. Loeffler, and J. P. Mutul. Efficient gene-transfer into mammalian primary endocrine-cells with lipopolyamine-coated DNA. *Proc. Natl. Acad. Sci. USA* **86**:6982–6986 (1989).
25. G. Byk, C. Dubertret, V. Escriou, M. Frederic, G. Jaslin, R. Rangara, B. Pitard, J. Crouzet, P. Wils, B. Schwartz, and D. Scherman. Synthesis, activity, and structure-activity relationship studies of novel cationic lipids for DNA transfer. *J. Med. Chem.* **41**:224–235 (1998).
26. B. Buchberger, E. Fernholz, H. v.d.Eltz, and M. Hinzepeter. DOSPER liposomal transfection reagent: a reagent with unique transfection properties. *Biochem. Inform.* **98**:27–29 (1996).
27. I. S. Blagbrough, A. J. Geall, and A. P. Neal. Polyamines and novel polyamine conjugates interact with DNA in ways that can be exploited in non-viral gene therapy. *Biochem. Soc. Trans.* **31**:397–406 (2003).
28. A. J. Geall, M. A. W. Eaton, T. Baker, C. Catterall, and I. S. Blagbrough. The regiochemical distribution of positive charges along cholesterol polyamine carbamates plays significant roles in modulating DNA binding affinity and lipofection. *FEBS Lett.* **459**:337–342 (1999).
29. B. G. Feuerstein, L. D. Williams, H. S. Basu, and L. J. Marton.

Implications and concepts of polyamine-nucleic acid interactions. *J. Cell. Biochem.* **46**:37–47 (1991).
30. A. J. Geall, D. Al-Hadithi, and I. S. Blagbrough. Spermine and thermine conjugates of cholic acid condense DNA, but lithocholic acid polyamine conjugates do so more efficiently. *Chem. Commun.* 2035–2036 (1998).
31. J. A. Heyes, D. Niculescu-Duvaz, R. G. Cooper, and C. J. Springer. Synthesis of novel cationic lipids: effect of structural modification on the efficiency of gene transfer. *J. Med. Chem.* **45**:99–114 (2002).
32. G. Ronsin, C. Perrin, P. Guedat, A. Kremer, P. Camilleri, and A. J. Kirby. Novel spermine-based cationic gemini surfactants for gene delivery. *Chem Commun.* 2234–2235 (2001).
33. I. Tranchant, B. Thompson, C. Nicolazzi, N. Mignet, and D. Scherman. Physicochemical optimisation of plasmid delivery by cationic lipids. *J. Gene Med.* **6**:S24–S35 (2004).
34. M. C. P. de Lima, S. Neves, A. Filipe, N. Duzgunes, and S. Simoes. Cationic liposomes for gene delivery: from biophysics to biological applications. *Curr. Med. Chem.* **10**:1221–1231 (2003).
35. I. S. Blagbrough and A. J. Geall. Practical synthesis of unsymmetrical polyamine amides. *Tetrahedron Lett.* **39**:439–442 (1998).
36. A. J. Geall and I. S. Blagbrough. Rapid and sensitive ethidium bromide fluorescence quenching assay of polyamine conjugate-DNA interactions for the analysis of lipoplex formation in gene therapy. *J. Pharm. Biomed. Anal.* **22**:849–859 (2000).
37. R. M. Tyrrell and M. Pidoux. Quantitative differences in host cell reactivation of ultraviolet-damaged virus in human skin fibroblasts and epidermal keratinocytes cultured from the same foreskin biopsy. *Cancer Res.* **46**:2665–2669 (1986).
38. D. Fischer, T. Bieber, Y. X. Li, H. P. Elsasser, and T. Kissel. A novel non-viral vector for DNA delivery based on low molecular weight, branched polyethylenimine: effect of molecular weight on transfection efficiency and cytotoxicity. *Pharm. Res.* **16**:1273–1279 (1999).
39. J. Y. Wu and C. H. Wu. Receptor-mediated *in vitro* gene transformation by a soluble DNA carrier system. *J. Biol. Chem.* **262**:4429–4432 (1987).
40. O. Boussif, F. Lezoualc'h, M. A. Zanta, M. D. Mergny, D. Scherman, and J. P. Behr. A versatile vector for gene and oligonucleotide transfer into cells in culture and *in vivo*: polyethylenimine. *Proc. Natl. Acad. Sci. USA* **92**:7297–7301 (1995).
41. J. M. Benns, R. I. Mahato, and S. W. Kim. Optimization of factors influencing the transfection effeciency of folate-PEG-folate-graft-polyethylenimine. *J. Control. Release* **79**:255–269 (2002).
42. K. Kunath, A. von Harpe, D. Fischer, H. Peterson, U. Bickel, K. Voigt, and T. Kissel. Low-molecular-weight polyethylenimine as a non-viral vector for DNA delivery: comparison of physicochemical properties, transfection efficiency and *in vivo* distribution with high-molecular-weight polyethylenimine. *J. Control. Release* **89**:113–125 (2003).
43. J. S. Remy, B. Abdallah, M. A. Zanta, O. Boussif, J. P. Behr, and B. Demeneix. Gene transfer with lipospermines and polyethylenimines. *Adv. Drug Deliv. Rev.* **30**:85–95 (1998).
44. L. C. Gosule and J. A. Schellman. Compact form of DNA induced by spermidine. *Nature* **259**:333–335 (1976).
45. R. W. Wilson and V. A. Bloomfield. Counterion-induced condesation of deoxyribonucleic acid. a light-scattering study. *Biochemistry* **18**:2192–2196 (1979).
46. H. S. Basu and L. J. Marton. The interaction of spermine and pentamines with DNA. *Biochem. J.* **244**:243–246 (1987).
47. L. C. Gosule and J. A. Schellman. DNA condensation with polyamines I. Spectroscopic studies. *J. Mol. Biol.* **121**:311–326 (1978).
48. T. Mosmann. Rapid colorimetric assay for cellular growth and survival: application to proliferation and cytotoxicity assays. *J. Immunol. Methods* **65**:55–63 (1983).
49. Q. L. Lu, G. Bou-Gharios, and T. A. Partridge. Non-viral gene delivery in skeletal muscle: a protein factory. *Gene Ther.* **10**:131–142 (2003).
50. T. Niidome and L. Huang. Gene therapy progress and prospects: nonviral vectors. *Gene Ther.* **9**:1647–1652 (2002).
51. L. Liu, M. A. Zern, M. E. Lizarzaburu, M. H. Nantz, and J. Wu. Poly(cationic lipid)-mediated *in vivo* gene delivery to mouse liver. *Gene Ther.* **10**:180–187 (2003).
52. H. Faneca, S. Simoes, and M. C. P. de Lima. Evaluation of lipid-based reagents to mediate intracellular gene delivery. *Biochim. Biophys. Acta, Biomembr.* **1567**:23–33 (2002).
53. S. P. Pantazatos and R. C. MacDonald. Real-time observation of lipoplex formation and interaction with anionic bilayer vesicles. *J. Membr. Biol.* **191**:99–112 (2003).
54. N. S. Templeton. Liposomal delivery of nucleic acids *in vivo*. *DNA Cell Biol.* **21**:857–867 (2002).
55. V. S. Trubetskoy, S. C. Wong, V. Subbotin, V. G. Budker, A. Loomis, J. E. Hagstrom, and J. A. Wolff. Recharging cationic DNA complexes with highly charged polyanions for *in vitro* and *in vivo* gene delivery. *Gene Ther.* **10**:261–271 (2003).
56. S. Simoes, C. Fonseca, H. Faneca, N. Duzgunes, and M. C. P. de Lima. Protein-associated lipoplexes: novel strategies to enhance gene delivery mediated by lipid-based particles. *STP Pharma Sci.* **12**:339–344 (2002).
57. E. Dauty, J. S. Remy, T. Blessing, and J. P. Behr. Dimerizable cationic detergents with a low cmc condense plasmid DNA into nanometric particles and transfect cells in culture. *J. Am. Chem. Soc.* **123**:9227–9234 (2001).
58. J. B. LePecq and C. Paoletti. A fluorescent complex between ethidium bromide and nucleic acids. Physical-chemical characterization. *J. Mol. Biol.* **27**:87–106 (1967).
59. D. Niculescu-Duvaz, J. Heyes, and C. J. Springer. Structure-activity relationship in cationic lipid mediated gene transfection. *Curr. Med. Chem.* **10**:1233–1261 (2003).
60. K. Fabio, J. Gaucheron, C. Di Giorgio, and P. Vierling. Novel galactosylated polyamine bolaamphiphiles for gene delivery. *Bioconjug. Chem.* **14**:358–367 (2003).
61. Y. Xu and F. C. Szoka, Jr. Mechanism of DNA release from cationic liposome/DNA complexes used in cell transfection. *Biochemistry* **35**:5616–5623 (1996).
62. V. Vijayanathan, T. Thomas, A. Shirahata, and T. J. Thomas. DNA condensation by polyamines: a laser light scattering study of structural effects. *Biochemistry* **40**:13644–13651 (2001).
63. V. Vijayanathan, T. Thomas, and T. J. Thomas. DNA nanoparticles and development of DNA delivery vehicles for gene therapy. *Biochemistry* **41**:14085–14094 (2002).
64. X. H. Zhou and L. Huang. DNA transfection mediated by cationic liposomes containing lipopolylysine – characterization and mechanism of action. *Biochim. Biophys. Acta, Biomembr.* **1189**:195–203 (1994).
65. I. S. Blagbrough, N. Adjimatera, O. A. A. Ahmed, A. P. Neal, and C. Pourzand. Spermine and lipopolyamines as gene delivery agents. In D. J. Beadle, I. R. Mellor, and P. N. R. Usherwood (eds.), *Neurotox '03: Neurotoxicological targets from functional genomics and proteomics*, SCI, London, 2004, pp. 147–159.
66. A. L. Coulberson, N. V. Hud, J. M. Ledoux, I. D. Vilfan, and M. R. Prausnitz. Gene packaging with lipids, peptides and viruses inhibits transfection by electroporation *in vitro*. *J. Control. Release* **86**:361–370 (2003).
67. J. Weyermann, D. Lochmann, and A. Zimmer. Comparison of antisense oligonucleotide drug delivery systems. *J. Control. Release* **100**:411–423 (2004).
68. F. Sakurai, R. Inoue, Y. Nishino, A. Okuda, O. Matsumoto, T. Taga, F. Yamashita, Y. Takakura, and M. Hashida. Effect of DNA/liposome mixing ratio on the physicochemical characteristics, cellular uptake and intracellular trafficking of plasmid DNA/cationic liposome complexes and subsequent gene expression. *J. Control. Release* **66**:255–269 (2000).
69. H. Bell, W. L. Kimber, M. Li, and I. R. Whittle. Liposomal transfection efficiency and toxicity on glioma cell lines: *in vitro* and *in vivo* studies. *Neuroreport* **9**:793–798 (1998).
70. J. Wu, M. E. Lizarzaburu, M. J. Kurth, L. Liu, H. Wege, M. A. Zern, and M. H. Nantz. Cationic lipid polymerization as a novel approach for constructing new DNA delivery agents. *Bioconjug. Chem.* **12**:251–257 (2001).

12 Fluorescence Techniques in Non-Viral Gene Therapy

N. Adjimatera, A. P. Neal and I. S. Blagbrough

Keywords: Non-viral gene therapy; Fluorescent lipopolyamines; (in vivo) FCS, DNA condensation, Fluorescence microscopy, FRET, Polyamines, Spermine

Abbreviations

1,4-DHP	1,4-Dihydropyridine
DOPE	Dioleoylphosphatidylethanolamine
DOTAP	*N*-[1-(2,3-Dioleoyloxy)propyl]-*N,N,N*-trimethylammonium chloride
DOTMA	*N*-[1-(2,3-Dioleyloxy)propyl]-*N,N,N*-trimethylammonium chloride
EGFP	(Enhanced) green fluorescent protein
EthBr	Ethidium bromide
FACS	Fluorescence-activated cell sorting
FCS	Fluorescence correlation spectroscopy
FLIM	Fluorescence lifetime microscopy
FRET	Fluorescence resonance energy transfer
GFP	Green fluorescent protein
HTAB	Hexadecyltrimethylammonium bromide
LS	Light scattering
NBD-PE	*N*-4-Nitrobenzo-2-oxa-1,3-diazole phosphatidylethanolamine
N/P	Ammonium/phosphate charge ratio
NPC	Nuclear pore complex
N-Rh-PE	1,2-Dioleoyl-*sn*-glycero-3-phosphatidylethanolamine-*N*-lissamine rhodamine B sulphonyl
NVGT	Non-viral gene therapy
PEI	Polyethylenimine
PNA	Peptide nucleic acid
Ru-BD	$[Ru(bpy)_2(dppz)]^{2+}$ (bpy=2,2′-bipyridine, dppz=dipyrido[3,2-*a*:2′,3′-*c*]phenazine)

12.1 Introduction to Non-Viral Gene Therapy and its Development

Gene therapy has been defined as "the opportunity for the treatment of genetic disorders in adults and children by genetic modification of human body cells" (UK Health Minister's Advisory Committee, 1995) [1]. There have been 636 clinical gene therapy studies run worldwide, mostly in the USA (79.4%) and in the UK (6.8%) [2]. Recent experiments show that gene therapy is not exclusive to genetic diseases such as cystic fibrosis, cancer, melanoma, or severe recombined immunodeficiencies, but it is also possible for other types of diseases including viral infections [1, 2]. These new opportunities make gene therapy research challenging in a highly competitive area.

The delivery of a DNA medicine into target cells is currently (mainly) achieved by two means: viral vectors and non-viral vectors. Though viral vectors are found to be highly efficient in transfection, the severe immune response/toxicity from the viral genome and the limited DNA packing size (the "payload") are major therapeutic problems. As a result, non-viral gene therapy (NVGT) vectors have been synthesized as an alternative safe system with possible control over their DNA payload and their manufacture, suitable for clinical use [1, 3–10]. According to Felgner et al.'s NVGT nomenclature guidelines, the two major synthetic gene delivery systems are: lipoplex (cationic lipids-nucleic acid complex), e.g. lipopolyamines, cationic liposomes; and polyplex (cationic polymer-nucleic acid complex), e.g. polyethylenimine (PEI), polylysine [11]. Though initially the efficiency of NVGT vectors was less than that of viral vectors [1, 3–10, 12, 13], the performance gap has been rapidly closed [14].

Gene therapy is a complex pro-drug strategy [15]. It is currently believed that the delivered plasmid DNA must dissociate, at some point, from the lipoplex for gene expression, transcription and translation to the desired therapeutic protein. There are intracellular barriers to these processes [16–18]. Polyamines and lipopolyamines have recently been developed from a natural DNA condensing agent, spermine, for applications in NVGT (Fig. 12.1). The mechanisms involved and the rate-limiting steps are still not well understood [3].

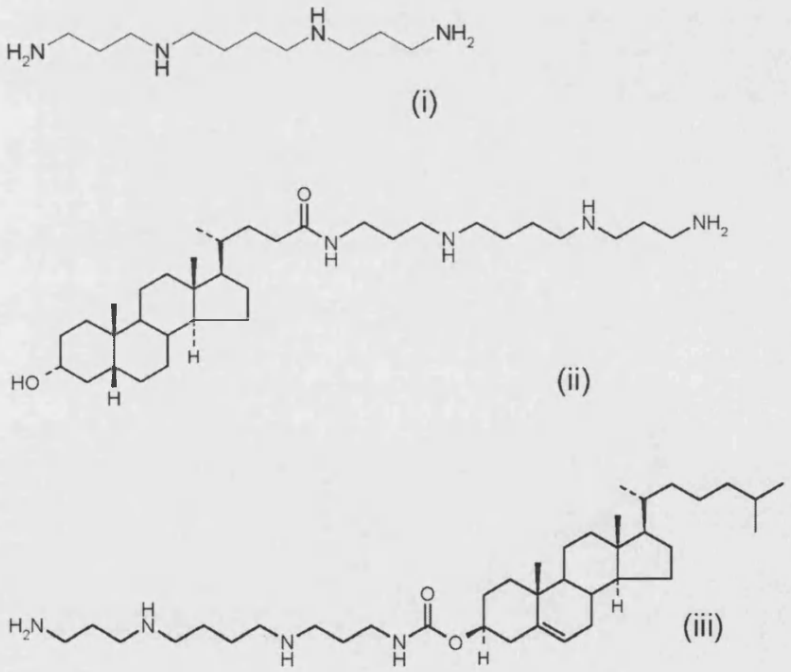

Fig. 12.1. Spermine (i) and two lipopolyamines based on lithocholic acid amide (ii) and cholesteryl carbamate (iii)

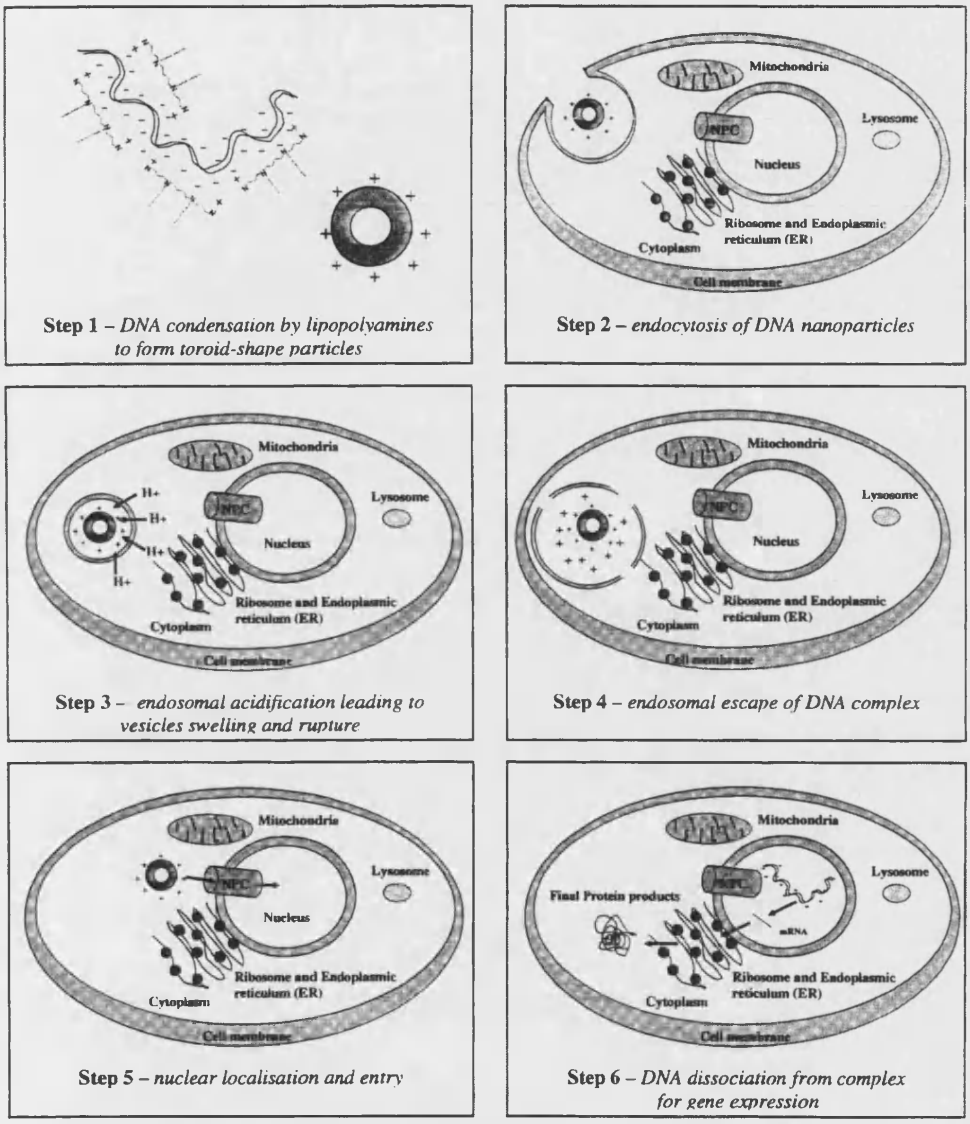

Fig. 12.2. The key steps in the mechanism of non-viral gene therapy

In the first step in the mechanism of NVGT (Fig. 12.2), the phosphate anions of DNA are neutralized by lipopolyamines (ammonium ions) to form condensed nanoparticles [3, 19, 20]. DNA complexes then enter cells by endocytosis. Endosomal escape, involving proton pumping, releases the delivered complexes to the cytoplasm. Nuclear entry, a crucial step for gene expression in NVGT, is achieved by nuclear localization and then transport through the nuclear pore complex (NPC) [3, 17].

12.2 Using Fluorescence Techniques to Determine the Efficiency of DNA Condensing Agents: an Important First Step in the Mechanism of NVGT

The development of gene-based medicines as a new class of pharmaceuticals is clearly important. DNA condensation by polyamine conjugates is a key first step, and fluorimetric, high-throughput assays have been developed to aid in the characterization of NVGT delivery systems. Negatively charged (due to the phosphate groups) DNA was bent by the addition of NVGT delivery agents carrying positive charges. This change in conformation (bending) presumably starts at certain specific nucleic acid sequences, as studied by Hud and co-workers [21], and results in condensed nanometre-sized particles in the range 10–180 nm, typically 50–150 nm in outer diameter. Nanoparticles, toroidal in shape, were observed in polyamine-induced DNA condensation [19, 22]. This DNA compaction facilitates the stability in extracellular compartments, cellular uptake and other intracellular processes such as nuclear entry [17, 19]. Additionally, the aggregation issue of DNA particles is important to the bioavailability of therapeutic DNA. The adjustment of complex charge and ionic strength is critical to their colloidal stability. However, the presence of an excess of positive charges may lead to undesired interactions with negatively charged extracellular molecules such as serum albumin [23, 24].

DNA intercalating agents have been widely used to determine DNA conformational changes, including the characterization of NVGT delivery systems, e.g. ethidium bromide (EthBr) (Fig. 12.3), YOYO-1, acridine orange and PicoGreen [25]. The EthBr assay, first introduced by LePecq and Paoletti in 1967, has been mostly used by NVGT researchers to assess the DNA condensation efficiency

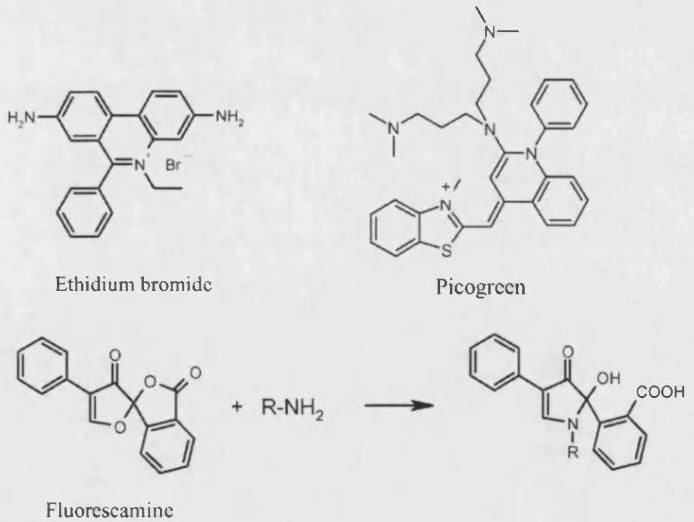

Fig. 12.3. Ethidium bromide, Picogreen, fluorescamine, and the reaction of fluorescamine with a primary amine

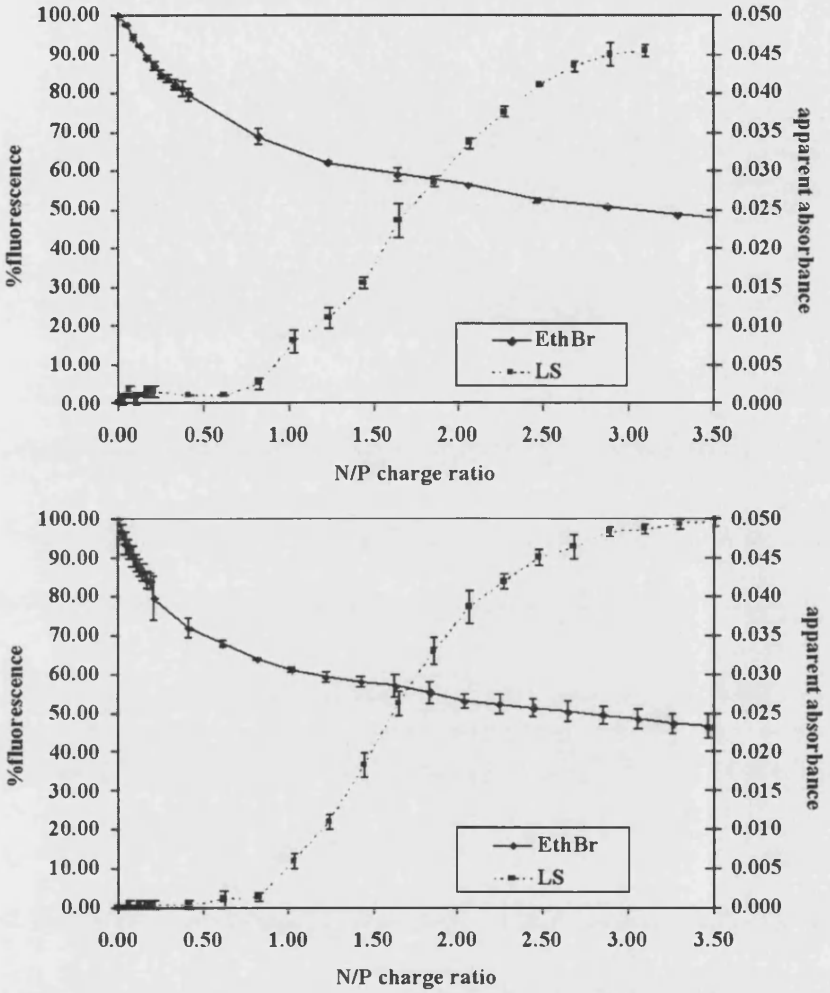

Fig. 12.4. EthBr and LS assay of pEGFP (*above*) and pGL3 (*below*) by spermine

of vector systems. EthBr, intercalated in stacks of DNA base pairs, fluoresces at 600 nm by direct excitation at 546 nm, or more efficiently through energy transfer from DNA base by excitation at 260 nm. On DNA condensation at increasing ammonium/phosphate (N/P) charge ratio [11], a decrease in EthBr fluorescence intensity was measured [26, 27]. This improved methods reported by Geall and Blagbrough [26] offers a rapid and sensitive analysis of lipoplex formation.

Fluorescamine, a non-fluorescent molecule, is also useful in studying NVGT [28, 29]. Fluorescamine easily reacts with primary amine functional groups of polyamines, forming a fluorescent molecule (Fig. 12.3). On salt formation between DNA phosphates and polyammonium ions, the reactivity to fluorescamine of these primary amine groups is eliminated. This observation allowed

a study of DNA-polyamine interactions [30], including polyamine-mediated DNA condensation. Thus, the reaction between free (i.e. unbound to DNA) primary amines on polyamines and added fluorescamine was used to determine the level of condensation. There is fluorescence from the product formed between fluorescamine and these amine functional groups, observed using λ_{ex}=392 nm and λ_{em}=480 nm.

PicoGreen, an (expensive commercial) cyanine dye, becomes intensely fluorescent with high quantum yield and molar extinction coefficient when binding to as little as 25 pg/ml dsDNA [31, 32]. The binding between chitosan (i.e. copolymers of glucosamine and *N*-acetyl glucosamine) and DNA was confirmed by PicoGreen, a fluorescent nucleic acid stain which only reacts with free (uncomplexed) DNA. Free DNA was extracted by gradient centrifugation and mixed with PicoGreen to form a fluorescent complex (λ_{ex}=480 nm and λ_{em}=520 nm) [28]. The unbound DNA level was used to determine the condensation performance of chitosan. Additionally, DNA loading can be studied by the PicoGreen assay of DNA after the digestion of nanocomplexes with chitosanase and lysozyme [33]. PicoGreen was compared to a large number of common nucleic acid stains based on EthBr, acridine orange, YOYO-1, etc. Fluorescence spectroscopy was compared to agarose gel electrophoresis for the biophysical characterization of DNA condensation [25]. In addition to these fluorescence techniques, the formation of nanoparticles by DNA condensation can be observed in a light scattering (LS) assay [34, 35]. This is complementary to the DNA condensation assay (Fig. 12.4); UV apparent absorption is measured at λ>300 nm (where there is no absorption by DNA). Precipitation after aggregation follows a plateauing of the LS signal, and it does not increase the absorption above 300 nm. However, the DNA concentration used in this assay was in tenfold excess compared to the EthBr assay, given the low sensitivity of this experiment and the lack of a fluorescence indicator.

12.3 Conjugation of Lipopolyamines to Fluorophores: Probes Derived from DNA Delivery Agents

Fluorescent lipopolyamines were synthesized by Fmoc (fluoren-9-ylmethoxycarbonyl) chemistry in order to label a specific position with a chosen fluorophore [3, 36, 37]. Fluorescence techniques, such as fluorescence correlation spectroscopy (FCS) [38–40], fluorescence resonance energy transfer (FRET) [41, 42] and confocal fluorescence microscopy [43], have recently been applied in NVGT. Thus, by introducing these probes to the DNA to be delivered during the condensation process, NVGT events can be followed by a range of available fluorescence techniques either spectroscopically or microscopically. Our designed fluorescent lipopolyamines (Fig. 12.5) are important tools for studying the intracellular fate of DNA nanoparticles (Fig. 12.6) [3, 36, 37].

Byk, Scherman and co-workers [44–46] have designed and synthesized polyamine–hydrocarbon lipid conjugates. A rhodamine derivative of a lipopolyamine (RPR 121653) was also synthesized and studied as an NVGT probe

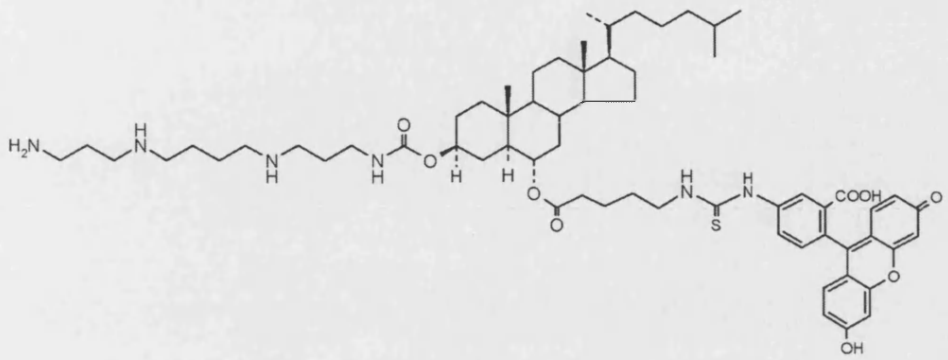

Fig. 12.5. An example of our novel fluorescent lipopolyamine conjugates, carrying a DNA condensing moiety (from spermine), a lipophilic steroid (a *trans*-AB-oxygenated cholestane), and coupled to a fluorescent tag

(Fig. 12.7) [44]. Structure modification was also carried out by introducing a disulphide bridge (a reduction-sensitive functional group) at different positions in the backbone of the lipids. The disulphide is incorporated in order to afford another escape mechanism for the DNA from the lipopolyamine carrier, taking advantage of the cytosolic cellular reducing medium, such as the plasma membrane or cytoplasmic reductases. Early reduction led to undesirable DNA release, i.e. total disruption of the particles in the early phase of delivery yielded total loss of transfection, but some positions for the disulphide bridge afforded increased transfection efficiency [45, 46].

Fluorescent derivatives of a small lipid molecule such as *N*-Rh-PE (1,2-dioleoyl-*sn*-glycero-3-phosphatidylethanolamine-*N*-lissamine rhodamine B sulphonyl) and NBD-PE (*N*-4-nitrobenzo-2-oxa-1,3-diazole phosphatidylethanolamine) are commercially available (Avanti Polar Lipids, AL, USA). These molecules (Fig. 12.7), incorporated into cationic liposomes in NVGT, enable the ability to track fluorescently the progress of transfection from liposomes (*vide infra*) [42, 47]. Fluorescent labelling of polyplex NVGT carriers has also recently been reported, with Oregon Green-PEI [43] and Texas Red-chitosan (*vide infra*) [48].

Ideal fluorophores are primarily chosen for their photostability profile. Naylor et al. [49] showed in interesting experiments that the cellular uptake and metabolism of fluorescent fatty acid analogues were different. The polar fluorophore has poor cellular uptake, and anthracene or pyrene fluorophores were regarded as the most extensively incorporated into cellular lipids. From these findings, it is expected that the molecular hydrophobicity of fluorophores may play an important role in fluorescent lipid (fatty acid)-based NVGT vector design.

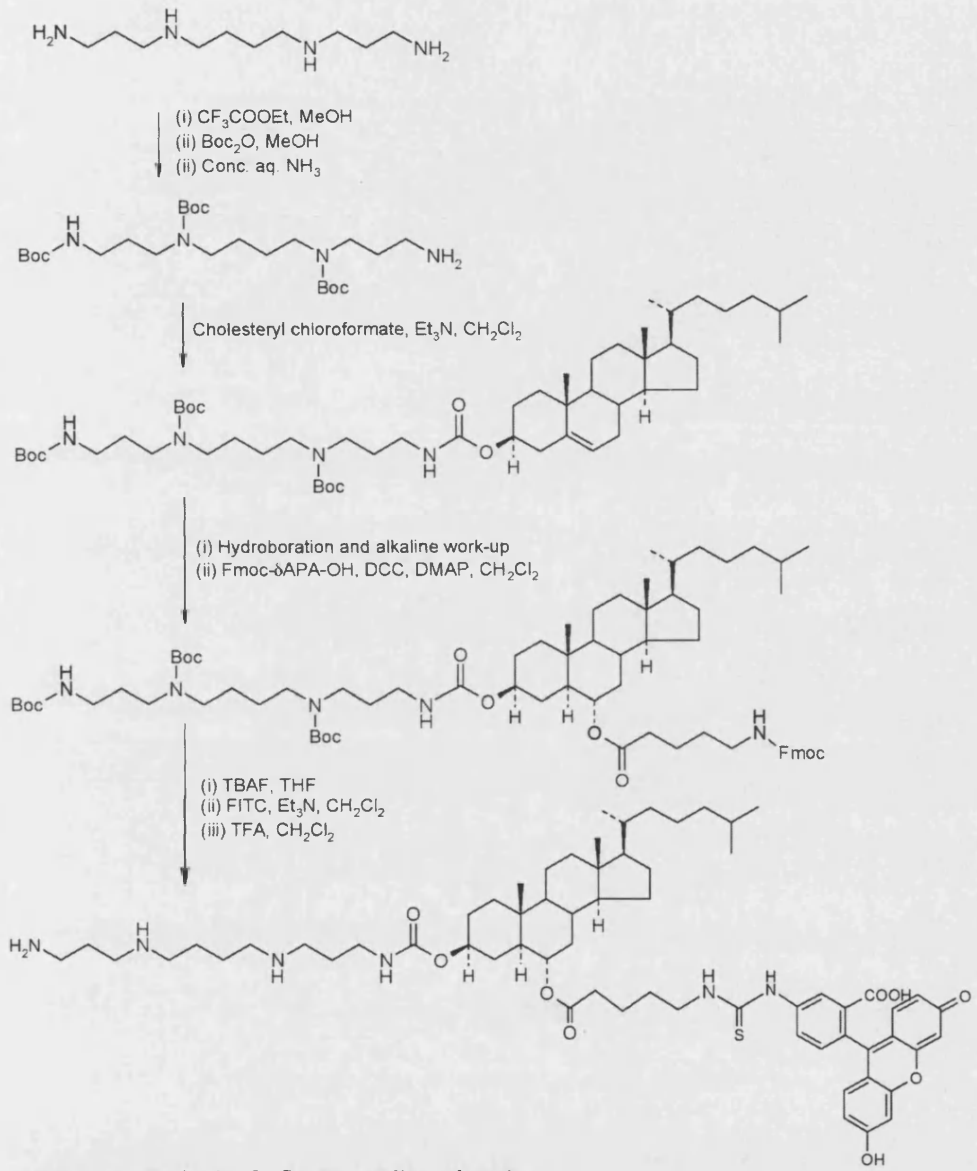

Fig. 12.6. Synthesis of a fluorescent lipopolyamine

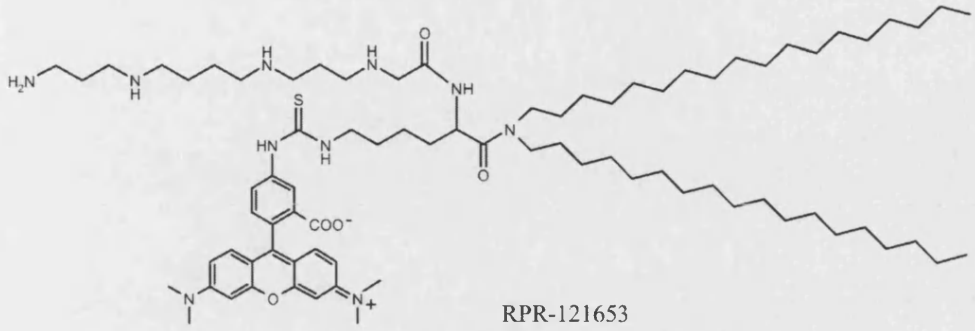

RPR-121653
(Byk and co-workers[44])

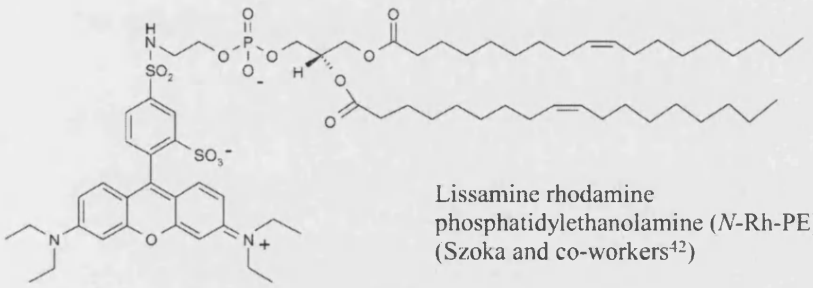

Lissamine rhodamine
phosphatidylethanolamine (*N*-Rh-PE)
(Szoka and co-workers[42])

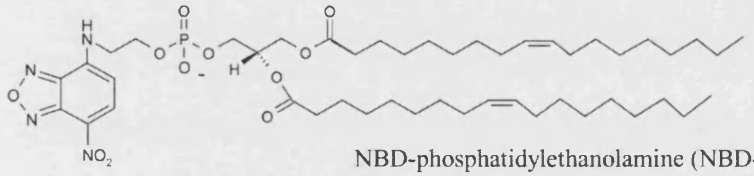

NBD-phosphatidylethanolamine (NBD-PE)
(Szoka and co-workers[42])

Fig. 12.7. Recently reported fluorescent probes

12.4 Preparation of Fluorescent Macromolecules

DNA can be labelled with fluorescent molecules by chemical techniques such as photocrosslinking (e.g. ethidium monoazide [50–52], *p*-azido-tetrafluoro-benzyl-lissamine [53], or dinitrophenyl [54]). Aryl azides can be photoactivated with UV light to generate highly reactive aryl nitrenes which bind to the aromatic bases of DNA. Covalent labelling without photoactivation is also possible, such as the Label IT kit (Mirus Ltd.) [41, 55]. Fluorescent DNA has also been used to study NVGT barriers, such as cell entry [52, 56] and nuclear entry [52, 57].

Some fluorophores for DNA labelling are sequence specific, for example Hoechst 33258 for AT-bases and minor groove [58–61], and 7-aminoactinomycin D for GC-bases [58–61]. Lakowicz and co-workers reported the imaging of cell nuclei based on fluorescence resonance energy transfer (FRET) and fluorescence lifetime microscopy (FLIM) to obtain unbiased maps of spatial distribution of the AT- and GC-rich DNA regions in nuclei. In FLIM, the image contrast is insensitive to concentration, but sensitive to the local environment and interactions of fluorophores such as FRET, allowing examination of the proximity between donors and acceptors. This selective labelling may lead to a better understanding of the starting point for DNA bending, the first step for condensation to form nanoparticles [58–61]. This labelling strategy can also be used together with DNA intercalating dyes, such as propidium iodide, to form a FRET pair [62]. Better fluorophores are being continually developed to increase sensitivity and photostability. Recent studies have demonstrated that silver metallic particles can increase the quantum yield and decrease the lifetimes of nearby fluorophores, including double-stranded DNA oligomers labelled with Cy3 or Cy5 in close proximity to silver particles [63]. The metal-ligand complex, $[Ru(bpy)_2(dppz)]^{2+}$ (bpy=2,2′-bipyridine, dppz=dipyrido-[3,2-*a*:2′,3′-*c*]phenazine) (Ru-BD), was utilized to study nucleic acid dynamics. This Ru-BD complex has both a long lifetime and a molecular light switch property on DNA binding, due to protection of its dppz ligand from water. The slow rotational correlation times appeared to be consistent with the bending motions of the plasmids [64, 65].

In addition to using fluorescent plasmids as a probing strategy for NVGT, protein markers have been employed to follow the transfection outcome, i.e. gene expression. Such protein markers include: (enhanced) green fluorescent protein (EGFP), which fluoresces naturally; β-galactosidase, which can turnover a pro-fluorescent substrate, e.g. one based on umbelliferone; and luci-

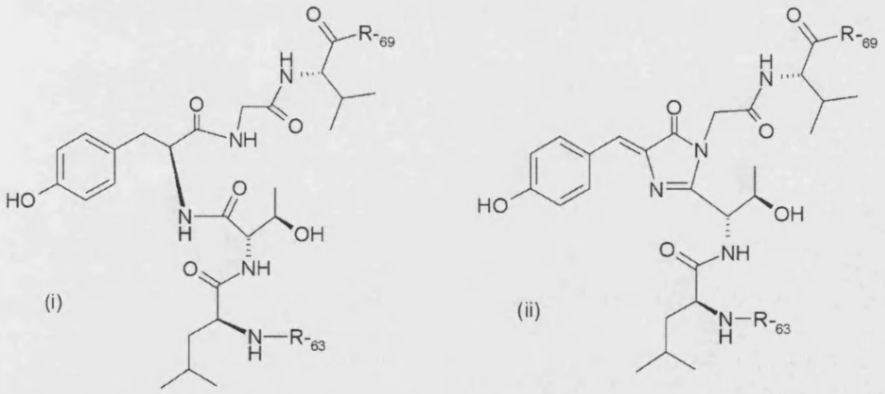

Fig. 12.8. The fluorophore in EGFP. (i) EGFP amino acid sequence L(64)TYGV(68) shown. (ii) Post-translational cyclization of amino acids 65–67 forming hydroxybenzylidene-imidazolidinone, an EGFP fluorophore with λ_{ex}=488 nm (red-shifted from wild GFP protein) and λ_{em}=507 nm

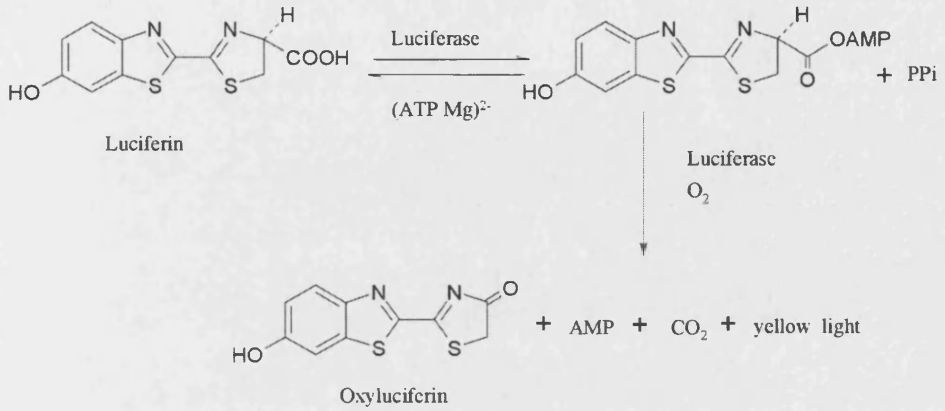

Fig. 12.9. The biochemical reaction of luciferin oxidation by luciferase to oxyluciferin

ferase, which drives luciferin oxidation and generates light. The chemistry that underpins the use of these reporter systems is highlighted below. By using pEGFP [66] as delivered DNA, the EGFP chromophore (a substituted 4-hydroxybenzylidene imidazolidinone Fig. 12.8) was detected in successfully transfected cells by FACS (fluorescence-activated cell sorting). Luminescence involves chemical reactions producing structurally different products which emit light. This bioluminescence method has also been used to quantify NVGT efficiency [67]. Firefly luciferase (*Photinus pyralis*) [67], which is widely used for gene expression, catalyses luciferin oxidation (Fig. 12.9) generating oxyluciferin and detectable yellow light.

12.5 Lipopolyamines and Cationic Lipids Used in Transfection

LipoGen (Invivogen) (Fig. 12.10) is a lipospermine with two oleoyl groups at N^2 and N^3 of spermine and therefore only two positively charged (primary) amines. It was prepared as a non-liposomal formulation. The lipophilic modification aims to facilitate the transfection process (e.g. potentially through enhanced DNA condensation, cell entry, endosomal escape). This lipophilic modification of the spermine structure resulted in a more efficient pEGFP cDNA condensation (Fig. 12.11) (15% residual fluorescence in the EthBr assay, at N/P charge ratio 2.5) compared to tetracationic spermine (50% at N/P charge ratio 3.0). The in vivo transfection of pEGFP (2 μg/well) with LipoGen was carried out using FEK4 [68] (2.5×10^4 cells/well at 50% confluence), incubated for 4 h, then the transfection was stopped by removal of the DNA complex and replacement with foetal calf serum-containing media; FACS analysis was performed 48 h post-transfection. Lipofectin (DOTMA/DOPE=1:1 w/w, Invitrogen) (Fig. 12.10), the commonly used transfection liposomal reagent containing cationic lipid (with one positive charge) and helper lipid (DOPE), was also used in this experiment for a comparison. The fluorescent cell counts observed in all N/P ratios were higher in LipoGen-

Fig. 12.10. LipoGen and Lipofectin

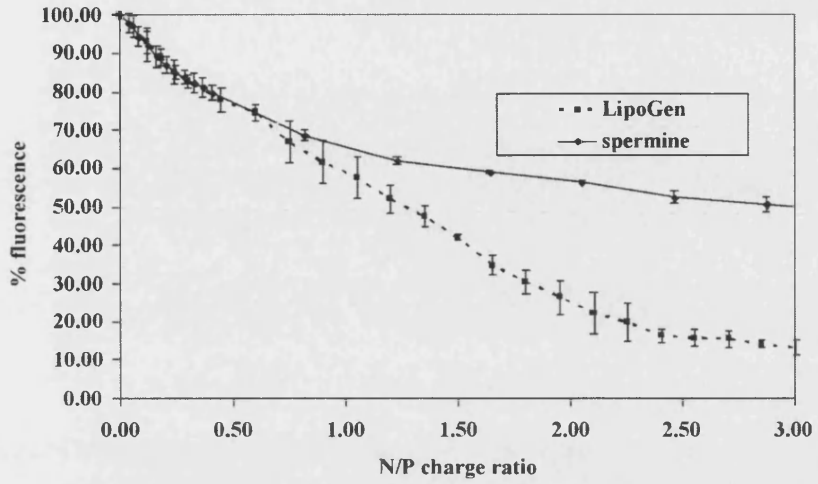

Fig. 12.11. pEGFP-EthBr fluorescence quenching by LipoGen and spermine

mediated transfection. Thus, the lipid moiety in lipospermine is playing an important role in in vitro transfection. The optimal charge ratio for FEK4 transfection with pEGFP-LipoGen complex is around 2.5, which corresponds to the optimal DNA condensation N/P ratio (from the EthBr assay). Though increased condensation leads to higher transfection efficacy (Fig. 12.12), the high N/P ratio (more than 5.0) results in less efficient gene delivery overall. A similar relationship between N/P charge ratio and transfection efficiency was also observed in Lipofectin-mediated transfection.

A highly fluorescent preparation of plasmid DNA was generated by hybridizing a fluorescently labelled peptide nucleic acid (PNA) to the plasmid and using this to study the biodistribution of conformationally and functionally intact plasmid DNA in living cells after cationic lipid-mediated transfection. This method enables the mechanism of plasmid delivery and nuclear import by synthetic gene delivery systems to be elucidated [69]. Using a fluorescent plasmid expressing GFP enabled simultaneous co-localization of both plasmid and expressed protein in living cells and in real time. GFP was shown to be expressed in cells containing detectable nuclear fluorescent plasmid; though conjugated, it still underwent transcription and translation [69].

Double-charged 1,4-dihydropyridine (1,4-DHP) amphiphiles condense ethidium monoazide-crosslinked fluorescent DNA and efficiently transfect cells in vitro. Confocal laser fluorescence microscopy was used to investigate the intracellular distribution of these nanoparticles. The biophysical properties, as a function of structure–activity relationships, determine the intracellular kinetics and transfection efficiency. Not one property among high cellular uptake, membrane destabilizing activity or buffering capacity alone is sufficient to achieve high transfection yields. Overall, there is a complex interplay of various factors that determine intracellular kinetics and, consequently, transfection [70, 71].

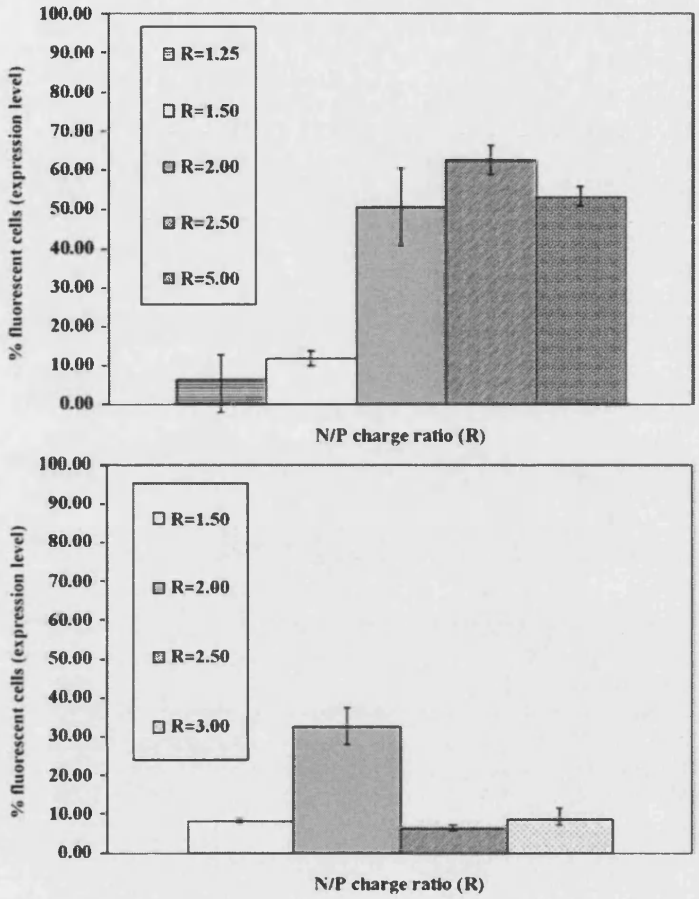

Fig. 12.12. FEK4 transfection of pEGFP complexes by LipoGen (*above*) and Lipofectin (*below*)

Cationic liposomes are useful to transfer genes into eukaryotic cells in vitro and in vivo. However, liposomes with good transfection efficiency are often cytotoxic, and often require serum-free conditions for optimal activity. A new cationic liposome formulation efficiently delivered a plasmid DNA for GFP into more than 80% of the cultured human cell hybrids derived from HeLa cells and normal fibroblasts. FACS analysis revealed that the efficiency of the GFP gene expression was 40–50% in a tumour-suppressed cell hybrid, while it was greatly reduced in the tumorigenic counterpart. The enhanced GFP expression in tumour-suppressed cell hybrids was quantitatively well correlated with a prolonged presence of the plasmid DNA, which had been labelled with the fluorescent probe ethidium monoazide, within the cells. The stability of the plasmid DNA inside the cell is a crucial step in this liposome-mediated gene expression. The mechanisms by which cationic liposomes mediate gene transfer into eukaryotic cells are being studied [72].

Polylysine-molossin is a 31 amino acid synthetic peptide that acts as a DNA vector in vitro for cell lines and for the cornea. It incorporates the 15 amino acid integrin-binding domain of the venom of the American pit viper, *Crotalus molossus* molossus, as the targeting moiety and a chain of 16 lysines as the DNA-binding moiety. Binding and tissue distribution of the vector-DNA complexes were followed using fluorescein-labelled DNA. Long exposure times (2–3 h) to the transfection medium were essential for substantial gene transfer. Although exposure to chloroquine for 8–10 h after uptake of vector/DNA complexes was essential for optimal gene transfer, exposure of complexes to even 1% serum before transfection markedly inhibited gene transfer. Careful attention to several parameters of little importance in vitro needs to be paid for optimal in vivo application of DNA vector systems [73].

12.6 Association and Dissociation Studies of DNA Complexes Through Fluorescence Correlation Spectroscopy (FCS)

FCS is a technique where fluctuations in the detected fluorescence from small molecules (such as DNA intercalating probes) are used to study the dynamic processes on the molecular scale, including DNA conformational changes resulting from polycation-mediated condensation [74]. This technique, first introduced by Magde et al. in 1972, to measure the EthBr diffusion and binding to double-stranded DNA, has been undergoing major technical improvements following the implementation of confocal microscopy in 1993 [74]. The count rate, diffusion time and particle numbers observed by FCS at the single molecule level and their correlations can be used to differentiate the nature of polycation-DNA [38–40, 75, 76] and oligonucleotide condensation [77]. Kral et al. reported the DNA complex association mediated by spermine. The pHbetaAPr-1-neo (10 kbp; contour length 3.4 μm) was labelled with EthBr and propidium iodide, and then titrated with spermine to form condensed DNA particles. The diffusion time, count rate and particle number decreased when the charge ratio (N/P) was increased, suggesting the dissociation of dyes from condensed DNA [38, 40]. The correlation plots of these FCS parameters versus condensing agent concentration can be a source of additional information about the nature of cationic compound–DNA interactions. In similar experiments, hexadecyltrimethylammonium bromide (HTAB)-mediated DNA condensation showed different correlation plots from spermine, and possible differences in DNA conformation were deduced [39].

FCS with two-photon excitation was used to characterize the complexes formed by rhodamine-labelled 25-kDa PEI or DNA plasmid molecules by Clamme et al. [75, 78]. FCS results revealed that fluorescent PEI in the complex solution at the N/P ratio used in transfection was 86% in a free PEI form leading to cell toxicity. As an application, FCS was also used to monitor the purification of PEI/DNA complexes by ultrafiltration as well as the heparin-induced dissociation of the complexes. Purification of the complexes is therefore important in lowering possible toxicity from uncomplexed polycations along NVGT vectors [75].

12.7 DNA Complexes and Their Intracellular Trafficking: Monitoring by Fluorescence (Förster) Resonance Energy Transfer (FRET)

FRET is gaining in importance as a technique for studying the mechanism and barriers in NVGT. A change in conformation on condensing DNA leads to a change in the distance between two fluorophores, which can be demonstrated through the random double labelling of DNA for FRET [41] or double labelling of the DNA and carriers [79, 80]. The stability in physiological media (in the presence of 20% serum) of polyplex- and lipoplex–non-viral gene delivery vectors, e.g. Lipofectamine, poly-L-lysine and poly(ethylene glycol)-poly(L-lysine) block copolymer, has been evaluated by detecting the conformational change in plasmid DNA labelled simultaneously with fluorescein (energy donor) and X-rhodamine (energy acceptor) and examining the condensation by FRET [41, 81]. FRET was also used to estimate the distance of closest approach of supercoiled plasmid DNA to the lipid bilayer of cationic liposomes. The structure of the negatively charged complexes is consistent with DNA extending from the surface of the particles, whereas those possessing an excess of positive charge were multi-lamellar aggregates with the DNA effectively condensed between lipid bilayers. Complexes between these two states consisted of weighted fractions of these two species [79].

FRET has also been used to monitor interactions between Cy3-labelled plasmid DNA and NBD-labelled cationic liposomes. Significantly, the time allowed for complex formation affected the in vitro luciferase transfection efficiencies of DOPE-based lipoplexes. Lipoplexes prepared with a 1 h incubation had much higher transfection efficiencies than samples with 1 min or 5 h incubations. The molar charge ratio of DOTAP to negatively charged phosphate in the DNA also affected the interaction between liposomes and plasmid DNA, and interactions stabilized more rapidly at higher positive charge ratios. Lipoplexes formulated with DOPE were more resistant to high ionic strength than complexes formulated with cholesterol [80].

Prior to cell entry of DNA nanoparticles, binding of DNA complexes with extracellular serum, which results in lower NVGT bioavailability, can also be studied by FRET [23]. Clear implications for clinical intravenous lipofection come from FRET and EthBr intercalation studies of intravenous gene delivery using cationic lipid vectors to achieve systemic gene expression in the (mouse) lung. DOPE vectors stayed poorly in the lung and were barely active in transfecting cells. However, cholesterol-containing vectors had a rapid aggregation, a slow disintegration, and were highly efficient in transfecting cells in vivo [23]. Endosome escape is also a key barrier to study microscopically. Fluorescent lipids in the bilayer membranes, as a FRET probe complementary pair to the fluorescent DNA carriers, were used in membrane fusion/leakage studies [82, 83]. FRET interaction of fluorescent lipopolyamine-DNA complexes with NLS can be studied to gain insights into nuclear localization, nuclear entry processes and the timing of DNA release from the lipoplex [42].

12.8
Fluorescence Microscopy in NVGT

The intracellular processes in NVGT can be imaged by scanning and confocal fluorescence microscopy [42, 47, 48, 84]. Szoka and co-workers were pre-eminent in this research area. They proposed a mechanism for fluorescein-labelled oligonucleotide (ODN) release from cationic rhodamine-labelled liposome complexes, showing that the fluorescent lipid remained in the cytoplasm. ODN displacement from the complex was studied by FRET. They proposed that the complex, after internalization by endocytosis, induces flip-flop of anionic lipids from the cytoplasmic facing monolayer. Anionic lipids laterally diffuse into the complex and form a charged neutralized ion pair with the cationic lipids. This leads to displacement of the ODN from the cationic lipid and its release into the cytoplasm (Fig. 12.13) [42].

A lung inflation-fixation protocol to examine the distribution and gene transfer efficiency of fluorescently tagged lipoplexes using fluorescence confocal microscopy within thick lung tissue sections was used to investigate the observation that intravenous (i.v.) administration of lipoplex was superior to intratracheal (i.t.) administration for gene transfer in the murine lung. A fluorescent ODN was used as a marker for cytoplasmic release of nucleic acids. Not unexpectedly, toxicity was associated with high local concentrations of

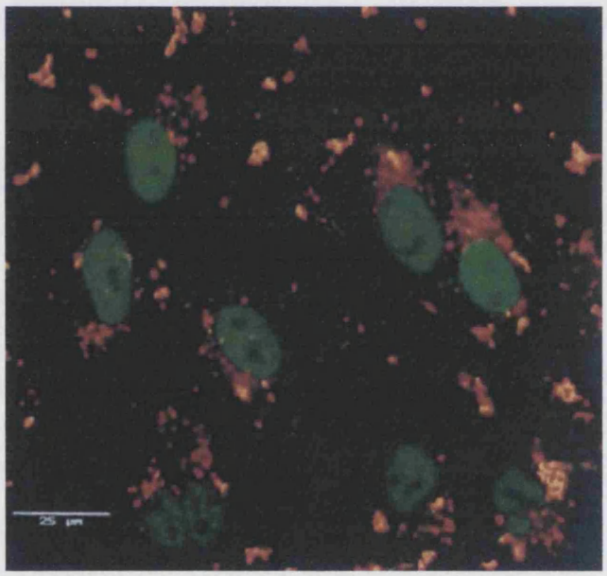

Fig. 12.13. Intracellular distribution of fluorescent lipids and fluorescent oligonucleotide (F-ODN). F-ODN were associated with DOTAP/N-Rh-PE at a 10:1 charge ratio. CV-1 cells were incubated in serum-free medium with complexes for 3 h at 37 °C and imaged using a confocal microscope. (Zelphati O, Szoka FC Jr, Proc Natl Acad Sci USA, 1996, 93:11493–11498; Copyright (1996) National Academy of Sciences, USA)

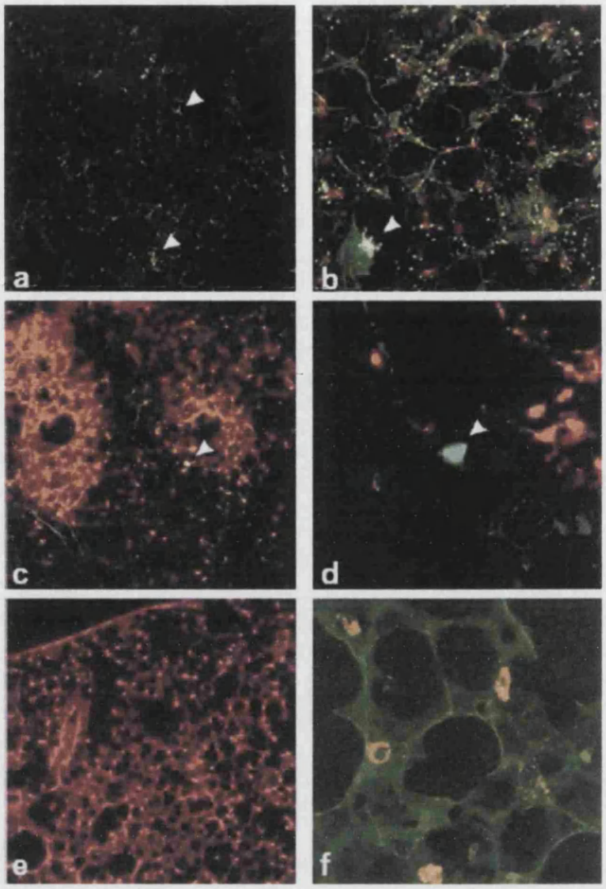

Fig. 12.14a–f. Simultaneous fluorescent oligonucleotide (*red*) localization and GFP (*green*) expression in the mouse lung after i.v. lipoplex administration (**a, b**), i.t. lipoplex administration (**a, c, e** at ×100) and high magnification (**b** at ×400, **d** and **f** at ×600). GFP expression shown by *arrowheads*. In panels **a** and **b**, a fluorescein-PE marker was also used and can be distinguished as green punctuates, distinct from GFP expression (*arrowheads*). The green reticular fluorescence observed in panels **b** and **f** is due to autofluorescence that is visualized at the gain used to image the section. No fluorescent lectin was used in these studies [47]. (Used with permission of Nature)

cationic lipoplexes. The ratio of GFP-expressing cells to fluorescent nuclei indicated that capillary endothelial cells were more efficient in gene expression per delivery event than were pulmonary epithelial cells. Thus, the greater gene expression efficiency of i.v.-administered lipoplexes was due not only to the initial distribution, but also to the greater efficiency of the vascular endothelial cells to appropriately traffic and express the foreign gene (Fig. 12.14) [47].

The seminal work carried out by Godbey, Wu and Mikos, reported in 1999, on PEI stands as a major contribution in this research area of NVGT [43].

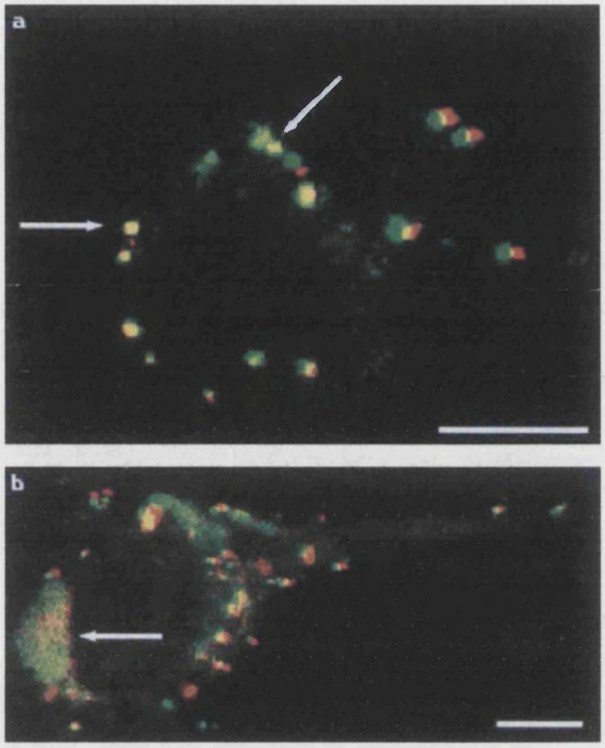

Fig. 12.15a, b. Tracking of double-labelled PEI/DNA complexes. The fluorescence patterns for single-labelled complexes are also seen for double-labelled complexes. **a** At 2 h post-transfection, visible complexes appear as clumps on the cell's exterior, as indicated by *arrows*. **b** At 3 h post-transfection, both surface aggregation and endosomes are visible. The *arrow* indicates endosomal formation. **c, d** s. p. 220

Their rigorous proof of mechanism, using fluorescent labelling and confocal microscopy, followed PEI/DNA complexes from endocytosis to gene expression. Significantly, the cationic polymer PEI (with or without DNA) underwent nuclear localization (Fig. 12.15) [43].

Chitosan, a polymer of glucosamine and *N*-acetylglucosamine, is useful as a non-viral vector for gene delivery. Although there are several reports of chitosan in gene delivery, studies of the effects on transfection and the chitosan-specific transfection mechanism are still few. Sato and co-workers have recently studied the transfection mechanism of plasmid/chitosan complexes as well as the relationship between transfection activity and cell uptake using fluorescein isothiocyanate-labelled plasmid and Texas Red-labelled chitosan. Factors that increased transfection activity and cell uptake included: molecular mass of chitosan (40 or 84 kDa), stoichiometry of the chitosan nitrogen to DNA phosphate (N/P ratio) in the complex was 5, and the transfection medium contained 10% serum at pH 7.0. For details of the transfec-

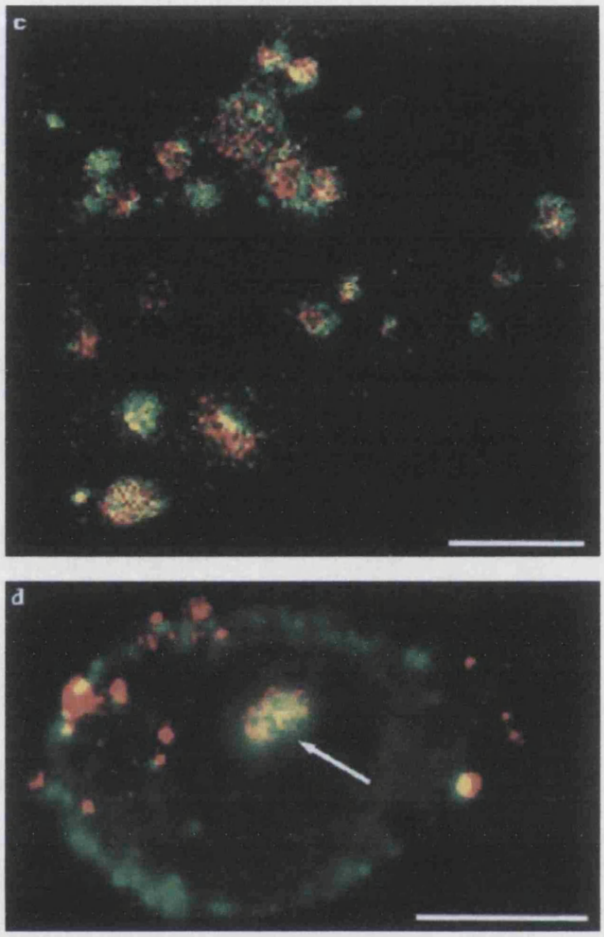

Fig. 12.15c,d. **c** At 4 h post-transfection, endosomes containing both PEI and DNA are visible throughout the cell cytoplasm. **d** At 4.5 h post-transfection, fluorescent structures containing both PEI and DNA inside the cell nucleus are present, as indicated by the *arrow*. (*Bar*=10 μm). (Godbey WT, Wu KK, Mikos AG, Proc Natl Acad Sci USA, 1999, 96:5177–5181; Copyright (1999) National Academy of Sciences, USA)

tion mechanism, they found that plasmid/chitosan complexes condense to form large aggregates (5–8 μm) which absorb to the cell surface. Plasmid/chitosan complexes are endocytosed and then released from endosomes due to osmotic swelling of endosome, in addition to possible swelling of plasmid/chitosan complex, causing the endosome to rupture. These complexes were observed to accumulate in the nucleus using confocal laser scanning microscopy (Fig. 12.16) [48].

Polyethylenimine (PEI) is one of the most efficient polymeric non-viral vectors for gene therapy, but one suffering from the serious limitation of

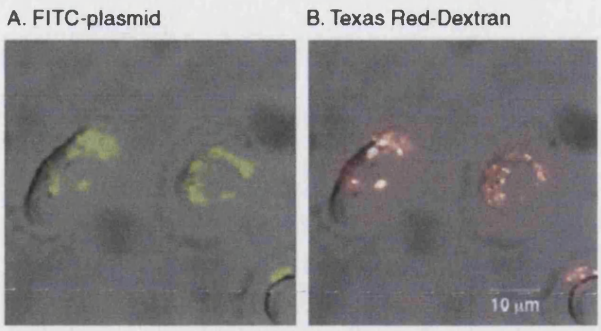

Fig. 12.16 A, B. Intracellular distribution of FITC-plasmid/chitosan complexes (**A**, *green*) and Texas Red-dextran (**B**, *red*) were observed by a confocal fluorescence microscope at 1 h post-incubation in SOJ cells. The confocal images show overlaid images of the fluorescent probe and the phase contrast. Molecular mass of chitosan was 40 kDa. (*Bar*=10 μm) [48]. (Used with permission of Elsevier)

significant cytotoxicity when used in large amounts for transfection. What is the role of endocytosis in the transfection of synchronized L929 fibroblasts by PEI/DNA complexes? Employing a combination of confocal microscopy and FACS, using the endocytosis marker FM4-64 and PEI/DNA complexes labelled either with the DNA intercalator YOYO-1 or with fluorescein covalently linked to PEI, Mely and co-workers showed that nanoparticles were typically taken up within 10 min in endosomes that did not exceed 200 nm in diameter. The location then became perinuclear and fusion between late endosomes was shown to occur. In L929 cells, escape of the complexes from the endosomes is a major barrier in transfection [84]. Comparison with the intracellular trafficking of the same complexes in EA.hy 926 cells (Godbey, Wu and Mikos [43]) revealed that endocytosis of PEI/DNA complexes is strongly cell-dependent (Fig. 12.17) [84].

Mely and co-workers [85] have recently reported their continuing studies on PEI. Fluorescence probes such as Nile red, cSNARF-1 and cyanine dye $DiSC_2(3)$, coupled with the technique of picosecond time-resolved fluorescence microscopy, were used to show that cytoplasmic pH increased by 0.1–0.4 units when cells were treated with PEI. Mely, Behr and co-workers [86] have also developed and studied a new cysteine detergent, ornithinyl-cysteinyl-tetradecylamide (C-14-CO), able to convert itself, via oxidative dimerization, into a cationic cystine lipid. Using fluorescence techniques, they characterized the structures of plasmid DNA lipoplexes [86].

12.8.1
New Emerging Fluorescence Techniques to Explore in NVGT Research

The non-invasive technique of FCS, with its high spatial resolution of less than 0.5 μm, extracts information about molecular dynamics from the tiny fluctuations that can be observed in the emission of small ensembles of fluorescent

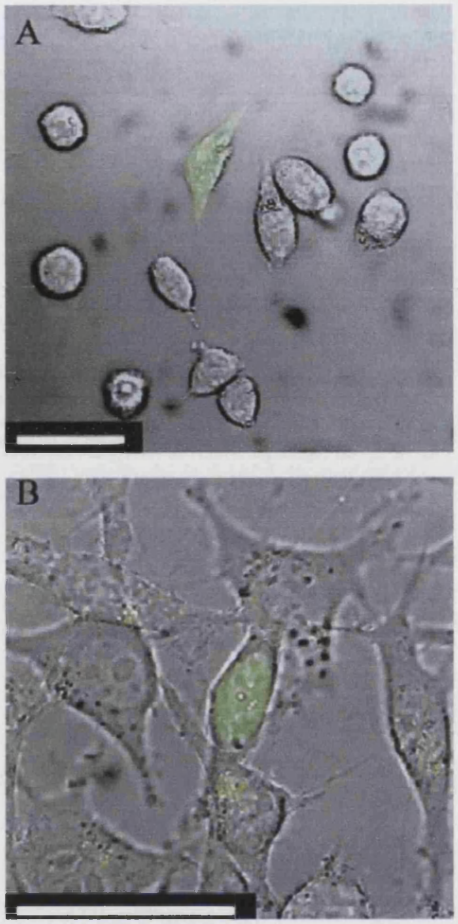

Fig. 12.17A, B. Transfection of L929 fibroblasts with a GFP-coding plasmid complexed with PEI. The cells were incubated with a GFP-coding plasmid complexed with either unlabelled (**A**) or FITC-labelled PEI (**B**). At 24 h post-transfection, a positive transfection is noted by the expression of the diffuse fluorescence of the green fluorescent protein (**A**) that could be easily differentiated from the fluorescence of the FITC-labelled complexes (**B**). (*Bar*= 50 μm) [84]. (Used with permission of Elsevier)

molecules in thermodynamic equilibrium. More non-invasive fluorescence techniques were developed and this allows NVGT research to be performed with intact cells directly, such as in vivo FCS [87, 88]. FCS is becoming increasingly popular as a technique to add chemical and biophysical information, e.g. particle mobility, local concentrations, rate constants for association and dissociation processes, enzyme kinetics and molecular interactions, to live cell images obtained by microscopy or other techniques. Recent examples of both auto- and cross-correlation applications further demonstrate the potential of FCS for cell

biology [87]. Thus, FCS is a versatile technique, particularly attractive for affording quantitative assessment of interactions and dynamics of small molecular quantities in biologically relevant systems [88]. Additionally, the combination of fluorescence techniques is a newly emerging strategy to obtain more information for a better understanding of the complex biological events in NVGT, e.g. the FCS measurement of FRET between the donor (Alexa488) and acceptor (Cy5) fluorophores, and in particular studying fluctuations generated by *trans-cis* isomerization of the acceptor dye, which can be conveniently measured by FCS [89]. The dissociation events of rhodamine green-labelled oligonucleotide (ODN 20-mer) and DNA from rhodamine green- or Cy5 red-labelled cationic polymer carriers (e.g. PLL) can also be studied by dual-colour fluorescence fluctuation spectroscopy (FFS), as recently reported by Lucas et al. [90]. In their studies, both the ODN and the cationic polymers were fluorescently labelled, and the results were compared with data obtained from single-colour FFS in which only the ODN or the cationic polymers were fluorescently marked [90].

Single-molecule fluorescence techniques have been increasingly used in biomolecular studies [91, 92]. The kinetics of spermidine-mediated linear DNA condensation were monitored by optical tweezers and fluorescence imaging at the single molecule level. Two steps, i.e. medium flow speed-dependent lag period and collapse, were observed in the DNA condensation process. The observed lag time suggests that loop formation at the end of the DNA may be a prerequisite for DNA condensation [93].

12.9 Conclusions

Fluorescence techniques can potentially play important roles in all areas of NVGT research. EthBr and other DNA intercalating dyes (as a simple, rapid analytical screen) contribute to the discovery of novel DNA condensing agents. The NVGT efficiency can be evaluated by using plasmid carrying fluorescent protein and luminescence-associated enzymes. Fluorescent lipopolyamines were designed and synthesized, enabling the intracellular tracking of DNA complexes to reveal (both spectroscopically and microscopically) the key steps and barriers in gene delivery. Fluorescence microscopy (e.g. GFP monitoring) has been intensively employed in NVGT imaging. Since the introduction of confocal microscopy, FCS has undergone major developments and has been used to monitor biological events including transfection. Moreover, fluorescent labelling of DNA can be used together with lipopolyamine probes for studies of fluorophore interactions, e.g. by FRET for studies of the (diss-)association of DNA and its cationic carrier, NLS or other biomolecules or intracellular organelles. Newly developed fluorescence techniques, e.g. in vivo FCS and FRET by FCS, are certainly valuable tools for ongoing research towards the goal of efficient NVGT. Designed small molecule probes will play their part in this.

Acknowledgements
We acknowledge the financial support of the EPSRC (a studentship to APN) and an ORS award from Universities U.K. (partial support of studentship fees to NA). We are grateful to Dr C. Pourzand (University of Bath) for cell biology skills and useful discussions and to Prof. R.M. Tyrrell (University of Bath) for the FEK4 cell line. In particular, we are grateful for the generous agreement to reproduce the colour plates (Figs. 12.13–12.17) provided by Profs. Mely, Mikos, Sato and Szoka, and their respective publishers.

References

1. Brooks G (2002) Gene therapy: the use of DNA as a drug. Pharmaceutical Press, London
2. Wiley (2003)http://www.wiley.com/legacy/wileychi/genmed/clinical/
3. Blagbrough IS, Geall AJ, Neal AP (2003) Polyamines and novel polyamine conjugates interact with DNA in ways that can be exploited in non-viral gene therapy. Biochem Soc Trans 31:397–406
4. Kumar VV, Singh RS, Chaudhuri A (2003) Cationic transfection lipids in gene therapy: successes, set-backs, challenges and promises. Curr Med Chem 10:1297–1306
5. Schmidt-Wolf GD, Schmidt-Wolf IGH (2003) Non-viral and hybrid vectors in human gene therapy: an update. Trends Mol Med 9:67–72
6. Liu F, Huang L (2002) Development of non-viral vectors for systemic gene delivery. J Control Release 78:259–266
7. Godbey WT, Mikos AG (2001) Recent progress in gene delivery using non-viral transfer complexes. J Control Release 72:115–125
8. Li S, Huang L (2000) Non-viral gene therapy: promises and challenges. Gene Ther 7:31–34
9. Lollo CP, Banaszczyk MG, Chiou HC (2000) Obstacles and advances in non-viral gene delivery. Curr Opin Mol Ther 2:136–142
10. MacLachlan I, Cullis P, Graham RW (1999) Progress towards a synthetic virus for systemic gene therapy. Curr Opin Mol Ther 1:252–259
11. Felgner PL, Barenholz Y, Behr JP, Cheng SH, Cullis P, Huang L, Jessee JA, Seymour L, Szoka F, Thierry AR, Wagner E, Wu G (1997) Nomenclature for synthetic gene delivery systems. Hum Gene Ther 8:511–512
12. El Aneed A (2004) An overview of current delivery systems in cancer gene therapy. J Control Release 94:1–14
13. Roux D, Cheneviera P, Pott T, Navailles L, Regev O, Monval OM (2004) Conception and realization of a non-cationic non-viral DNA vector. Curr Med Chem 11:169–177
14. Russell SJ (2003) Rise of the nanomachines. Nat Biotechnol 21:872–873
15. Kamiya H, Akita H, Harashima H (2003) Pharmacokinetic and pharmacodynamic considerations in gene therapy. Drug Discov Today 8:990–996
16. Ruponen M, Honkakoski P, Ronkko S, Pelkonen J, Tammi M, Urtti A (2003) Extracellular and intracellular barriers in non-viral gene delivery. J Control Release 93:213–217
17. Wiethoff CM, Middaugh CR (2003) Barriers to nonviral gene delivery. J Pharm Sci 92: 203–217
18. Ferrari S, Geddes DM, Alton EWFW (2002) Barriers to and new approaches for gene therapy and gene delivery in cystic fibrosis. Adv Drug Deliv Rev 54:1373–1393
19. Vijayanathan V, Thomas T, Thomas TJ (2002) DNA nanoparticles and development of DNA delivery vehicles for gene therapy. Biochemistry 41:14085–14094
20. Vijayanathan V, Thomas T, Shirahata A, Thomas TJ (2001) DNA condensation by polyamines: a laser light scattering study of structural effects. Biochemistry 40:13644–13651
21. Hud NV, Plavec J (2003) A unified model for the origin of DNA sequence-directed curvature. Biopolymers 69:144–159
22. Golan R, Pietrasanta LI, Hsieh W, Hansma HG (1999) DNA toroids: stages in condensation. Biochemistry 38:14069–14076
23. Li S, Tseng WC, Stolz DB, Wu SP, Watkins SC, Huang L (1999) Dynamic changes in the characteristics of cationic lipidic vectors after exposure to mouse serum: implications for intravenous lipofection. Gene Ther 6:585–594

24. Oupicky D, Konak C, Dash PR, Seymour LW, Ulbrich K (1999) Effect of albumin and polyanion on the structure of DNA complexes with polycation containing hydrophilic nonionic block. Bioconjug Chem 10:764–772
25. Welz C, Fahr A (2001) Spectroscopic methods for characterization of nonviral gene delivery systems from a pharmaceutical point of view. Appl Spectrosc Rev 36:333–397
26. Geall AJ, Blagbrough IS (2000) Rapid and sensitive ethidium bromide fluorescence quenching assay of polyamine conjugate–DNA interactions for the analysis of lipoplex formation in gene therapy. J Pharm Biomed Anal 22:849–859
27. Gershon H, Ghirlando R, Guttman SB, Minsky A (1993) Mode of formation and structural features of DNA-cationic liposome complexes used for transfection. Biochemistry 32: 7143–7151
28. Corsi K, Chellat F, Yahia L, Fernandes JC (2003) Mesenchymal stem cells, MG63 and HEK293 transfection using chitosan-DNA nanoparticles. Biomaterials 24:1255–1264
29. Read ML, Etrych T, Ulbrich K, Seymour LW (1999) Characterisation of the binding interaction between poly(L-lysine) and DNA using the fluorescamine assay in the preparation of non-viral gene delivery vectors. FEBS Lett 461:96–100
30. Bode J, Willmitzer L (1975) Application of fluorescamine to the study of protein-DNA interactions. Nucleic Acids Res 2:1951–1965
31. Cosa G, Focsaneanu KS, Mclean JRN, McNamee JP, Scaiano JC (2001) Photophysical properties of fluorescent DNA-dyes bound to single- and double-stranded DNA in aqueous buffered solution. Photochem Photobiol 73:585–599
32. Singer VL, Jones LJ, Yue ST, Haugland RP (1997) Characterization of PicoGreen reagent and development of a fluorescence-based solution assay for double-stranded DNA quantitation. Anal Biochem 249:228–238
33. Leong KW, Mao HQ, Truong L, Roy K, Walsh SM, August JT (1998) DNA-polycation nanospheres as non-viral gene delivery vehicles. J Control Release 53:183–193
34. Geall AJ, Taylor RJ, Earll ME, Eaton MAW, Blagbrough IS (2000) Synthesis of cholesteryl polyamine carbamates: pKa studies and condensation of calf thymus DNA. Bioconjug Chem 11:314–326
35. Wilson RW, Bloomfield VA (1979) Counterion-induced condensation of deoxyribonucleic acid. A light-scattering study. Biochemistry 18:2192–2196
36. Neal AP, Blagbrough IS (2001) Design and synthesis of fluorescent cholesterol and lithocholic acid polyamine conjugates. Abstr Pap Am Chem Soc 221:332–MEDI
37. Neal AP, Blagbrough IS (2001) Fluorescent steroidal lipopolyamine conjugates for monitoring gene delivery. Abstr Pap Am Chem Soc 221:352–MEDI
38. Kral T, Hof M, Langner M (2002) The effect of spermine on plasmid condensation and dye release observed by fluorescence correlation spectroscopy. Biol Chem 383:331–335
39. Kral T, Hof M, Jurkiewicz, P, Langner M (2002) Fluorescence correlation spectroscopy (FCS) as a tool to study DNA condensation with hexadecyltrimethylammonium bromide (HTAB). Cell Mol Biol Lett 7:203–211
40. Kral T, Langner M, Benes M, Baczynska D, Ugorski M, Hof M (2002) The application of fluorescence correlation spectroscopy in detecting DNA condensation. Biophys Chem 95:135–144
41. Itaka K, Harada A, Nakamura K, Kawaguchi H, Kataoka K (2002) Evaluation by fluorescence resonance energy transfer of the stability of nonviral gene delivery vectors under physiological conditions. Biomacromolecules 3:841–845
42. Zelphati O, Szoka FC Jr (1996) Mechanism of oligonucleotide release from cationic liposomes. Proc Natl Acad Sci USA 93:11493–11498
43. Godbey WT, Wu KK, Mikos AG (1999) Tracking the intracellular path of poly(ethylenimine)/DNA complexes for gene delivery. Proc Natl Acad Sci USA 96:5177–5181
44. Byk G, Dubertret C, Escriou V, Frederic M, Jaslin G, Rangara R, Pitard B, Crouzet J, Wils P, Schwartz B, Scherman D (1998) Synthesis, activity, and structure–activity relationship studies of novel cationic lipids for DNA transfer. J Med Chem 41:224–235
45. Byk G, Scherman D (2000) Genetic chemistry: tools for gene therapy coming from unexpected directions. Drug Dev Res 50:566–572

46. Byk G, Wetzer B, Frederic M, Dubertret C, Pitard B, Jaslin G, Scherman D (2000) Reduction-sensitive lipopolyamines as a novel nonviral gene delivery system for modulated release of DNA with improved transgene expression. J Med Chem 43:4377–4387
47. Uyechi LS, Gagne L, Thurston G, Szoka FC (2001) Mechanism of lipoplex gene delivery in mouse lung: binding and internalization of fluorescent lipid and DNA components. Gene Ther 8:828–836
48. Ishii T, Okahata Y, Sato T (2001) Mechanism of cell transfection with plasmid/chitosan complexes. Biochim Biophys Acta Biomembr 1514:51–64
49. Naylor BL, Picardo M, Homan R, Pownall HJ (1991) Effects of fluorophore structure and hydrophobicity on the uptake and metabolism of fluorescent lipid analogs. Chem Phys Lipids 58:111–119
50. Bolton PH, Kearns DR (1978) Spectroscopic properties of ethidium monoazide: a fluorescent photoaffinity label for nucleic acids. Nucleic Acids Res 5:4891–4903
51. Cantrell CE, Yielding KL, Pruitt KM (1979) Efficiency of photolytic binding of ethidium monoazide to nucleic acids and synthetic polynucleotides. Mol Pharmacol 15:322–330
52. Zabner J, Fasbender AJ, Moninger T, Poellinger KA, Welsh MJ (1995) Cellular and molecular barriers to gene transfer by a cationic lipid. J Biol Chem 270:18997–19007
53. Neves C, Byk G, Escriou V, Bussone F, Scherman D, Wils P (2000) Novel method for covalent fluorescent labeling of plasmid DNA that maintains structural integrity of the plasmid. Bioconjug Chem 11:51–55
54. Keller GH, Huang DP, Manak MM (1989) Labeling of DNA probes with a photoactivatable hapten. Anal Biochem 177:392–395
55. Slattum PS, Loomis AG, Machnik KJ, Watt MA, Duzeski JL, Budker VG, Wolff JA, Hagstrom JE (2003) Efficient in vitro and in vivo expression of covalently modified plasmid DNA. Mol Ther 8:255–263
56. Yoshinaga T, Yasuda K, Ogawa Y, Takakura Y (2002) Efficient uptake and rapid degradation of plasmid DNA by murine dendritic cells via a specific mechanism. Biochem Biophys Res Commun 299:389–394
57. Byrnes CK, Nass PH, Shim J, Duncan MD, Lacy B, Harmon JW (2002) Novel nuclear shuttle peptide to increase transfection efficiency in esophageal mucosal cells. J Gastrointest Surg 6:37–42
58. Murata S, Herman P, Lin HJ, Lakowicz JR (2000) Fluorescence lifetime imaging of nuclear DNA: effect of fluorescence resonance energy transfer. Cytometry 41:178–185
59. Murata S, Herman P, Mochizuki K, Nakazawa T, Kondo T, Nakamura N, Lakowicz JR, Katoh R (2003) Spatial distribution analysis of AT- and GC-rich regions in nuclei using corrected fluorescence resonance energy transfer. J Histochem Cytochem 51:951–958
60. Murata S, Herman P, Lakowicz JR (2001) Texture analysis of fluorescence lifetime images of AT- and GC-rich regions in nuclei. J Histochem Cytochem 49:1443–1451
61. Murata S, Herman P, Lakowicz JR (2001) Texture analysis of fluorescence lifetime images of nuclear DNA with effect of fluorescence resonance energy transfer. Cytometry 43:94–100
62. Murata S, Kusba J, Piszczek G, Gryczynski I, Lakowicz JR (2000) Donor fluorescence decay analysis for energy transfer in double-helical DNA with various acceptor concentrations. Biopolymers 57:306–315
63. Malicka J, Gryczynski I, Maliwal BP, Fang JY, Lakowicz JR (2003) Fluorescence spectral properties of cyanine dye labeled DNA near metallic silver particles. Biopolymers 72: 96–104
64. Kang JS, Abugo OO, Lakowicz JR (2002) Dynamics of supercoiled and relaxed pTZ18U plasmids probed with a long-lifetime metal-ligand complex. J Biochem Mol Biol 35:389–394
65. Kang JS, Abugo OO, Lakowicz JR (2002) Dynamics of supercoiled and linear pTZ18U plasmids observed with a long-lifetime metal-ligand complex. Biopolymers 67:121–128
66. Cormack BP, Valdivia RH, Falkow S (1996) FACS-optimized mutants of the green fluorescent protein (GFP). Gene 173:33–38
67. Deluca M, McElory WD (1978) Purification and properties of firefly luciferase. Meth Enzymol 57:3–15

68. Vile GF, Tyrrell RM (1993) Oxidative stress resulting from ultraviolet-A irradiation of human skin fibroblasts leads to a heme oxygenase-dependent increase in ferritin. J Biol Chem 268:14678–14681
69. Zelphati O, Liang XW, Hobart P, Felgner PL (1999) Gene chemistry: functionally and conformationally intact fluorescent plasmid DNA. Hum Gene Ther 10:15–24
70. Hyvonen Z, Plotniece A, Reine I, Chekavichus B, Duburs G, Urtti A (2000) Novel cationic amphiphilic 1,4-dihydropyridine derivatives for DNA delivery. Biochim Biophys Acta 1509: 51–466
71. Hyvonen Z, Ruponen M, Ronkko S, Suhonen P, Urtti A (2002) Cellular and intracellular factors influencing gene transfection mediated by 1,4-dihydropyridine amphiphiles. Eur J Pharm Sci 15:449–460
72. Serikawa T, Suzuki N, Kikuchi H, Tanaka K, Kitagawa T (2000) A new cationic liposome for efficient gene delivery with serum into cultured human cells: a quantitative analysis using two independent fluorescent probes. Biochim Biophys Acta Biomembr 1467:419–430
73. Collins L, Sawyer GJ, Zhang XH, Gustafsson K, Fabre JW (2000) In vitro investigation of factors important for the delivery of an integrin-targeted nonviral DNA vector in organ transplantation. Transplantation 69:1168–1176
74. Krichevsky O, Bonnet G (2002) Fluorescence correlation spectroscopy: the technique and its applications. Rep Progr Phys 65:251–297
75. Clamme JP, Azoulay J, Mely Y (2003) Monitoring of the formation and dissociation of polyethylenimine/DNA complexes by two-photon fluorescence correlation spectroscopy. Biophys J 84:1960–1968
76. Van Rompaey E, Engelborghs Y, Sanders N, De Smedt SC, Demeester J (2001) Interactions between oligonucleotides and cationic polymers investigated by fluorescence correlation spectroscopy. Pharm Res 18:928–936
77. Jurkiewicz P, Okruszek A, Hof M, Langner M (2003) Associating oligonucleotides with positively charged liposomes. Cell Mol Biol Lett 8:77–84
78. Clamme JP, Krishnamoorthy G, Mely Y (2003) Intracellular dynamics of the gene delivery vehicle polyethylenimine during transfection: investigation by two-photon fluorescence correlation spectroscopy. Biochim Biophys Acta Biomembr 1617:52–61
79. Wiethoff CM, Gill ML, Koe GS, Koe JG, Middaugh CR (2002) The structural organization of cationic lipid-DNA complexes. J Biol Chem 277:44980–44987
80. Zhang Y, Garzon-Rodriguez W, Manning MC, Anchordoquy TJ (2003) The use of fluorescence resonance energy transfer to monitor dynamic changes of lipid-DNA interactions during lipoplex formation. Biochim Biophys Acta Biomembr 1614:182–192
81. Itaka K, Harada A, Yamasaki Y, Nakamura K, Kawaguchi H, Kataoka K (2004) In situ single cell observation by fluorescence resonance energy transfer reveals fast intra-cytoplasmic delivery and easy release of plasmid DNA complexed with linear polyethylenimine. J Gene Med 6:76–84
82. Pal R, Barenholz Y, Wagner RR (1988) Pyrene phospholipid as a biological fluorescent probe for studying fusion of virus membrane with liposomes. Biochemistry 27:30–36
83. Struck DK, Hoekstra D, Pagano RE (1981) Use of resonance energy transfer to monitor membrane fusion. Biochemistry 20:4093–4099
84. Remy-Kristensen A, Clamme JP, Vuilleumier C, Kuhry JG, Mely Y (2001) Role of endocytosis in the transfection of L929 fibroblasts by polyethylenimine/DNA complexes. Biochim Biophys Acta 1514:21–32
85. Ira A, Mely Y, Krishnamoorthy G (2003) DNA vector polyethylenimine affects cell pH and membrane potential: a time-resolved fluorescence microscopy study. J Fluoresc 13: 339–347
86. Lleres D, Dauty E, Behr JP, Mely Y, Duportail G (2001) DNA condensation by an oxidizable cationic detergent. Interactions with lipid vesicles. Chem Phys Lipids 111:59–71
87. Bacia K, Schwille P (2003) A dynamic view of cellular processes by in vivo fluorescence auto- and cross-correlation spectroscopy. Methods 29:74–85
88. Haustein E, Schwille P (2003) Ultrasensitive investigations of biological systems by fluorescence correlation spectroscopy. Methods 29:153–166

89. Widengren J, Schweinberger E, Berger S, Seidel CAM (2001) Two new concepts to measure fluorescence resonance energy transfer via fluorescence correlation spectroscopy: theory and experimental realizations. J Phys Chem A 105:6851–6866
90. Lucas B, Van Rompaey E, De Smedt SC, Demeester J, Van Oostveldt P (2002) Dual-color fluorescence fluctuation spectroscopy to study the complexation between poly-L-lysine and oligonucleotides. Macromolecules 35:8152–8160
91. Weiss S (1999) Fluorescence spectroscopy of single biomolecules. Science 283:1676–1683
92. Sako Y, Yanagida T (2003) Single-molecule visualization in cell biology. Nat Cell Biol SS1–SS5
93. Su TJ, Theofanidou E, Arlt J, Dryden DTF, Crain J (2004) Single molecule fluorescence imaging and its application to the study of DNA condensation. J Fluoresc 14:65–69

Neurotox'03: Neurotoxicological Targets from Functional Genomics and Proteomics
D.J. Beadle, I.R. Mellor & P.N.R. Usherwood, editors

CHAPTER 16

SPERMINE AND LIPOPOLYAMINES AS GENE DELIVERY AGENTS

I.S. BLAGBROUGH, N. ADJIMATERA, O.A.A. AHMED, A.P. NEAL and C. POURZAND

Department of Pharmacy and Pharmacology, University of Bath, Bath, BA2 7AY, U.K.

1. INTRODUCTION TO SPERMINE AND LIPOPOLYAMINES

Polyamines are polycationic at physiological pH and play a variety of important biological roles. Many mammalian cells also possess an active polyamine uptake system, although little is known about its function.[1] Spermine (Fig. 1i) (3.4.3 methylene count between the amine groups) and spermidine (Fig. 1ii) (4.3 methylene spacings) were first discovered in the nuclei of sperm, where these polycations help histone proteins to package DNA by charge neutralization of the phosphate anions along the DNA backbone. Most cells use histone proteins and polyamines to condense DNA in the nucleus. The histones found in chromatin are categorized as core histone (subunit H2A, H2B, H3, H4) (Fig. 1) and linker histone (H1), forming an octomer (108kDa) that binds to DNA. Lysine (Lys, K) and arginine (Arg, R), the most important of the positively charged amino acids, are found in significant sequences along most histone proteins. Lys has its $(CH_2)_4NH_3^+$ (basic) side-chain, and Arg is the naturally occurring (mammalian) amino acid containing a guanidine functional group, the most basic functional group in biological chemistry. Thus, the side-chains of these amino acids (together with ornithine and histidine) can be positively charged in the cell. The pK_as of Lys and Arg (side-chains) are 10.5 and 12.5 respectively. DNA-histone complexes are dissociated on treatment with acids or dilute salt solutions.[2] This is evidence of ionic and non-covalent interactions; the phosphate anions are titrated by the ammonium cations. Of course, there also has to be some consideration of spermine (i) and spermidine (ii) and their conjugates as neurotoxins; such neurotoxication can be due to high levels of free polyamines, or similar effects achieved by polyamine amides in the mammalian brain by mechanisms involving glutamate receptors. This latter process parallels the modes of action of the spider and wasp polyamine amide (invertebrate) neurotoxins.

2. OVERVIEW OF NON-VIRAL GENE THERAPY (NVGT)

Gene therapy is a new treatment strategy for some difficult-to-cure diseases, introducing a therapeutic gene into body cells and aiming for desired gene expression. The therapeutic outcome is not only limited to missing proteins in patients (such as a chloride ion channel in

the lungs of patients with cystic fibrosis), but also an inhibitory protein signal to stop the progression of disease, especially as a potential treatment for certain cancers.[4] The design and synthesis of efficient DNA delivery vectors are major research areas in non-viral gene therapy (NVGT). Lentiviral and other viral vectors show efficient transfection, however, there is the possibility of severe toxicity from the viral genome, as well as immunogenicity, and there is the drawback of a limited DNA payload. Naked DNA is used even in current clinical trials. NVGT vectors have been produced to retain or to improve upon the performance of viral vectors and to provide a safe alternative for clinical gene therapy.[4] Recently, Felgner *et al.* reported a system of NVGT nomenclature guidelines to aid in NVGT research, dividing the vectors into the two major synthetic gene delivery systems: lipoplex (cationic lipid-nucleic acid complex) e.g. lipopolyamines, cationic liposomes, and polyplex (cationic polymer-nucleic acid complex) e.g. polyethylenimine (PEI), poly-L-lysine (PLL) etc.[5] Gene therapy is a complex drug (DNA) delivery strategy which must overcome intracellular barriers. The contributions from these barriers in blocking efficient NVGT are not well understood. We are aiming to understand (Fig. 2) and, thereby, to design a significant improvement over current transfection yields.

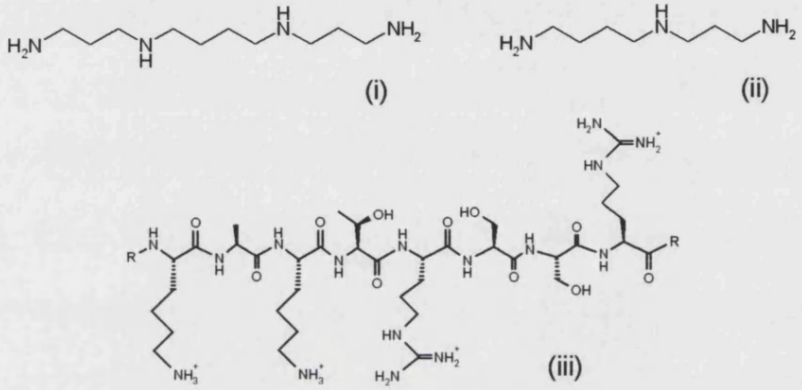

Figure 1 *Spermine (i), spermidine (ii) and histone 2A (iii) K(13)AKTRSSR(20) (underlined amino acids representing some DNA contact sites of histone 2A are shown).*[3]

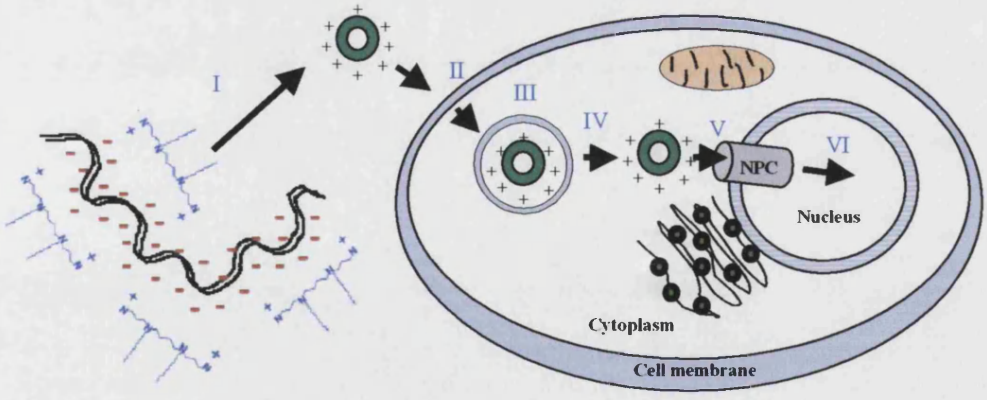

Figure 2 *Barriers to NVGT (I – DNA condensation and particle formation, II – endocytosis, III – endosome escape, IV - nuclear localization, V - nuclear entry and VI - gene expression).*

Negatively charged DNA (due to the phosphate anions), when neutralized by salt formation with positively charged lipopolyamine vectors, results in condensed nanometer-sized particles typically 50-150nm in outer diameter (Fig. 4). Nanoparticles, toroidal in shape, were observed in polyamine-induced DNA condensation.[6,7] This DNA compaction facilitates its stability in extracellular compartments, cellular uptake, and other intracellular process such as nuclear entry.[7,8] The electrostatic interactions between the surface of DNA particles and cell membranes is expected to be an initial process leading to internalization by endocytosis of DNA nano-complexes, with the involvement of clathrin-coated pits on the cell membrane.[9,10] It has been shown that endosome escape of the DNA is one major critical barrier to efficient transfection.[8] Early endosomes are formed by the inversed cell membrane upon DNA particles endocytosis, which are eventually degraded into late endosomes by internalization into lysosome vesicles. The "proton sponge" hypothesis has been proposed for endosome escape of NVGT cationic polymer. The protons are pumped into endosomes (at pH 7.4) by V-ATPase proton pump at their membrane, while polycations (the pK_a of a primary amine is around 10.5)[11] work as a pH buffer material. This results in an increased proton/water flux and lower pH at 5.5. Membrane disruption by swelling and finally osmotic lysis allows DNA complexes to escape from these vesicles prior to enzymatic degradation. Alternatively, the mechanism of lipid membrane mixing between endosomal membrane and lipidic gene carrier has also been hypothesized as an alternative means by which cationic lipids/liposomes might facilitate the endosome escape process, although this process is not well understood.[8,12,13]

Also, the mechanism of DNA nuclear translocation is not well understood. However, the transport through nuclear pores has been considered as the most likely possible route in conjunction with help from nuclear localization signals (NLS). NLS are peptides that help DNA complexes (which are typically bigger than 50kDa and cannot pass through the nuclear pore complex) to reach the nucleus. NLS binds with the α-subunit of the cytosolic importin receptor, then the β-subunit of the importin binds to the nuclear pore complex with the help of GTP binding protein (called Ran). The β-subunit will be retained at the inner face of pore complex.[14] Based on amino acid sequence analysis of NLS such as SV40 T-antigen, HIV-tat protein etc., positively charged amino acids are also found as their unique characteristic.[14] The nuclear envelope contains double phospholipid layers, with the membrane space directly connecting to the endoplasmic reticulum lumen. The inner and outer membranes join together at the nuclear pore complex (NPC). The NPC is a large structure with an assembly of eight spokes attached to rings on the cytoplasmic and nuclear sides of the nuclear envelope, accordingly named "the cytoplasmic ring" and "the nuclear ring", with a formed central channel approximately 40nm in diameter for the transportation of large particles across the nuclear membrane. The pore diameter is 120nm and the molecular mass is about 125 million Da. The small molecules (size of 9nm diameter, size less than 50kDa), for example, ions, metabolites and small proteins, use passive diffusion to get in and out of the nucleus freely. Bigger molecules, including DNA, are transported by an energy-dependent mechanism through this NPC. The selective transport of these macromolecules to and from the nucleus requires a NLS to direct their traffic through the NPC.[14]

3. SPERMINE MEDIATED DNA CONDENSATION AND PARTICLE FORMATION

Spermine (i) is a natural biomolecule involved in cell growth and differentiation control. *In vitro* studies have shown that the binding of spermine to DNA induces structural changes in DNA. The spermine cations neutralize the negatively charged phosphodiester groups of DNA, initiating the DNA helix's axis bending resulting in DNA condensation. This gene

packing enables efficient gene therapy by non-viral vectors. The results show that the nanoparticle (50-150nm) is able to go across the cell membrane and lead to the gene expression of delivered DNA.[7,15] The ethidium bromide (EthBr) assay was used to measure DNA condensation. EthBr is a cationic dye (Fig. 3) that intercalates between DNA base pairs. This intercalation increases the fluorescence yield of EthBr (excitation 546nm, emission 595nm). Many compounds that bind to DNA, including spermine, can displace EthBr from the EthBr-DNA complex. The EthBr displacement by these chemicals is related to DNA bases as well as environmental conditions (e.g. buffer composition, ionic strength). So, EthBr fluorescence quenching can be used to measure the DNA-polyamine binding efficiently.[15,16]

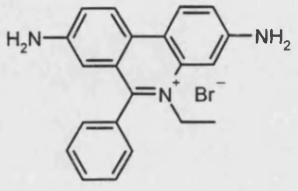

Figure 3 *Ethidium bromide.*

The EthBr assay method is a modified literature protocol of Cain and co-workers[17], regarded as an "exclusion assay" requiring the pre-forming of DNA and DNA binding drugs, before EthBr is added. The excitation wavelength used is 546nm, which is based on the excitation of EthBr. In 2000, the modified reproducible EthBr "displacement assay" was reported by Geall and Blagbrough.[16] The excitation wavelength was optimized at 260nm, so (only) intercalated EthBr is indirectly excited by energy transfer from the DNA. The proposed protocol also allows the experiment to be run without pre-complexing DNA and its binding molecule. This method is named as "displacement assay".[16] Additionally, the EthBr-DNA complex formation restricts the internal rotational freedom of EthBr. The fluorescence polarization is calculated from the emission intensity from polarizer and analyzer in a spectrofluorimeter. The polarization increase is observed when DNA is condensed due to the limited movement of EthBr. The measurement of steady-state fluorescence polarization can be used to indicate the EthBr-DNA complex conformation upon binding of spermine.[15]

In addition to the intercalating assay using EthBr, the UV absorbance at over 300nm (e.g. 320nm) was useful in confirming the formation of nanoparticles. The double helix DNA was bound by polyamines and formed the nanoparticles which scatter the light resulting in the UV absorbance increase above 300nm.[18] So, light scattering (LS) is being measured rather than (apparent) UV absorption. Some precipitation of the DNA may be visible, but it does not increase the absorption above 300nm. However, the DNA concentration used in this assay was in a 10-fold excess compared to the EthBr assay given the low sensitivity of this experiment and the lack of fluorescent indicator.[11]

DNA used in gene therapy research is normally prepared as plasmids, usually with a protein marker that can be followed in the gene expression quantification. pEGFP[19] (4.7 kilobasepairs) is the plasmid encoding for enhanced green fluorescent protein, under CMV (cytomegalovirus) promoter, obtained from Clontech. Successfully transfected cells with pEGFP shows the distinct fluorescence detectable by a Fluorescent Activated Cell Sorter (FACS). Modified firefly (*Photinus pyralis*) luciferase pGL3 control vector[20] (5.2 kilobasepairs), with SV-40 promoter, was from Promega. In this luciferase assay, luciferin was added to transfected cells that underwent oxidation and generated the yellow light, measured by a luminometer.

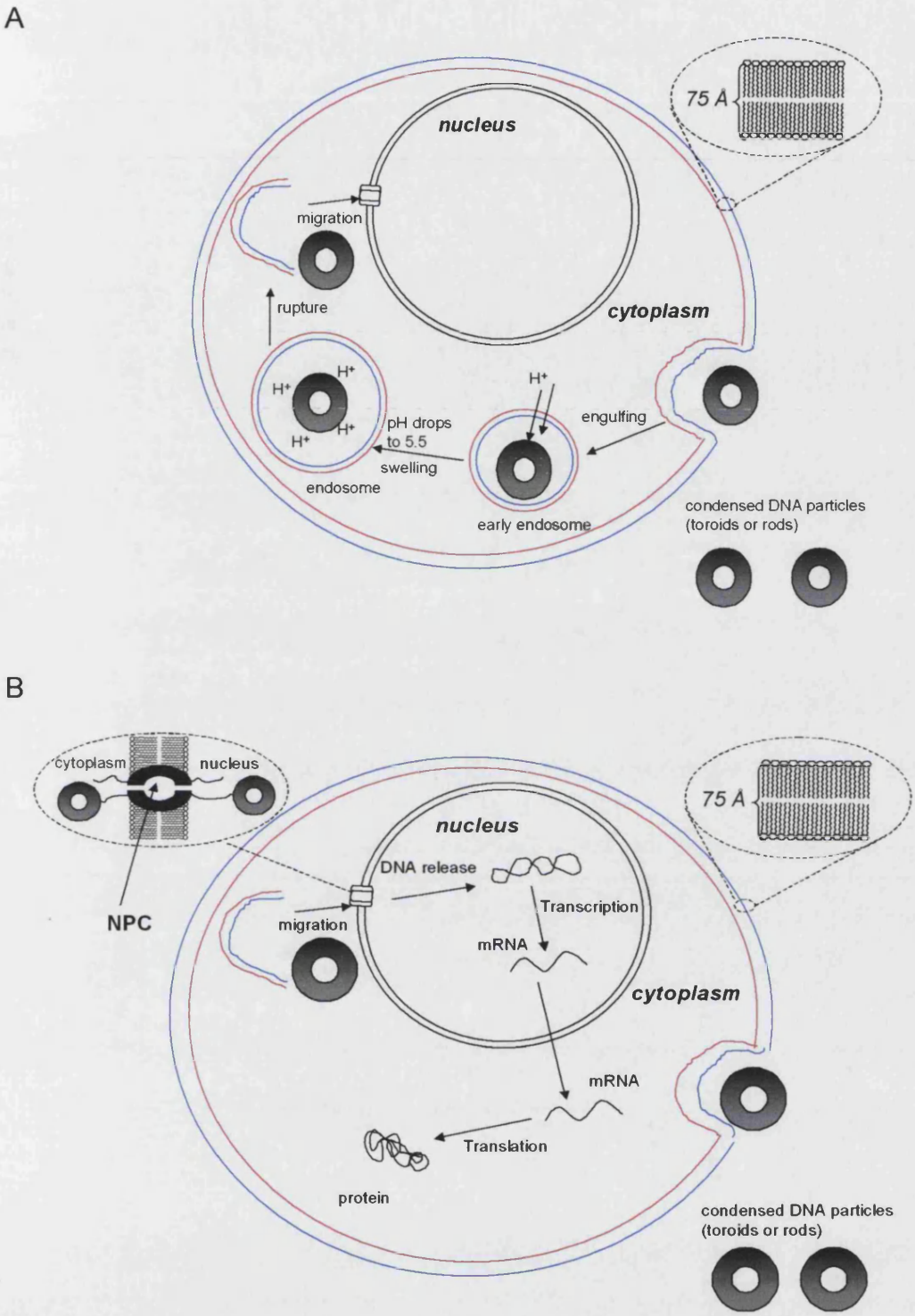

Figure 4 *Detailed NVGT mechanism. A: endocytosis process. B: nuclear entry and gene expression process.*

pEGFP and pGL3 were condensed by spermine to about 50%, measured using the EthBr assay (Fig. 5). Particle formation was also confirmed by the LS assay, with significantly increased apparent absorbance at an N/P ratio > 3.00. We conclude that (simple) spermine-mediated condensation may provide less compacted particles; also these are only really significant at high N/P ratios. Additionally, the condensation profiles of both plasmids were found to be similar, possibly relative to their similar plasmid sizes. We and others have shown that lipopolyamines are more efficient DNA condensers (though not necessarily NVGT vectors) than these simple polyamines.[21]

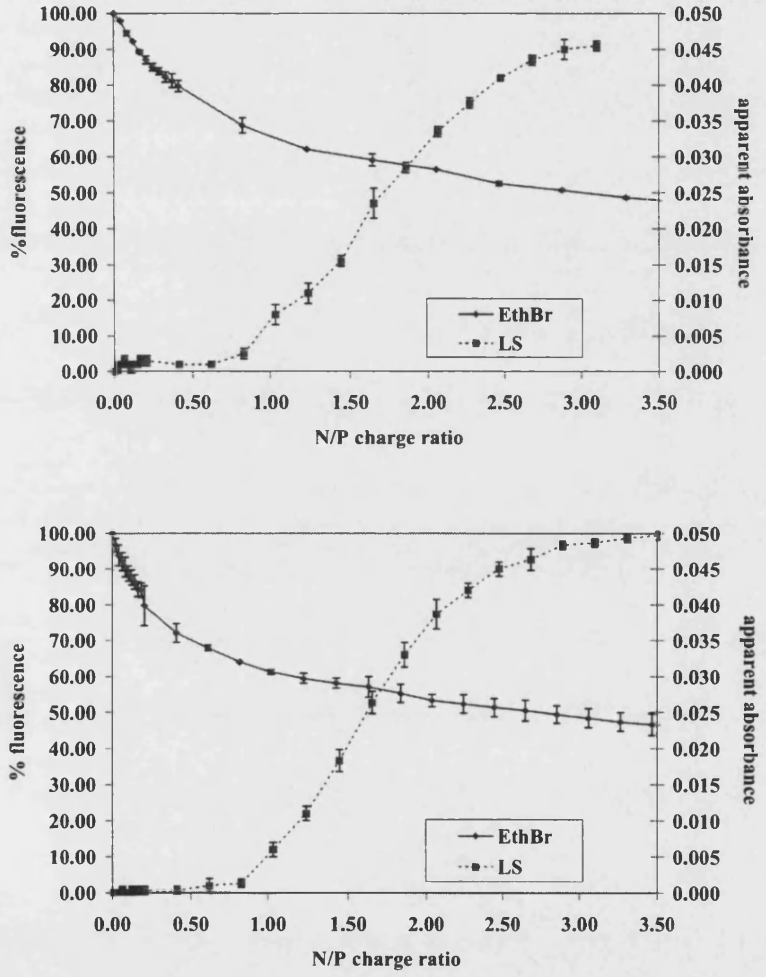

Figure 5 *DNA condensation and light scattering of nanoparticles (above – pEGFP plasmid vs spermine, below – pGL3 vs spermine).*

4. DEVELOPMENT OF POLYCATION VECTORS IN NVGT

A variety of polycations, but nevertheless small molecules compared to histones or DNA, have now been reported for studies in NVGT (Fig. 6). The examples chosen serve to illustrate the current range of molecular diversity within lipopolyamines. From one of the earliest steroid conjugates, DC-Chol containing only one positively charged N-atom, through

Genzyme's GL#67, Behr's Transfectam (DOGS), Scherman and co-workers' RPR-120535 and DOSPA (all containing spermine in different ways), through to vitamin D and modified buckyball (C60) conjugates. The most recent lipopolyamine is KanaChol from Lehn and co-workers.[23]

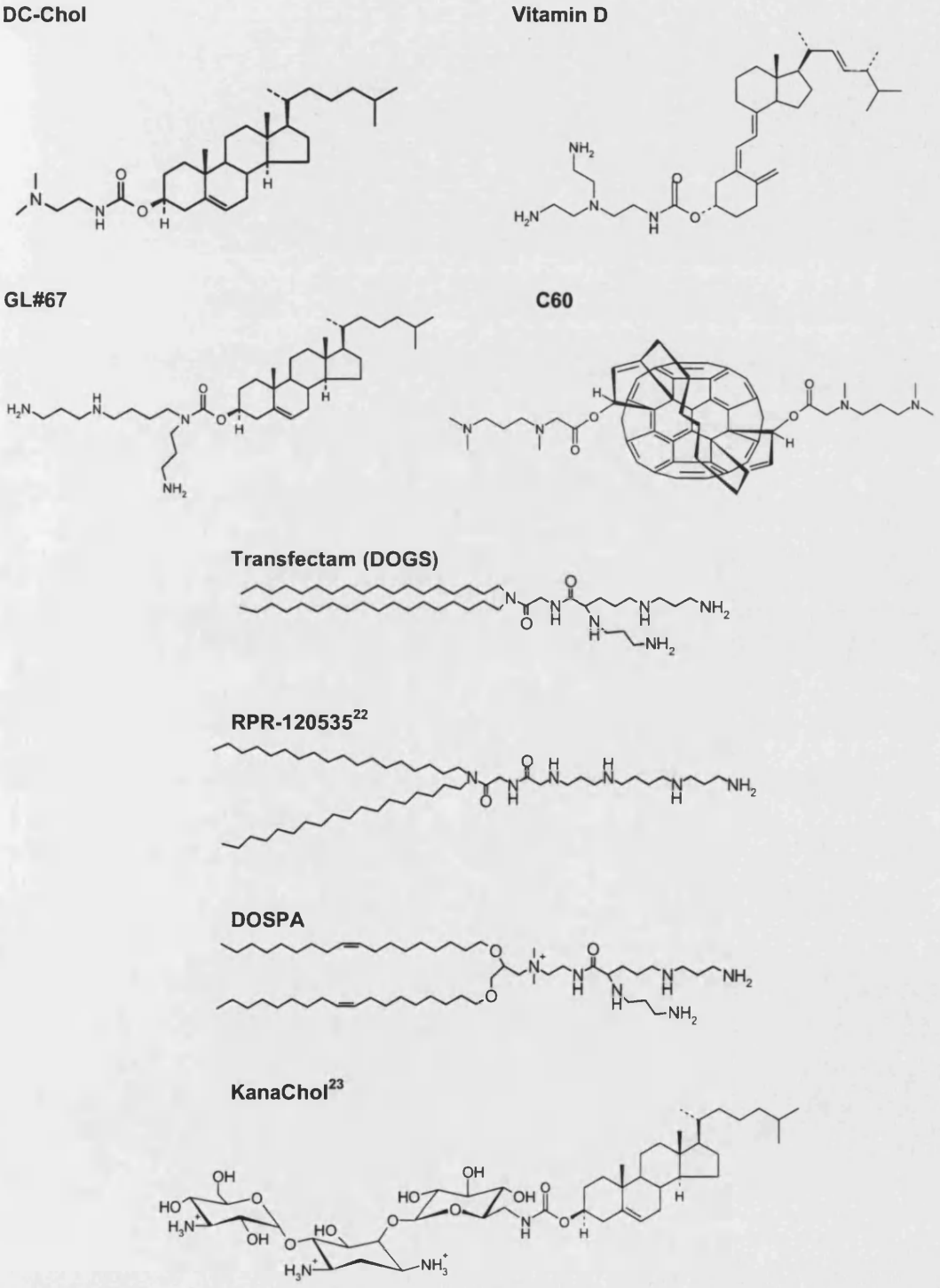

Figure 6 *A selection of lipopolyamine-based NVGT vectors (lipoplex).*[21]

Polymer polycationic NVGT vectors (Fig. 7) for the formation of polyplexes are based upon linear and branched polyethylenimines, PLL, poly-L-arginine and poly-L-histidine. These representative examples demonstrate the distribution of positive charge in the presence of a lipid region, cationic lipids.

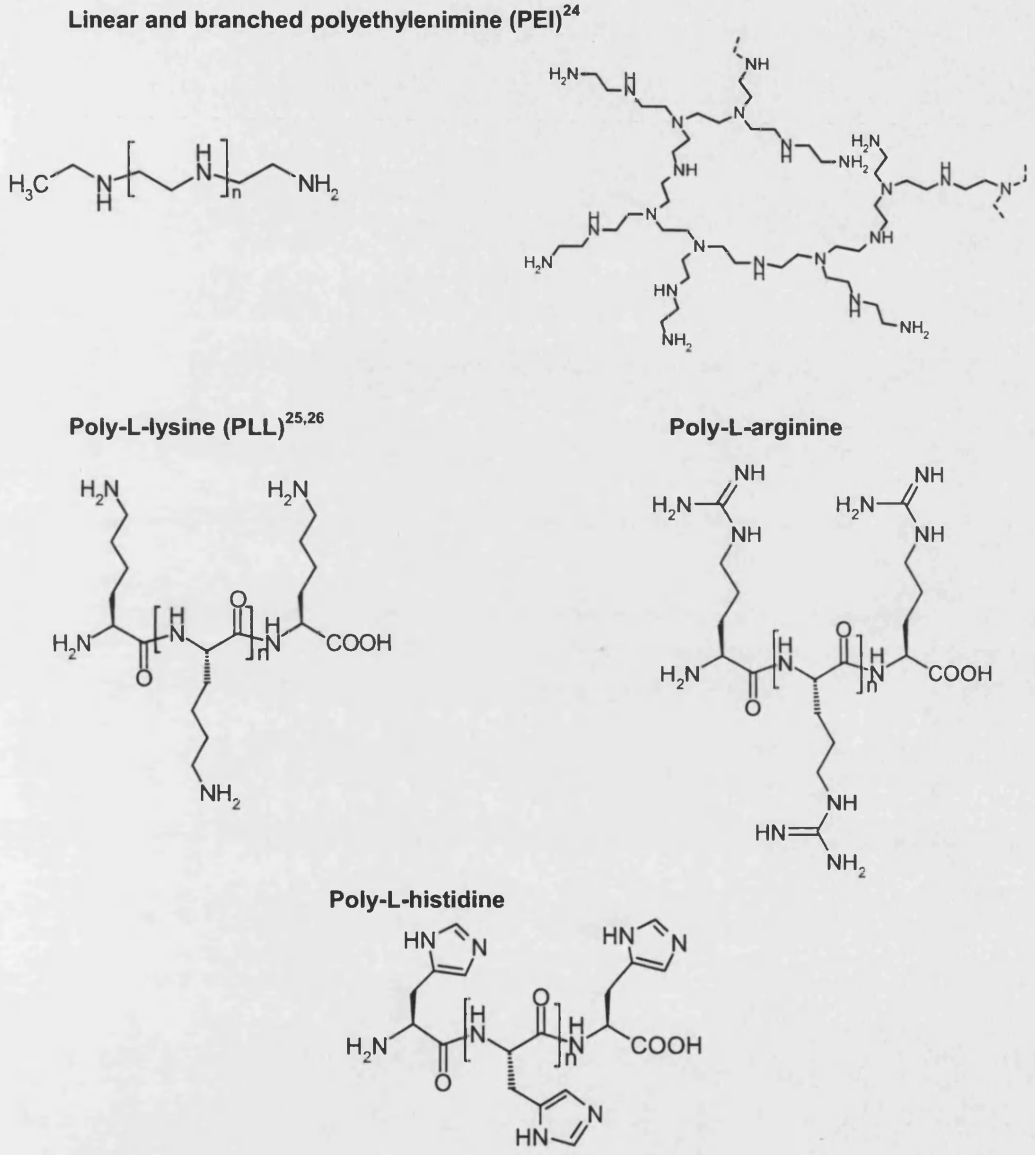

Figure 7 *Polymer polycationic NVGT vectors (polyplex).*

5. PHYSICOCHEMICAL PROPERTIES OF POLYAMINES-BASED DNA CONDENSING AGENTS

The effects of the regiochemical distribution of positive charges along the polyamine moiety in DNA condensing agents were studied by Geall *et al.*[11,27] DNA condensation is dependent upon

three characteristic properties of polyamines: the number of positive charges, the regiochemical distribution of charges (determined by the pK_a of each amino group), and the local salt concentration. From the pK_a investigation and calculation, spermine (i) carries 3.8 charges and its cholesterol conjugate has a positive charge distribution similar to that found in spermidine (ii) (4.3) (Fig. 8). Such spermidine mimics (lipospermidines) are still effective as DNA condensing agents, significantly more so than spermidine itself, which is but a weak DNA condensing agent.

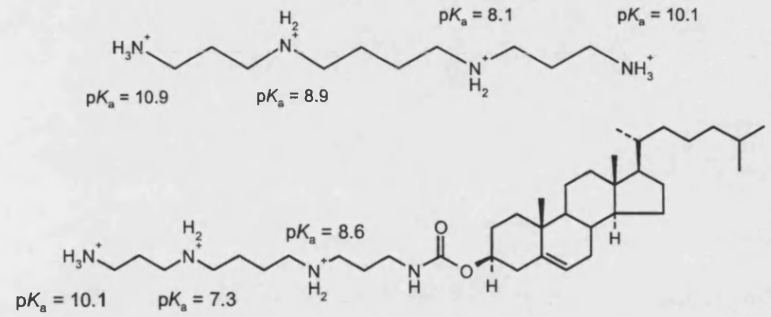

Figure 8 *p*K$_a$ *of spermine and a cholesteryl lipopolyamine.*[11]

We have designed and prepared lipopolyamines (Fig 9) and monitored their efficiency in DNA condensation into particles by LS and their salt-dependent binding affinity for DNA by fluorescence quenching.[11,27] Lipopolyamines were prepared from cholesterol, lithocholic and cholic acids (5β-cholanes) by acylation of tri-Boc-protected tetra-amines spermine and thermine. These ligands are polyammonium ions at physiological pH.[28]

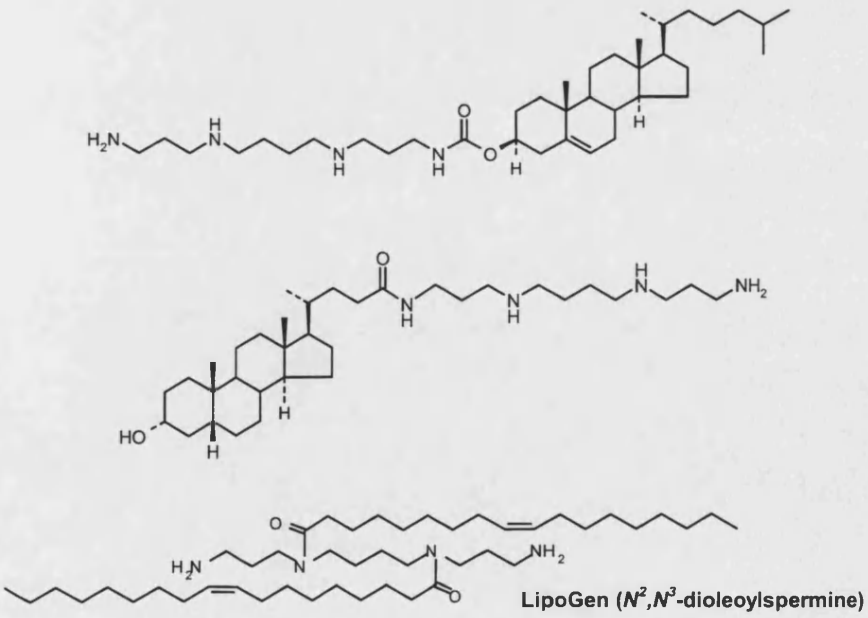

Figure 9 *Lipopolyamines based on cholesterol*[11]*, bile acids*[28] *and fatty acids.*

LipoGen (from InvivoGen) is an example of a lipopolyamine with two oleoyl groups at N^2 and N^3 of spermine, therefore with only two positively charged nitrogens. Modifying the lipophilicity of spermine (3.4.3) led to efficient DNA condensation (15% residual fluorescence at N/P charge ratio 2.5) comparing to the tetracationic spermine (50% at charge ratio more than 3.50) (Fig 10). According to Vijayanathan *et al.*[29] the λ–phage DNA condensed particles (by spermine) are in the size range 50-100 nm. Lipospermine was shown to condense pSfiSVneo, pSifiSV19 and pCISfi-γIFN DNA to smaller particle sizes at 50-70nm.[30] The efficient condensation of DNA by lipospermine over spermine, resulting in smaller sized particles, may promote more effective transfection.

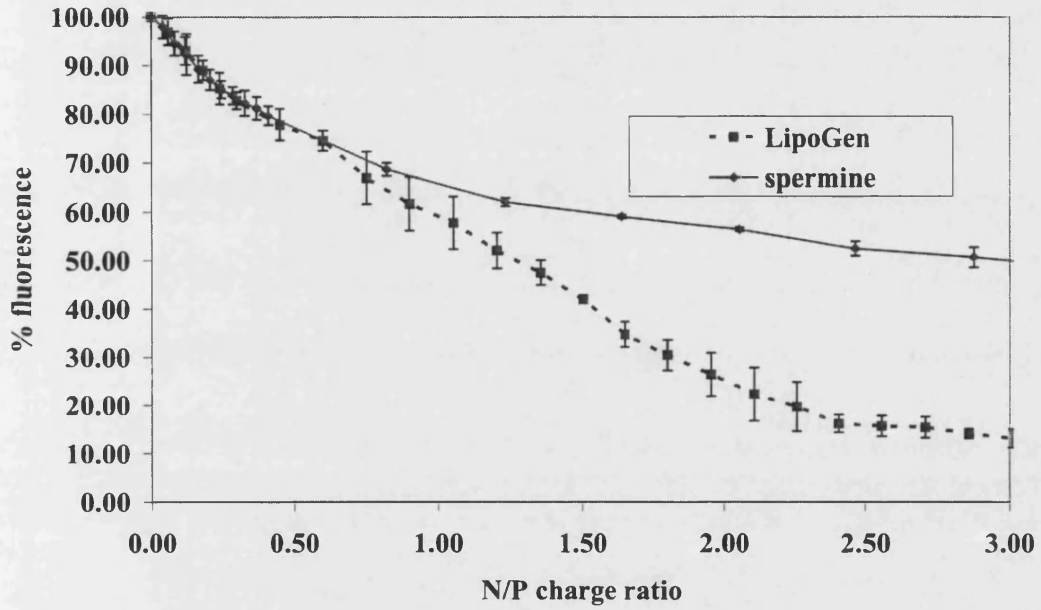

Figure 10 *pEGFP condensation by LipoGen vs spermine.*

6. TRANSFECTION IN HUMAN SKIN FIBROBLAST CELLS (FEK4)

LipoGen (Invivogen) is a lipospermine with two oleoyl groups at N^2 and N^3 of spermine (i) and, therefore, only two positively charged primary amines. It was prepared as a non-liposomal formulation. The lipophilic modification aims to facilitate the transfection process (e.g. potentially through enhanced DNA condensation, cell entry, endosomal escape). This lipophilic modification of the spermine structure resulted in a more efficient pEGFP DNA condensation (15% residual fluorescence, in the EthBr assay, at N/P charge ratio 2.5) compared to tetracationic spermine (50% at N/P charge ratio 3.0). The *in vivo* transfection of pEGFP (2μg/well) with LipoGen was carried out using FEK4[31] (2.5 x 10^4 cells/well at 50% confluence), incubated for 4h, then the transfection was stopped by removal of the DNA complex and replacement with foetal-calf serum containing media; FACS analysis was performed 48h post-transfection. By using pEGFP as delivered DNA, the EGFP chromophore (a substituted 4-hydroxybenzylidene imidazolidinone) was detected in successfully transfected cells by FACS (fluorescent-activated cell sorting). The EGFP amino acid sequence L(64)TYGV(68) transcribed from pEGFP was cyclised in the post-translational

steps (at amino acids 65-67) forming an EGFP fluorophore with λ ex = 488nm (red-shifted from wild GFP protein) and λ em = 507nm.[19] Lipofectin (DOTMA/DOPE = 1:1 w/w, Invitrogen), the commonly used transfection liposomal reagent containing cationic lipid (with one positive charge) and helper lipid (DOPE), was also used in this experiment for a comparison. The fluorescent cell counts observed in all N/P ratios were higher in LipoGen-mediated transfection. Thus, the lipid moiety in lipospermine is playing an important role in *in vitro* transfection. The optimal charge ratio for FEK4 transfection with pEGFP-LipoGen complex is around 2.5, which corresponds to the optimal DNA condensation N/P ratio (from the EthBr assay). However, from Fig. 11 it appears that increased condensation leads to higher transfection efficacy. The high N/P ratio (more than 5.0) results in less efficient gene delivery overall. A similar relationship between N/P charge ratio and transfection efficiency was also observed in Lipofectin-mediated transfection.

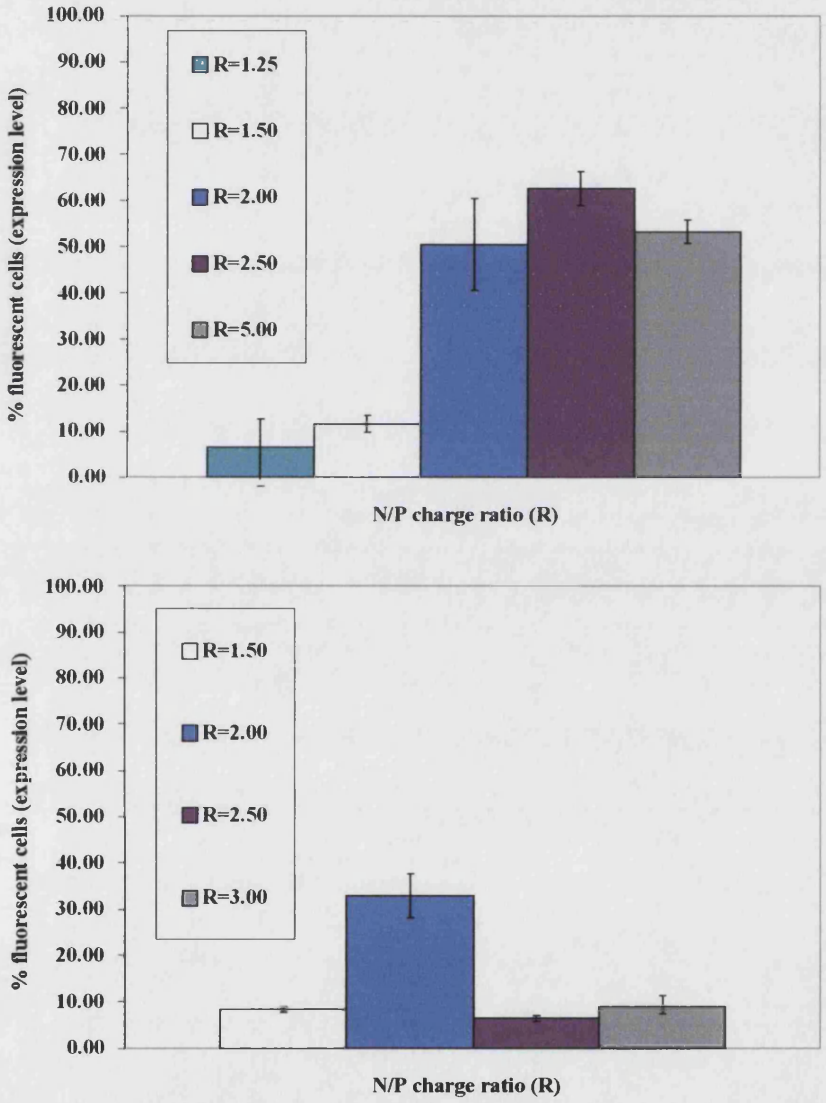

Figure 11 *FEK4 Transfection of pEGFP complexed by LipoGen (above) and Lipofectin (below).*

7. CONCLUSIONS

Our research has advanced neurotoxic polyamine amides from spider and wasp natural products,[32] with their exquisite sensitivity in modulating glutamate receptors, from pharmacological tools towards therapeutic neurochemistry,[33] thereby highlighting their potential as therapeutic agents.[34] So, whilst polyamines and polyamine amides are potent and selective receptor probes for a variety of voltage- and especially for ligand-gated cation channels,[35] they also are now seen to have potential as synthetic vectors and can be exploited in NVGT.[21,35] Using our designed steroidal lipopolyamine probes (Fig. 9), we are studying DNA-lipopolyamine complexes with respect to their formation by DNA condensation. Comparable DNA-binding efficiency to that of the unlabelled lipopolyamines and robust fluorescent spectral properties across the varying cellular pH range are desirable properties in fluorescent ligands, but this requires experimental verification. Have we designed and prepared fluorophore-substituted lipopolyamines or lipopolyamine-substituted fluorophores? Only time and experimental results will tell. However, we have achieved a controlled chain extension of suitably protected polyamines using reductive alkylation to mimic spermine (i) rather than spermidine (ii) in the target molecules.[21] A practical method for the efficient hydroboration of cholesteryl carbamates has allowed us to prepare our designed *trans*-AB steroidal lipopolyamines, together with the corresponding *cis*-AB ring junction as the minor product of hydroboration or from naturally occurring bile acids.[21] We are able to introduce fluorophores of choice by our Fmoc-chemistry route. The design in our versatile synthetic route to Fmoc protected aminoesters of cholesteryl carbamate and lithocholic acid polyamine amides allows a range of selected fluorophores to be readily incorporated. The design and synthesis of these novel fluorescent lipopolyamines allows us to study the intracellular events during transfection. As well as our studies on lipopolyamine-mediated DNA condensation, we are optimising these probes to employ them monitoring the intracellular hurdles to NVGT. At present, a poor understanding of the molecular mechanisms of action of non-viral vectors remains an important, but unresolved issue. With a greater knowledge of these mechanisms, new (possibly spermine based) lipopolyamine vectors with improved transfection efficiency can be rationally designed and used as gene delivery agents *in vivo*.

Acknowledgements

We thank the Embassy of the Arab Republic of Egypt and the EPSRC for PhD studentships to O.A.A.A. and A.P.N. respectively. We acknowledge the support of Universities U.K. through an ORS award to N.A. We are also grateful to Prof R.M. Tyrrell (University of Bath) for the FEK4 cell line.

References

1. Cullis, P.M., Green, R.E., Merson-Davies, L. and Travis, N., *Chem. Biol.* **6** (1999), 717-729.
2. Berg, J.M., Tymoczko, J.L. and Stryer, L., *Biochemistry* (1995), pp 977-982.
3. Balicki, D., Putnam, C.D., Scaria, P.V. and Beutler, E., *Proc. Natl. Acad. Sci. U.S.A* **99** (2002), 7467-7471.
4. Gelvin, B. *Gene therapy : the use of DNA as a drug*, Pharmaceutical Press: (2002).
5. Felgner, P.L. *et al.*, *Hum. Gene Ther.* **8** 1997, 511-512.

6. Golan, R., Pietrasanta, L.I., Hsieh, W. and Hansma, H.G., *Biochemistry* **38** (1999), 14069-14076.
7. Vijayanathan, V., Thomas, T. and Thomas, T.J., *Biochemistry* **41** (2002), 14085-14094.
8. Wiethoff, C.M. and Middaugh, C.R., *J. Pharm. Sci.* **92** (2003), 203-217.
9. Friend, D.S., Papahadjopoulos, D. and Debs, R.J., *Biochim. Biophys. Acta* **1278** (1996), 41-50.
10. Zuhorn, I.S., Kalicharan, R. and Hoekstra, D., *J. Biol. Chem.* **277** (2002), 18021-18028.
11. Geall, A.J. *et al.*, *Bioconjug. Chem.* **11** (2000), 314-326.
12. Cho, Y.W., Kim, J.D. and Park, K., *J. Pharm. Pharmacol.* **55** (2003), 721-734.
13. Langner, M., *Cell Mol. Biol. Lett.* **5** (2000), 295-313.
14. Cooper, G.M. The Cell, A Molecular Approach, 2nd ed. (2000), pp 315-327.
15. Delcros, J.G. *et al.*, *Biochem. J.* **291** (1993), 269-274.
16. Geall, A.J. and Blagbrough, I.S., *J. Pharm. Biomed. Anal.* **22** (2000), 849-859.
17. Cain, B.F., Baguley, B.C. and Denny, W.A., *J. Med. Chem.* **21** (1978), 658-668.
18. Wilson, R.W. and Bloomfield, V.A., *Biochemistry* **18** (1979), 2192-2196.
19. Cormack, B.P., Valdivia, R.H. and Falkow, S., *Gene* **173** (1996), 33-38.
20. Deluca, M. and McElory, W.D., *Meth. Enzymol.* **57** (1978), 3-15.
21. Blagbrough, I.S., Geall, A.J. and Neal, A.P., *Biochem. Soc. Trans.* **31** (2003), 397-406.
22. Byk, G. *et al.*, *J. Med. Chem.* **41** (1998), 229-235.
23. Belmont, P. *et al.*, *J. Gene Med.* **4** (2002), 517-526.
24. Boussif, O. *et al.*, *Proc. Natl. Acad. Sci. U.S.A.* **92** (1995), 7297-7301.
25. Pouton, C. W. *et al.*, *J. Control Release* **53** (1998), 289-299.
26. Wu, G.Y. and Wu, C.H., *J. Biol. Chem.* **262** (1987), 4429-4432.
27. Geall, A.J. *et al.*, *FEBS Lett.* **459** (1999), 337-342.
28. Geall, A.J., Al Hadithi, D. and Blagbrough, I.S., *Bioconjug. Chem.* **13** (2002), 481-490.
29. Vijayanathan, V., Thomas, T., Shirahata, A. and Thomas, T.J., *Biochemistry* **40** (2001), 13644-13651.
30. Dunlap, D.D., Maggi, A., Soria, M.R. and Monaco, L., *Nucleic Acids Res.* **25** (1997), 3095-3101.
31. Vile, G.F. and Tyrrell, R.M., *J. Biol. Chem.* **268** (1993), 14678-14681.
32. Blagbrough, I.S., Moya, E. and Taylor, S., *Biochem. Soc. Trans.* **22** (1994), 888-893.
33. Usherwood, P.N.R. and Blagbrough, I.S., *Pharmacology and Therapeutics* **52** (1991), 245-268.
34. Blagbrough, I.S. and Usherwood, P.N.R., *Proc. Roy. Soc. Edin.* **99B** (1992), 67-81.
35. Blagbrough, I.S., Carrington, S. and Geall, A.J., *Pharmaceutical Sciences* **3** (1997), 223-233.

1. BPC2005 (ORAL)

Analysis of Single Lipopolyamine-DNA Nanoparticle Formation in Non-viral Gene Therapy by Fluorescence Correlation Spectroscopy using PicoGreen

Noppadon Adjimatera, Teresa Kral[1,2], Martin Hof[1] and Ian S. Blagbrough

Department of Pharmacy and Pharmacology, University of Bath, Bath BA2 7AY, U.K.
[1] J. Heyrovský Institute of Physical Chemistry, Academy of Sciences of the Czech Republic, Dolejškova 3, Cz-18223 Prague 8, Czech Republic.
[2] Department of Physics and Biophysics, Agricultural University, Norwida 25, 50-375 Wrocław, Poland.
prsisb@bath.ac.uk

Non-viral gene therapy (NVGT) has the potential to revolutionize the way difficult-to-cure diseases are treated, by inserting genes coding for missing proteins (e.g. enzymes or signals) into patients' target cells. DNA nanocomplex formation is the first crucial step in NVGT. This enables lengthy polynucleotides to be stored as nanoparticles which it is feasible to deliver to target cells. DNA nanostructures (50-150 nm in outer diameter) can self-assemble by the interactions of the cationic lipid vectors with the negative charges of DNA phosphate. This DNA compaction protects DNA from degradation and facilitates gene delivery.

Small molecule sensors for DNA intercalation, e.g. ethidium bromide (EthBr), PicoGreen® (PG), have been widely used to determine polycation-DNA interactions, by measuring the fluorescence intensity of probes during condensation. As well as these fluorescent techniques, the formation of DNA nanoparticles can be observed in a light scattering (LS) assay, measuring UV apparent absorption at $\lambda >$ 300 nm.

Fluorescence correlation spectroscopy (FCS) is a new technique where fluctuations in the detected fluorescence from small sensors are also used to study dynamic processes of DNA nanocomplex formation (Kral et al 2002; Adjimatera et al 2005). The advantages of the FCS approach in comparison to standard fluorescence techniques are: a) use of lower dye concentration; b) use of lower (nM range) DNA concentration; c) information about possible condensed plasmid sub-populations; d) the possibility of monitoring the condensation process at the single molecule level. Employing PicoGreen® (PG), a high affinity DNA intercalating agent that only fluoresces when intercalated, we have used FCS to provide more insight e.g. diffusion time and particle number (PN), than the steady-state fluorimetric method. PG does not change the hydrodynamic properties of DNA and does not influence the lipopolyamine concentrations necessary for condensation. Additionally, PG requires 10-fold lower staining when compared with previously used markers because of the polyamine moiety structural modification which efficiently forms salt bridges with DNA phosphate anions, and taken together with the DNA intercalation, this is higher affinity from biphasic binding.

We have studied the condensation of linear calf thymus DNA (ct DNA, 13 kilobase pairs) and circular plasmid DNA (pEGFP, 4.7 kilobase pairs) using two lipopolyamines, N^4,N^9-dioleoylspermine (Ahmed et al 2005) and N^1-cholesteryl spermine carbamate. N^4,N^9-Dioleoylspermine efficiently condensed both ct DNA and pEGFP into point-like molecules with diffusion coefficient (D) = 1.8×10^{-12} m^2/s and 2.3×10^{-12} m^2/s, and particle number (PN) = 0.7 and 0.9 (the theoretical PN under this point-like molecular model is 0.6). Cholesteryl spermine carbamate showed poorer DNA condensation efficiency, even at higher N/P (ammonium/phosphate) charge ratios. Ultimately, a better understanding of DNA condensation, using new probes and analytical techniques, will lead to the development of more efficient DNA condensing agents.

We acknowledge the financial support of Universities U.K. (ORS award to N. A.) and of the Grant Agency of the Czech Republic (203/05/2308).

Adjimatera, N.; Neal, A. P.; Blagbrough, I. S. (2005) Fluorescence Techniques in Non-Viral Gene Therapy. In: Hof, M., Hutterer, R., Fidler, V., (eds) *Fluorescence Spectroscopy in Biology*. Berlin: Springer-Verlag, pp 201-228
Ahmed, O. A. A. et al (2005) *Pharm. Res.*, **22**: 12 pp in press
Kral, T. et al (2002) *Biophys. Chem.*, **95**: 135-144

2. BPC2005 (POSTER)

Synthesis and Biological Testing of Lipopolyamine N^4,N^9-Dioleoylspermine – Self-Assembly of a Nanopharmaceutical for Plasmid Delivery

N. Adjimatera, C. Pourzand and I. S. Blagbrough

Department of Pharmacy and Pharmacology, University of Bath, Bath BA2 7AY, U.K.

prsisb@bath.ac.uk

We are designing novel, small molecule DNA-condensing agents, modified synthetic polyamine-conjugates (lipopolyamines) (Blagbrough et al 2003) using spermine as the polyammonium ion moieties conjugated with lipophilic groups (such as steroids e.g. cholesterol, bile acids, long alkyl or alkenyl chains e.g. C_{18} fatty acids), to develop more efficient non-viral gene delivery systems in order to improve DNA uptake by target cells for safe non-viral gene therapy (NVGT). Non-viral vector mediated cell transfection remains a poorly understood phenomenon, but it is inherently safer (less immunogenic)and can transport a significantly larger DNA payload than using a viral vector.

N^4,N^9-Dioleoylspermine (LipoGen) (Ahmed et al 2005) is a lipospermine with two oleoyl chains acylating both secondary amines. This small molecule combines the characteristics of both a cationic lipid and a fusogenic (lipid bilayer disrupting) lipid in its structure. Trifluoroacetylation with ethyl trifluoroacetate (2.0 eq) was successfully used to protect only the primary amino functional groups in spermine (1.0 eq). N^1,N^{12}-Di-(trifluoroacetyl)spermine was reacted with oleic acid (2.2 eq) to form N^4,N^9-dioleoyl-N^1,N^{12}-di-(trifluoroacetyl)spermine using 1,3-dicyclohexylcarbodiimide (DCC) (2.4 eq) and catalyzed by 1-hydroxybenzotriazole (HOBt) (1.0 eq). The removal of the protecting groups was easily carried out at alkaline pH (11.0) in methanolic ammonia. Given N^4,N^9-dioleoylspermine carries two positive charges at neutral pH, the removal of unreacted starting materials and by-products (e.g. oleic acid, dicyclohexylurea etc) was carried out by column chromatographic elution over flash silica gel with DCM/MeOH (5/2 v/v) as mobile phase. Then, N^4,N^9-dioleoylspermine was collected by elution with DCM/MeOH/NH_4OH (25/10/1 v/v/v) and characterised by NMR and MS.

The ammonium ions interact with and then condense DNA, so we are studying the formulation and analytical chemistry of these polyamine conjugates acting as histone mimics. DNA condensation, the first step in gene delivery achieved by DNA phosphate charge neutralisation with cationic lipopolyamines, was studied by the fluorescence quenching of ethidium bromide (EthBr) (Geall & Blagbrough 2000) to monitor the formation of nanoparticles and to determine the efficiency of the condensation process. The fluorescence yield of EthBr (λ_{ex} = 260 nm, λ_{em} = 600 nm) increased on intercalation between adjacent base-pairs, and then gradually decreased as the DNA phosphate anions were neutralised by titration with increasing ammonium/phosphate (N/P) charge ratio. We showed that lipophilic modification of spermine resulted in a more efficient Enhanced Green Fluorescent Protein (pEGFP) cDNA condensation (15% residual fluorescence, in the EthBr assay, at N/P charge ratio 2.5) compared to tetracationic spermine (50% at N/P charge ratio 3.0). Particle formation was confirmed by measuring UV light scattering (LS), recorded as increased absorption at λ = 320 nm. This can be compared to the efficiency of primary FEK4 cell line transfection with plasmid DNA encoding EGFP condensed by the same lipopolyamine; transfection efficiency (62% at optimal charge ratio 2.5) is significantly higher than in the control cells transfected with cationic lipid (DOTMA/DOPE) (10-40%). Thus, this is an efficient novel lipopolyamine for NVGT in vitro.

We thank Universities U.K. for an ORS award to N. A. and Prof R. M. Tyrrell (University of Bath) for the FEK4 cell line.

Ahmed, O. A. A. et al (2005) *Pharm. Res.*, **22**: 12 pp in press
Blagbrough, I. S. et al (2003) *Biochem. Soc. Trans.* **31**: 397-406
Geall, A. J., Blagbrough, I. S. (2000) *J. Pharm. Biomed. Anal.* **22**: 849-859

3. MAF9 (POSTER)

MONITORING SINGLE LIPOPOLYAMINE-DNA NANOPARTICLE FORMATION IN NON-VIRAL GENE THERAPY BY FLUORESCENCE CORRELATION SPECTROSCOPY USING PICOGREEN

Noppadon Adjimatera[1], Teresa Kral[2,3], Martin Hof[2], and Ian S. Blagbrough[1]

[1] *Department of Pharmacy and Pharmacology, University of Bath, Bath BA2 7AY, U.K.*

[2] *J. Heyrovský Institute of Physical Chemistry, Academy of Sciences of the Czech Republic, Dolejškova 3, Cz-18223 Prague 8, Czech Republic.*

[3] *Dept. of Physics and Biophysics, Agricultural Univ., Norwida 25, 50-375 Wrocław, Poland.*

Non-viral gene therapy (NVGT) has the potential to revolutionize the way difficult-to-cure diseases are treated. DNA nanocomplex formation is the first crucial step in NVGT. DNA nanostructures (50-150 nm in diameter) can be self-assembled by the interactions of cationic lipids with DNA phosphate negative charges. This DNA compaction protects DNA from degradation and facilitates gene delivery. Fluorescence Correlation Spectroscopy (FCS) fluctuations in the detected fluorescence from small sensors e.g. ethidium bromide (EthBr), PicoGreen® (PG), are used to study dynamic processes of DNA nanocomplex formation [1,2]. The advantages of the FCS approach in comparison to standard fluorescence techniques are: a) use of lower dye concentrations; b) use of low (nM) DNA concentrations; c) information about possible condensed plasmid sub-populations; d) the possibility of monitoring the condensation process at the single molecule level. Employing PG, a high affinity DNA intercalating agent that only fluoresces when intercalated, we have used FCS to provide more insight e.g. diffusion time and particle number (PN), than the steady-state fluorimetric method.

We have studied two circular plasmid DNAs (pGL3 and pEGFP) using two lipopolyamines. N^4,N^9-Dioleoylspermine efficiently condensed both plasmid DNAs into point-like molecules with similar diffusion coefficient (D) = 4 x 10^{-12} m^2/s, and particle number (PN) = 1.6 and 1.0 (theoretical PN under this point-like molecular model is 0.6). N^1-Cholesteryl spermine carbamate showed poorer DNA condensation efficiency at similar N/P (ammonium/phosphate) charge ratios. A better understanding of DNA condensation, using new probes and fluorescence techniques will lead to the development of more efficient DNA condensing agents.

We acknowledge the financial support of Universities U.K. (ORS award to N.A.) and of the Grant Agency of the Czech Republic (203/05/2308).

[1] T. Kral, M. Langner, M. Benes, D. Baczynska, M. Ugorski, M. Hof, *Biophys. Chem.* **95** (2002) 135-144.

[2] N. Adjimatera, A.P. Neal, I.S. Blagbrough, Fluorescence Techniques in Non-Viral Gene Therapy in: *Fluorescence Spectroscopy in Biology*, Eds., M. Hof, R. Hutterer, V. Fidler, Springer-Verlag, Berlin (2005) 201-228.

4. MAF9 (POSTER)

FLUORESCENT LIPOPOLYAMINES: A NEW CLASS OF MOLECULAR PROBES IN NON-VIRAL GENE THERAPY

Noppadon Adjimatera, Adrian P. Neal, Chararеh Pourzand and Ian S. Blagbrough

Department of Pharmacy and Pharmacology, University of Bath, Bath BA2 7AY, U.K.

Spermine is a natural polyamine which plays important roles in DNA condensation. We are studying lipospermines, spermine conjugated with lipophilic groups (such as steroids e.g. cholesterol or long alkyl or alkenyl chains e.g. C_{18} fatty acids), as part of a programme to develop more efficient non-viral gene delivery systems for effective and safe non-viral gene therapy (NVGT). The use of a variety of fluorescence techniques enable the intracellular monitoring of NVGT at the molecular level. DNA condensation, the first step in the gene delivery mechanism, was studied by the fluorescence quenching of ethidium bromide (EthBr) to monitor the formation of nanoparticles [1-3]. The fluorescence yield of EthBr (λ_{ex} = 260 nm, λ_{em} = 600 nm) increased on intercalation between adjacent base-pairs, and then gradually decreased when DNA phosphate anions were neutralised by increasing the ammonium/phosphate (N/P) charge ratio. Formation of DNA complexes was confirmed by UV light scattering (LS) at λ = 320 nm. The plasmid encoding enhanced green fluorescent protein (pEGFP) under the control of CMV promoter (Clontech) was chosen as the DNA to be delivered. Transfected cells with fluorescent imidazolidinone-labelled protein were analysed by fluorescent-activated cell sorting (FACS). Similar experiments were also conducted using the luciferase plasmid (pGL3). N^2, N^3-Dioleoyl spermine (i.e. LipoGen®) showed more effective DNA condensation than spermine, at all N/P charge ratios. The *in vitro* transfection results using LipoGen were also significantly higher in both primary cell lines (skin fibroblast) and carcinoma, comparing to Lipofectin® (liposomal cationic lipid). Designed fluorescent-tagged lipopolyamines were prepared by Fmoc chemistry [1]. These probes are designed for studies tracking the major intracellular barriers to efficient NVGT, e.g. cell entry, endosome escape, nuclear localisation. The trafficking of DNA complexes can be monitored by fluorescence microscopy. These conjugate probes can be reporters at different stages of plasmid delivery by the use of Fluorescence Correlation Spectroscopy (FCS) studying the change in fluorophore diffusion behaviour within DNA complexes. Fluorescent tagged plasmid DNA was also prepared by non-enzymatic (random) covalent conjugation and shown to transfect as efficiently. With fluorophores labelling both DNA and vector, the Fluorescence Resonance Energy Transfer (FRET) effect may be observed to offer more insights about NVGT kinetics and barriers, with even the possibility of in vivo studies. A clearer understanding of the complexity of the barriers to NVGT is crucial in the development of novel efficient vectors.

We acknowledge the financial support of the EPSRC (studentship to A.P.N.) and an ORS award from Universities U.K. (to N.A.). We are grateful to Prof R. M. Tyrrell (University of Bath) for the FEK4 cell line.

[1] I.S. Blagbrough, A.J. Geall, A.P. Neal, *Biochem. Soc. Trans.* **31** (2003) 397-406.

[2] A. J. Geall, I.S. Blagbrough, *J. Pharm. Biomed. Anal.* **22** (2000) 49-859.

[3] H. Gershon, R. Ghirlando, S.B. Guttman , A. Minsky, *Biochemistry* **32** (1993) 7143-7151.

5. 229th ACS (ORAL)

Sensing DNA nanocomplex delivery by fluorescent probes

Noppadon Adjimatera, Adrian P. Neal, and Ian S. Blagbrough.
Department of Pharmacy and Pharmacology, University of Bath, Bath BA2 7AY, United Kingdom

DNA condensation, an important molecular event in life, enables lengthy polynucleotides to be stored as chromosomes. We have designed and prepared biomimetic lipopolyamines conjugated to fluorescent probes as sensors to aid in the development of novel and more efficient therapeutics for gene therapy. These DNA nanostructures (50-150 nm outer diameter) are prepared by the interaction of cationic lipid vectors with the negative charges of the DNA phosphate i.e. self-assembled nanostructures. This DNA compaction facilitates gene delivery, and the fluorescent sensors allow us to monitor stability in extracellular compartments, cellular uptake, and other intracellular processes such as endosome escape and nuclear entry, eventually leading to protein synthesis (which can be another biosensor). Small molecule DNA intercalators have been used as sensors to determine the polycation-DNA phosphate interaction, e.g. ethidium bromide, and a cyanine dye, (a polyamine conjugate of benzo-1,3-thiazole and 1-phenylquinoline) PicoGreen, by measuring the steady state fluorescence intensity over the condensation process. In addition to these fluorescence techniques, the formation of nanoparticles by DNA condensation was observed in a light scattering assay. Fluorescence correlation spectroscopy (FCS), a new technique where fluctuations in the detected fluorescence from small sensors is monitored, was also used to study dynamic processes at the single molecule level. Using these probes, we were able to obtain more insight by FCS than by the steady-state fluorimetric method, such as change in diffusion time of the complex, and "particle number" (photons). Ultimately, a better understanding of DNA condensation will come from new sensors and techniques leading to the development of more efficient DNA condensing agents for therapeutic non-viral gene therapy. Designed small molecule fluorescent sensors will play an important part in this nanoparticle research area. We acknowledge the financial support of the EPSRC (studentship to A.P.N.) and an ORS award from Universities U.K. (to N.A.).

6. 229th ACS (ORAL)

Monitoring formulation and intracellular delivery of plasmids by lipopolyamines

Noppadon Adjimatera, Ian S. Blagbrough, and Charareh Pourzand.
Department of Pharmacy and Pharmacology, University of Bath, Bath BA2 7AY, United Kingdom

There remain significant challenges in the development of biopharmaceutical formulations for efficient non-viral gene therapy. The mechanisms of the initial intracellular steps are currently poorly understood, making the effectiveness of therapeutic gene delivery difficult to predict and manage. Transfection efficiency cannot be improved without a greater knowledge of the molecular detail of these important intracellular events. Our novel delivery agents, lipopolyamines N^2,N^3-dioleoylspermine and N^1-cholesterylspermine carbamate, are developed from the tetra-amine spermine conjugated with a lipophilic moiety (e.g. long-chain oleic or other unsaturated fatty acids, steroids e.g. cholesteryl or cholic and other bile acids, and other research groups have incorporated lipophilic vitamin D). These lipopolyamine vectors are produced and purified on a gram scale for our formulation and gene delivery research. These excipients have been developed by considering the optimal positive charge number and the regiochemical distribution of those charges, as well as the important role of the lipid moiety in aiding DNA complexation. DNA condensation, that is nanoparticle formation (including characterization at 50-150 nm diameter), is a critical first step in NVGT formulation. When successful, this condensed formulation helps to protect the plasmid DNA from physical, chemical, and biological degradation, and it facilitates cell entry with integrity for gene delivery. We used spectroscopic assays for monitoring DNA condensation in our novel formulations, including a fluorescence quenching ethidium bromide assay and a light scattering assay. Using these techniques, we have shown that our synthetic lipopolyamine excipients condense DNA more efficiently than the natural polyamines spermidine and spermine. Transfection efficiency was monitored in carcinoma and in primary skin cell lines which confirmed the novel formulation's improved biological integrity in plasmid delivery (generating 70% fluorescent cells compared with Lipofectin's typical 10% efficiency). We thank Universities U.K. for an ORS award to N.A.

7. 229th ACS (POSTER)

Synthesis and biological testing of lipopolyamine N^2,N^3-dioleoylspermine: Self-assembly of a nanopharmaceutical for plasmid delivery

Noppadon Adjimatera, Charareh Pourzand, and Ian S. Blagbrough.
Department of Pharmacy and Pharmacology, University of Bath, Bath BA2 7AY, United Kingdom

Novel gene delivery excipients have been designed based upon modified synthetic polyamine-conjugates (lipopolyamines), using spermine as the polyammonium ion moiety conjugated with lipophilic groups (steroids e.g. cholesterol, bile acids, long alkyl or alkenyl chains), to develop more efficient non-viral gene delivery systems in order to improve DNA uptake by target cells for effective non-viral gene therapy (NVGT). N2,N3-Dioleoylspermine (LipoGen®) is a lipospermine with two oleoyl chains acylating both secondary amines. This small molecule combines the characteristics of both a cationic lipid and a fusogenic (lipid bilayer disrupting) lipid in its structure. Selective protection of the primary amino groups was achieved with ethyl trifluoroacetate (2.0 eq). N1,N4-Bis-trifluoroacetylspermine was reacted with oleic acid (2.2 eq) to form the N^1,N^4-bis-protected N^2,N^3-dioleoylspermine using 1,3-dicyclohexylcarbodiimide (DCC) (2.4 eq) and catalyzed by 1-hydroxybenzotriazole (HOBt) (1.0 eq). Facile deprotection at alkaline pH (11.0) preceded purification over silica gel yielded N^2,N^3-dioleoylspermine. DNA-bending was monitored by fluorescence quenching to analyse and quantify the efficiency of DNA condensation. The fluorescence yield of ethidium bromide increased on intercalation between adjacent base-pairs, and then gradually decreased when the DNA phosphate anions were neutralised by increasing the ammonium/phosphate (N/P) charge ratio. We showed that lipophilic modification (dioleoyl addition) of spermine resulted in a more efficient Enhanced Green Fluorescent Protein cDNA condensation (15% residual fluorescence, in the EthBr assay, at N/P charge ratio 2.5) compared to tetracationic spermine (50% at N/P charge ratio 3.0). Particle formation was confirmed by UV light scattering, increased absorption at l = 320 nm. The transfection efficiency (70% at optimal charge ratio 2.5) is significantly higher than in the control cells transfected with cationic lipid DOTMA/DOPE (10-40%). Given the superiority of this novel lipopolyamine (to spermine), we are studying its mechanisms and kinetics in NVGT. We thank Universities U.K. for an ORS award to N.A.

8. BPC2004 (POSTER)

Fluorescent lipopolyamines: a new class of molecular probes in non-viral gene therapy

N. Adjimatera, A. P. Neal, C. Pourzand and I. S. Blagbrough

Department of Pharmacy and Pharmacology, University of Bath, Bath BA2 7AY, U.K.

prsisb@bath.ac.uk

Spermine is a natural polyamine which plays important roles in DNA condensation. We are studying lipospermines, spermine conjugated with lipophilic groups (such as steroids e.g. cholesterol or long alkyl or alkenyl chains e.g. C_{18} fatty acids), as part of a programme to develop more efficient non-viral gene delivery systems for effective and safe non-viral gene therapy (NVGT). The use of a variety of fluorescence techniques enable the intracellular monitoring of NVGT at the molecular level. DNA condensation, the first step in the gene delivery mechanism, was studied by the fluorescence quenching of ethidium bromide (EthBr) to monitor the formation of nanoparticles (Gershon et al 1996, Geall & Blagbrough 2000). The fluorescence yield of EthBr (λ_{ex} = 260 nm, λ_{em} = 600 nm) increased on intercalation between adjacent base-pairs, and then gradually decreased when DNA phosphate anions were neutralised by increasing the ammonium/phosphate (N/P) charge ratio. Formation of DNA complexes was confirmed by UV light scattering (LS) at λ = 320 nm. The plasmid encoding enhanced green fluorescent protein (pEGFP) under the control of CMV promoter (Clontech) was chosen as the DNA to be delivered. Transfected cells with fluorescent imidazolidinone-labelled protein were analysed by fluorescent-activated cell sorting (FACS). Similar experiments were also conducted using the luciferase plasmid (pGL3). N^2, N^3-Dioleoyl spermine (i.e. LipoGen®) showed more effective DNA condensation than spermine, at all N/P charge ratios. The *in vitro* transfection results using LipoGen were also significantly higher in both primary cell lines (skin fibroblast) and carcinoma, comparing to Lipofectin® (liposomal cationic lipid). Designed fluorescent-tagged lipopolyamines were prepared by Fmoc chemistry (Blagbrough et al 2003). These probes are designed for studies tracking the major intracellular barriers to efficient NVGT, e.g. cell entry, endosome escape, nuclear localisation. The trafficking of DNA complexes can be monitored by fluorescence microscopy. These conjugate probes can be reporters at different stages of plasmid delivery by the use of Fluorescence Correlation Spectroscopy (FCS) studying the change in fluorophore diffusion behaviour within DNA complexes. Fluorescent tagged plasmid DNA was also prepared by non-enzymatic (random) covalent conjugation and shown to transfect as efficiently. With fluorophores labelling both DNA and vector, the Fluorescence Resonance Energy Transfer (FRET) effect may be observed to offer more insights about NVGT kinetics and barriers, with even the possibility of in vivo studies. A clearer understanding of the complexity of the barriers to NVGT is crucial in the development of novel efficient vectors.

We acknowledge the financial support of the EPSRC (studentship to A.P.N.) and an ORS award from Universities U.K. (to N.A.). We are grateful to Prof R. M. Tyrrell (University of Bath) for the FEK4 cell line.

Blagbrough, I. S. et al (2003) *Biochem. Soc. Trans.* **31**: 397-406
Geall, A. J., Blagbrough, I. S. (2000) *J. Pharm. Biomed. Anal.* **22**: 49-859
Gershon, H. et al (1993) *Biochemistry* **32**: 7143-7151

FLUORESCENCE CORRELATION SPECTROSCOPY OF SPERMINE-DNA INTERACTIONS – NANOSTRUCTURE AND PHYSICAL SUPRAMOLECULAR CHEMISTRY OF DNA CONDENSATION

TERESA KRAL[1], MAREK LANGNER[2], MARTIN HOF[1], NOPPADON ADJIMATERA[3], and IAN S. BLAGBROUGH[3]*

[1] *J. Heyrovský Institute, Academy of Sciences of the Czech Republic and Center for Complex Molecular Systems and Biomolecules, Dolejškova 3, Cz-18223 Prague 8, Czech Republic.*
[2] *Wrocław University of Technology, Institute of Physics, Wyb. Wyspiańskiego 27, 50-370, Wrocław, Poland.*
[3] *Department of Pharmacy and Pharmacology, University of Bath, Bath BA2 7AY, U.K.*

martin.hof@jh-inst.cas.cz
prsisb@bath.ac.uk

DNA condensation, one of the important events in life, enables lengthy polynucleotides to be stored as chromosomes in the nucleus of a cell, but utilising a minimum of space. This nanostructure can be achieved by the interactions of cationic lipids with the negative charges of DNA phosphate. Naturally occurring histones (lysine and arginine rich protein) and spermine help to maintain the folded conformations of DNA in cells. The use of spermine and its conjugates to compact DNA by condensation has been recently studied[1-5], with an aim to use self-assembled DNA nanoparticles in gene therapy. The condensed DNA particles are in the range 10-180 nm, typically 50-150 nm in outer diameter. This DNA compaction facilitates several key aspects of self assembly: its stability in extracellular compartments, cellular uptake, and other intracellular processes such as nuclear entry.

Spermine

DNA intercalating agents have been widely used to determine the polycation-DNA interaction. e.g. ethidium bromide (EthBr), propidium iodide, PicoGreen. EthBr steady state fluorescence assay is the mostly used simple technique to monitor the conformation change of DNA over the condensation process[3]. EthBr, intercalated in stacks of DNA base pairs, fluoresces at 600 nm by direct excitation at 546 nm, or more efficiently through energy transfer from DNA base by excitation at 260 nm[4]. On DNA condensation at increasing ammonium/phosphate (N/P) charge ratio, a decrease in EthBr fluorescence intensity was measured. Spermine-mediated DNA condensation occurred at N/P charge ratios ranging from 0.25 to 3.00. In addition to these fluorescence techniques, the formation of nanoparticles by DNA condensation can be observed in a light scattering (LS) assay, measuring UV apparent absorption at $\lambda > 300$ nm. DNA complexes were formed at N/P charge ratios ranging from 0.50 to 3.00. The optimal N/P charge ratio for both EthBr and LS assays was 3.0[5].

Fluorescence correlation spectroscopy (FCS) is a technique where fluctuations in the detected fluorescence from small molecules (such as DNA intercalating probes) are used to study dynamic processes on the molecular scale. We have demonstrated for the first time that FCS is able to monitor the condensation process of DNA-plasmids on a single molecule level[6-8]. DNA plasmids are loaded with fluorescent dyes: ethidium bromide, propidium iodide, or PicoGreen and the diffusion coefficient of single plasmids are determined by FCS. Condensation induced by positively charged condensing agents like e.g. spermine leads to a dramatic increase in the diffusion coefficient. The advantages of the FCS approach in comparison to standard fluorescence techniques are: a) use of lower dye concentration, b) information of possible plasmid sub-populations, c) the possibility to monitor the condensation process on a single molecule level.

Considering the success in using FCS, more fluorescence techniques have been developed from FCS e.g. in vivo FCS, fluorescence resonance energy transfer (FRET) by FCS. These would reveal more detailed nanostructure and physical chemistry of DNA condensation. Ultimately a better understanding of DNA condensation will lead to the development of more efficient DNA condensing agents. Designed small molecule fluorescent probes will play an important part in this[2,5].

We thank Universities U.K. for an ORS award to N.A.

REFERENCES

1. Böttcher C., Endisch C., Fuhrhop J.H., Catterall C., Eaton M. J. Am. Chem. Soc. *120*, 12 (1998).
2. Blagbrough I.S., Geall A.J., Neal A.P. Biochem. Soc. Trans. *31*, 397 (2003).
3. Geall A.J., Blagbrough I.S. J. Pharm. Biomed. Anal. *22*, 849 (2000).
4. Gershon H., Ghirlando R, Guttman S.B., Minsky A. Biochemistry *32*, 7143 (1993).
5. Adjimatera N., Neal A.P., Blagbrough I.S. in: *Fluorescence Methods and Applications, Vol. 3,* Spectroscopy, Imaging and Probes, (Eds. Hof M., Hutterer R., Fidler V.) Book Chapter, in press (2004).
6. Kral T., Hof M., Langner M. Biol. Chem. *383*, 331 (2002).
7. Kral T., Hof, M., Jurkiewicz P., Langner M. Cell Mol. Biol. Lett. *7*, 203 (2002).
8. Kral T., Langner M., Benes M., Baczynska D., Ugorski M., Hof, M. Biophys. Chem. *95*, 135 (2002).

MOLECULAR MODELLING OF DNA-ETHIDIUM BROMIDE-POLYAMINE WEAK INTERACTIONS – DNA BENDING AND CONDENSATION LEADING TO SELF-ASSEMBLY OF A NANOPHARMACEUTICAL

NOPPADON ADJIMATERA[1], IAN S. BLAGBROUGH[1]*, and IAN S. HAWORTH[2]
[1] *Department of Pharmacy and Pharmacology, University of Bath, Bath BA2 7AY, U.K.*
[2] *Department of Pharmaceutical Sciences, University of Southern California, Los Angeles CA 90033, U.S A.*

prsisb@bath.ac.uk

Polyamines and their conjugates electrostatically interact with DNA to form self-assembled nanoparticles[1]. Spermidine, a tri-amine, was first reported to condense DNA[2]. The DNA collapse was explained by the counterion condensation theory further developed by Manning[3]. Naturally occurring and biologically useful polycations (such as the tetra-amine spermine and spermidine) were found to lower the energy of transition for DNA nanoparticle self-assembly[4]. From structure-activity relationships (SAR) within naturally occurring and synthetic polyamines, the importance of positive charge distribution in DNA condensation efficacy has been highlighted[1]. In addition to this polyamine SAR, DNA bending (conformational change) seems to exhibit selectivity for certain base sequences. Toroidal DNA particles were formed in which the DNA is organized within a series of equally sized contiguous loops that precess about the toroid axis[5-9]. The size of the nucleation loop has a direct effect on the diameter of the formed toroid, whereas solution conditions govern toroid thickness[5-9].

Ethidium bromide (EthBr) intercalates between base pairs of DNA and fluoresces at 600 nm when excited (indirectly through the DNA bases) at 260 nm or at 546 nm (direct excitation of EthBr). Upon changes to the DNA conformation, the fluorescence is decreased due to a complex mechanism for the loss of EthBr intercalation binding sites. Thus, EthBr has been widely used in DNA-polyamine interaction studies including polyamine vector-based gene therapy. The fluorescence assay was performed by titrating polyamine against DNA to achieve different interactions. In addition to these fluorescence techniques, the formation of nanoparticles by DNA condensation was also confirmed by a light (320 nm) scattering assay[10].

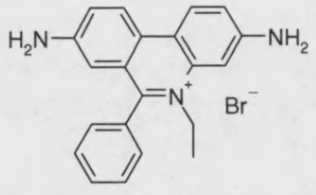

Ethidium bromide

Computer modelling of bent DNA containing intercalated ethidium was performed to obtain theoretical data to complement the above experimental results. Bent DNA was constructed using a newly designed algorithm, NASDAC (Nucleic Acids: Structure, Dynamics, and Conformation), using an algorithm for the computation of 2'-deoxyribose-phosphodiester backbone conformations that are stereochemically compatible with a given arrangement of nucleic acid bases along a DNA structure. The algorithm involves the sequential computation of 2'-deoxyribose and phosphodiester conformers beginning at the 5'-end of a DNA strand. Regardless of the conformational complexity of these structures, we are able to compute backbone conformations for each structure. Hence the algorithm, which is currently implemented within the new computer program NASDAC, should have generally applicability to the computation of DNA structures[11]. Intercalation sites based on X-ray data were included at regular intervals in the duplex, and ethidium was docked into these sites. The duplex was progressively bent in a systematic manner, and the affinity of ethidium for each bent duplex was calculated. The results provide a basis for the interpretation of the fluorescence quenching data, and the modelling provides insights into the mechanisms of DNA bending as found in the bending by polyamines and especially by lipopolyamines leading to the self-assembly of nanoparticles.

We thank Universities U.K. for an ORS award to N.A.

REFERENCES

1. Blagbrough I.S., Geall A.J., Neal A.P. Biochem. Soc. Trans. *31*, 397 (2003).
2. Gosule L.C., Schellman J.A. Nature *259*, 333 (1976).
3. Manning G.S. Q. Rev. Biophys. *11*, 179 (1978).
4. Bloomfield V.A. Biopolymers *44*, 269 (1997).
5. Hud N.V., Downing K.H., Balhorn R.A. Proc. Natl. Acad. Sci. USA *92*, 3581 (1995).
6. Hud N.V., Downing K.H. Proc. Natl. Acad. Sci. USA *98*, 14925 (2001).
7. Shen, M.R., Downing, K.H., Balhorn, R., Hud, N.V. J. Am. Chem. Soc *122*, 4833 (2000).
8. Conwell C.C., Vilfan I.D., Hud N.V. Proc. Natl. Acad. Sci. USA *100*, 9296 (2003).
9. Hud N.V., Plavec J.A. Biopolymers *69*, 144 (2003).
10. Geall A.J., Blagbrough I.S. J. Pharm. Biomed. Anal. *22*, 849 (2000).
11. Chambers E.J., Price E.A., Bayramyan M.Z., Haworth I.S. J. Biomol. Struct. Dyn. *21*, 111 (2003).

11. ICCS&T2004 (POSTER)

SYNTHESIS AND BIOLOGICAL TESTING OF LIPOPOLYAMINE N^2,N^3-DIOLEOYLSPERMINE – SELF-ASSEMBLY OF A NANOPHARMACEUTICAL FOR PLASMID DELIVERY

NOPPADON ADJIMATERA, CHARAREH POURZAND, and IAN S. BLAGBROUGH*
Department of Pharmacy and Pharmacology, University of Bath, Bath BA2 7AY, U.K.

prsisb@bath.ac.uk

Spermine is a natural tetra-cation polyamine which plays important roles in DNA condensation, and especially (together with histones, naturally occurring polymers of lysine and arginine) in maintaining the folded conformations of DNA in the nucleus. We are designing novel small molecule DNA-condensing agents, modified synthetic polyamine-conjugates (lipopolyamines), using spermine as the polyammonium ion moieties conjugated with lipophilic groups (such as steroids e.g. cholesterol, bile acids, long alkyl or alkenyl chains e.g. C_{18} fatty acids), as part of a programme to develop more efficient non-viral gene delivery systems in order to improve DNA uptake by target cells for safe and effective non-viral gene therapy (NVGT). Non-viral vector mediated cell transfection remains a poorly understood phenomenon both *in vitro* and *in vivo*, but it is inherently safer and can transport a significantly larger DNA payload than using a viral vector[1].

N^2,N^3-Dioleoylspermine (LipoGen) is a lipospermine with two oleoyl chains acylating both secondary amines. This simple, small molecule combines the characteristics of both a cationic lipid and a fusogenic (lipid bilayer disrupting) lipid, such as dioleoyl phosphatidylethanolamine (DOPE), in its structure. Protection of amino groups is crucial to efficient synthetic control of polyamines[2,3]. Trifluoroacetylation with ethyl trifluoroacetate (2.0 eq) was successfully used to protect only the primary amino functional groups in spermine (1.0 eq)[2-4]. N^1,N^4-Trifluoroacetylspermine was reacted with oleic acid (2.2 eq) to form N^2,N^3-dioleoylspermine using 1,3-dicyclohexylcarbodiimide (DCC) (2.4 eq) and catalyzed by 1-hydroxybenzotriazole (HOBt) (1.0 eq). The removal of this protecting group was easily carried out at alkaline pH (11.0). Given N^2,N^3-dioleoylspermine carries two positive charges at neutral pH, the removal of unreacted starting materials and by-products (e.g. oleic acid, dicyclohexylurea etc) was carried out by column chromatographic elution over flash silica gel with DCM/MeOH (5/2 v/v) as mobile phase. Then, N^2,N^3-dioleoylspermine was collected by elution with DCM/MeOH/NH_4OH (25/10/1 v/v/v). The obtained sample was pre-column derivatized with dansyl chloride and its homogeneity analysed by HPLC with fluorescence detection[5,6]; full spectroscopic identification was carried out by using NMR and MS.

DNA-bending experiments were monitored by UV-fluorescence spectroscopic techniques to analyse and quantify the efficiency of DNA condensation. This condensation was achieved by DNA phosphate charge neutralisation with cationic lipopolyamines. The ammonium ions interact with and then condense DNA, so we study the formulation and analytical chemistry of these polyamine conjugates acting as histone mimics. DNA condensation, the first step in gene delivery, was studied by the fluorescence quenching of ethidium bromide (EthBr) to monitor the formation of nanoparticles[7]. The fluorescence yield of EthBr (λ_{ex} = 260 nm, λ_{em} = 600 nm) increased on intercalation between adjacent base-pairs, and then gradually decreased when the DNA phosphate anions were neutralised by increasing the ammonium/phosphate (N/P) charge ratio. We showed that lipophilic modification of spermine resulted in a more efficient Enhanced Green Fluorescent Protein (pEGFP) cDNA condensation (15% residual fluorescence, in the EthBr assay, at N/P charge ratio 2.5) compared to tetracationic spermine (50% at N/P charge ratio 3.0). Particle formation was confirmed by measuring UV light scattering (LS)[8], recorded as increased absorption at λ = 320 nm. This is compared to the efficiency of cell line transfection with plasmid DNA encoding EGFP, and condensed by the same lipopolyamine. The transfection efficiency (62% at optimal charge ratio 2.5) is significantly higher than in the control cells transfected with cationic lipid (DOTMA/DOPE) (10-40%). Given the superiority of this novel lipopolyamine (to spermine), we are studying its mechanisms and kinetics in NVGT.

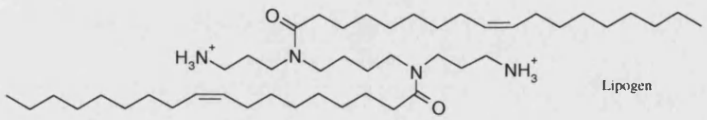

Lipogen

We thank Universities U.K. for an ORS award to N.A.

REFERENCES

1. Blagbrough I.S., Geall A.J., Neal A.P. Biochem. Soc. Trans. *31*, 397 (2003).
2. Geall A.J., Blagbrough I.S. Tetrahedron *56*, 2449 (2000).
3. Blagbrough I.S., Al-Hadithi D., Geall A.J. Tetrahedron *56*, 3439 (2000).
4. O'Sullivan M.C., Dalrymple, D.M. Tetrahedron Lett. *36*, 3451 (1995).
5. Hawel L., Byus C.V. Anal. Biochem. *311*, 127 (2002).
6. Escribano M. I., Legaz M. E. Plant Physiol. *87*, 519 (1988).
7. Geall A.J., Blagbrough I.S. J. Pharm. Biomed. Anal. *22*, 849 (2000).
8. Geall A.J., Taylor R.J., Earll M.E., Eaton M.A.W., Blagbrough I.S. Bioconjug. Chem. *11*, 314 (2000).

12. MAF8 (POSTER)

FLUORESCENCE TECHNIQUES IN NON-VIRAL GENE THERAPY: USING SPERMINE AND LIPOPOLYAMINES AS DNA DELIVERY AGENTS

Noppadon Adjimatera, Adrian P. Neal, Charareh Pourzand, and Ian S. Blagbrough (e-mail: ***prsisb@bath.ac.uk***)

Department of Pharmacy and Pharmacology, University of Bath, Bath BA2 7AY, U.K.

Spermine is a natural polyamine which plays important roles in DNA condensation. We are studying lipospermines, spermine conjugated with lipophilic groups (such as steroids e.g. cholesterol or long alkyl or alkenyl chains e.g. C18 fatty acids), as part of a programme to develop more efficient non-viral gene delivery systems for effective and safe non-viral gene therapy (NVGT). Designed fluorescent probes and the use of a variety of fluorescence techniques will enable the intracellular monitoring of NVGT. DNA condensation, the first step in the gene delivery mechanism, was studied by the fluorescence quenching of ethidium bromide (EthBr) to monitor the formation of nanoparticles. The fluorescence yield of EthBr (λ_{ex} = 260 nm, λ_{em} = 600 nm) increased on intercalation between adjacent base-pairs, and then gradually decreased when DNA phosphate anions were neutralised by increasing the N/P charge ratio with spermine. DNA condensation occurred at N/P ratios ranging from 0.25 to 3.00. Particle formation was confirmed by UV light scattering (LS), recorded as increased absorption at λ = 320 nm. The particles of condensed DNA were formed at N/P ratios ranging from 0.50 to 3.00. The optimal N/P ratio for both EthBr and LS assays was 3.00. The plasmid encoding enhanced green fluorescent protein (p-EGFP) under control of CMV promoter (Clontech) (1-6 μg/μl) was chosen as the DNA to be delivered. Different charge ratios of N^2, N^3-dioleic acid-spermine conjugate (LipoGen from InvivoGen) to DNA (2.0 μg /well) were used in a primary human skin fibroblast cell line at 2.5 x 104 cells/well. Transfected cells with fluorescent imidazolidinone-labelled protein (λ_{ex} = 488 nm, λ_{em} = 507 nm) were analysed by fluorescent-activated cell sorting (FACS). The transfection efficiency (62%) is significantly higher than in the control cells transfected with cationic lipid (DOTMA/DOPE) (10-40%). Similar experiments were also conducted using the luciferase plasmid (pGL3). A novel lipopolyamine fluorescent tagging strategy is being used to study the major intracellular barriers, e.g. endosome escape, nuclear localisation, to efficient NVGT. We thank the EPSRC for a PhD studentship to A.P.N.